A dynamical study of the chirally rotated Schrödinger functional in lattice QCD

by

Mattia Dalla Brida

supervised by

Stefan Sint

A Project submitted to

The University of Dublin

for the degree of

Doctor in Philosophy

School of Mathematics

University of Dublin

Trinity College

February 2015
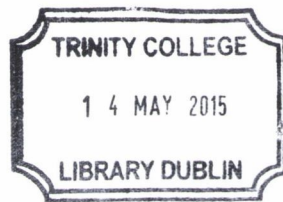
This project has not been submitted as an exercise for a degree at any other University. Except where otherwise stated, the work described herein has been carried out by the author and by Dr. Stefan Sint. This project may be borrowed or copied upon request with the permission of the Librarian, University of Dublin, Trinity College. The copyright belongs jointly to the University of Dublin and Mattia Dalla Brida.

Signature of Author: _Mattia Dalla Brida_

Summary

In this work, we present first results from dynamical simulations of the chirally rotated Schrödinger functional (SF) in lattice QCD. More specifically, we discuss the determination of renormalization constants of quark-bilinears, and show evidence for the expected automatic $O(a)$ improvement of these determinations. After a short introduction on the topics of non-perturbative renormalization and improvement in lattice field theory, we recall the technical advantages of renormalization schemes based on the SF. We then motivate and discuss the lattice regularization of the SF with chirally rotated boundary conditions, and present details and tests on the simulation algorithm. Finally, we comment on the results and on future possible applications of the method.

Acknowledgements

A Enrico Dallabrida

Contents

1

Introduction

The Standard Model (SM) of particle physics gives a unified theoretical description of all known phenomena governed by the strong, weak, and electromagnetic interactions. Extraordinarily accurate predictions have been confirmed so far for an incredibly wide range of experiments, and up to the highest energies reachable in current accelerators. The discovery of a possibly fundamental scalar field made at CERN in July 2012, might even corroborate the most debated sector of the SM. The generation of the fermion and gauge boson masses through the Higgs-mechanism, provides indeed an elegant and accurate description of the present experimental evidence. The SM then passes another crucial test, and this makes it more difficult to predict what is beyond.

A way to capture the physics beyond the SM consists in exploring higher and higher energy scales, where new degrees of freedom might become active and manifest explicitly in the dynamics. On the other hand, the existence of as yet undetected high-energy excitations might be unveiled at low-energy through their effects as virtual particles. To this end, however, unprecedented precision is needed in both theoretical and experimental determinations.

In this respect, the strongly interacting sector of the SM plays a crucial rôle. Indeed, at energies much below the mass of the W-bosons, the SM can be accurately described by a theory of strongly coupled quarks and gluons and some effective electro-weak interactions.[1] As a result, precise SM predictions require first of all control on the strong interaction contributions, which are in general the dominant ones and most difficult to treat.

---

[1]We recommend (Donoghue, Golowich and Holstein, 1994) for an introduction to the effective low-energy descriptions of the SM. A discussion in the context of lattice field theory techniques can then be found in (Lellouch, 2011).

The aim of our work is to develop techniques in the context of lattice field theory which can lead to precise theoretical determinations of strong interaction contributions. In order to introduce our study in more detail, we start in the next section with a brief review of the theory of the strong interactions, namely, Quantum Chromo Dynamics (QCD).[2] This simply serves us to fix some of the notation, and recall some basic concepts needed in the following. Later, we introduce the lattice formulation of QCD and thus contextualize our study. We then conclude with an outline of this work.

1.1   Quantum Chromo Dynamics

QCD is a quantum field theory characterized by a gauge invariance under the color group $SU(3)_c$. It is defined in terms of a gluon field A_μ, and quark and anti-quark fields ψ and $\overline{\psi}$. The latter are taken to be a column and row vector of length N_f, respectively, where N_f corresponds to the number of quark flavours $f = u, d, s, c, b, t$, considered. For reasons that will become clear shortly, the theory is set-up in Euclidean space-time.

The dynamics of QCD is determined by the action,

$$S[A, \psi, \overline{\psi}] = S_G[A] + S_F[A, \psi, \overline{\psi}], \tag{1.1}$$

where S_G is the action for the gluon field, while S_F is the action for the quark fields.

The action for the gluon field is given by,

$$S_G[A] = -\frac{1}{2g_0^2} \int d^4x \, \text{tr}\{F_{\mu\nu}(x)F_{\mu\nu}(x)\}, \tag{1.2}$$

where $F_{\mu\nu}$ is the field strength tensor defined by (cf. (A.23)),

$$F_{\mu\nu}(x) = \partial_\mu A_\nu(x) - \partial_\nu A_\mu(x) + [A_\mu(x), A_\nu(x)], \tag{1.3}$$

and g_0 is the (bare) gauge coupling of the theory.

The action for the quark fields instead is defined as,

$$S_F[A, \psi, \overline{\psi}] = \int d^4x \, \overline{\psi}(x)(\slashed{D} + M_0)\psi(x), \tag{1.4}$$

---

[2]For an introduction please see e.g. (Ellis, Stirling and Webber, 1996; Aitchison and Hey, 2004).

where $\not{D}$ is the massless Dirac operator, $\not{D} = \gamma_\mu(\partial_\mu + A_\mu)$, and M_0 is a $N_f \times N_f$ diagonal matrix which diagonal elements are the (bare) quark masses, m_0^f, of the quark flavours f. The Euclidean Dirac matrices, γ_μ, are collected in Appendix A.2.

Given the classical action and field content of the theory, its formal quantization is specified by the Euclidean partition function,

$$\mathcal{Z} = \int [\mathcal{D}A][\mathcal{D}\psi][\mathcal{D}\overline{\psi}]\, e^{-S[A,\psi,\overline{\psi}]}, \tag{1.5}$$

where the integration measures are given by,

$$[\mathcal{D}A] = \prod_{x,\mu,a} \mathrm{d}A_\mu^a(x), \quad [\mathcal{D}\psi] = \prod_f \prod_{x,A,a} \mathrm{d}\psi_{A,a}^f(x) \quad [\mathcal{D}\overline{\psi}] = \prod_f \prod_{x,A,a} \mathrm{d}\overline{\psi}_{A,a}^f(x). \tag{1.6}$$

We refer the reader to Appendix A.1 for the index definitions.

The quantum mechanical expectation value of a generic product of local fields, $\mathcal{O} \equiv \mathcal{O}[A, \psi, \overline{\psi}]$, is then obtained from the Euclidean correlation functions,[3]

$$\langle \mathcal{O} \rangle = \frac{1}{\mathcal{Z}} \int [\mathcal{D}A][\mathcal{D}\psi][\mathcal{D}\overline{\psi}]\, \mathcal{O}[A, \psi, \overline{\psi}]\, e^{-S[A,\psi,\overline{\psi}]}. \tag{1.7}$$

Apart from the aforementioned gauge invariance and manifest SO(4) global invariance, the theory posses a series of exact discrete symmetries, namely: parity, charge conjugation, and Euclidean time-reflection (see Appendix A.6). In addition, there are some approximate continuous global symmetries which are described by the chiral-flavour group $\mathrm{SU}(N_f)_L \times \mathrm{SU}(N_f)_R$, where L and R stand for the left- and right-handed chiral components of the quark fields.[4,5]

The chiral-flavour symmetries will be studied in more detail in the next chapter. Here we just want to note that if the quark masses m_0^f are all degenerate, then the

---

[3] A rigorous discussion on the reconstruction of quantum mechanical expectation values from Euclidean correlation functions can be found in (Lüscher, 1977; Osterwalder and Seiler, 1978), where the lattice formulation of QCD is employed.

[4] Just for completeness, we recall that the L (left) and R (right) handed chiral components of the quark fields ψ and $\overline{\psi}$ are defined as: $\psi_R = P_R\psi$, $\psi_L = P_L\psi$, $\overline{\psi}_R = \overline{\psi}P_L$, and $\overline{\psi}_L = \overline{\psi}P_R$, where the projectors P_R and P_L are given in Appendix A.2.

[5] In the following we will not discuss the exact U(1) vector symmetry associated with the baryon number conservation, nor the anomalous U(1) axial symmetry (see e.g. (Aitchison and Hey, 2004)).

mass matrix M_0 is proportional to the identity, and the action (1.4) is invariant under the flavour (or vector) transformations,

$$\psi(x) \rightarrow \psi'(x) = e^{-\alpha^a T^a} \psi(x),$$
$$\overline{\psi}(x) \rightarrow \overline{\psi}'(x) = \overline{\psi}(x) e^{\alpha^a T^a}, \tag{1.8}$$

where α^a, $a = 1, \ldots, N_{\mathrm{f}}^2 - 1$, are real constants, and T^a are algebra elements of $\mathrm{SU}(N_{\mathrm{f}})$ (see Appendix A.3). In the case where the quark masses are all zero, the action (1.4) is also invariant under the chiral (or axial) transformations,

$$\psi(x) \rightarrow \psi'(x) = e^{-\alpha^a \gamma_5 T^a} \psi(x),$$
$$\overline{\psi}(x) \rightarrow \overline{\psi}'(x) = \overline{\psi}(x) e^{-\alpha^a \gamma_5 T^a}, \tag{1.9}$$

where γ_5 is defined in Appendix A.2. In the next chapter, we will show how these symmetries of the QCD action are in fact symmetries of the whole quantum theory.

Given these observations, it might come as a surprise that the plethora of strong interactions phenomena can be described by such an apparently simple theory with relatively few parameters and extended symmetry properties. The dynamics of QCD, however, is highly non-trivial and a solution of the theory is generally difficult to obtain. In fact, at high-energies the (renormalized) QCD coupling becomes smaller and smaller as the energy of the considered process increases. This is the property of *asymptotic freedom* (Gross and Wilczek, 1973; Politzer, 1973). In this regime, the strong interactions can be described in terms of nearly free quarks and gluons, and accurate determinations can be obtained through a perturbative approximation of the QCD path-integral. On the other hand, at intermediate and low energies the strong coupling is not small, and a perturbative treatment of the strong interactions is not valid anymore. A non-perturbative solution of the theory is then generally needed in order to obtain meaningful predictions.

1.2   Lattice QCD

The lattice formulation of QCD is so far the only known method to obtain a non-perturbative solution of the theory (Wilson, 1974).[6] Starting from the Euclidean path-integral (1.7), the lattice formulation is defined by introducing a space-time lattice and

---

[6]For an introduction to lattice field theory we suggest (Montvay and Münster, 1997; Rothe, 2012).

discretizing the fields and the action. The finite lattice spacing effectively works like a momentum cutoff that eliminates all energy frequencies of the theory above $\sim a^{-1}$, where a is the lattice spacing. The lattice hence provides a non-perturbative regulator, which makes the theory finite and mathematically well-defined.

Nowadays, essentially all quantitative results in lattice QCD are obtained through numerical simulations. Considering a finite space-time volume, the theory has a finite number of degrees of freedom and numerical methods can be applied to solve it. Due to the extensive number of degrees of freedom, Monte Carlo (MC) methods are used to estimate the discretized path-integrals: representative gauge field configurations are generated stochastically, and the expectation values of generic observables are computed as ensemble averages.[7] For the given lattice parameters lattice QCD gives exact answers within the statistical uncertainties. Physical results are then expected to be obtained once the infrared and ultraviolet cutoffs have been removed or, equivalently, the infinite volume and continuum limits have been taken.

The effects of a finite physical volume are generally easier to handle. For example if one considers particle masses, general field theoretical considerations show that in a theory with a mass gap the corrections due to the finite volume are exponentially suppressed with the system size, where the exponential decay rate is given by the mass gap itself. In QCD, this means that finite volume hadron masses differ w.r.t. their infinite volume counterparts by corrections of $O(e^{-m_\pi L})$, where m_π is the pion mass and L is the finite size of the system.[8] Similar conclusions can be drawn for many other quantities of interest.

In practice, another infrared cutoff than the volume needs to be handled in lattice simulations. This is given by the quark masses. Without entering too much into the details, the problem can be tracked down to the difficultly of inverting the lattice Dirac operator numerically for relatively light quark masses. This computation is required for example in the generation of the field ensembles through MC simulations, as well as in the evaluation of fermionic correlation functions. The quark masses in fact provide an

---

[7]We will discuss the current simulations algorithms for lattice QCD in Chapter 4.

[8]We refer to (Lüscher, 1986*a*; Lüscher, 1986*b*) for the details on the derivation and conditions under which this result holds. A shorter introduction can be found in (Lüscher, 1988).

infrared cutoff for the Dirac spectrum, and the numerical computation of the inverse operator clearly suffers from the removal of this cutoff. Here we just want to mention that significant improvement has been achieved in this respect, and relatively small if not physical quark masses can now be simulated. In addition, the tools developed in the context of chiral perturbation theory can help in extrapolating lattice results at unphysical quark masses to their physical values.[9] The problem of determining our observables at the physical quark masses is then generally under control.

More delicate is the issue of taking the continuum limit. In numerical simulations this is done by simulating the theory at different values of the lattice spacing a, and then extrapolate the results for $a \to 0$. This procedure, however, is very demanding in terms of computational effort. The cost of current simulations indeed scales as a^{-7} towards the continuum limit, if the physical volume is kept fixed and for comparable statistical precision (Schaefer, 2012). This means that in practice the lattice spacing can be varied only by a modest factor. Considering that, as we shall see, lattice observables can differ from their continuum values by corrections of $O(a)$, it is not obvious that reliable and precise extrapolations can be performed. A theoretical understanding of the approach to the continuum limit of lattice observables is certainly needed, as well as techniques to control and eventually accelerate the convergence.

Related to the problem of taking the continuum limit there is the problem of the renormalization of the theory. As we remove the cutoff, the bare lattice correlation functions will develop divergences that need to be cancelled by the usual parameter and field renormalization. In this respect, note that renormalization is an ultraviolet phenomenon with relevant energy scales of $O(a^{-1})$. Since the continuum limit of lattice QCD is expected to be reached by tuning the bare coupling $g_0 \to 0$,[10] one is tempted to conclude that the renormalization of the theory can be performed perturbatively in terms of the bare coupling.[11] Bare lattice perturbation theory, however, is known

---

[9]For an introduction to chiral perturbation theory and its applications to lattice QCD see e.g. (Sharpe, 2006; Golterman, 2009).

[10]From asymptotic freedom we expect $g_0^2(a) \overset{a \to 0}{\sim} \frac{-1}{\log(a\Lambda_{\text{QCD}})}$, where Λ_{QCD} is some hadronic scale.

[11]We ignore for the moment the case of power-divergences where a perturbative treatment is not even possible a priori. We will return to this issue in the next chapter.

to be poorly convergent (Parisi, 1980; Lepage and Mackenzie, 1993). Even though the situation can be improved, it is still difficult to estimate the systematic errors one is introducing with this approximation. In fact, the crucial question is whether one is in a regime of lattice spacings fine enough for this approach to be reliable at all. In present simulations this is generally difficult to achieve since the lattice spacing a can not be taken much smaller than the relevant physical scales of the observables considered, as otherwise the computation becomes too expensive. In conclusion, in order not to introduce uncontrolled approximations in renormalized lattice observables, the renormalization has to be performed non-perturbatively! As any other non-perturbative determination, the renormalization has then to deal with the systematic effects we discussed, namely, finite-volume effects, discretization effects, and quark-mass effects. It is the aim of this work to develop methods for the non-perturbative renormalization of lattice QCD where all these systematic effects are under control.

Given these general considerations, the details of the renormalization will depend on the specific lattice regularization employed. Note that in lattice QCD there is quite some freedom in choosing the regularization. At least in perturbation theory and for some classes of actions, it has then been proven that the specific choice does not matter once the continuum limit is taken (Reisz, 1989; Reisz and Rothe, 2000). This property is referred to as the *universality* of the continuum limit, and it is assumed to be valid also at the non-perturbative level. In this work we consider the original formulation of lattice QCD as proposed by Wilson (Wilson, 1974). This discretization is theoretically robust, practically simple, and relatively cheap to simulate. All these nice properties make this alternative a concrete possibility to obtain precise and solid determinations.

The well-known drawback of Wilson's formulation is the explicit breaking of chiral symmetry at finite lattice spacing. Since chiral symmetry is a fundamental property of QCD this might be a source of concern. The effect of the breaking, however, is theoretically well-understood, and the correct chiral symmetry relations are recovered in the continuum limit after a proper renormalization of the theory (Karsten and Smit, 1981; Bochicchio *et al.*, 1985; Testa, 1998). On the other hand, as discussed in detail in the next chapter, the absence of this symmetry at finite lattice spacing implies that

the renormalization of the theory is more complicated, and the leading discretization effects are of $O(a)$. Ideas are then needed in order to obtain precise continuum limit extrapolations of renormalized lattice observables using this regularization.

In this respect, we just want to mention that chiral symmetry is a delicate issue on the lattice (Nielsen and Ninomiya, 1981a; Nielsen and Ninomiya, 1981b; Nielsen and Ninomiya, 1981c). In fact, lattice formulations that preserve (a lattice version of) chiral symmetry do exist,[12] and have been recently exploited for large scale simulations (see (Chiu, 2013)). On the other hand, even though major progress has been achieved in simulating chiral lattice fermions, these formulations are still very demanding from the computational point of view, and are not yet feasible for most computations. For this reason Wilson fermions remain a popular choice especially when precision is required.

1.3 Outline

In this work we study non-perturbative renormalization schemes based on the chirally rotated Schrödinger functional (SF) of QCD (Sint, 2006; Sint, 2011). Renormalization schemes based on the SF (Lüscher, Narayanan, Weisz and Wolff, 1992; Sint, 1994) have proven to be powerful tools in solving non-perturbative renormalization problems in lattice QCD. For the case of Wilson-quarks, we argue that the chirally rotated version of the SF is a valuable and interesting alternative to be considered. The aim is to improve our control on discretization effects, and offer novel approaches for the renormalization of operators that might be complicated by the absence of chiral symmetry. In order to motivate and introduce these renormalization schemes, as well as present the results of our investigation, several tools and concepts need to be discussed first. A general outline of this work is then the following:

Chapter 2 We start by introducing the standard Wilson formulation of lattice QCD. In particular, we focus on the consequences of chiral symmetry breaking on the renormalization of the theory. Secondly, we analyze the approach to the continuum

---

[12]Some original references on chiral lattice fermions are (Kaplan, 1992; Narayanan and Neuberger, 1995; Neuberger, 1998; Lüscher, 1998b). For an introduction instead we recommend (Lüscher, 2000; Kaplan, 2009).

limit of renormalized lattice observables through Symanzik's effective continuum theory. After a short introduction on the latter, we study how the leading $O(a)$ discretization effects of Wilson fermions can be systematically removed from our observables. Next, the general difficulties of performing non-perturbative renormalization on the lattice are discussed in detail. As we shall see, the requirements of controlled finite-volume effects and discretization effects put severe constraints on the determination of scale-dependent renormalization factors and parameters from lattice QCD. In this respect, we present how finite-volume renormalization schemes in combination with finite-size scaling techniques provide a general and elegant solution to the problem.

Chapter 3 We introduce the Schrödinger functional (SF) of QCD as a practical tool to define non-perturbative finite-volume renormalization schemes. Through its formal continuum definition we motivate this choice, and present its nice features. Secondly, we discuss the standard lattice formulation of the SF, paying particular attention to the renormalization and $O(a)$-improvement of the theory. This will lead us to introduce an alternative regularization of the SF based on the chirally rotated Schrödinger functional (χSF). The connection with the standard SF is discussed, and the lattice regularization, renormalization, and $O(a)$-improvement of the χSF are presented in detail. The crucial property of the novel formulation is that, differently from the standard SF regularization, the $O(a)$-improvement of the theory is (almost) automatic. As we shall see, the χSF thus does not only provide an interesting test of universality for the SF, but also alternative methods for the renormalization of operators where $O(a)$ cutoff effects are automatically absent.

Chapter 4 We shortly review the general algorithmic strategies for simulating lattice QCD. We then present the details of the algorithms that we have implemented to simulate the χSF. Finally, some consistency checks are discussed in order to support the correctness of our implementation.

Chapter 5 We present results from dynamical simulations of $N_f = 2$ $O(a)$-improved Wilson-fermions with chirally rotated boundary conditions. More precisely, we

consider the renormalization of several quark-bilinears including the non-singlet axial and vector currents, and pseudo-scalar density. After a short presentation of the set-up, we discuss how the expected universality between the χSF and SF can be exploited to define renormalization conditions for these operators. The results are then compared with previous SF determinations, and their automatic $\mathrm{O}(a)$ improvement is demonstrated. We conclude the chapter with a detailed analysis of the robustness of our simulations.

2
Non-perturbative renormalization

In this chapter we want to review some of the basic concepts of non-perturbative renormalization in the context of lattice field theory. As said, the aim of this work is to study a set-up for the non-perturbative renormalization of operators and fundamental parameters where all systematic effects are under control. The concepts that will be presented here are the building blocks for introducing and motivating our set-up in the next chapter. Through the next sections we will also fix some of the notation, and define several quantities which are central for our analyze later on.

More precisely, we start in the next section with a presentation of the standard Wilson formulation of lattice QCD (Wilson, 1974). In particular, we are interested in understanding the additional renormalization originating from the explicit breaking of chiral symmetry by the regularization. To this scope, the Ward identities of the theory will be studied in detail. Secondly, we introduce Symanzik's effective theory. This powerful tool allows us to systematically study and eventually improve the approach to the continuum limit of renormalized lattice observables. We conclude discussing the general problems in performing non-perturbative renormalization on the lattice, and present how finite-volume renormalization schemes and finite-size scaling techniques provide an elegant solution.

Note that most of the material presented in this chapter is by now standard wisdom in lattice field theory. The author then recommends the references that will be provided for a more detailed an complete discussion.

2.1 Wilson fermions and chiral symmetry

2.1.1 The Wilson formulation of lattice QCD

In the standard Wilson formulation of lattice QCD, the quark and anti-quark fields $\psi(x)$ and $\overline{\psi}(x)$ live on the sites x of the lattice and carry color, flavor and Dirac indices as in the continuum. We assume ψ and $\overline{\psi}$ to be isospin doublets of mass-degenerate light quarks since this will be the case of most interest for us. The gauge field instead is represented through a field of SU(3) matrices $U_\mu(x)$ associated with the links of the lattice $(x, x + a\hat{\mu})$, where $\mu = 0, \ldots, 3$, labels the four space-time directions, and $\hat{\mu}$ is the unit vector in the direction μ. The index $\mu = 0$ is conventionally associated with the time direction, while the indices $k = 1, 2, 3$, are associated with the spatial ones. If not specified otherwise, we consider the theory to be defined on a hyper-cubic lattice with lattice spacing a, and infinite extent in all directions.

The dynamics of theory is determined by the action,

$$S[U, \psi, \overline{\psi}] = S_{\mathrm{G}}[U] + S_{\mathrm{F}}[U, \psi, \overline{\psi}], \tag{2.1}$$

where S_{G} is the Wilson (or plaquette) gauge action, and S_{F} the Wilson quark action.

The gauge action S_{G} is defined by,

$$S_{\mathrm{G}}[U] = \frac{1}{g_0^2} \sum_x \sum_{\mu,\nu=0}^{3} \mathrm{tr}\{1 - P_{\mu\nu}(x)\}, \tag{2.2}$$

where g_0 is the bare gauge coupling of the theory, and $P_{\mu\nu}(x)$ is the plaquette field: $P_{\mu\nu}(x) = U_\mu(x)U_\nu(x + a\hat{\mu})U_\mu(x + a\hat{\nu})^{-1}U_\nu(x)^{-1}$.

In order to define the fermionic action S_{F}, we introduce the Wilson Dirac operator,

$$D_{\mathrm{w}} = \tfrac{1}{2} \sum_\mu \left\{ \gamma_\mu (\nabla_\mu^* + \nabla_\mu) - a\nabla_\mu^* \nabla_\mu \right\}, \tag{2.3}$$

where the lattice covariant derivatives ∇_μ and ∇_μ^* are defined in Appendix A.4. The second term in curly brackets is the Wilson term. This is included in order to avoid the well-known doubling problem on the lattice (see e.g. (Montvay and Münster, 1997)). As we shall see shortly, however, it is source of other concerns.

The action for the quark fields S_F is then defined by,

$$S_\mathrm{F}[U, \psi, \overline{\psi}] = a^4 \sum_x \overline{\psi}(x)\big(D_\mathrm{w} + m_0\big)\psi(x), \qquad (2.4)$$

where m_0 is the bare quark-mass of the degenerate quark-doublet.

Given the definitions (2.2) and (2.4), it is easy to show that the lattice action (2.1) shares all the discrete symmetries of the continuum QCD action (1.1), viz., parity, charge conjugation, and Euclidean time reflection (see Appendix A.6).[1] This, however, is not true for the continuous global symmetries. The SO(4) symmetry of continuum QCD is unavoidably broken down to the discrete hyper-cubic group H(4). Moreover, not all internal symmetries are preserved, as we now show.

The non-singlet vector (flavour) transformations (1.8) can be analogously defined on the lattice, and for $N_\mathrm{f} = 2$ Wilson-quarks read,

$$\begin{aligned}
\psi(x) &\to \psi'(x) = e^{i\alpha_V^a \frac{\tau^a}{2}}\psi(x), \\
\overline{\psi}(x) &\to \overline{\psi}'(x) = \overline{\psi}(x)e^{-i\alpha_V^a \frac{\tau^a}{2}},
\end{aligned} \qquad (2.5)$$

where τ^a, $a = 1, 2, 3$, are Pauli matrices acting on the isospin indices of the quark fields (cf. Appendix A.3), and α_V^a are some real parameters. The gauge action (2.2) is trivially invariant under any fermionic transformation, and does not need to be discussed. It is then immediate to conclude that the Wilson quark action (2.4) is invariant under the transformations (2.5) since the bare quark masses are degenerate. Vector symmetry is thus preserved by the Wilson action.

Secondly, we consider the non-singlet axial (chiral) transformations (1.9), which for $N_\mathrm{f} = 2$ Wilson-quarks are given by,

$$\begin{aligned}
\psi(x) &\to \psi'(x) = e^{i\alpha_A^a \frac{\tau^a}{2}\gamma_5}\psi(x), \\
\overline{\psi}(x) &\to \overline{\psi}'(x) = \overline{\psi}(x)e^{i\alpha_A^a \frac{\tau}{2}\gamma_5},
\end{aligned} \qquad (2.6)$$

where α_A^a are some real parameters. In this case, even if the bare quark mass m_0 is zero, the presence of the Wilson term $(a\overline{\psi}\nabla_\mu^* \nabla_\mu \psi)$ makes the Wilson action not invariant

---

[1]The lattice action (2.1) satisfies the property of reflection positivity (Lüscher, 1977). This is a fundamental property for the quantum mechanical interpretation of the theory, which includes the existence of a Hilbert space of states for the theory, and a positive self-adjoint Hamiltonian operator.

under the axial transformations (2.6). The Wilson term thus explicitly breaks chiral symmetry, which is not a symmetry of the Wilson action.

Chiral symmetry is a fundamental aspect of the low-energy dynamics of QCD. The explicit breaking of this symmetry by the regularization might then be a source of concern. In order to better understand this issue, in the next two subsections we investigate the breaking of chiral symmetry through the Ward identities of the theory. Dealing with a quantum field theory, we need to extend our analyze from the simple action to the correlation functions of the theory in order to fully capture the effects of the breaking. As we shall see, chiral symmetry is restored in the continuum limit if the lattice theory is properly renormalized (Karsten and Smit, 1981; Bochicchio *et al.*, 1985; Lüscher, Sint, Sommer and Wittig, 1997*b*; Testa, 1998). In fact, the requirement of chiral symmetry restoration in the continuum limit can be used as a condition to fix this renormalization.

2.1.2 Chiral Ward identities

In this subsection we want to study the Ward identities (WIs) of the theory, and specifically those related to chiral symmetry. The idea is first to discuss these relations in the formal continuum theory.[2] In the next subsection we will then repeat their derivation in the lattice theory with Wilson fermions. This will allow us to better understand the consequences of the breaking of chiral symmetry by the regularization on the renormalization of the theory. Note that we will skip most of the technical details, and basically summarize the main results. We thus recommend the original references that will be given for a more complete discussion. For an introduction instead we suggest (Sommer, 1997; Lüscher, 1998*a*; Vladikas, 2011).

As introduced, in Euclidean space-time the expectation value of any product of local fields $\mathcal{O}$ is given in terms of the functional integral (cf. (1.7)),

$$\langle \mathcal{O} \rangle = \frac{1}{\mathcal{Z}} \int [\mathcal{D}A][\mathcal{D}\psi][\mathcal{D}\overline{\psi}] \, \mathcal{O}[A, \psi, \overline{\psi}] \, e^{-S[A,\psi,\overline{\psi}]}. \tag{2.7}$$

---

[2]For a more rigorous derivation instead of the formal continuum theory one could consider a chirally preserving lattice formulation. The bare lattice correlation functions would then respect WIs analogous to the formal continuum ones (Hasenfratz, 1998; Kikukawa and Yamada, 1999). Since, however, we did not present chiral lattice fermions in detail, we will proceed less rigorously.

In order to obtain WIs, we simply consider suitable changes of variables in the functional integral, of the form,

$$\psi(x) \to \psi(x) + \delta\psi(x), \qquad \overline{\psi}(x) \to \overline{\psi}(x) + \delta\overline{\psi}(x). \tag{2.8}$$

Specifically, we consider infinitesimal local versions of the flavour and chiral transformations (2.5) and (2.6), which are given by,

$$\delta_V \psi(x) = i\left[\alpha_V^a(x)\frac{\tau^a}{2}\right]\psi(x), \qquad \delta_V\overline{\psi}(x) = -i\overline{\psi}(x)\left[\alpha_V^a(x)\frac{\tau^a}{2}\right], \tag{2.9}$$

$$\delta_A \psi(x) = i\left[\alpha_A^a(x)\frac{\tau^a}{2}\gamma_5\right]\psi(x), \qquad \delta_A\overline{\psi}(x) = i\overline{\psi}(x)\left[\alpha_A^a(x)\frac{\tau^a}{2}\gamma_5\right], \tag{2.10}$$

where $\alpha_{V,A}(x)$ are smooth functions that vanish outside some bounded region of spacetime we will denote by R.

Since the Pauli matrices are traceless, the integration measure in (2.7) is trivially invariant under these transformations, and we then conclude that,

$$\langle \mathcal{O}\, \delta_X S \rangle = \langle \delta_X \mathcal{O} \rangle, \tag{2.11}$$

where $\delta_X S$ and $\delta_X \mathcal{O}$, with $X = V, A$, are the infinitesimal variations of the continuum action S and observable $\mathcal{O}$ corresponding to the transformations (2.9) and (2.10), respectively. By considering different transformations, observables $\mathcal{O}$, and functions $\alpha_X(x)$, many useful relations among correlation functions can be obtained. These are collectively referred to as WIs. The relations that follow from the local chiral-flavour transformations we are considering are just a special case that goes under the name of *chiral-flavour WIs* (or axial-vector WIs).

We first consider the vector WIs that derive from the vector transformations (2.9). In this case, the variation of the action (1.1) is given by,[3]

$$\delta_V S = -i \int_R \mathrm{d}^4x\, \alpha_V(x)\partial_\mu V_\mu^a(x), \tag{2.12}$$

---

[3]Note that the derivation of this result involves a partial integration. Hence, if as in Chapter 3 one considers the case of compact space-time manifolds with boundaries, it is important that $\alpha_V(x)$ smoothly goes to zero outside some bounded domain R that does not contain the boundaries, as otherwise additional terms might arise. If this condition is met, then the result holds regardless of the boundary conditions for the fields.

where we defined the non-singlet local vector current $V_\mu^a(x)$ as,

$$V_\mu^a(x) = \overline{\psi}(x)\frac{\tau^a}{2}\gamma_\mu\psi(x). \tag{2.13}$$

Given this result, it is now convenient to decompose the product of local fields $\mathcal{O}$ as $\mathcal{O} \equiv \mathcal{O}_{\text{int}}\mathcal{O}_{\text{ext}}$, where $\mathcal{O}_{\text{int}}$ and $\mathcal{O}_{\text{ext}}$ are products of fields localized in the interior and exterior of R, respectively. Using the general relation (2.11), we then immediately obtain the *vector WIs*,

$$\int_R \mathrm{d}^4 x\,\alpha_V^a(x)\langle\partial_\mu V_\mu^a(x)\,\mathcal{O}_{\text{int}}\mathcal{O}_{\text{ext}}\rangle = i\langle(\delta_V\mathcal{O}_{\text{int}})\mathcal{O}_{\text{ext}}\rangle. \tag{2.14}$$

If we consider the fields in the product $\mathcal{O}$ to be localized outside the region R, i.e., $\mathcal{O}_{\text{int}} = 1$ and $\mathcal{O} = \mathcal{O}_{\text{ext}}$, the variation $\delta_V\mathcal{O}_{\text{int}}$ vanishes, and so the r.h.s. of (2.14). Since the resulting equation is valid for any choice of R, we can choose R to be a single space-time point x, and thus conclude that,

$$\langle\partial_\mu V_\mu^a(x)\mathcal{O}_{\text{ext}}\rangle = 0. \tag{2.15}$$

Note that in the more general case of non-degenerate quark-masses, the above relation is modified, and reads,

$$\langle\partial_\mu V_\mu^a(x)\mathcal{O}_{\text{ext}}\rangle = i\epsilon^{3ab}\delta m_0\langle S^b(x)\,\mathcal{O}_{\text{ext}}\rangle, \tag{2.16}$$

where δm_0 is the mass difference between the two light quarks, and $S^a(x)$ is the non-singlet scalar-density,

$$S^a(x) = \psi(x)\frac{\tau^a}{2}\psi(x). \tag{2.17}$$

This is the partially conserved vector current (PCVC) relation, and $V_\mu^a(x)$ is generally referred to as the PCVC. The relations (2.15) and (2.16) are the Euclidean versions of the corresponding operator relations in Minkowski space-time. Different fields $\mathcal{O}_{\text{ext}}$ then correspond to different matrix elements of the operator relation.

Moving to the case of the axial transformations (2.10), the variation of the action (1.1) is now given by,

$$\delta_A S = -i\int_R \mathrm{d}^4 x\,\alpha_A^a(x)\big(\partial_\mu A_\mu^a(x) - 2m_0 P^a(x)\big), \tag{2.18}$$

where we introduced the non-singlet local axial current $A_\mu^a(x)$,

$$A_\mu^a(x) = \overline{\psi}(x)\frac{\tau^a}{2}\gamma_\mu\gamma_5\psi(x), \qquad (2.19)$$

and the non-singlet pseudo-scalar density $P^a(x)$,

$$P^a(x) = \overline{\psi}(x)\frac{\tau^a}{2}\gamma_5\psi(x). \qquad (2.20)$$

Using again the general relation (2.11), we can derive the *axial WIs*,

$$\int_R \mathrm{d}^4x\,\alpha_A^a(x)\langle\partial_\mu A_\mu^a(x)\mathcal{O}_\mathrm{int}\mathcal{O}_\mathrm{ext}\rangle = i\langle(\delta_A\mathcal{O}_\mathrm{int})\mathcal{O}_\mathrm{ext}\rangle$$
$$+ 2m_0\int_R \mathrm{d}^4x\,\alpha_A^a(x)\langle P^a(x)\,\mathcal{O}_\mathrm{int}\mathcal{O}_\mathrm{ext}\rangle. \qquad (2.21)$$

Analogously to the vector case (2.16), if we consider a product of fields $\mathcal{O}$ localized outside the region R, and take R to be a single space-time point x, the expression (2.21) reduces to the familiar partially conserved axial current (PCAC) relation,

$$\langle\partial_\mu A_\mu^a(x)\mathcal{O}_\mathrm{ext}\rangle = 2m_0\langle P^a(x)\mathcal{O}_\mathrm{ext}\rangle. \qquad (2.22)$$

The local axial current is thus conserved only for vanishing quark-masses.

The above relations have been formally obtained in the continuum theory. However, analogous relations can be derived among the corresponding bare correlation functions in a regularization that preserves chiral-flavour symmetry. This said, it is possible to show that, in general, (partially) conserved currents do not need any renormalization (see e.g. (Collins, 1986; Vladikas, 2011)).[4,5] Hence, if we define the renormalized vector and axial currents,

$$(A_R)_\mu^a = Z_A A_\mu^a, \qquad (V_R)_\mu^a = Z_V V_\mu^a, \qquad (2.23)$$

we conclude that $Z_A = Z_V = 1$. Using standard arguments, the finiteness of the axial current implies through (2.22) that the product of the bare quark mass m_0 and the pseudo-scalar density $P^a(x)$ is also finite (see e.g. (Testa, 1998)). Consequently, the

---

[4]If the conserved current is associated with a gauge symmetry, this conclusion is not always true. The vector current in QED for example requires renormalization (Collins, Manohar and Wise, 2006).

[5]For the specific case of the axial and vector currents, and a chirally preserving lattice regularization of QCD, a detailed proof can be found in (Hasenfratz, 1998; Kikukawa and Yamada, 1999).

bare quark mass m_0 renormalizes multiplicatively and inversely proportional to the pseudo-scalar density,

$$(P_R)^a = Z_P P^a, \qquad m_R = Z_{\mathrm{m}} m_0 = Z_P^{-1} m_0. \qquad (2.24)$$

Analogously, the finites of the vector current implies through (2.16) that the quark-mass difference and the scalar-density renormalize with inverse renormalization factors (see e.g. (Vladikas, 2011)),

$$(S_R)^a = Z_S S^a, \qquad \delta m_R = Z_{\delta\mathrm{m}} \delta m_0 = Z_S^{-1} \delta m_0. \qquad (2.25)$$

From the above equations, one is tempted to conclude also that $Z_P = Z_S$. In fact, using the more general chiral WIs (2.21) one can show that operators in the same chiral multiplet renormalize with the same multiplicative factor (see e.g. (Bochicchio *et al.*, 1985)). The same can be shown for operators in the same flavour multiplet using the WIs (2.14) instead.[6]

2.1.3 Lattice Ward identities

After the discussion of the chiral-flavour WIs in the continuum, in this subsection we want to study how the relations (2.15) and (2.22) get modified on the lattice with Wilson fermions.

On the lattice the generic expectation value for a product of fields, $\mathcal{O} \equiv \mathcal{O}[U, \psi, \overline{\psi}]$, is given by the lattice path-integral,

$$\langle \mathcal{O} \rangle = \frac{1}{\mathcal{Z}} \int [\mathcal{D}U][\mathcal{D}\psi][\mathcal{D}\overline{\psi}] \, \mathcal{O}[U, \psi, \overline{\psi}] \, e^{-S[U, \psi, \overline{\psi}]}, \qquad (2.26)$$

where S is the Wilson action (2.1), while the partition function $\mathcal{Z}$ is defined by the normalization condition $\langle 1 \rangle = 1$. The integration measures instead are given by,

$$[\mathcal{D}U] = \prod_{x,\mu,a} \mathrm{d}U_\mu^a(x), \quad [\mathcal{D}\psi] = \prod_{x,A,a} \mathrm{d}\psi_{A,a}(x) \quad [\mathcal{D}\overline{\psi}] = \prod_{x,A,a} \mathrm{d}\overline{\psi}_{A,a}(x), \qquad (2.27)$$

where $\mathrm{d}U$ is the Haar-measure over the group SU(3), while $\mathrm{d}\psi$ and $\mathrm{d}\overline{\psi}$ are differentials of the Grassmann algebra (Montvay and Münster, 1997).

---

[6]Two or more operators are said to be in the same chiral (flavour) multiplet if they transform into each other under the chiral (flavour) transformations (2.6) (or (2.5)). The operators P^a and S^a for example are in the same chiral multiplet. The corresponding operators with a different index a instead belong to the same flavour multiplet.

Starting from this definition, one can derive WIs for the lattice theory in complete analogy with the continuum case already discussed. As a results, one finds essentially the same equations, but with additional contributions to $\delta_{V,A}S$ which come from the variation of the Wilson term under the local chiral-flavour transformations (2.9) and (2.10). More precisely, considering the case of the PCAC relation (2.22), one obtains (Bochicchio *et al.*, 1985),

$$\langle \partial_\mu^* A_\mu^a(x)\mathcal{O}_{\text{ext}}\rangle = 2m_0\langle P^a(x)\mathcal{O}_{\text{ext}}\rangle + a\langle X^a(x)\mathcal{O}_{\text{ext}}\rangle, \tag{2.28}$$

where ∂_μ^* is the backward lattice derivative (A.17), and X^a is a dimension 5 operator. Its explicit form can be easily worked out (see e.g. (Vladikas, 2011)).[7]

Naively, one might conclude that the corresponding term contributes only at $\mathrm{O}(a)$, and then simply vanishes when $a \to 0$. However, in order to understand what happens to (2.28) when the continuum limit is taken, one first needs to consider the renormalization of the operator X^a, as this conclusion might not be correct. On the lattice indeed the operator X^a can mix under renormalization with operators of lower or equal dimension, and same quantum numbers (Testa, 1998). The mixing with operators of equal dimension involves coefficients that only diverge logarithmically with a. These contributions are thus suppressed in the continuum limit by the explicit factor of a in (2.28). The mixing with lower dimensional operators instead, is given by coefficients which are inverse powers of the lattice spacing multiplied by finite functions of the bare coupling i.e. renormalization scale-independent (Testa, 1998). The inverse powers of the lattice spacing can thus cancel the explicit factor a in (2.28) and generate finite, if not divergent, contributions. The key observation however is that the operator X^a only mixes with lower dimensional operators that are already present in (2.28), since all the operators with the legitimate quantum numbers are there. The effect of the renormalization of X^a can thus be recast into a renormalization of the fields in the WIs. In fact, one can show that this renormalization is all what is needed to make the

---

[7]We note that in the lattice PCAC relation the separation between the lattice regularization of $\partial_\mu A_\mu^a$ and the definition of the operator X^a is not unique. In (2.28) for example we consider the local definition of the axial current (2.19). The form of X^a thus differs from the one of the given reference where the point-split axial current $\widetilde{A}_\mu^a$ is considered (Vladikas, 2011). It is however easy to convert between the two definitions.

PCAC relation finite (Testa, 1998). The resulting renormalized lattice PCAC relation then reads,[8]

$$\langle \tilde{\partial}_\mu (A_R)^a_\mu(x) \mathcal{O}_{\text{ext}} \rangle = 2m_R \langle (P_R)^a(x) \mathcal{O}_{\text{ext}} \rangle + \mathrm{O}(a), \tag{2.29}$$

where the $\mathrm{O}(a)$ terms denote contributions that vanish (up to logarithms) linearly with a in the continuum limit i.e. discretization effects. As before, the renormalized axial current is defined as $(A_R)^a_\mu = Z_A A^a_\mu$. However, since the conservation of the current is now spoiled by discretization effect, we expect $Z_A \neq 1$. In fact, the renormalization constant Z_A is a finite function of the bare coupling g_0 (Testa, 1998),[9] which only goes to 1 in the continuum limit, i.e., $Z_A(g_0) \overset{g_0 \to 0}{\to} 1$. The correctly normalized continuum WIs (2.22) are then recovered for $a \to 0$. Secondly, we note that the bare quark mass m_0 is not protected by an additive renormalization, hence: $m_R = Z_\mathrm{m}(m_0 - \overline{m})$, where $Z_m = Z_P^{-1}$, and $\overline{m}(am_0, g_0) = \frac{c(am_0, g_0)}{a}$, with $c(g_0, am_0)$ a regular function of am_0 and g_0 (Testa, 1998). In practice, it is thus convenient to introduce the (bare) PCAC mass,

$$m_{\text{PCAC}} \equiv \frac{\langle \tilde{\partial}_\mu A^a_\mu(x) \mathcal{O}_{\text{ext}} \rangle}{2 \langle P^a(x) \mathcal{O}_{\text{ext}} \rangle}, \tag{2.30}$$

which renormalizes multiplicatively, and inversely proportional to the pseudo-scalar density, i.e.,

$$(P_R)^a = Z_P P^a, \qquad m_R = Z_P^{-1} Z_A \, m_{\text{PCAC}}. \tag{2.31}$$

We stress that different choices of $\mathcal{O}_{\text{ext}}$ or flavour index a in (2.30) will give definitions for m_{PCAC} that differ by $\mathrm{O}(a)$ effects (cf. (2.29)). Only in the continuum limit all these definitions are expected to coincide.

An analogous discussion as for the PCAC relation can now be done for the PCVC relation (2.15). In this case, one obtains the lattice vector WIs (see (Vladikas, 2011)),

$$\langle \partial^*_\mu V^a_\mu(x) \mathcal{O}_{\text{ext}} \rangle = a \langle Y^a(x) \mathcal{O}_{\text{ext}} \rangle, \tag{2.32}$$

where the expression for the dimension 5 operator Y^a can again be easily worked out.

---

[8]Note that we substituted the backward lattice derivative ∂^*_μ with $\tilde{\partial}_\mu$ defined in (A.16) since the two coincide up to $\mathrm{O}(a)$ terms.

[9]This is true if a mass-independent renormalization scheme is chosen for Z_A, as otherwise one also has a finite am_0 dependence (Testa, 1998). The important point, however, is that a dependence on a renormalization scale $a\mu$ is excluded by general considerations.

Considering the renormalization of the above relation, we note that the only lower dimensional operator that Y^a mixes with is given by $\partial_\mu V_\mu^a$. A finite renormalized expression is then given by,

$$\langle \tilde{\partial}_\mu (V_R)_\mu^a(x) \mathcal{O}_{\text{ext}} \rangle = \mathrm{O}(a), \tag{2.33}$$

where up to $\mathrm{O}(a)$ terms we replaced ∂_μ^* by $\tilde{\partial}_\mu$, and where we defined the renormalized local vector current as before, i.e., $(V_R)_\mu^a = Z_V V_\mu^a$. Similarly to the axial case, the renormalization factor Z_V is a finite function of the bare coupling, and in general, $Z_V(g_0) \neq 1$. The main difference w.r.t. the axial case, however, is that in this case the operator Y^a can be written as the divergence of a dimension 4 operator Δ_μ^a, i.e., $Y^a = -\partial_\mu^* \Delta_\mu^a$. Using (2.32) one can then define a conserved lattice vector current $\widetilde{V}_\mu^a$ which satisfies,[10]

$$\langle \partial_\mu^* \widetilde{V}_\mu^a(x) \mathcal{O}_{\text{ext}} \rangle = 0, \tag{2.34}$$

where,

$$
\begin{aligned}
\widetilde{V}_\mu^a(x) &= V_\mu^a(x) + a\Delta_\mu^a(x) \\
&= \frac{1}{2}\left[\bar{\psi}(x)(\gamma_\mu - 1)U_\mu(x)\frac{\tau^a}{2}\psi(x + a\hat{\mu}) + \bar{\psi}(x + a\hat{\mu})(\gamma_\mu + 1)U_\mu^\dagger(x)\frac{\tau^a}{2}\psi(x) \right].
\end{aligned}
\tag{2.35}
$$

The conservation of this lattice current in the bare theory allows one to show that the corresponding renormalization factor is given by $Z_{\widetilde{V}} = 1$ (see e.g. (Vladikas, 2011)). The conserved current $\widetilde{V}_\mu^a$ thus does not need renormalization, as expected. In addition, the difference between the matrix elements of $(V_R)_\mu^a$ and $\widetilde{V}_\mu^a$ are purely discretization effects (cf. (2.33) and (2.34)). Since, $\widetilde{V}_\mu^a \overset{a \to 0}{\to} V_\mu^a$, we then conclude that, $Z_V(g_0) \overset{g_0 \to 0}{\to} 1$, and the continuum vector WIs (2.15) are recovered in both cases.

Before concluding we want to mention that by investigating more general lattice WIs (cf. (2.21)), one can infer other important consequences of the explicit breaking of chiral symmetry by Wilson's regularization. In particular, one can show that the overall multiplicative renormalization factors of operators that belong to the same chiral

---

[10]Note that in the expression (2.34) one can either use ∂_μ^* or $\tilde{\partial}_\mu$ since the conserved vector current $\widetilde{V}_\mu^a$ is time independent.

multiplet generally differ by finite functions of the bare coupling (Testa, 1998). This means that for example $(Z_P/Z_S)(g_0) \neq 1$, where this function only approaches 1 for $g_0 \to 0$. Note also that the renormalization of the individual operators is in general complicated by the mixing with operators of different chirality. The mixing pattern is in fact only restricted by parity and flavour symmetry (Bochicchio *et al.*, 1985). This additional renormalization can be particularly difficult for more complicated operators as for example many interesting four-quark operators responsible for electro-weak hadronic transitions (Donini *et al.*, 1995).

To summarize the results of this subsection, first of all we have seen that by properly (re)normalizing the local axial and vector currents we recover, up to cutoff effects, the continuum WI. In particular, in the case of the vector current we found a conserved lattice definition that does not need renormalization, and respect continuum-like WIs. Secondly, the PCAC relation suggested us a valid definition for a renormalized quark mass through (2.31). This allows us to define the chiral point where the quark-masses are zero by simply requiring $m_{\mathrm{PCAC}} = 0$. Note however that at zero quark-mass the renormalized axial current is only conserved up to discretization effects. Moreover, the critical value of the bare quark-mass m_0 for which $m_{\mathrm{PCAC}} = 0$ is implicitly defined by the equation: $m_{\mathrm{crit}}(g_0) = \overline{m}(am_{\mathrm{crit}}, g_0)$, and it is then a function of g_0. Finally, as mentioned above, we commented on the fact that operators in the same chiral multiplet do not renormalize with the same multiplicative factors, but a finite rescaling is needed.

To conclude, since Z_V and Z_A go to 1 in the continuum limit, one might ask the question whether these finite renormalization factors are needed at all. The answer is that, as we have seen, properly normalized matrix elements of the local axial or vector current differ from their continuum limit by powers of the lattice spacing. On the other hand, omitting Z_A (or Z_V) implies that the same bare matrix elements will converge to their continuum limits as power series in g_0 (Bochicchio *et al.*, 1985), which is only logarithmic in the lattice spacing.[11] This convergence is much slower than any power of a, and reliable continuum extrapolations of unrenormalized bare matrix elements can be very difficult if only a few lattice spacings are available over a limited range.

---

[11] We remind that close to the continuum limit, $g_0^2(a) \sim \frac{-1}{\ln(a\Lambda_{\mathrm{QCD}})}$.

Through these examples, we can appreciate the importance of non-perturbative renormalization. For example, if we had Z_A only at 1-loop order in perturbation theory, a perturbatively renormalized matrix element of the axial current would converge to its continuum limit with $O(g_0^4)$ corrections. As said, however, any power of the bare coupling is much slower than any positive power of the lattice spacing a as $a \to 0$. Secondly, we want to note that there are cases where a perturbative treatment of the renormalization would fail altogether. The renormalization of the bare quark-mass, and more generally of any power-divergence, is an example where the renormalization can only be performed non-perturbatively. In fact, in order to identify the chiral point, one could think of determining the value of the critical mass $m_{\mathrm{crit}}(g_0)$ using a perturbative estimate for the function $c(g_0, am_0)$ in $\overline{m}$. If, however, such function is known only up to $O(g_0^n)$ corrections, this would lead to uncancelled $O(\frac{g_0^n}{a})$ divergences in the PCAC mass for example. While this is perfectly fine in perturbation theory, it is certainly not in a non-perturbative determination.

As a last remark we want to mention that, once the correct WIs have been shown to be recovered in the continuum limit through a proper renormalization of the theory, one can actually turn the tables and impose the validity of a set of WIs at finite lattice spacing in order to determine the necessary renormalization constants (Bochicchio *et al.*, 1985; Maiani and Martinelli, 1986; Martinelli *et al.*, 1993; Lüscher, Sint, Sommer and Wittig, 1997*b*). It is important to note at this point that in principle any relation among correlation functions which is dictated by chiral symmetry can be used to fix this renormalization. We will explore these ideas in detail in Chapter 5.

2.2   Symanzik's effective theory and O(a)-improvement

As seen in the previous section, renormalized lattice observables computed with Wilson fermions generally suffer from $O(a)$ discretization effects (cf. (2.29)). Since long ago, these effects are known to be rather large in the range of lattice spacings considered in current simulations (see e.g. (Jansen, *et al.*, 1996)). This can make continuum limit extrapolations difficult, and ultimately not very precise. In order to better control these extrapolations and eventually devise strategies to accelerate the convergence, a theoretical understanding of how renormalized lattice observables approach their

continuum limit is then needed. As we present in the next subsection, a quantitative analysis can be obtained through Symanzik's effective theory, which will lead us to introduce Symanzik's improvement programme for lattice field theory (Symanzik, 1981b; Symanzik, 1983a; Symanzik, 1983b). The presentation will follow closely the one of (Lüscher, Sint, Sommer and Weisz, 1996). For a more introductory discussion we recommend (Lüscher, 1998a; Weisz, 2010).

2.2.1 Symanzik's effective theory

Despite being difficult to prove rigorously, the idea of Symanzik is in principle simple.[12] It is well-known that the effect of as yet unknown high-energy degrees of freedom can be described at low-energy by adding higher-dimensional interaction terms to the original Lagrangian. The new Lagrangian so constructed defines an effective low-energy description for the underlying more fundamental theory. A similar situation occurs in lattice QCD. In purely formal terms, we can regard the momentum cutoff a^{-1} as a scale of new physics, and our lattice theory as the fundamental theory defined at this scale. The associated low-energy effective theory is then a continuum theory with action,

$$S_{\text{eff}} = S_0 + aS_1 + a^2 S_2 + \ldots, \tag{2.36}$$

where S_0 denotes the continuum QCD action, while the S_k's, $k \geq 1$, contain higher-order terms. More precisely, these contributions are of the form,

$$S_k = \int \mathrm{d}^4 x \, \mathcal{L}_k(x), \tag{2.37}$$

where the Lagrangians $\mathcal{L}_k(x)$ are linear combinations of local composite operators of dimension $4 + k$.[13] Among the list of all possible such fields, only those that are invariant under the symmetries of the lattice theory need to be considered.[14]

---

[12]The existence of Symanzik's effective theory is only conjectured (Weisz, 2010). However, it is supported by low-order perturbative calculations, and non-perturbative numerical results.

[13]The dimension counting eventually includes (non-negative) powers of the quark mass which may multiply some of the fields.

[14]We remind that for $N_{\text{f}} = 2$ (mass-degenerate) Wilson fermions these are: gauge invariance, $\mathrm{U}(1) \times \mathrm{SU}(2)$ vector symmetry, and all exact discrete symmetries of the lattice action including space-time symmetries (cf. Section 2.1.1).

In addition to the effective action, we need an effective description for the lattice operators. In a lattice correlation function, indeed, cutoff effects do not only originate from the action but also from the local composite operators inserted. For simplicity, in the following we consider a generic local gauge invariant lattice field $\phi(x)$, which renormalizes only multiplicatively, i.e., $(\phi_R)(x) = Z_\phi \phi(x)$. In the effective theory the renormalized lattice field ϕ_R is then represented through an effective field,

$$\phi_{\text{eff}}(x) = \phi_0(x) + a\phi_1(x) + a^2\phi_2(x) + \dots, \tag{2.38}$$

where $\phi_0(x)$ is the corresponding continuum field, while the fields $\phi_k(x)$, $k \geq 1$, are linear combinations of local fields of dimension $d_\phi + k$, where d_ϕ is the engineering dimension of $\phi(x)$. Analogously to the case of the effective action, only local fields with the appropriate dimensions and symmetry properties enter in the combination $\phi_k(x)$.

Given the effective action and fields, we have to discuss how lattice correlation functions are actually described by the effective theory. In the following, we restrict ourselves to on-shell correlation functions. These are all position space correlation functions of local composite operators at non-zero physical distance. The reason for this terminology is that all on-shell quantities in QCD, as for example hadron masses, or matrix elements of local operators between particle states, can be extracted from these correlation functions. This restriction is hence not severe, and meets most practical purposes.[15] To simplify the discussion, we also restrict to analyze the leading $O(a)$ effects. Terms proportional to higher-powers of the lattice spacing are anyhow expected to be suppressed if the lattice spacing is fine enough.

As an example of correlation function we consider the connected n-point Green function of the operator $\phi(x)$ introduced above. The generalization to more general correlation functions involving several types of fields is straightforward. Specifically, since we want to study the approach to the continuum limit of this observable, the properly renormalized quantity needs to be considered. In this case, this is given by,

$$(G_R)_n(x_1, \dots, x_n) = \langle(\phi_R)(x_1) \cdots (\phi_R)(x_n)\rangle_c, \tag{2.39}$$

---

[15]Note that if this assumption is not made, additional cutoff effects can arise when the composite fields in the correlation functions are brought at coinciding space-time points. These effects are specific of the correlation function considered, and are not taken into account by the effective action and fields.

where $\langle \cdots \rangle_c$ refers to the connected part of the Green function. Note that we assume the space-time points $x_1, \ldots, x_n$, to be at a non-zero physical distance from each others.

In the effective theory, the lattice correlation function (2.39) is then represented through the asymptotic expansion (see e.g. (Lüscher, 1998a)),

$$
\begin{aligned}
(G_R)_n(x_1, \ldots, x_n) = & \ \langle \phi_0(x_1) \cdots \phi_0(x_n) \rangle_{\mathrm{c}}^{\mathrm{cont}} \\
& - a \int \mathrm{d}^4 y \langle \phi_0(x_1) \cdots \phi_0(x_n) \mathcal{L}_1(y) \rangle_{\mathrm{c}}^{\mathrm{cont}} \\
& + a \sum_{k=1}^{n} \langle \phi_0(x_1) \cdots \phi_1(x_k) \cdots \phi_0(x_n) \rangle_{\mathrm{c}}^{\mathrm{cont}} + \mathrm{O}(a^2),
\end{aligned}
\tag{2.40}
$$

where the expectation values $\langle \cdots \rangle_c^{\mathrm{cont}}$ are taken w.r.t. the continuum action S_0.[16] The second term on the r.h.s. of the equation is given by the $\mathrm{O}(a)$ contribution of the effective action, here considered as an operator insertion in the correction function. Due to the integral over y, this insertion can possibly generate contact terms when y coincides with the points x_k. In principle, one should then analyze the potential divergences that arise from the operator product expansion of the operators involved, and provide proper renormalization prescriptions for the non-integrable singularities that survive. These contact terms, however, can always be reabsorbed into a redefinition of the operator $\phi_1(x)$, which contains all the fields with the correct symmetry properties and dimensions. This, as we shall see, is all we need to know in practice.

To conclude we want to comment on a couple of technical points regarding (2.40). First of all, the a dependence of lattice correlation functions is not only expressed by the explicit factors of a in (2.40). It is clear that, while the general form of the basis fields in $\mathcal{L}_1(y)$ and $\phi_1(x)$ is only dictated by the field content and symmetries of the lattice theory, the coefficients that multiply them clearly depend on the details of the latter. Consequently, even though the basis elements in $\mathcal{L}_1(y)$ and $\phi_1(x)$ are independent of a, the coefficients that multiply them are in general functions of the lattice spacing. In fact, in perturbation theory, they are calculable polynomials in $\ln(a)$ (Lüscher, 1998a).

---

[16]In the following we can imagine the effective theory to be regularized on a space-time lattice with a very fine lattice spacing $\varepsilon \ll a$. The fields in $\mathcal{L}_1$, ϕ_0 and ϕ_1, are then renormalized ones.

Secondly, the basis of operators in $\mathcal{L}_1(y)$ and $\phi_1(x)$ can in general be reduced using the field equations of motion (Lüscher, 1998*a*). In principle, the field equations are only valid in correlation functions up to contact terms.[17] These again can arise when y gets close to one of the points x_k in (2.40). As discussed, however, these contact terms simply amount to a redefinition of the field $\phi_1(x)$. The latter thus depends on exactly which basis of operators has been considered for the effective action. When the field equations are used to simplify ϕ_1 instead, no contact terms can arise since all points x_k are kept at physical distance.

2.2.2 Symanzik's improvement programme

Symanzik's effective theory provides an effective description of our lattice theory when the cutoff scale is well above the relevant energy scales of the observables we are considering. In particular, the form and nature of the discretization effects is made explicit in terms of irrelevant operators contributing to the effective action and fields. This suggests the idea that one can try to modify the original lattice theory in such a way that the corresponding effective theory is free from such contributions. The way this is realized in practice is what is referred to as the Symanzik's improvement programme (Symanzik, 1981*b*; Symanzik, 1983*a*; Symanzik, 1983*b*), which aims at systematically removing cutoff effects order by order in the lattice spacing. The general idea of this strategy goes as follows.

One starts by adding to the lattice action and fields, lattice representatives of the irrelevant operators in S_1 and ϕ_1. As long as the lattice symmetries are respected, the specific discretization does not really matter and will only affect higher-orders in a. At this point, the crucial observation is that by adjusting the coefficients of these operators one is able to modify the size of the corresponding $O(a)$ contributions in the

---

[17]The relations between the basis fields in $\mathcal{L}_1(y)$ or $\phi_1(x)$ can be easily derived at tree-level, using the classical field equations. In principle, however, the renormalization and mixing of the basis operators should be taken into account when deriving these relations. The simple relations determined at tree level are then replaced in general by more complicated equations involving more basis fields, and with coefficients that depend on the coupling and the chosen renormalization conditions. On the other hand, the only information that is used in practice is that, given a fixed number of constrains, some of the basis fields can be expressed in terms of the others (Lüscher, 1998*a*).

effective theory. The coefficients can then be fixed by imposing suitable improvement conditions. These are obtained by considering some combinations of lattice observables which are pure lattice artifacts, and are hence expected to vanish in the continuum limit. In general, a given combination is chosen such that the contribution of a specific irrelevant operator is isolated. The corresponding coefficient is then determined as a function of the lattice spacing by simply requiring the given combination to vanish. Once the lattice action and fields have been improved, any renormalized on-shell lattice correlation function of these fields is then expected to be free of $O(a)$ discretization effects. In fact, Symanzik's improvement programme can be seen as an extension of the renormalization of the theory at the level of irrelevant operators. Of course, the modification of the theory so obtained does not alter the continuum limit of the theory, since the latter is only redefined at the cutoff level.[18]

In perturbation theory, improvement coefficients can be easily obtained from any (renormalized) lattice observable by comparing it with its continuum limit. This is particularly simple at tree-level, where one simply compares the lattice action and fields with their continuum counterparts. The improvement coefficients so determined are universal, and independent from the observable considered. On the other hand, in a non-perturbative determination taking the continuum limit is generally demanding. It is then convenient to define improvement conditions based on symmetries which are broken by the discretization, but are expected to be recovered in the continuum limit. In this respect, note that improvement coefficients determined through non-perturbative simulations suffer in general from $O(a)$ ambiguities. This means that different improvement conditions will give coefficients that differ by $O(a)$ effects. These ambiguities, however, are consistent with $O(a)$ improvement since they only affect improved lattice observables at $O(a^2)$.

Given these considerations, one may ask whether a perturbative estimate of the improvement coefficients is good in practice. Note that, in the case of improvement the situation is more relaxed than for the renormalization of marginal or relevant operators. Even if the computation of the improvement coefficients is not accurate,

---

[18]Reflection positivity however might be compromised (Lüscher and Weisz, 1985a; Parisi, 1985).

no systematic effects are introduced in the results if these are extrapolated to the continuum limit. The answer to the above question then very much depends on the specific observable, and irrelevant operator considered. The effect of the latter has thus to be studied in some detail (e.g. by varying its coefficient in simulations), in order to conclude if a perturbative estimate of the corresponding improvement coefficient is satisfactory.

To conclude, one has to keep in mind that as any effective theory Symanzik's theory is only an asymptotic concept. This means that it is not known a priori the range of lattice spacings at which this description really sets in. It could well be that current simulations are far very far from its regime of applicability. In practice, however, Symanzik's effective theory provides a very robust and effective description.

2.2.3 O(a) improvement of Wilson fermions

Having introduced the general principles of Symanzik's effective theory and associated improvement programme, in this subsection we consider its application to Wilson's formulation. Specifically, we consider the case of (two) massless fermions. As we will motivate in the next section, this is the set-up we are most interested in. In addition, when restricting to zero quark-masses, the improvement programme is simplified, since one does not need to consider any reparametrization of the bare lattice theory.[19]

As seen, the first ingredient of Symanzik's effective theory is given by the effective action (2.36). In the massless case, this starts with the massless continuum QCD action (cf. (1.1)),[20]

$$S_0 = -\frac{1}{2g^2} \int \mathrm{d}^4x \, \mathrm{tr}\{F_{\mu\nu}(x)F_{\mu\nu}(x)\} + \int \mathrm{d}^4x \, \overline{\psi}(x) \slashed{D}\psi(x). \tag{2.41}$$

The terms that appear in the O(a) correction, S_1, must then be integrals over local composite fields of dimension 5 that respect all symmetries of the massless lattice action. In fact, there are only two terms that can contribute to S_1, these are given by (see e.g. (Lüscher, 1998a)),

---

[19]We refer to (Lüscher, Sint, Sommer and Weisz, 1996) for a detailed discussion about this point.

[20]We remind that in order to define Wilson's theory in the massless limit, one has to tune the bare quark masses to their critical value e.g. by requiring the PCAC mass to vanish (cf. Section 2.1.3).

$$S_1 = c_1 \int \mathrm{d}^4x \, \overline{\psi}(x) \tfrac{i}{4} \sigma_{\mu\nu} F_{\mu\nu} \psi(x) + c_2 \int \mathrm{d}^4x \, \overline{\psi}(x) D_\mu D_\mu \psi(x), \qquad (2.42)$$

where c_1, c_2 are some given coefficients, and $\sigma_{\mu\nu}$ is defined in Appendix A.2.[21] First of all, note that both terms in S_1 explicitly break chiral symmetry. These contributions are hence present because of the explicit breaking of chiral symmetry by Wilson's regularization.[22] Secondly, note that the two operators can be reduced to a single operator by using the field equations of motion (Lüscher, 1998a). In the following we then choose to consider the operator proportional to c_1, as it is conventionally done in the literature.

Having the form of the effective action, the second step is to introduce lattice representatives of the corresponding $O(a)$ contributions to the original lattice action. Specifically, the improved Wilson-action can be defined as (see e.g. (Lüscher, 1998a)),

$$S_I = S + a^5 \sum_x c_{\mathrm{sw}}(g_0) \, \overline{\psi}(x) \tfrac{i}{4} \sigma_{\mu\nu} \widehat{F}_{\mu\nu} \psi(x), \qquad (2.43)$$

where S is the standard Wilson action (2.1), and $\widehat{F}_{\mu\nu}$ is a lattice regularization of the continuum field strength tensor $F_{\mu\nu}$. A possible definition for $\widehat{F}_{\mu\nu}$ is given by the clover discretization specified in (A.26). The additional term in (2.43) is known as the Sheikholeslami-Wohlert (SW) term (Sheikholeslami and Wohlert, 1985). As discussed in the previous subsection, the corresponding coefficient $c_{\mathrm{sw}}(g_0)$ needs to be tuned according to some improvement condition in order to remove the corresponding $O(a)$ discretization effects from lattice observables.

The value of $c_{\mathrm{sw}}(g_0)$ is easily obtained at tree-level in perturbation theory, and is given by $c_{\mathrm{sw}}^{(0)} = 1$ (Sheikholeslami and Wohlert, 1985). In fact, the coefficient has also been computed in perturbation theory to the 1-loop order (Wohlert, 1987; Lüscher and Weisz, 1996). As mentioned at the beginning of the section, however, the $O(a)$ discretization effects of Wilson fermions are generally large at the lattice spacings considered in current simulations. In particular, a perturbative estimate of c_{sw} turns

---

[21] No purely gluonic terms are present. Indeed, in the pure gauge theory the leading discretization effects are expected to be of $O(a^2)$ (Lüscher and Weisz, 1985b).

[22] Lattice regularizations that preserve chiral symmetry do not posses any $O(a)$ discretization effects (see e.g. (Niedermayer, 1999)).

out to be not very effective in most cases. This led to devise a strategy for the non-perturbative determination of c_{sw}. This determination has been obtained through the Schrödinger functional of QCD, introduced in the next chapter. The corresponding improvement condition is based on the restoration of the PCAC relation (2.29) up to $O(a^2)$ corrections. We refer to the original references for the details of this computation (Lüscher, Sint, Sommer and Weisz, 1996; Lüscher, Sint, Sommer, Weisz and Wolff, 1997a; Jansen and Sommer, 1998), and to (Lüscher, 1998a; Sommer, 1997) for an introduction.

Through the $O(a)$ improvement of the lattice action, one obtains that spectral quantities like for example particle masses, approach their continuum limit with $O(a^2)$ corrections (Lüscher and Weisz, 1985b).[23] As discussed in Section 2.2, however, in order to achieve full $O(a)$ improvement of generic on-shell correlation functions, one needs to improve the corresponding fields as well. In the following we present the $O(a)$ improved definitions for the quark-bilinear fields introduced in Section 2.1.2. These in fact will be needed for our discussion in Chapter 5. We remind that, similarly to the improvement of the action, in order to improve the fields one first needs to identify the $O(a)$ contributions to the corresponding effective operators. In this case, these are given by operators of dimension 4 with the same symmetry transformations as the lattice operator considered. Again, one can use the equations of motion to reduce the number of terms that appear. Finally, given the continuum basis of counterterms so obtained, one adds lattice representatives to the original lattice fields with arbitrary coefficients. The latter need then to be fixed by requiring the absence of $O(a)$ lattice artifacts in some on-shell correlation functions of the improved fields.

Starting from the local axial current (2.19), one can show that after using the equations of motion, its $O(a)$ improvement can be obtained in the chiral limit by considering the operator (see e.g. (Lüscher, 1998a)),

$$(A_I)^a_\mu \equiv A^a_\mu + a\,c_A(g_0)\tilde{\partial}_\mu P^a, \tag{2.44}$$

where, we remind, $\tilde{\partial}_\mu$ is defined by (A.16), and P^a is the pseudo-scalar density (2.20). The coefficient $c_A(g_0)$ is chosen in order to achieve the $O(a)$ improvement of correlation

---

[23]Spectral quantities indeed do not depend on the interpolating fields employed for their extraction.

functions of the local axial current. This coefficient has been computed for example using the Schrödinger functional, and enforcing the restoration of chiral symmetry through the PCAC relation (2.29). This allowed its determination first in perturbation theory (Lüscher and Weisz, 1996), and later also non-perturbatively (Lüscher, Sint, Sommer, Weisz and Wolff, 1997a; Della Morte, Hoffmann and Sommer, 2005c).

Considering the local vector current (2.13), an O(a) improved definition is given by (see e.g. (Sint and Weisz, 1997)),

$$(V_I)^a_\mu \equiv V^a_\mu + a\,c_V(g_0)\tilde{\partial}_\nu T^a_{\nu\mu},\tag{2.45}$$

where the tensor operator $T^a_{\mu\nu}(x)$ is defined as,

$$T^a_{\mu\nu}(x) = i\overline{\psi}(x)\frac{\tau^a}{2}\sigma_{\mu\nu}\psi(x).\tag{2.46}$$

In the case of the point-split discretization of the vector current (2.35), one can take the same O(a) counterterm as for the local one. The corresponding improvement coefficient though will change i.e. $c_V(g_0) \rightarrow c_{\tilde{V}}(g_0)$. For completeness, we mention that the value of $c_V(g_0)$ is known to 1-loop order in perturbation theory (Sint and Weisz, 1997). A non-perturbative determination instead has only been attempted in the quenched approximation (Guagnelli and Sommer, 1998).

Differently from the axial and vector currents, the pseudo-scalar and scalar densities do not have any operator of dimension 4 that can contribute to their Symanzik's effective expansion. Consequently, they are already O(a) improved, i.e.,

$$(P_I)^a = P^a, \qquad (S_I)^a = S^a.\tag{2.47}$$

Finally, the O(a) counterterm to the tensor operator (2.46) is given in terms of the local vector current as (see e.g. (Sint and Weisz, 1998)),

$$(T_I)^a_{\mu\nu} = T^a_{\mu\nu} + a\,c_T(g_0)\big(\tilde{\partial}_\mu V^a_\nu - \tilde{\partial}_\nu V^a_\mu\big),\tag{2.48}$$

where $c_T(g_0)$ is only known to 1-loop order in perturbation theory.

2.2.4 Automatic O(a) improvement of massless Wilson fermions

To conclude this section on the O(a) improvement of Wilson fermions, we want to present the somehow surprising feature that massless Wilson fermions in a finite physical volume are automatically O(a) improved. This means that the O(a) counterterms to the effective action and operators are not needed to obtain O(a) improved definitions of physically interesting observables (Frezzotti and Rossi, 2004).[24] Even though this is not the physical regime one is generally interested in, this fact had been overlooked for more than 20 years! It is crucial, however, for our study. Indeed, as we will motivate in the next section, this is the regime where we want to perform the renormalization of the theory. Before presenting the argument, we note that since we are considering a finite space-time volume, some boundary conditions for the fields need to be chosen. In the following we will assume (some sort of) periodic boundary conditions for all fields. We anticipate, however, that the argument is not insensitive to the boundary conditions imposed.

In order to start presenting the argument, let us consider a generic lattice observable $\mathcal{O}$ given by a finite product of multiplicatively renormalized local fields at non-zero physical distances. The corresponding Symanzik's expansion (2.40) is then given by,

$$\langle \mathcal{O} \rangle_c = \langle \mathcal{O}_0 \rangle_c^{\text{cont}} - a \langle S_1 \mathcal{O}_0 \rangle_c^{\text{cont}} + a \langle \delta \mathcal{O}_0 \rangle_c^{\text{cont}} + \mathrm{O}(a^2), \qquad (2.49)$$

where $\mathcal{O}_0$ is the continuum (renormalized) field corresponding to the renormalized lattice operator $\mathcal{O}$, while $\delta \mathcal{O}_0$ is a shorthand notation for the associated O(a) operator counterterm. The argument now relies on the following observations.

First of all, the continuum massless QCD action S_0 of (2.41) is chirally symmetric. In particular, if we consider the discrete γ_5-transformation,

$$\psi \to \gamma_5 \psi, \qquad \overline{\psi} \to -\overline{\psi} \gamma_5, \qquad (2.50)$$

the action S_0 is invariant under this transformation. The counterterm action S_1 in (2.42) instead changes sign.

---

[24]The proof of this result has been completed by several authors in later works (Aoki and Bär, 2006; Shindler, 2006; Sint, 2006; Frezzotti, Martinelli, Papinutto and Rossi, 2006).

Secondly, if one considers the transformation (2.50) as a change of variables in the functional integral, it is possible to show that the transformation is non-anomalous and leaves the functional integral measure invariant, at least for an even number of quark-flavors (Sint, 2011). The transformation properties of a given expectation value $\langle \mathcal{O}_0 \rangle_c^{\text{cont}}$ under the transformation (2.50), are then dictated by those of the operator $\mathcal{O}_0$ considered. In particular, since the γ_5-transformation squares to the identity, any composite field $\mathcal{O}_0$ can be decomposed into parts which are even, $\mathcal{O}_0^{\text{even}}$, or odd, $\mathcal{O}_0^{\text{odd}}$, under this transformation, where we define,

$$\mathcal{O}_0^{\text{even}} \xrightarrow{\gamma_5} \mathcal{O}_0^{\text{even}}, \qquad \mathcal{O}_0^{\text{odd}} \xrightarrow{\gamma_5} -\mathcal{O}_0^{\text{odd}}. \tag{2.51}$$

Note that, this mapping can be carried over to the lattice even though there the γ_5-transformation is not a symmetry. Also on the lattice we can then talk about γ_5-even and odd fields $\mathcal{O}$, similarly defined as in (2.51). In particular, once this decomposition is considered, the corresponding O(a) counterterms of a γ_5-even observable, $\delta \mathcal{O}_0^{\text{even}}$, can be shown to be γ_5-odd, and vice versa interchanging even with odd (Frezzotti and Rossi, 2004; Aoki and Bär, 2006). Given these observations we conclude that,

$$\langle S_1 \mathcal{O}_0^{\text{even}} \rangle_c^{\text{cont}} = -\langle S_1 \mathcal{O}_0^{\text{even}} \rangle_c^{\text{cont}} = 0,$$
$$\langle \delta \mathcal{O}_0^{\text{even}} \rangle_c^{\text{cont}} = -\langle \delta \mathcal{O}_0^{\text{even}} \rangle_c^{\text{cont}} = 0. \tag{2.52}$$

In turn, this means that for γ_5-even lattice observables, $\mathcal{O}^{\text{even}}$, we have (cf. (2.49)),

$$\langle \mathcal{O}^{\text{even}} \rangle_c = \langle \mathcal{O}_0^{\text{even}} \rangle_c^{\text{cont}} + O(a^2). \tag{2.53}$$

γ_5-even observables are then automatically O(a) improved. This does not mean that O(a) effects are absent from the theory, but rather that these effects are confined in correlation functions of γ_5-odd observables, for which we have,

$$\langle \mathcal{O}^{\text{odd}} \rangle_c = -a \langle S_1 \mathcal{O}_0^{\text{odd}} \rangle_c^{\text{cont}} + a \langle \delta \mathcal{O}_0^{\text{odd}} \rangle_c^{\text{cont}} + O(a^3), \tag{2.54}$$

where we used the fact that: $\langle \mathcal{O}_0^{\text{odd}} \rangle_c^{\text{cont}} = -\langle \mathcal{O}_0^{\text{odd}} \rangle_c^{\text{cont}} = 0$. Note that the corrections in (2.54) are of order a^3 rather than a^2. In fact, the mechanism of automatic O(a) improvement more generally implies that lattice effects in γ_5-even (γ_5-odd) correlation

functions only come with even (odd) powers of the lattice spacing (Frezzotti and Rossi, 2004; Aoki and Bär, 2006). In conclusion, the main result is that we can get rid of the $O(a)$ effects in our lattice observables by projecting them on their even components. The odd components do not anyway contribute in the continuum limit, and only contain the leading discretization effects.

To conclude, as discussed in Section 2.1.3, the chiral limit of Wilson fermions can be identified through the condition $m_{\text{PCAC}} = 0$. In the unimproved lattice theory, however, this condition can be satisfied only within the intrinsic $O(a)$ ambiguities in the determination of m_{PCAC}. One may then ask whether this $O(a)$ ambiguity in the definition of the chiral point can invalidate the result here presented, for which we require the quark-masses to be zero. In fact, it can be show that the $O(a)$ ambiguity in the determination of the critical line $m_{\text{crit}}(g_0)$ only affects γ_5-even observables at $O(a^2)$. The reason is that this ambiguity can be effectively described by an $O(a)$ mass-counterterm in the effective action (see e.g. (Sint, 2006)). This counterterm, similarly to the ones already present in S_1, is γ_5-odd, and thus does not contribute at leading order to a in γ_5-even observables.

Some other subtle points in the proof of automatic $O(a)$ improvement are the following. As emphasized at the beginning of the subsection, it is crucial that the physical volume of the lattice is finite. The reason is that no spontaneous breaking of chiral symmetry can occur in this case (see e.g. (Weinberg, 2005)). This guarantees that expectation values which are expected to vanish because of the chiral symmetry of the action do not acquire non-trivial values (cf. (2.52)). In addition, as mentioned, also the boundary conditions for the fields in finite volume matter for automatic $O(a)$ improvement to hold. The boundary conditions for the quark-fields, indeed, need to be compatible with the transformation (2.50) in order to be able to prove this result.

Finally, we note that a mass term for the fermions would unavoidably spoil the argument of automatic $O(a)$ improvement since in this case the γ_5-transformation is not a symmetry of the continuum QCD action. On the other hand, the argument can be restored by introducing a twisted-mass term (Frezzotti, Grassi, Sint and Weisz, 2001; Frezzotti and Rossi, 2004). In this case the continuum QCD symmetry exploited

to prove the argument is not spontaneously broken, and the then result holds also in an infinite physical volume.

2.3 Scale dependent renormalization

In Section 2.1, we studied in detail the renormalization of Wilson's theory originating from the explicit breaking of chiral symmetry by the regularization. In this case, the necessary renormalization is given in terms of finite functions of the bare coupling g_0, that do not depend on any renormalization scale μ, e.g. Z_A, Z_P/Z_S, ... The most common case of renormalization in lattice QCD, however, is scale-dependent. The first important example is given by the renormalization of the fundamental parameters of QCD i.e. the gauge coupling and quark-masses. Scale-dependent renormalization is then necessary for local composite quark-fields which are not (partially) conserved currents. Of particular interest for us are the quark-bilinears discussed in Section 2.2.3. In all these cases, the connection between the bare quantity and the renormalized one is expressed in terms of a scale-dependent renormalization factor $Z \equiv Z(g_0, am_0, a\mu)$, which has to be fixed by some suitable renormalization condition.[25] The aim of this section is to present the problem of scale-dependent renormalization in lattice QCD.[26] More precisely, we want to discuss how to compute the non-perturbative running of a given renormalization factor Z w.r.t. the renormalization scale μ.

We start in the next subsection presenting some interesting physical applications where this problem comes about. We then try to understand how one could eventually work on the lattice to perform these computations. As it will become clear shortly, a straightforward approach to the problem has to face some intrinsic limitations in order to keep systematic effects under control. We thus conclude the section showing how these limitations can be overcome by considering finite-volume renormalization schemes, together with finite-size scaling techniques.

---

[25]For simplicity we assume that any power divergence in our observables has been taken care of. We are then left only with the problem of the overall multiplicative renormalization.

[26]For an introduction to the topic of non-perturbative renormalization on the lattice we recommend the following set of lectures (Sommer, 1997; Lüscher, 1998a; Weisz, 2010; Vladikas, 2011).

Before moving to the discussion, we note that if one considers QCD with only light quarks (i.e. u, d and s), it is convenient to adopt mass-independent schemes for the renormalization factors Z (Weinberg, 1973). In this case, the renormalization constants do not depend on the quark-masses, i.e., $Z \equiv Z(g_0, a\mu)$. Their renormalization group equations are then easier to solve since the running of the quark-masses in disentangled.

2.3.1 Connecting low-and-high-energies

In lattice QCD, one generally renormalizes the theory through some hadronic scheme (see e.g. (Lüscher, 1998a)). Indeed, it is natural to fix the bare parameters by requiring a set of observables, as for example some hadron masses or decay constants, to take on their physical values. Analogously, it is convenient to renormalize the bare operators by demanding some matrix elements between hadronic states to assume prescribed values. At high-energy, however, perturbation theory is commonly applied to make predictions of strong interaction contributions. In this case, the renormalization schemes in use are generally different. A popular and technically advantageous scheme, for example, is given by the $\overline{\text{MS}}$ scheme of dimensional regularization ('t Hooft, 1973; Collins, 1986).[27]

The problem of non-perturbative renormalization can now be defined as matching a given hadronic scheme to some perturbative scheme. In more physical terms, this means connecting the low- and high-energy sectors of QCD. In principle, this presents no fundamental obstacles. Once the theory is renormalized in a given hadronic scheme, any quantity that did not enter in the renormalization conditions is a prediction of the theory. In particular, this includes the high-energy behavior of renormalized matrix elements and parameters in any other scheme.

Apart from the purely theoretical appeal of the problem, there are several instances where this connection would be desirable in practice. The renormalized coupling and quark-masses, for example, are generally extracted at high-energy by fitting the results of some scattering processes to their perturbative predictions. The values so obtained are then used as an input for the perturbative computation of any other quantity

---

[27] From now on we choose the $\overline{\text{MS}}$ scheme as our perturbative scheme of reference. At high-energy, the connection between different schemes can then be made through perturbative computations.

of interest. It is clear, however, that this procedure suffers from several systematics which are difficult to quantify. In particular, these include the truncation of the perturbative series in the corresponding expansions, as well as the contamination of non-perturbative effects which might not be completely suppressed at the energies considered.[28] Having more systematic methods for these determinations is then important not only to corroborate, but also to improve the results. In this respect, we note that lattice QCD allows in principle for a determination of the fundamental parameters of QCD where all systematic effects are under control. Indeed, matching a given hadronic scheme to a perturbative scheme would permit the non-perturbative determination of the strong coupling and quark masses at high-energy in terms of some well-known low-energy constants of the theory (see e.g. (Sommer, 1997)).

Establishing a connection between perturbative and non-perturbative schemes is also important in the context of operator renormalization (see e.g. (Weisz, 2010; Vladikas, 2011; Lellouch, 2011)). In particular, many interesting cases where operator renormalization is necessary are related to the determination of electro-weak transition amplitudes between hadronic states. In these computations, the electro-weak interactions are described by effective low-energy interactions between quarks and gluons. More precisely, the virtual contributions corresponding to the electro-weak bosons, and heavy-quarks (i.e. t, b, and eventually c), are integrated out using perturbative methods, resulting in some effective interactions between the light quarks. The generic transition amplitude, $\mathcal{A}$, between the hadronic states $|i\rangle$ and $|f\rangle$ is then schematically represented as,

$$\mathcal{A} = \langle f|\mathcal{H}_{\text{eff}}|i\rangle = C_W(\mu)\langle f|(\mathcal{O}_R)(\mu)|i\rangle, \tag{2.55}$$

where $\mathcal{H}_{\text{eff}}$ is the effective electro-weak Hamiltonian. $\mathcal{H}_{\text{eff}}$ is generally given in terms of some Wilson coefficients C_W, and corresponding renormalized operators $\mathcal{O}_R$ (see e.g. (Donoghue, Golowich and Holstein, 1994)). The Wilson coefficients incorporate the short distance effects of the electro-weak transition under consideration. The operators

---

[28]This comes without mentioning the practical difficulties in extracting these parameters from this class of observables, the precision of which is already limited by many systematic effects (see e.g. (Donoghue, Golowich and Holstein, 1994)).

$\mathcal{O}_R$ instead describe the low-energy effective interactions among quarks and gluons. Their matrix elements between the initial and final hadronic states $|i\rangle$ and $|f\rangle$, encode the long-range non-perturbative contributions of the strong-interactions to the process.

The renormalization scale μ effectively separates the two energy scales above. In practice, this scale has to be chosen high enough such that a perturbative estimate of the Wilson coefficients C_W is possible, and reliable. In this respect, we note that the renormalization scheme of the operators $\mathcal{O}_R$ is fixed by the perturbative scheme employed in the computation of the Wilson coefficients. Indeed, the scale and scheme dependence of the coefficients and hadronic matrix elements have to cancel each other in order to give a physical amplitude $\mathcal{A}$ independent of any renormalization scale and condition.

While the computation of the Wilson coefficients is naturally performed using perturbation theory, in order to capture the non-perturbative effects of the strong-interactions one would like to determine the hadronic matrix elements of $\mathcal{O}_R$ using lattice techniques. The renormalized electro-weak matrix elements in (2.55), are then generally given by,

$$\langle f|(\mathcal{O}_R)(\mu)|i\rangle = \lim_{a\to 0} Z_{\mathcal{O}}(g_0(a), a\mu)\langle f|\mathcal{O}(g_0(a))|i\rangle_{\text{bare}}, \qquad (2.56)$$

where $\langle f|\mathcal{O}|i\rangle_{\text{bare}}$ denotes the bare matrix element computed on the lattice. We remind that the matrix element on the l.h.s. must be renormalized in the perturbative scheme of the corresponding Wilson coefficients. The renormalization factor $Z_{\mathcal{O}} \equiv Z_{\mathcal{O}}(g_0, a\mu)$, then *defines* the non-perturbative bare matrix element in the perturbative scheme.

The most naive approach to determine $Z_{\mathcal{O}}$ is to rely on bare lattice perturbation theory. In this case, one would simply compute $Z_{\mathcal{O}}$ in a convenient perturbative lattice scheme, and then match directly to the $\overline{\text{MS}}$ scheme at a given order in perturbation theory. The resulting matching factor, $Z_{\mathcal{O}} \equiv Z_{\mathcal{O}}^{\overline{\text{MS}},\text{LAT}}$, is then of the general form,

$$Z_{\mathcal{O}}^{\overline{\text{MS}},\text{LAT}}(g_0(a), a\mu) = 1 + \frac{g_0^2(a)}{(4\pi)^2}\{\gamma_{\mathcal{O}}^{(0)} \log(a\mu)^2 + k\} + \text{O}(g_0^4), \qquad (2.57)$$

where $\gamma_{\mathcal{O}}^{(0)}$ is the anomalous dimension of the operator $\mathcal{O}$ at the lowest order, μ is the renormalization scale in the $\overline{\text{MS}}$ scheme, and k is a constant that depends on the lattice regularization employed for the computation of the bare matrix element.

This strategy, however, is not very reliable since it is hard to quantify the systematics effects one is introducing with this approximation.[29] Apart from the generally bad convergence of bare lattice perturbation theory (Parisi, 1980), it is indeed difficult to estimate the size of discretization (and finite volume) effects in these determinations. In (2.57), in fact, these effects are unavoidably entangled with the renormalization effects, since the renormalization scale is effectively given in terms of the lattice cut-off a^{-1}. For a trustable determination of $Z_{\mathcal{O}}$, and thus of (2.56), one then needs to proceed non-perturbatively. As a result, the renormalization constant $Z_{\mathcal{O}}$ factorizes in two parts: $Z_{\mathcal{O}} \equiv Z_{\mathcal{O}}^{\text{NPT}} \times X_{\mathcal{O}}^{\text{NPT}-\overline{\text{MS}}}$, where $Z_{\mathcal{O}}^{\text{NPT}}$ is defined in some non-perturbative scheme, while $X_{\mathcal{O}}^{\text{NPT}-\overline{\text{MS}}}$ is the finite matching coefficient between this scheme and the perturbative one.

2.3.2 The necessity of a renormalization window

Given the observations of the previous subsection, we now want to understand which are the general difficulties that one encounters in the determination of $Z_{\mathcal{O}}$ using lattice techniques. To this scope, we will consider an explicit example given by a popular approach to the problem. Discussing the limitations of such an approach, will help us in motivating finite-volume renormalization schemes, which are presented in the next subsection. As we shall see, the combination of this class of schemes with finite-size scaling methods, offers a general solution for the determination of $Z_{\mathcal{O}}$ where these limitations are absent.

Moving to our presentation, the basic principle of any of these strategies is to rely on an intermediate non-perturbative renormalization scheme. In the specific example we want to consider, this is given by a regularization independent momentum subtraction scheme (RI-MOM) (Martinelli *et al.*, 1995).[30] The key idea in this case, is to mimic non-perturbatively what is done in continuum perturbation theory to renormalize the operators. More precisely, one imposes the renormalization conditions by considering

---

[29]We refer to (Lüscher, 1998*a*) for a more detailed discussion including also some explicit examples.
[30]For an introduction we recommend (Vladikas, 2011).

matrix elements of the operator $\mathcal{O}$ between quark states $|p\rangle$ with given momenta p.[31] Specifically, the renormalization conditions require these matrix elements to be equal to their tree-level values, i.e.,

$$\langle p|(\mathcal{O}_R)(\mu)|p\rangle|_{p^2=\mu^2} = \langle p|\mathcal{O}|p\rangle|_{\text{tree}} \quad \Rightarrow \quad Z_{\mathcal{O}}^{\text{RI}}(g_0, a\mu) = \left.\frac{\langle p|\mathcal{O}|p\rangle|_{\text{tree}}}{\langle p|\mathcal{O}(g_0)|p\rangle_{\text{bare}}}\right|_{\mu^2=p^2}.$$
$$(2.58)$$

This defines the renormalization factor $Z_{\mathcal{O}}^{\text{RI}}$ in the RI-MOM scheme at the renormalization scale $\mu^2 = p^2$. In the following we will thus use the notation $Z_{\mathcal{O}}^{\text{RI}} \equiv Z_{\mathcal{O}}^{\text{RI}}(g_0, ap)$.

The matrix elements in (2.58) are then computed non-perturbatively for several momenta p at the relevant values of bare coupling g_0 in large physical volumes. Once the renormalization factor $Z_{\mathcal{O}}^{\text{RI}}$ is determined, the generic bare matrix element $\langle f|\mathcal{O}(g_0)|i\rangle_{\text{bare}}$ can be renormalized, and extrapolated to the continuum limit. The result obtained is now independent of the regularization employed. The renormalized operator and corresponding matrix element, can then be converted from the RI-MOM scheme, to any other perturbative scheme using continuum perturbation theory.

In conclusion, the desired renormalized matrix element of (2.56), is given by,

$$\langle f|(\mathcal{O}_R^{\overline{\text{MS}}})(\mu)|i\rangle = X_{\mathcal{O}}^{\overline{\text{MS}},\text{RI}}(g_{\overline{\text{MS}}}, p/\mu) \lim_{a\to 0} Z_{\mathcal{O}}^{\text{RI}}(g_0(a), ap)\langle f|\mathcal{O}(g_0(a))|i\rangle_{\text{bare}}$$
$$= X_{\mathcal{O}}^{\overline{\text{MS}},\text{RI}}(g_{\overline{\text{MS}}}, p/\mu)\langle f|(\mathcal{O}_R^{\text{RI}})(p)|i\rangle,$$
$$(2.59)$$

where μ denotes the renormalization scale in the $\overline{\text{MS}}$ scheme, $g_{\overline{\text{MS}}}$ is the corresponding renormalized coupling, and $X_{\mathcal{O}}^{\overline{\text{MS}},\text{RI}}$ is the perturbative matching factor between the RI-MOM, and $\overline{\text{MS}}$ scheme. The latter is generally known to several orders in perturbation theory (see e.g. (Martinelli *et al.*, 1995)). The nice features of this approach are that one does not involve any perturbative approximation in the determination of $Z_{\mathcal{O}}^{\text{RI}}$, and the matching factor $X_{\mathcal{O}}^{\overline{\text{MS}},\text{RI}}$ is computed using continuum perturbation theory at high orders.

---

[31] Working with quark states at the non-perturbative level implies some difficulties. First of all, one has to deal with the problem of Gribov copies (Gribov, 1978), and more generally of gauge fixing on the lattice (see e.g. (Giusti *et al.*, 2001)). In additional, the O(a) improvement of the theory needs to be reconsidered since the correlation functions employed are not on-shell (Martinelli *et al.*, 1995). A similar method to the one discussed here but which uses gauge-invariant on-shell correlation functions is described in (Martinelli *et al.*, 1997; Becirevic *et al.*, 2003).

From our discussion, it is clear that the practical success of the program outlined above depends on several conditions. First of all, in order to obtain reliable continuum extrapolations of the renormalized matrix elements in (2.59), the momenta p at which we evaluate $Z_{\mathcal{O}}^{\mathrm{RI}}$ need to be well below the lattice cutoff a^{-1}, as otherwise discretization effects can be large. On the other hand, the range of p's explored determines the scale at which in the continuum one connects the RI-MOM scheme with the perturbative scheme. In order for this connection to be safe, the matching needs to be performed at an energy scale μ where perturbation theory can be trusted. The control over discretization effects and non-perturbative effects, thus requires the existence of a "renormalization window" given by,

$$\Lambda_{\mathrm{QCD}} \ll \mu \ll a^{-1}, \qquad (2.60)$$

where Λ_{QCD} is a typical scale of non-perturbative QCD effects (lets say a few GeV).

These conditions, however, are not always easy to be satisfied within the above strategy. The values of the lattice spacing a, indeed, are generally limited by the fact that the physical size of the lattice, L, has to be large enough such that finite volume effects are negligible. In this approach, this is crucial for a reliable determination of both the bare matrix element $\langle f|\mathcal{O}|i\rangle_{\mathrm{bare}}$, *and* the renormalization factor $Z_{\mathcal{O}}^{\mathrm{RI}}$. In this respect, we note that in current large volume lattice simulations one generally has: $a^{-1} \leq 5\,\mathrm{GeV}$ (see e.g. (Schaefer, 2012)). This means that a perturbative matching between the non-perturbative scheme and the perturbative one has to be trusted at this relatively low energy scale.[32]

To conclude, in this subsection we have learned which are the conditions for a reliable non-perturbative scale-dependent renormalization. These can be summarized by the following chain of inequalities,

$$L^{-1} \ll \Lambda_{\mathrm{QCD}} \ll \mu \ll a^{-1}. \qquad (2.61)$$

Once again, going from right to left, we have: first, the cutoff scale a^{-1} must be much higher than all other physical length scales in the problem, as in particular

---

[32]In practice, many technical improvements have been developed in order to make this matching more and more reliable with such a constraint (see e.g. (Vladikas, 2011) and references therein). Here, however, we are stressing on the basic principles of this approach.

the perturbative scale μ at which we match the two schemes. This is necessary in order to control cutoff effects. Secondly, the renormalization scale μ must be much higher than the typical scale of non-perturbative QCD effects Λ_{QCD}, such that the matching between the non-perturbative and perturbative schemes can be safely made through perturbation theory. Finally, the physical size of the lattice L must be large enough such that all relevant non-perturbative scales are contained without sizable finite volume effects. A rough estimate of (2.61) shows that the lattices required need a great resolution: $L/a \gg 50$, which is generally difficult to achieve with present computer and algorithmic resources.

2.3.3 Finite-volume schemes and scaling techniques

The problem with the type of strategy discussed in the previous subsection, is that one is trying to fit two very separate energy scales into a single lattice simulation, namely: the non-perturbative scale set by the hadronic matrix element, and the perturbative scale set by the matching between the non-perturbative renormalization scheme and the perturbative one. As we now present, however, this is not necessary in practice.

The key idea is to use as an intermediate non-perturbative renormalization scheme a *finite-volume* scheme (Wolff, 1986; Lüscher, Weisz and Wolff, 1991).[33] The peculiarity of this class of schemes is that one identifies the renormalization scale with the inverse size of the physical volume, i.e.,

$$\mu = L^{-1}. \tag{2.62}$$

In order words, one uses finite volume effects to define renormalized parameters and operators. The main advantage of these schemes is that the problem of connecting low- an high-energy scales can be split over several volumes, each of which covers only a limited range of energies. This allows the conditions (2.61) to be easily satisfied at each step of the computation. In order to disclose a bit more the strategy, we now present in detail how the renormalized matrix elements of (2.56) can be computed

---

[33]For an introduction to finite-volume renormalization schemes and their use in lattice field theory we recommend the set of lectures (Sommer, 1997; Lüscher, 1998a; Weisz, 2010).

using these methods. More precisely, we will start by giving the master formula for this type of computations. We will then discuss in detail each key step.

The determination of (2.56) using finite-volume techniques, can be summarized as (cf. (2.59)),

$$\langle f|(\mathcal{O}_R^{\overline{\text{MS}}})(\mu)|i\rangle = X_{\mathcal{O}}^{\overline{\text{MS}},\text{FVS}}(g_{\overline{\text{MS}}}, \mu L_{\min})U_{\mathcal{O}}(L_{\min}^{-1}, L_{\max}^{-1})\langle f|(\mathcal{O}_R^{\text{FVS}})(L_{\max}^{-1})|i\rangle, \quad (2.63)$$

where,

$$\langle f|(\mathcal{O}_R^{\text{FVS}})(L_{\max}^{-1})|i\rangle = \lim_{a\to 0} Z_{\mathcal{O}}^{\text{FVS}}(g_0(a), aL_{\max}^{-1})\langle f|\mathcal{O}(g_0(a))|i\rangle_{\text{bare}}. \quad (2.64)$$

The first ingredient is, of course, the bare matrix element $\langle f|\mathcal{O}(g_0)|i\rangle_{\text{bare}}$. This, we recall, must be computed in a large physical volume of spatial extent L_∞, for several values of the bare coupling g_0. The latter should be chosen such that L_∞ can be taken large enough that finite volume corrections are negligible within the statistical accuracy of the matrix element, i.e. $L_\infty \gg m_\pi^{-1}$. On the other hand, however, a must be small enough that discretization effects are under control, i.e. $a \ll \Lambda_{\text{QCD}}^{-1}$, but large enough that simulations are affordable, i.e. $L_\infty/a \lesssim 100$.

Secondly, the renormalization factor $Z_{\mathcal{O}}^{\text{FVS}} \equiv Z_{\mathcal{O}}^{\text{FVS}}(g_0, a/L)$, is obtained as follows. One considers some matrix element of the operator $\mathcal{O}$ in a lattice with given resolution L/a, and fixed bare coupling g_0. Note that all dimensionfull parameters in the system must be rescaled in fixed proportions with L such that L is the only scale in the problem. The finite-volume renormalization factor $Z_{\mathcal{O}}^{\text{FVS}}$ is then defined by requiring the chosen renormalized matrix element to assume some prescribed value e.g. its tree-level value. This implicitly defines the renormalization factor $Z_{\mathcal{O}}^{\text{FVS}}$ at the bare coupling g_0, and renormalization scale $\mu = L^{-1}$. In particular, at high enough energy (small enough L), i.e. $\mu \gg \Lambda_{\text{QCD}}$, the finite-volume renormalization factor can be evaluated in perturbation theory. The finite-volume scheme can thus be matched to any conventional perturbative scheme in infinite volume (see e.g. (Lüscher, 1998a)). The finite matching factor $X_{\mathcal{O}}^{\overline{\text{MS}},\text{FVS}}$ is determined in this way.

Given the renormalization condition for $Z_{\mathcal{O}}^{\text{FVS}}$, the renormalization of the bare matrix element (2.64) at low-energy proceeds as follows. One starts by considering the renormalization condition for $Z_{\mathcal{O}}^{\text{FVS}}$ at the values of the bare coupling g_0 where the bare

matrix element $\langle f|\mathcal{O}(g_0)|i\rangle_{\text{bare}}$ has been computed. Note that the discretization effects in the determination of $Z_{\mathcal{O}}^{\text{FVS}}$ are under control once the simple condition $L/a \gg 1$ is satisfied. Choosing a suitable L_{max}/a at the largest value of g_0, then implicitly defines the renormalization scale $\mu_{\text{min}} = L_{\text{max}}^{-1}$. Given the typical values of the lattice spacing in simulations, and assuming $L_{\text{max}}/a = \mathrm{O}(10)$, one generally has $\mu_{\text{min}} = \mathrm{O}(100)$ MeV. The continuum limit in (2.64) must now be taken keeping μ_{min} fixed, which in turn requires to adjust L_{max}/a as a function of g_0, i.e. $L_{\text{max}}/a \equiv (L_{\text{max}}/a)(g_0)$. Finally, given the values of g_0 and $(L_{\text{max}}/a)(g_0)$ so defined, one computes $Z_{\mathcal{O}}^{\text{FVS}}$ accordingly, and performs the limit in (2.64). As a result, the renormalized matrix element in the finite-volume scheme, $\langle f|(\mathcal{O}_R^{\text{FVS}})(\mu_{\text{min}})|i\rangle$, is obtained at the renormalization scale $\mu_{\text{min}} = L_{\text{max}}^{-1}$.

The last step of the determination (2.63) requires the running of the renormalized matrix element $\langle f|(\mathcal{O}_R^{\text{FVS}})|i\rangle$ from the low-energy scale μ_{min}, up to the high-energy scale $\mu_{\text{max}} = L_{\text{min}}^{-1}$, where the connection to the $\overline{\text{MS}}$ scheme can be safely made using $X_{\mathcal{O}}^{\overline{\text{MS}},\text{FVS}}$. To this end, the idea is to determine the non-perturbative evolution operator $U_{\mathcal{O}}(\mu',\mu)$ defined by (see e.g. (Guagnelli *et al.*, 2006)),

$$(\mathcal{O}_R)(\mu') = U_{\mathcal{O}}(\mu',\mu)(\mathcal{O}_R)(\mu), \qquad U_{\mathcal{O}}(\mu',\mu) = \lim_{a \to 0} \frac{Z_{\mathcal{O}}^{\text{FVS}}(g_0, a\mu')}{Z_{\mathcal{O}}^{\text{FVS}}(g_0, a\mu)}. \qquad (2.65)$$

The way this is constructed in practice is through a finite-size scaling technique, i.e. *step-scaling*. More precisely, one first introduces the continuum step-scaling function $\sigma_{\mathcal{O}}$, defined by,

$$\sigma_{\mathcal{O}}(u) = \lim_{a \to 0} \Sigma_{\mathcal{O}}(u, a/L), \qquad \Sigma_{\mathcal{O}}(u, a/L) = \left. \frac{Z_{\mathcal{O}}^{\text{FVS}}(g_0(a), a/2L)}{Z_{\mathcal{O}}^{\text{FVS}}(g_0(a), a/L)} \right|_{\bar{g}^2(L^{-1})=u}. \qquad (2.66)$$

As emphasized in the above equation, $\sigma_{\mathcal{O}}(u)$ is obtained as the continuum limit of the lattice step-scaling function $\Sigma_{\mathcal{O}}(u, a/L)$. This is computed by determining $Z_{\mathcal{O}}^{\text{FVS}}(g_0, a/L)$ and $Z_{\mathcal{O}}^{\text{FVS}}(g_0, a/2L)$ for several values of g_0 and resolutions L/a, at fixed renormalization scale $\mu = L^{-1}$. The latter is kept fixed by tuning g_0 and L/a such that a given renormalized finite-volume coupling $\bar{g}^2(L^{-1})$ is constant. Once the step-scaling $\sigma_{\mathcal{O}}(u)$ is obtained, this allows to run the renormalized operator $(\mathcal{O}_R)(\mu)$ from the renormalization scale μ down to $\mu/2$, where $\mu = L^{-1}$ is specified by $u = \bar{g}^2(L^{-1})$.

The energy range $[\mu_{\min}, \mu_{\max}]$ can thus be split in a number of steps k, where the renormalization scale is varied by a factor of two at each step, i.e. $\mu_{\max} = 2^k \mu_{\min}$. The step-scaling function $\sigma_{\mathcal{O}}(u)$ then needs to be determined at the corresponding values of the finite-volume coupling $u \in [u_0, \ldots, u_{k-1}]$, where $u_0 \equiv \bar{g}^2(2L_{\max}^{-1})$, and $u_{k-1} \equiv \bar{g}^2(L_{\min}^{-1})$. Finally, the evolution operator $U(\mu_{\max}, \mu_{\min})$ is obtained as,

$$U_{\mathcal{O}}(\mu_{\max}, \mu_{\min}) = \prod_{l=0}^{k-1} \sigma_{\mathcal{O}}^{-1}(u_l). \tag{2.67}$$

To conclude, finite-volume renormalization schemes provide a general solution to non-perturbative renormalization problems. The practical success of the program outlined above, however, very much depends on the details of the specific scheme chosen. In particular, some basic criteria should be met by the finite-volume scheme in order to make this program feasible:

- The finite-volume scheme should be relatively simple to compute in perturbation theory, such that the matching at high-energy with other perturbative schemes can performed easily and accurately.

- The given scheme should be relatively easy compute numerically, and have a good statistical precision once estimated through Monte Carlo methods.

- Discretization effects should be mild, such that relatively small lattice sizes L/a can be considered for the running, and safe continuum limit extrapolations can be obtained for renormalized quantities like for example the lattice step-scaling function $\Sigma_{\mathcal{O}}$.

Careful consideration of the above points led to the introduction of renormalization schemes based on the Schrödinger functional of QCD (Lüscher, Narayanan, Weisz and Wolff, 1992). This powerful tool will be the central topic of the next chapter.

3
The Schrödinger functional

In the last chapter, we presented the advantages of using finite-volume renormalization schemes for the non-perturbative renormalization of the lattice theory. In particular, we discussed that several practical criteria have to be satisfied by the specific scheme in order to make this renormalization feasible (cf. Section 2.3.3). In this chapter, we want to introduce a family of schemes that enjoy many attractive features in this respect. These schemes are based on the Schrödinger functional (SF) of QCD (Lüscher, Narayanan, Weisz and Wolff, 1992; Sint, 1994; Sint, 1995).

We thus begin the chapter presenting the SF in the continuum. Starting from the pure Yang-Mills theory, we later introduce fermions. Note that, although only formal, the continuum formulation will allow us to discuss many of the crucial properties of the set-up on fairly general grounds. Secondly, given the continuum definition, we present the lattice regularization of the SF. After a short discussion of the pure gauge theory, we will discuss the inclusion of fermions in detail. More precisely, we will first review the standard lattice formulation of the SF based on Wilson-fermions. In particular, we will investigate the $O(a)$ improvement of the theory, and show how the SF boundary conditions for the quark fields break the argument of automatic $O(a)$ improvement presented in Section 2.2.4. This will lead us to introduce an alternative discretization of the SF where this nice feature is recovered. The formulation is based on the chirally rotated Schrödinger functional (χSF) (Sint, 2011), which is the main focus of this work. Finally, the chapter is concluded with an analysis of the novel set-up including the details of the regularization, renormalization, and $O(a)$ improvement of the theory.

3.1 The Schrödinger functional: formal definition

3.1.1 Yang-Mills theory

The Schrödinger functional is given by the quantum-mechanical propagation kernel from some field configuration at time $x_0 = 0$, to some other configuration at $x_0 = T$. In Euclidean space-time, this can be written as a functional integral over all fields with given boundary conditions (Lüscher, Narayanan, Weisz and Wolff, 1992). In particular, since we are interested in studying the theory in finite volume, we consider space to be a $L \times L \times L$ torus. The space-time manifold is then given by a hyper-cylinder, with finite spatial extent L, and finite temporal extent T. The gauge potential $A_\mu(x) \in \mathfrak{su}(3)$, is defined accordingly for all $0 \leq x_0 \leq T$. It is periodic in the spatial directions, and satisfies Dirichlet boundary conditions in the time direction. The latter are specified by,

$$A_k(\mathbf{x}) = \begin{cases} C_k^\Lambda(\mathbf{x}), & \text{at } x_0 = 0, \\ C_k'(\mathbf{x}), & \text{at } x_0 = T, \end{cases} \tag{3.1}$$

where C, and C' are classical gauge potentials, and $A_k^\Lambda(\mathbf{x})$ denotes the gauge transform of $A_k(\mathbf{x})$, which is defined as,

$$A_k^\Lambda(\mathbf{x}) = \Lambda(\mathbf{x}) A_k(\mathbf{x}) \Lambda(\mathbf{x})^{-1} + \Lambda(\mathbf{x}) \partial_k \Lambda(\mathbf{x})^{-1}, \quad \Lambda(\mathbf{x}) \in \text{SU}(3). \tag{3.2}$$

Note that in order to preserve periodicity, only periodic functions $\Lambda(\mathbf{x})$ are permitted.

Given these definitions, the functional integral representation of the Schrödinger functional can be written as (Lüscher, Narayanan, Weisz and Wolff, 1992),

$$\mathcal{Z}[C, C'] = \int \mathcal{D}[\Lambda] \int \mathcal{D}[A] \, e^{-S_G[A]}, \tag{3.3}$$

where the gauge action S_G is given by,

$$S_G[A] = -\frac{1}{2g_0^2} \int_0^T dx_0 \int_0^L d^3\mathbf{x} \, \text{tr} \{F_{\mu\nu}(x) F_{\mu\nu}(x)\}, \tag{3.4}$$

with $F_{\mu\nu}$ defined in (A.23), while the integral measures are defined by,

$$\mathcal{D}[A] = \prod_{x,\mu,a} dA_\mu^a(x), \qquad \mathcal{D}[\Lambda] = \prod_{\mathbf{x}} d\Lambda(\mathbf{x}), \tag{3.5}$$

where $d\Lambda$ is the Haar measure over the gauge group SU(3).

The integral over the gauge group in (3.3) guarantees that $\mathcal{Z}[C', C]$ is invariant under arbitrary gauge transformations of the boundary value fields C and C'.

3.1.2 Induced background field

A characteristic property of the SF is given by the following observation. The boundary value fields C and C', can be chosen in such a way that, up to gauge transformations, the action S_G has a unique global minimum field configuration (Lüscher, Narayanan, Weisz and Wolff, 1992). This field configuration is generally referred to as the induced *background field*, and it will be denoted as B in the following. The existence of this unique minimal action configuration, is an essential ingredient for the perturbative expansion of the SF. Indeed, in the weak coupling regime, $g_0 \to 0$, the fields close to B will dominate the path integral, and the SF can be computed by performing a saddle point approximation around B. In particular, the corresponding effective action,[1]

$$\Gamma[B] = -\ln \mathcal{Z}[C, C'], \tag{3.6}$$

has a regular perturbative expansion of the form,

$$\Gamma[B] = \frac{1}{g_0^2}\Gamma_0[B] + \Gamma_1[B] + g_0^2\Gamma_2[B] + \dots, \tag{3.7}$$

where the leading term is given by,

$$\Gamma_0[B] = g_0^2 S_{\mathrm{G}}[B], \tag{3.8}$$

where $S_{\mathrm{G}}[B]$ is the action of the background field. The higher-order terms in the expansion, are then given by sums of vacuum bubble Feynmann diagrams with an increasing number of loops.

Given this nice property, the perturbative evaluation of the effective action can proceed as usual (Lüscher, Narayanan, Weisz and Wolff, 1992). First, a regularization is chosen in order to regularize the divergent loop integrals. This can be either a continuum regularization, like dimensional regularization, or a lattice regularization

---

[1]Note that we can unambiguously label the effective action in terms of the background field, instead of the boundary value fields. The background field and the boundary fields, indeed, are in a one-to-one correspondence.

for example. Secondly, gauge fixing has to be performed taking care of imposing the correct boundary conditions on the gauge and ghost fields. The Feynmann rules can then be derived in standard fashion, where the vertices and propagators will now depend on the background field, similarly to a background field method.[2] Some degree of complication is certainly introduced by the loss of translation invariance in the time direction. In general, however, perturbation theory in the SF has been shown to be feasible up to two loops, with several explicit continuum and lattice computations, both in pure Yang-Mills theory and full QCD.[3] In addition, several automated tools have been developed over the last years in order to help performing these calculations on the lattice (Takeda, 2009*b*; Hesse and Sommer, 2013; Brambilla *et al.*, 2013). In conclusion, the SF offers a robust and practical framework for perturbative computations in finite volume.

At this point, the reader might wonder whether such an elaborate set-up as the SF is in fact needed to obtain a regular perturbative expansion in finite volume. Why not simply consider for example finite-volume schemes defined in a hyper-tours? The answer to this question is rather technical. Here we just want to mention that the problem in this case is that in a finite volume with periodic boundary conditions, the perturbative expansion of the path-integral is greatly complicated due to the presence of gauge zero-modes (Gonzalez-Arroyo, Jurkiewicz and Korthals-Altes, 1981). These modes are constant gauge field configurations of minimal action that dominate the low-energy dynamics of the theory in a finite volume. In particular, in the perturbative evaluation of the path-integral one has to treat the non-zero modes and the zero-modes differently, where for the latter a standard perturbative approach is not possible. Here we do not want to enter into the details of this technical subject. We thus refer the reader to the review in (Fodor *et al.*, 2012) for a detailed discussion about these points, and how to deal properly with gauge zero-modes in perturbation theory.

To conclude, we note that alternative boundary conditions do exist, which eliminate

---

[2]For an introduction to background field methods we refer to (Abbott, 1982).

[3]A list of early computations is given by (Lüscher, Narayanan, Weisz and Wolff, 1992; Narayanan and Wolff, 1995; Sint, 1995; Sint and Sommer, 1996; Bode, Weisz and Wolff, 1999; Bode, Weisz and Wolff, 2000).

the gauge zero-modes of Yang-Mills theory in finite volume. An example is given by twisted periodic boundary conditions ('t Hooft, 1979). A nice feature of these boundary conditions is that translation invariance is preserved in all space-time directions. One the other hand, these boundary conditions impose some restrictions on the matter content of the theory (Parisi, 1984). In particular, matter fields in the fundamental representation of the gauge group $SU(N)$ are forced to come in multiples of the number of colors N. This, unfortunately, is not very convenient for studies of QCD.[4]

3.1.3 Renormalization

Through the perturbative study of the SF, one can analytically investigate the nature and form of the divergences that appear in the formulation, and thus understand its renormalization. In this respect, a relevant and non-trivial question is whether a local quantum field theory formulated on a manifold with boundaries develops additional ultra-violet divergences. In fact, the presence of the boundaries can be described by additional interaction terms in the Lagrangian, which effectively impose on the fields the given boundary conditions. The renormalization of the theory can then in principle be altered by the presence of these additional terms.

The first studies in this direction have been conducted by Symanzik in the massless ϕ_4^4 theory (Symanzik, 1981a). In particular, in this work Symanzik expressed the expectation that all divergences in the SF could be removed by renormalizing the bare coupling constant, and by including in the bare action the boundary counterterms,

$$\int_{x_0=T} \mathrm{d}^3\mathbf{x} \left\{ Z_1 \phi^2 + Z_2 \phi \partial_0 \phi \right\} + \int_{x_0=0} \mathrm{d}^3\mathbf{x} \left\{ Z_1 \phi^2 - Z_2 \phi \partial_0 \phi \right\}, \qquad (3.9)$$

where Z_1 and Z_2 are some divergent renormalization factors. In fact, Symanzik conjectured that this result is generic, and the SF of any renormalizable theory can be made finite by the usual parameter and field renormalization, and by adding a few boundary counterterms to the action. These boundary counterterms are given as local composite fields of mass dimension less or equal to 3 integrated over the boundaries at

---

[4]Note however that quark fields in the adjoin representation of the gauge group, do not suffer from any restriction. Other interesting theories than QCD can then be studied in finite-volume with these boundary conditions, see e.g. (Gonzlez-Arroyo and Okawa, 2013).

$x_0 = 0$ and $x_0 = T$. In particular, only the counterterms that respect the symmetries of the theory are allowed.[5]

In the case of the pure Yang-Mills theory, we then expect the SF to be finite after the renormalization of the bare coupling. Indeed, we note that there are no non-trivial gauge invariant polynomials in the gauge potential with mass dimension less or equal to 3. Even though this conjecture has never been proven, quite some evidence has been accumulated over the years confirming this expectation.[6] In particular, several 1-loop and even 2-loop computations have been performed where this has been shown explicitly (Lüscher, Narayanan, Weisz and Wolff, 1992; Narayanan and Wolff, 1995; Bode, Weisz and Wolff, 1999). Similar results have been obtained for QCD. In this case, as we shall see, the situation is even less trivial since the renormalization of the SF requires in general some dimension 3 boundary counterterms (Sint, 1995; Sint and Sommer, 1996; Bode, Weisz and Wolff, 2000; Sint, 2006).

To conclude, we note that in addition to the perturbative results, many non-perturbative studies of the SF have been conducted so far using several different lattice regularizations, and considering many different theories. The numerical results show that a universal continuum limit of the SF exists, and it is obtained after the expected renormalization of the theory. There is thus little doubt that Symanzik's conjecture is correct in these cases, and most likely in general.

3.1.4   Quarks

The introduction of fermions in the SF was first considered in (Sint, 1994). There, starting from the lattice theory with Wilson-fermions, the boundary conditions and action of the continuum theory could be inferred. Specifically, the Euclidean action of the SF of QCD is given by,

$$S[A, \overline{\psi}, \psi] = S_{\mathrm{G}}[A] + S_{\mathrm{F}}[A, \overline{\psi}, \psi], \tag{3.10}$$

---

[5]Of course the relevant symmetries to be considered depend on the specific regulator employed. For the case of gauge theories, we will always assume that the regularization preserves gauge symmetry.

[6]A prove of Symanzik's conjecture to all order in perturbation theory is complicated by the loss of time translation invariance in the SF. A standard application of power counting in momentum space is thus not possible in this case.

where the gauge action S_G has been already introduced in (3.4), while the fermionic action S_F is defined as,

$$
\begin{aligned}
S_F[A, \overline{\psi}, \psi] = &\int_0^T dx_0 \int_0^L d^3\mathbf{x}\, \overline{\psi}(x)(\slashed{D} + m)\psi(x) \\
&- \int_0^L d^3\mathbf{x}\, \left[\overline{\psi}(x)P_-\psi(x)\right]\big|_{x_0=0} - \int_0^L d^3\mathbf{x}\, \left[\overline{\psi}(x)P_+\psi(x)\right]\big|_{x_0=T}.
\end{aligned}
\tag{3.11}
$$

The projectors $P_\pm = \frac{1}{2}(1 \pm \gamma_0)$ are used to project on the Dirichlet components of the quark fields. More precisely, the Dirichlet boundary conditions for the quark fields are given by,

$$
\begin{aligned}
P_+\psi(x)|_{x_0=0} = \rho_+(\mathbf{x}), \qquad & P_-\psi(x)|_{x_0=T} = \rho'_-(\mathbf{x}), \\
\overline{\psi}(x)P_-|_{x_0=0} = \overline{\rho}_-(\mathbf{x}), \qquad & \overline{\psi}(x)P_+|_{x_0=T} = \overline{\rho}'_+(\mathbf{x}),
\end{aligned}
\tag{3.12}
$$

where ρ_+, $\overline{\rho}_-$, ρ'_-, and $\overline{\rho}'_+$, are some given source fields. It is then general practice to take the quark fields to be periodic in the spatial directions, but allow for a constant $U(1)$ background field in the covariant derivative, i.e.,

$$
D_\mu = \partial_\mu + A_\mu + i\frac{\theta_\mu}{L}, \qquad \theta_\mu = (1 - \delta_{\mu 0})\theta, \qquad \theta \in [0, 2\pi].
\tag{3.13}
$$

This Abelian field can be eliminated by an Abelian gauge transformation of the quark fields, but as a consequence the spatial boundary conditions of the fields would change, and be periodic up to a phase factor. These boundary conditions are interesting, since they offer some additional freedom in probing the quark dynamics in finite volume.

Given these definitions, some observations are in order. The first thing that we want to note is that the boundary conditions (3.12) only constrain half of the components of the quark fields at the boundary. From a classical point of view, this can be understood by noticing that the Dirac equation is a first order differential equation. A given solution is then uniquely determined when half of the components of the fields are specified at each boundary. The second remark concerns the boundary terms that appear in the quark action (3.11). Naively, one might have expected that similarly to the case of the gauge action, the quark action would have been given by the standard action (1.4), supplemented with the boundary conditions (3.12). The origin of these terms, however, is easily explained. Once the boundary conditions (3.12), and parity

invariance of the action are assumed, these terms guarantee that the action has smooth, i.e. C^∞, solutions to the classical field equations of motion (Sint, 1994). Finally, one can prove that the boundary conditions for the quark fields introduce a gap in the spectrum of the Dirac operator. More precisely, for any smooth gauge potential, the spectrum of the massless SF Dirac operator is purely discrete and with no zero modes (Lüscher, 2006). As we shall see, this property is very important in practice since it allows numerical simulations of the SF directly in the chiral limit.

Having introduced the classical action and boundary conditions, the path-integral representation of the SF of QCD can be defined as (Sint, 1995),

$$\mathcal{Z}[\overline{\rho}'_+, \rho'_-, C'; \overline{\rho}_-, \rho_+, C] = \int \mathcal{D}[\Lambda] \int \mathcal{D}[A]\mathcal{D}[\psi]\mathcal{D}[\overline{\psi}]\, e^{-S[A,\psi,\overline{\psi}]}, \tag{3.14}$$

where the functional integral is over all fields which satisfy the boundary conditions (cf. (3.1)),

$$
\begin{aligned}
A_k(\mathbf{x})|_{x_0=0} &= C_k^\Lambda(\mathbf{x}), & A_k(\mathbf{x})|_{x_0=T} &= C_k'(\mathbf{x}), \\
P_+\psi(x)|_{x_0=0} &= \Lambda(\mathbf{x})\rho_+(\mathbf{x}), & P_-\psi(x)|_{x_0=T} &= \rho'_-(\mathbf{x}), \\
\overline{\psi}(x)P_-|_{x_0=0} &= \overline{\rho}_-(\mathbf{x})\Lambda(\mathbf{x})^{-1}, & \overline{\psi}(x)P_+|_{x_0=T} &= \overline{\rho}'_+(\mathbf{x}).
\end{aligned}
\tag{3.15}
$$

Including the quark fields, the renormalization of the SF has to be reconsidered. In particular, differently from the case of the pure Yang-Mills theory, gauge invariant composite fields of mass dimension 3 are present in QCD (Sint, 1995). More precisely, taking into account the boundary conditions for the fields, one finds that the boundary counterterms,

$$\overline{\psi}(x)P_-\psi(x)\big|_{x_0=0}, \qquad \overline{\psi}(x)P_+\psi(x)\big|_{x_0=T}, \tag{3.16}$$

need to be added to the action in order to obtain a finite renormalized SF. Inspecting (3.11), it is easy to see that these counterterms can be included through a multiplicative renormalization of the quark boundary values, namely,

$$(\rho_R)_+ = Z_\zeta^{-1/2}\rho_+, \ \ldots, \ (\overline{\rho}'_R)_+ = Z_\zeta^{-1/2}\overline{\rho}'_+, \tag{3.17}$$

where Z_ζ is a logarithmically divergent factor. This means that for homogeneous boundary conditions, i.e. vanishing boundary values $\rho_+, \ldots, \overline{\rho}'_+$, the SF of QCD is finite after the usual coupling and quark-mass renormalization.

Even in the case of vanishing boundary values, however, the renormalization (3.17) is important once one considers correlation functions in the SF. The generic correlation function of an operator $\mathcal{O}$ in the SF is defined as,

$$\langle \mathcal{O} \rangle = \left\{ \frac{1}{\mathcal{Z}} \int \mathcal{D}[\Lambda] \int \mathcal{D}[A] \mathcal{D}[\psi] \mathcal{D}[\overline{\psi}] \, \mathcal{O}[A, \psi, \overline{\psi}] \, e^{-S[A, \psi, \overline{\psi}]} \right\}_{\rho = \overline{\rho} = \rho' = \overline{\rho}' = 0} , \qquad (3.18)$$

and is thus evaluated at vanishing boundary values. On the other hand, apart from operators made out of quark and gluon fields that live in the bulk, $\mathcal{O}$ may also involve the "boundary quark fields" defined by,

$$
\begin{aligned}
\zeta(\mathbf{x}) &= \frac{\delta}{\delta \overline{\rho}_-(\mathbf{x})}, & \zeta'(\mathbf{x}) &= \frac{\delta}{\delta \overline{\rho}'_+(\mathbf{x})}, \\
\overline{\zeta}(\mathbf{x}) &= \frac{\delta}{\delta \rho_+(\mathbf{x})}, & \overline{\zeta}'(\mathbf{x}) &= \frac{\delta}{\delta \rho'_-(\mathbf{x})}.
\end{aligned}
\qquad (3.19)
$$

Note that, these functional derivatives are well-defined objects since they act on the Boltzmann factor e^{-S} before we set the boundary values to zero. In fact, taking these functional derivatives effectively corresponds to considering the insertion in correlation functions of the non-Dirichlet components of the quark fields infinitesimally close to the boundaries (Lüscher and Weisz, 1996), i.e.,

$$
\begin{aligned}
\zeta(\mathbf{x}) &= P_- \psi(0_+, \mathbf{x}), & \zeta'(\mathbf{x}) &= P_+ \psi(T_-, \mathbf{x}), \\
\overline{\zeta}(\mathbf{x}) &= \overline{\psi}(0_+, \mathbf{x}) P_+, & \overline{\zeta}'(\mathbf{x}) &= \overline{\psi}(T_-, \mathbf{x}) P_-,
\end{aligned}
\qquad (3.20)
$$

where the arguments $x_0 = 0_+$ and $x_0 = T_-$ indicate that the fields are located in the bulk, infinitesimally away from the time boundaries at $x_0 = 0$ and $x_0 = T$, respectively.

In particular, one can consider operators made out of finite products of Fourier components of these fields. A simple example is given by the operator,

$$\mathcal{O}_5^a = \int d^3\mathbf{y} \, d^3\mathbf{z} \, \overline{\zeta}(\mathbf{y}) \frac{\tau^a}{2} \gamma_5 \zeta(\mathbf{z}). \qquad (3.21)$$

We will consider these operators in more detail in the context of the lattice theory. Here we just want to mention that, firstly these operators are gauge invariant quantities. Secondly, single insertions of these boundary operators in on-shell correlation functions are made finite by multiplying the bare operators with the appropriate number of renormalization factors, $(Z_\zeta)^{\frac{n}{2}}$, where n is the total number of ζ and $\overline{\zeta}$ fields that

appear in the given composite field. This is certainly a non-trivial result which is related to the fact that once the bare parameters and boundary values are renormalized, the SF is completely finite (Lüscher, Sint, Sommer and Weisz, 1996).

3.2 The Schrödinger functional: lattice formulation

In the previous section, we formally introduced the SF in the continuum, and discussed its main features. In order to perform a concrete non-perturbative study, however, a lattice regularization needs to be specified. In this section, we will start discussing the lattice regularization of the SF for the pure Yang-Mills theory, as originally proposed in (Lüscher, Narayanan, Weisz and Wolff, 1992). We will then present the standard formulation of the SF of QCD with Wilson-fermions (Sint, 1994).

3.2.1 Yang-Mills theory

We set-up our theory by considering an hyper-cubic lattice with finite spatial extent L and finite temporal extent T, both are assumed to be integer multiples of the lattice spacing a. As usual, our gauge field is defined by assigning an SU(3) matrix $U_\mu(x)$ to every pair $(x, x + a\hat{\mu})$ of points of the lattice. In particular, the temporal link variables $U_0(x)$ are defined for all lattice points with $0 \leq x_0 < T$. As in the continuum, we then require the gauge fields as well as the gauge transformation functions to be periodic in the spatial directions with period L.

The action for the gauge field is taken to be the Wilson action,

$$S_{\mathrm{G}}[U] = \frac{1}{g_0^2} \sum_{\mathbf{x} \in \Gamma} \sum_{x_0=0}^{T} \sum_{\mu,\nu=0}^{3} \omega(P) \operatorname{tr}\{1 - P_{\mu\nu}(x)\}, \tag{3.22}$$

where Γ is defined as the set of spatial points on a given time-slice, i.e.,

$$\Gamma = \left\{\mathbf{x} \,\middle|\, \mathbf{x}/a \in \mathbb{Z}^3,\, 0 \leq x_k < L,\, k = 1, 2, 3\right\}. \tag{3.23}$$

Comparing with the corresponding lattice action in infinite volume (cf. (2.2)), we note the additional weight factor $\omega(P)$ introduced by the presence of the boundaries. For the moment, $\omega(P)$ is taken equal to 1 in all cases except for the spatial plaquettes at $x_0 = 0$ and $x_0 = T$, which are given the weight $\frac{1}{2}$. The significance of this weight factor will be discussed in more detail in the next section.

Given the definition of the action, the lattice regularization of the SF for the pure Yang-Mills theory is now defined as (Lüscher, Narayanan, Weisz and Wolff, 1992),

$$\mathcal{Z}[C, C'] = \int \mathcal{D}[U] \, e^{-S_{\text{G}}[U]}, \qquad \mathcal{D}[U] = \prod_{x,\mu} dU_\mu(x), \qquad (3.24)$$

where dU denotes, as usual, the gauge invariant Haar measure on SU(3). Specifically, the integration in (3.24) is over the gauge fields $U_\mu(x)$ with $0 \leq x_0 < T$ for $\mu = 0$, and $0 < x_0 < T$ for $\mu = 1, 2, 3$. The links at the boundaries are then fixed, and have prescribed values,

$$W_k(\mathbf{x}) = U_k(x)|_{x_0=0}, \qquad W'_k(\mathbf{x}) = U_k(x)|_{x_0=T}. \qquad (3.25)$$

To make contact with the continuum definition of the SF (cf. Section 3.1.1), the link variables W and W' should be related with the continuum boundary values C and C'. The connection is made by recalling that $U_\mu(x)$ is the parallel transporter along the straight line connecting $x + a\hat{\mu}$ with x. We thus identify the link $W_k(\mathbf{x})$ with the corresponding parallel transporter determined by the continuum boundary field $C_k(\mathbf{x})$. In other words, we set,

$$W_k(\mathbf{x}) = \mathcal{P} \exp \left\{ a \int_0^1 dt C_k(\mathbf{x} + a\hat{\mathbf{k}} - ta\hat{\mathbf{k}}) \right\}. \qquad (3.26)$$

where the symbol $\mathcal{P}$ denotes the path ordered exponential.[7] $W'_k(\mathbf{x})$ is similarly given in terms of the field $C'_k(\mathbf{x})$. With this construction, if we perform a gauge transformation $C \to C^\Lambda$, the associated boundary field W transforms as a proper lattice gauge field. In this respect, we emphasize that the lattice SF has to be regarded as a functional of the continuum fields C and C', rather than the boundary link fields W and W'. In particular, the continuum limit of the lattice theory is taken by keeping C and C' fixed while sending the lattice spacing a to zero.

To conclude, comparing the lattice SF (3.24) with its continuum counterpart (3.3), we note that an integral over the gauge transformation functions is missing. The reason is that the lattice SF is already invariant under arbitrary gauge transformations of the boundary fields (Lüscher, Narayanan, Weisz and Wolff, 1992). Indeed, as discussed, a

---

[7]The path ordered exponential is such that the fields at larger integration variable t come first.

gauge transformation $C \to C^\Lambda$ induces a corresponding gauge transformation of the fields W. It is then easy to see that this transformation can always be compensated by a change of variables in the path-integral (3.24). Finally, we also want to mention that the lattice SF has a rigorous quantum mechanical interpretation as the propagation kernel from the field configuration W to the field configuration W' (Lüscher, Narayanan, Weisz and Wolff, 1992). In fact, this is the starting point for its construction in terms of the transfer matrix of the theory.

3.2.2   Quarks

Given the definition of the lattice SF for the pure Yang-Mills theory, in this subsection we discuss the inclusion of fermions. Specifically, we present the standard lattice formulation of the SF of QCD with Wilson-fermions (Sint, 1994).[8] As for the previous subsection, we will not enter into the details of the construction, but simply summarize the main results. We then refer the reader to the given references for the details.

Starting directly from the path-integral, the lattice regularization of the QCD SF with Wilson fermions is given by (Sint, 1994),

$$\mathcal{Z}[\overline{\rho}'_+, \rho'_-, C'; \overline{\rho}_-, \rho_+, C] = \int \mathcal{D}[U]\mathcal{D}[\psi]\mathcal{D}[\overline{\psi}]e^{-S}, \tag{3.27}$$

where the integration is over all quark and anti-quark fields at Euclidean times x_0 with $0 < x_0 < T$. The integral measure for the gauge fields, we remind, has been already specified in (3.24). In (3.27), the lattice action $S = S_\mathrm{G} + S_\mathrm{F}$ is given in terms of a pure gauge part S_G, defined in (3.22), and a fermionic part S_F given by,

$$
\begin{aligned}
S_\mathrm{F} = {}& a^3 \sum_{\mathbf{x}\in\Gamma} \overline{\psi}(x) P_- \Big\{ \sum_{k=1}^{3} a\gamma_k \tfrac{1}{2}\big(\nabla_k + \nabla_k^*\big)\psi(x) - U_0(x)\psi(x+a\hat{0}) \Big\}_{x_0=0} \\
& + a^4 \sum_{\mathbf{x}\in\Gamma} \sum_{x_0=a}^{T-a} \overline{\psi}(x)\Big\{ \tfrac{1}{2}\big\{ \gamma_\mu\big(\nabla_\mu + \nabla_\mu^*\big) - a\nabla_\mu^*\nabla_\mu \big\} + m_0 \Big\}\psi(x) \\
& + a^3 \sum_{\mathbf{x}\in\Gamma} \overline{\psi}(x) P_+ \Big\{ \sum_{k=1}^{3} a\gamma_k \tfrac{1}{2}\big(\nabla_k + \nabla_k^*\big)\psi(x) - U_0^\dagger(x-a\hat{0})\psi(x-a\hat{0}) \Big\}_{x_0=T},
\end{aligned}
\tag{3.28}
$$

where, we recall, $P_\pm = \tfrac{1}{2}(1 \pm \gamma_0)$.

---

[8]The SF of QCD has been later formulated with several other fermionic discretizations. Some examples are found in (Taniguchi, 2005; Lüscher, 2006; Takeda, 2009a; Perez-Rubio and Sint, 2010).

The first observation we want to make is that, by taking the classical continuum limit of (3.28), one recovers the corresponding continuum action (3.11). In particular, the correct boundary terms are obtained. Secondly, we note that the quark and anti-quark fields at the boundaries $x_0 = 0, T$, are not integration variables in (3.27). Hence, they are not active degrees or freedom. Some of their components, however, appear in the action (3.28). More precisely, these are given by,

$$
\begin{aligned}
P_+\psi(x)|_{x_0=0} = \rho_+(\mathbf{x}), && P_-\psi(x)|_{x_0=T} = \rho'_-(\mathbf{x}), \\
\overline{\psi}(x)P_-|_{x_0=0} = \overline{\rho}_-(\mathbf{x}), && \overline{\psi}(x)P_+|_{x_0=T} = \overline{\rho}'_+(\mathbf{x}),
\end{aligned}
\tag{3.29}
$$

where we specified their values in terms of the source fields ρ_+, $\overline{\rho}_-$, ρ'_-, and $\overline{\rho}'_+$. As one might have expected, the components that appear in (3.29) correspond to the Dirichlet quark field components introduced in the continuum theory (cf. (3.12)). In particular, it is interesting to note that the dependence on the boundary fields only enters through the components (3.29). The complementary components, instead, are completely decoupled from the dynamical fields, and thus from the theory. In this respect, we want to stress that, on the lattice, the relations (3.29) should not be regarded as specifying some boundary conditions for the fields. Rather, they define sources to which some particular combinations of field components near the boundary couple (cf. (3.35)). Indeed, strictly speaking, in lattice field theory boundary conditions are not really imposed on the fields, but instead they are encoded in the details of the lattice action close to the boundary (Lüscher, 2006).

Given these observations, for vanishing boundary values (3.29), the lattice quark action (3.28) reduces to the simple form,

$$
S_{\mathrm{F}} = a^4 \sum_{\mathbf{x} \in \Gamma} \sum_{x_0=a}^{T-a} \overline{\psi}(x)\big(D_{\mathrm{w}} + m_0\big)\psi(x),
\tag{3.30}
$$

where we recover the (infinite-volume) massless Wilson Dirac operator (cf. (2.3)),

$$
D_{\mathrm{w}} = \tfrac{1}{2} \sum_{\mu} \big\{ \gamma_\mu (\nabla_\mu + \nabla_\mu^*) - a\nabla_\mu^* \nabla_\mu \big\}.
\tag{3.31}
$$

Note that as we did in the continuum theory, we include in the covariant derivatives an additional Abelian field by defining (cf. (3.13)),

$$\nabla_\mu \psi(x) = \frac{1}{a}\left[e^{i\frac{a}{L}\theta_\mu}U_\mu(x)\psi(x+a\hat{\mu}) - \psi(x)\right],\tag{3.32}$$

and similarly for ∇_μ^* (see Appendix A.4).

Finally, the SF correlation function of a lattice operator $\mathcal{O}$ is given by (cf. (3.18)),

$$\langle\mathcal{O}\rangle = \left\{\frac{1}{\mathcal{Z}}\int \mathcal{D}[U]\mathcal{D}[\psi]\mathcal{D}[\overline{\psi}]\,\mathcal{O}[U,\psi,\overline{\psi}]\,e^{-S[U,\psi,\overline{\psi}]}\right\}_{\rho=\overline{\rho}=\rho'=\overline{\rho}'=0}.\tag{3.33}$$

As in the continuum theory, we can consider fields $\mathcal{O}$ constructed out of the boundary quark fields (3.19), analogously defined on the lattice. As an example, the lattice operator corresponding to (3.21), simply reads,

$$\mathcal{O}_5^a = a^6 \sum_{\mathbf{y},\mathbf{z}\in\Gamma} \overline{\zeta}(\mathbf{y})\frac{\tau^a}{2}\gamma_5\zeta(\mathbf{z}).\tag{3.34}$$

In particular, one can show that in the lattice theory the derivatives w.r.t. the boundary values (3.19) correspond to the insertion in correlation functions of the quark field components (cf. (3.20)) (Lüscher and Weisz, 1996),

$$\zeta(\mathbf{x}) = U_0(0,\mathbf{x})P_-\psi(a,\mathbf{x})\,,\qquad \zeta'(\mathbf{x}) = U_0(T-a,\mathbf{x})^\dagger P_+\psi(T-a,\mathbf{x}),$$
$$\overline{\zeta}(\mathbf{x}) = \overline{\psi}(a,\mathbf{x})P_+U_0(0,\mathbf{x})^\dagger,\qquad \overline{\zeta}'(\mathbf{x}) = \overline{\psi}(T-a,\mathbf{x})P_-U_0(T-a,\mathbf{x}).\tag{3.35}$$

Operators like (3.34) can then be argued to be gauge invariant (Lüscher, Sint, Sommer and Weisz, 1996; Lüscher and Weisz, 1996).

3.3   The Schrödinger functional and O(a) improvement

Having introduced the standard lattice discretization of the SF with Wilson-fermions, in this section we want to study the O(a) improvement of the theory. We thus start in the next subsection with a discussion of how Symanzik's effective description extends to the SF (Lüscher, Sint, Sommer and Weisz, 1996). As one expects, some modifications w.r.t. to the infinite volume analysis of Section 2.2 are in order due to the presence of the boundary. Symanzik's effective theory will then allow us to identify the sources of O(a) effects in the SF. More precisely, as we shall see, discretization effects come from two sources: firstly from O(a) counterterms localized in the interior of the space-time volume, and secondly from counterterms localized at the boundary. In particular, the O(a) counterterms localized in the bulk of the space-time are the same as the ones

identified in infinite volume, or equivalently, in a finite volume without boundary. It is thus natural to ask whether for these contributions the argument of automatic $O(a)$-improvement of massless Wilson fermions in finite volume also applies in the SF (cf. Section 2.2.4). As we shall see, unfortunately, this is not the case since the SF boundary conditions for the quark fields explicitly break this argument. As a result, all bulk $O(a)$ counterterms need to be taken into account in order to eliminate the corresponding effects in the standard SF regularization.

3.3.1   Symanzik's effective theory and the SF

Before presenting the details of Symanzik's effective description for the SF, we need to introduce the class of lattice observables we want to consider. Symanzik's effective theory will then allow us to describe the approach to the continuum limit of the properly renormalized quantities, and discuss their improvement.

In the following, we restrict our attention to correlation functions of products of local composite fields $\phi(x)$, and Fourier components of the boundary quark fields $\zeta(\mathbf{y}), \ldots \overline{\zeta}'(\mathbf{z})$. The fields $\phi(x)$ are assumed to be multiplicatively renormalizable, and inserted at non-zero physical distances from each other, and from the boundaries. The latter condition guarantees that contact terms between the fields $\phi(x)$, and the Fourier components of the boundary fields are avoided. The renormalization and improvement of this class of observables is then relatively simple since the bulk and boundary operators can be discussed separately.

In particular, we note that the insertion of the operator $\phi(x)$ in the interior of the volume requires the same renormalization as in on-shell correlation functions in infinite volume. Instead, the product of any finite number of Fourier components of the boundary fields $\zeta(\mathbf{y}), \ldots \overline{\zeta}'(\mathbf{z})$, is made finite by simply multiplying each boundary field with the corresponding renormalization factor Z_ζ (cf. Section 3.1.4). As already noticed, this is a non-trivial result, since one might expect short distance singularities to appear when considering products of more Fourier components. These singularities, however, are already taken care of at the level of the SF, and are thus cancelled by the renormalization of the boundary fields (Lüscher, Sint, Sommer and Weisz, 1996).

Given these observations, it is clear now how to proceed for the improvement of this class of observables. Similar conclusions as for their renormalization can in fact be drawn. Specifically, the improvement of the fields $\phi(x)$ is the same as in infinite volume, and hence does not need to be rediscussed (cf. Section 2.2.1). Correlation functions of the boundary quark fields, instead, are automatically improved once the SF is improved (Lüscher, Sint, Sommer and Weisz, 1996). In this respect, given the discussion on the renormalization of the SF (cf. Section 3.1.3), we expect that further terms need to be included in the corresponding Symanzik effective action in order to account for boundary effects. The general higher-order contribution to the Symanzik effective action of the SF, is then given by (Lüscher, Sint, Sommer and Weisz, 1996),

$$S_k = \int \mathrm{d}^4 x \, \mathcal{L}_k(x) + \int \mathrm{d}^3 \mathbf{x} \left\{ \mathcal{B}_k(x)|_{x_0=0} + \mathcal{B}'_k(x)|_{x_0=T} \right\}, \tag{3.36}$$

where the bulk Lagrangian $\mathcal{L}_k(x)$ is defined in (2.37), while the boundary operators $\mathcal{B}_k(x)$ and $\mathcal{B}'_k(x)$ are given by linear combinations of local composite fields of dimension $3 + k$.[9] Note that the basis fields in $\mathcal{B}_k(x)$ and $\mathcal{B}'_k(x)$ need to respect all internal symmetries of the lattice theory and the discrete space-time rotations and reflections. In particular, $\mathcal{B}_k(x)$ and $\mathcal{B}'_k(x)$ are related by time reflection, so that only one of them really needs to be discussed. In addition, as in the infinite volume case, the field equations of motion can be used to reduce the number of operators in the bulk Lagrangian $\mathcal{L}_k(x)$, and in the boundary terms $\mathcal{B}_k(x)$ and $\mathcal{B}'_k(x)$.

3.3.2 O(a) improved action

Starting from the general expression for the Symanzik effective action, one can now construct an improved lattice action for the SF with Wilson-fermions. In the following we present the main results of this construction, although leaving out most of the technical details. For the latter, we refer the reader to the discussion in (Lüscher, Sint,

---

[9]Technically the boundary operators are first defined in the bulk infinitesimally close to the boundaries, and then a proper limit has to be taken where the coefficients of the basis operators in $\mathcal{B}_k(x)$ and $\mathcal{B}'_k(x)$ are scaled in a precise way (Lüscher, Sint, Sommer and Weisz, 1996). For us, however, these details are unimportant, and we can consider the formal expression for the effective action given above. In fact, we are only interested in the form of the boundary terms, and this is determined only by symmetry considerations.

Sommer and Weisz, 1996). This said, considering only the leading $O(a)$ corrections, the improved lattice action for the SF with Wilson-fermions can be written as,

$$S_I = S + \delta S_v + \delta S_{G,b} + \delta S_{F,b}. \tag{3.37}$$

Here, $S = S_G + S_F$, is the unimproved lattice action given by the sum of the pure gauge action (3.22), and the quark action (3.28). The $O(a)$ volume counterterm, δS_v, related to $\mathcal{L}_1$, is then analogously defined as in the infinite volume case, i.e. (cf. (2.43)),

$$\delta S_v = a^5 \sum_{\mathbf{x} \in \Gamma} \sum_{x_0 = a}^{T-a} c_{\mathrm{sw}}(g_0) \, \overline{\psi}(x) \tfrac{i}{4} \sigma_{\mu\nu} \widehat{F}_{\mu\nu}(x) \psi(x). \tag{3.38}$$

The additional ingredients in (3.37) are the $O(a)$ boundary counterterms, which divide into a purely gluonic term, $\delta S_{G,b}$, and a fermionic term, $\delta S_{F,b}$. Considering first the gluonic contribution, we note that in the pure gauge theory any gauge invariant local composite operator has mass dimension greater or equal to 4. The only fields that can contribute to $\mathcal{B}_1$ and $\mathcal{B}_1'$ are then given by,

$$\mathrm{tr}\left\{F_{0k}F_{0k}\right\} \quad \text{and} \quad \mathrm{tr}\left\{F_{kl}F_{kl}\right\}. \tag{3.39}$$

In particular, for the corresponding lattice counterterms we can choose operators that are already present in the gauge action (3.22). In this case, these counterterms read,

$$\begin{aligned}
\delta S_{G,b} = {} & \frac{1}{2g_0^2}(c_s(g_0) - 1) \sum_{\mathbf{x} \in \Gamma} \sum_{x_0 = 0, T} \sum_{k,l=0}^{3} \mathrm{tr}\{1 - P_{kl}(x)\} \\
& + \frac{1}{g_0^2}(c_t(g_0) - 1) \sum_{\mathbf{x} \in \Gamma} \sum_{x_0 = 0, T-a} \sum_{k=0}^{3} \mathrm{tr}\{1 - P_{0k}(x)\},
\end{aligned} \tag{3.40}$$

where we introduced the corresponding improvement coefficients $c_s(g_0)$ and $c_t(g_0)$. Making this choice, the insertion of the gluonic counterterm $\delta S_{G,b}$ simply modifies the weight function $\omega(P)$ in the action. Specifically, $\omega(P)$ can be redefined as (cf. (3.22)),

$$\omega(P) = \begin{cases} \tfrac{1}{2}c_s(g_0) & \text{for spatial plaquettes at } x_0 = 0, \text{ and } T, \\ c_t(g_0) & \text{for time-like plaquettes } P \text{ attached to the boundaries,} \\ 1 & \text{otherwise.} \end{cases} \tag{3.41}$$

For completeness, we mention that the improvement coefficients $c_s(g_0)$ and $c_t(g_0)$ are only known in perturbation theory. Their tree-level values can be easily obtained by

expanding the gauge action (3.22) in a, and requiring the leading $O(a)$ effects to vanish. The values one obtains are $c_s(0) = c_t(0) = 1$. For the specific discretization of the SF we are considering, the value of $c_t(g_0)$ is in fact known at 2-loops order in perturbation theory (Bode, Weisz and Wolff, 1999; Bode, Weisz and Wolff, 2000). The value of $c_s(g_0)$, instead, is not known beyond tree-level. However, if one considers spatially constant boundary fields C_k and C'_k, $c_s(g_0)$ does not contribute to the action.

Having specified the gluonic $O(a)$ boundary counterterm $\delta S_{G,b}$, we now comment on the fermionic contribution $\delta S_{F,b}$. In this case, the presence of the quark fields allows to construct many more terms of mass dimension 4 with the right symmetry properties. A detailed analysis is then necessary in order to understand how to eventually reduce this basis of fields, and how to properly include them in the lattice action. In order to keep our presentation short, here we simply report the result of this study and refer the reader to (Lüscher, Sint, Sommer and Weisz, 1996) for the details. In particular, restricting ourselves to the case of massless quarks and vanishing boundary values ρ_+, $\bar{\rho}_-$, ρ'_-, and $\bar{\rho}'_+$, there is only a single term that needs to be added to the action. This is given by,

$$\delta S_{F,b} = (\tilde{c}_t(g_0) - 1) \sum_{\mathbf{x} \in \Gamma} \sum_{x_0 = a, T-a} \overline{\psi}(x)\psi(x), \tag{3.42}$$

where $\tilde{c}_t(g_0)$ is the corresponding improvement coefficient. In fact, note that the proper counterterm would also contribute in changing the weight of the time-like hopping term at the boundary from 1 to $\tilde{c}_t(g_0)$ (Lüscher, Sint, Sommer and Weisz, 1996). This contribution, however, does not appear in the action if the boundary values are set to zero (cf. (3.28)). On the other hand, it contributes when considering correlation functions of the boundary quark fields (3.19). Indeed, when we take derivatives of the lattice action with respect to the boundary source fields, this term is inserted in the correlation functions. As a result, the prescription (3.35) that defines the boundary quark fields in correlation functions has to be replaced by,

$$\zeta(\mathbf{x}) = \tilde{c}_t(g_0) U_0(0, \mathbf{x}) P_- \psi(a, \mathbf{x}) , \qquad \zeta'(\mathbf{x}) = \tilde{c}_t(g_0) U_0(T - a, \mathbf{x})^\dagger P_+ \psi(T - a, \mathbf{x}),$$

$$\overline{\zeta}(\mathbf{x}) = \tilde{c}_t(g_0) \overline{\psi}(a, \mathbf{x}) P_+ U_0(0, \mathbf{x})^\dagger, \qquad \overline{\zeta}'(\mathbf{x}) = \tilde{c}_t(g_0) \overline{\psi}(T - a, \mathbf{x}) P_- U_0(T - a, \mathbf{x}).$$

$$\tag{3.43}$$

For the lattice regularization we are considering, the value of $\tilde{c}_t$ is only known at 1-loop order in perturbation theory (Lüscher and Weisz, 1996; Sint and Weisz, 1998).

To conclude, for later convenience we write down the O(a) improved SF quark action for vanishing boundary values. This can be written as,

$$(S_I)_F = a^4 \sum_{\mathbf{x} \in \Gamma} \sum_{x_0=a}^{T-a} \overline{\psi}(x) D \psi(x), \tag{3.44}$$

where we introduced the improved Dirac operator,

$$D = D_{\mathrm{w}} + \delta D_{\mathrm{v}} + \delta D_{\mathrm{b}} + m_0. \tag{3.45}$$

This is defined in terms of the unimproved Dirac operator D_{w} (cf. (2.3)), and the O(a) counterterms δD_{v} and δD_{b}, which are given by,

$$\delta D_{\mathrm{v}} \psi(x) = a \, c_{\mathrm{sw}}(g_0) \sum_{\mu,\nu=0}^{3} \tfrac{i}{4} \sigma_{\mu\nu} \widehat{F}_{\mu\nu}(x) \psi(x), \tag{3.46}$$

$$\delta D_{\mathrm{b}} \psi(x) = a \, (\tilde{c}_t(g_0) - 1) \{ \delta_{x_0,a} + \delta_{x_0,T-a} \} \psi(x). \tag{3.47}$$

From the discussion of this subsection, it is clear that independently from the specific lattice regularization considered, the SF unavoidably introduces additional O(a) effects due to the boundary. The O(a) boundary counterterms here presented, indeed, do not break any internal symmetry of the continuum SF. They are thus expected to be present in any discretization of the SF.

3.3.3 Automatic O(a)-improvement and the SF

Given the results of the previous subsections, it comes natural to ask at this point whether the argument of automatic O(a)-improvement of massless Wilson-fermions in finite volume also applies to the bulk O(a) counterterms in the SF. As we shall see, this unfortunately is not the case (Frezzotti and Rossi, 2005; Sint, 2006; Sint, 2011), and all bulk O(a) counterterms are necessary to cancel the corresponding lattice artifacts in the standard SF regularization.

In order to show this, we start considering a generic multiplicatively renormalized lattice field $\mathcal{O}$ in a finite volume with SF boundary conditions. In particular, the field $\mathcal{O}$ may contain operators $\phi(x)$ inserted in the bulk of the lattice volume, as well as

operators made out of boundary quark fields $\zeta(\mathbf{y}), \ldots \overline{\zeta}'(\mathbf{z})$. The Symanzik effective description for the corresponding expectation value is then given by (cf. (2.40)),

$$\langle \mathcal{O} \rangle_{c\,(P_+)} = \langle \mathcal{O}_0 \rangle_{c\,(P_+)}^{\text{cont}} - a \langle S_1 \mathcal{O}_0 \rangle_{c\,(P_+)}^{\text{cont}} + a \langle \delta \mathcal{O}_0 \rangle_{c\,(P_+)}^{\text{cont}} + \mathrm{O}(a^2), \qquad (3.48)$$

where $\mathcal{O}_0$ is the continuum (renormalized) field corresponding to the renormalized lattice operator $\mathcal{O}$, while $\delta \mathcal{O}_0$ is a shorthand notation for the associated $\mathrm{O}(a)$ operator counterterm. The latter, we recall, only contains counterterms associated to the bulk operators $\phi(x)$. The $\mathrm{O}(a)$ counterterm to the action, S_1, instead, includes both bulk and boundary terms (cf. (3.37)). The expectation values in (3.48) are then taken w.r.t. the continuum SF action for massless quarks, which is given by (cf. (3.4) and (3.11)),

$$S_0 = -\frac{1}{2g^2} \int_0^T \mathrm{d}x_0 \int_0^L \mathrm{d}^3\mathbf{x} \, \mathrm{tr}\{F_{\mu\nu}(x) F_{\mu\nu}(x)\} + \int_0^T \mathrm{d}x_0 \int_0^L \mathrm{d}^3\mathbf{x} \, \overline{\psi}(x) \slashed{D} \psi(x). \quad (3.49)$$

Note that in (3.48) we emphasized with a subscript (P_+) that SF boundary conditions are imposed on the fields.[10] In particular, we remind that these expectation values are evaluated for vanishing boundary values (cf. (3.18)). The boundary conditions for the quark fields thus explicitly read,

$$\begin{aligned} P_+ \psi(x)|_{x_0=0} = 0, &\qquad P_- \psi(x)|_{x_0=T} = 0, \\ \overline{\psi}(x) P_-|_{x_0=0} = 0, &\qquad \overline{\psi}(x) P_+|_{x_0=T} = 0. \end{aligned} \qquad (3.50)$$

Given these definitions, we recall that the argument of automatic $\mathrm{O}(a)$-improvement presented in Section 2.2.4 relied on the following observation. If we considered the γ_5-transformation,

$$\psi \to \gamma_5 \psi, \qquad \overline{\psi} \to -\overline{\psi} \, \gamma_5, \qquad (3.51)$$

as a change of variables in the functional integral, both the action S_0 and the functional integral measure were invariant. This allowed us to catalog the expectation values of the observables as even or odd under the above transformation, and thus proceed with the proof. In the case of the SF, the action S_0 is still invariant under the transformation (3.51) (cf. (3.49)). On the other hand, in this case the transformation also affects the

---

[10]For notational convenience we indicate only the boundary conditions for the quark fields at $x_0 = 0$. The boundary conditions for the gauge field can be ignored in the present discussion.

boundary conditions (3.50). In particular, it is easy to see that the transformed fields satisfy the SF boundary conditions with the complementary projectors, e.g., at $x_0 = 0$,

$$P_+ \psi(x)|_{x_0=0} = 0, \qquad \overset{\gamma_5}{\longrightarrow} \qquad P_- \psi(x)|_{x_0=0} = 0,$$
$$\overline{\psi}(x) P_-|_{x_0=0} = 0, \qquad \qquad \overline{\psi}(x) P_+|_{x_0=0} = 0, \qquad (3.52)$$

and consequently,

$$\langle \mathcal{O}_0 \rangle_{c(P_+)}^{\text{cont}} \qquad \overset{\gamma_5}{\longrightarrow} \qquad \langle \mathcal{O}_0 \rangle_{c(P_-)}^{\text{cont}}. \qquad (3.53)$$

Thus, the transformed correlation functions can not be proportional to the original ones, and the proof of automatic $O(a)$-improvement can not go through. This may be taken as a property of the fermion measure that is not invariant under the γ_5-transformation (3.51), since the function space integrated over in the path-integral is not the same before and after the change of variables. However, we prefer to say that chiral symmetry is explicitly broken by the SF boundary conditions.[11] The γ_5-transformation (3.51) is then not a symmetry of the continuum massless SF, and the argument as it stands does not hold.

3.4   The chirally rotated Schrödinger functional

In the previous subsection we understood that in the standard lattice regularization of the SF with Wilson-fermions, the property of automatic bulk $O(a)$-improvement in the chiral limit is spoiled by the boundary conditions for the quark fields. The question then arises naturally whether it is possible to recover this nice feature by changing the boundary conditions for the fields. Essentially, one would need to find alternative SF boundary conditions and field transformations such that the latter are symmetries of the massless continuum theory, while the modified (homogeneous) boundary conditions are left invariant.[12] As we now present, at least in principle, there are several possibilities to achieve this.

---

[11] This can be properly seen by studying the WIs of the theory (Lüscher, 2006; Sint, 2011).

[12] In the following we refer in general to SF boundary conditions as Dirichlet boundary conditions in the time direction, supplemented with periodic boundary conditions in the spatial directions. The boundary conditions (3.50) are then referred to as the standard SF boundary conditions.

If one insists in keeping the γ_5-transformation (3.51) as a symmetry transformation, one could consider the boundary conditions specified by (Frezzotti and Rossi, 2005),[13]

$$P_\pm = \frac{1}{2}(1 \pm \gamma_0) \quad \longrightarrow \quad \Pi_\pm = \frac{1}{2}(1 \pm \gamma_5\tau^3). \tag{3.54}$$

Alternatively, one could choose a different symmetry transformation, as for example the γ_5-transformation (3.51) augmented by a flavour permutation (Sint, 2006), i.e.,

$$\psi \to \tau^1\gamma_5\psi, \qquad \overline{\psi} \to -\overline{\psi}\gamma_5\tau^1, \tag{3.55}$$

where τ^1 is a Pauli matrix. This flavour permutation does not affect the bulk action, and $O(a)$ improvement for $\gamma_5\tau^1$-even observables in the bulk can be shown as in Section 2.2.4. Boundary conditions invariant under this transformation can then be easily obtained by adding a flavour structure to the original projectors (Sint, 2011) e.g.,

$$P_\pm = \frac{1}{2}(1 \pm \gamma_0) \quad \longrightarrow \quad \tilde{P}_\pm = \frac{1}{2}(1 \pm \gamma_0\tau^3). \tag{3.56}$$

It is indeed easy to show that: $[\gamma_5\tau^1, \tilde{P}_\pm] = 0$.

Another possibility is again to consider the $\gamma_5\tau^1$-transformation above, but with the boundary projectors (Sint, 2006; Sint, 2011),

$$\tilde{Q}_\pm = \frac{1}{2}(1 \pm i\gamma_0\gamma_5\tau^3) \quad \Rightarrow \quad [\gamma_5\tau^1, \tilde{Q}_\pm] = 0. \tag{3.57}$$

In conclusion, it is relatively simple to come up with a set of boundary conditions and symmetry transformations that meet the basic requirements. Certainly, what is nontrivial is to show that the theory obtained is a sensible alternative to the standard SF. First of all, by modifying the boundary conditions arbitrarily and independently from the bulk action, it is not even clear a priori if the theory defined is sensible at all. The proposal made in (3.54), for example, suffers from several inconsistencies already at the classical level (Gonzalez-Lopez, 2011). Secondly, besides basic requirements such as a well-defined classical continuum theory, and the renormalizability of the quantum

---

[13]Note that the most generic boundary conditions for the quark fields are given by $\mathcal{B}\psi(x) = 0$, where $\mathcal{B}$ is a linear operator of non-maximal rank (Lüscher, 2006). We can then discuss different choices of boundary conditions in terms of different projector structures.

theory, one would like to maintain some of the characteristic features of the standard SF boundary conditions. These include in particular the absence of zero modes in the massless Dirac operator, that allows numerical simulations at zero quark-masses. Yet another difficultly is given by the actual implementation of the boundary conditions on the lattice. As we briefly commented, on the lattice one does not really impose the boundary conditions on the fields. These instead are encoded in the structure of the lattice action close to the boundaries. Thus, depending on the given boundary conditions, it might be relatively difficult to determine the proper structure.

In this respect, in (Sint, 2006; Sint, 2011) the author has shown that the boundary conditions specified by the projectors (3.57) provide a natural solution to all these problems. In fact, in the case of Wilson-fermions these boundary conditions simply lead to an alternative lattice regularization of the SF with the standard boundary conditions (3.50). We thus start in the next subsection motivating this result. The rest of the chapter is then dedicated to a detailed discussion of the resulting lattice theory. For the presentation we follow closely the original references (Sint, 2006; Sint, 2011). We then recommend (Sint, 2007a) for an introduction.

3.4.1 A chiral rotation to the Schrödinger functional

In order to understand the nature of the projectors (3.57), let us consider the formal massless continuum theory. As we now show, the projectors $\tilde{Q}_\pm$ naturally appear by applying a chiral rotation to the standard SF. More precisely, let ψ' and $\overline{\psi}'$ to be quark doublets satisfying the homogeneous SF boundary conditions (3.50). Performing then a non-singlet chiral field rotation,

$$\psi' = R(\alpha)\psi, \qquad \overline{\psi}' = \overline{\psi}R(\alpha), \qquad R(\alpha) = e^{i\alpha\gamma_5\frac{\tau^3}{2}}, \qquad (3.58)$$

the rotated fields satisfy the chirally rotated boundary conditions,

$$P_+(\alpha)\psi(x)|_{x_0=0} = 0, \qquad\qquad P_-(\alpha)\psi(x)|_{x_0=T} = 0,$$
$$\overline{\psi}(x)\gamma_0 P_-(\alpha)|_{x_0=0} = 0, \qquad\qquad \overline{\psi}(x)\gamma_0 P_+(\alpha)|_{x_0=T} = 0, \qquad (3.59)$$

where the projectors $P_\pm(\alpha)$ are defined as,

$$P_\pm(\alpha) = \frac{1}{2}\left[1 \pm \gamma_0 e^{i\alpha\gamma_5\tau^3}\right]. \qquad (3.60)$$

In particular, for $\alpha = \pi/2$, one finds,

$$P_\pm(\pi/2) = \frac{1}{2}(1 \pm i\gamma_0\gamma_5\tau^3) = \tilde{Q}_\pm, \tag{3.61}$$

and the boundary conditions (3.59) take the form,

$$
\begin{aligned}
\tilde{Q}_+\psi(x)|_{x_0=0} &= 0, & \tilde{Q}_-\psi(x)|_{x_0=T} &= 0, \\
\overline{\psi}(x)\tilde{Q}_+|_{x_0=0} &= 0, & \overline{\psi}(x)\tilde{Q}_-|_{x_0=T} &= 0.
\end{aligned}
\tag{3.62}
$$

As anticipated, the boundary conditions with the projectors $\tilde{Q}_\pm$ naturally appear when chirally rotating quark fields satisfying the standard SF boundary conditions. In the following we will thus refer to the formulation of the SF so obtained as the chirally rotated Schrödinger functional (χSF). In this respect, note that the non-singlet chiral rotation (3.58) is a non-anomalous symmetry transformation of the continuum massless QCD action. Considering this transformation as a change of variables in the functional integral, we then expect to obtain simple relations between correlation functions with standard and chirally rotated SF boundary conditions.

Specifically, performing such a change of variables for the case of interest $\alpha = \pi/2$, we derive the generic identities,

$$\langle \mathcal{O}[\psi, \overline{\psi}] \rangle_{(P_\pm)} = \langle \mathcal{O}[R(\pi/2)\psi, \overline{\psi}R(\pi/2)] \rangle_{(\tilde{Q}_\pm)}, \tag{3.63}$$

where the integration variables are assumed to be ψ and $\overline{\psi}$ on both sides. In particular, note that the operator $\mathcal{O}$ can contain in principle boundary quark fields $\zeta(\mathbf{y}), \ldots \overline{\zeta}'(\mathbf{z})$. These are naturally included in the mapping by identifying them with the non-Dirichlet components near the time boundaries, i.e. (cf. (3.20)),

$$
\begin{aligned}
\zeta(\mathbf{x}) &= \tilde{Q}_-\psi(0_+, \mathbf{x}), & \zeta'(\mathbf{x}) &= \tilde{Q}_+\psi(T_-, \mathbf{x}), \\
\overline{\zeta}(\mathbf{x}) &= \overline{\psi}(0_+, \mathbf{x})\tilde{Q}_-, & \overline{\zeta}'(\mathbf{x}) &= \overline{\psi}(T_-, \mathbf{x})\tilde{Q}_+.
\end{aligned}
\tag{3.64}
$$

In summary, we have seen that the continuum SF with chirally rotated boundary conditions merely corresponds to a "rewriting" of the original SF. Indeed, the two formulations are related by a non-anomalous field redefinition. On the other hand, the relation becomes non-trivial once we consider the lattice regularization of these formulations in terms of Wilson-fermions. In this case, the bulk action is not invariant

under the chiral rotation (3.58), and the two set-ups define different regularizations of the standard SF.[14] In particular, the relations (3.63) will not be exact at finite lattice spacing. Similarly to the chiral WIs, however (cf. Section 2.1.3), these relations are expected to hold up to discretization effects among properly renormalized lattice correlation functions. To conclude, the problem that is left to solve is to determine a lattice discretization of the SF with Wilson-fermions, such that the chirally rotated boundary conditions (3.62) are correctly implemented. Differently from the standard discretization of the SF, this formulation is then expected to benefit from the property of automatic bulk $O(a)$-improvement in the chiral limit.

3.4.2 χSF boundary conditions on the lattice

Defining a lattice field theory which reproduces the correct boundary conditions in the continuum limit is not automatic. As remarked several times by now, on the lattice one cannot really impose the boundary conditions directly on the fields. Rather, these are encoded in the specification of the dynamical field variables, and in the details of the lattice action close to the boundaries (Lüscher, 2006). Hence, one is in the situation where the boundary conditions in the continuum theory arise "dynamically" from the details of the lattice theory, once the continuum limit is taken. In particular, different lattice theories with different actions can give the same boundary conditions for the fields in the continuum limit.

Given these observations, the way one can proceed in the definition of the target lattice theory is the following (Lüscher, 2006). First one needs to define a lattice theory where the correct boundary conditions are obtained in the classical continuum limit i.e. in the free case. Secondly, the renormalization of the theory has to be studied. In particular, given the symmetries of the lattice regularization, one has to determine all possible boundary counterterms that can appear. Finally, given the list of these counterterms, one can conclude if the desired boundary conditions are obtained automatically in the continuum limit, or if the fine tuning of some counterterm is needed.

---

[14]The chirally rotated SF presents some interesting applications also in the case of chirally preserving bulk discretizations. In fact, it allows for a simple definition of the SF for overlap (or domain-wall) fermions (Sint, 2007b). For different approaches see (Taniguchi, 2005; Lüscher, 2006; Takeda, 2009a).

In the case of the χSF, the correct (homogeneous) boundary conditions for the free theory can be obtained through an orbifold construction (Sint, 2006; Sint, 2011).[15] This construction, however, is rather technical, and will not be discussed here. We thus refer the reader to the references for the details. For brevity of exposition, here we simply introduce the lattice discretization of the χSF resulting from this investigation. In particular, note that in (Sint, 2011) three different discretizations of the χSF have been proposed. In the following we present the one we believe is the most convenient for numerical applications. Given the lattice regularization, in the next subsection we will then study the renormalization and $\mathrm{O}(a)$ improvement of the χSF.

This said, the lattice regularization of the chirally rotated SF of QCD with Wilson-fermions is defined by,[16]

$$\mathcal{Z}[C';C] = \int \mathcal{D}[U]\mathcal{D}[\psi]\mathcal{D}[\overline{\psi}]e^{-S}, \tag{3.65}$$

where the integration is over all quark and anti-quark fields $\psi(x)$ and $\overline{\psi}(x)$ at Euclidean times $0 \le x_0 \le T$. The integral over the gauge fields is defined as usual (cf. (3.24)). Similarly, the gauge part S_{G} of the action $S = S_{\mathrm{G}} + S_{\mathrm{F}}$ has been already introduced in (3.22), while the fermionic part S_{F} is now given by,

$$S_{\mathrm{F}} = a^4 \sum_{\mathbf{x}\in\Gamma} \sum_{x_0=0}^{T} \overline{\psi}(x)\big(\mathcal{D}_W + m_0\big)\psi(x), \tag{3.66}$$

where we define the χSF Dirac operator $\mathcal{D}_W$ as,

$$\mathcal{D}_W\psi(x) = \begin{cases} -U_0(x)P_-\psi(x+a\hat{0}) + (K + i\gamma_5\tau^3 P_-)\psi(x) & \text{if } x_0 = 0, \\ D_{\mathrm{w}}\psi(x) & \text{if } 0 < x_0 < T, \\ (K + i\gamma_5\tau^3 P_+)\psi(x) - U_0(x-a\hat{0})^\dagger P_+\psi(x-a\hat{0}) & \text{if } x_0 = T. \end{cases} \tag{3.67}$$

In the above expression, D_{w} indicates as usual the (infinite-volume) Dirac operator (2.3), while K is the corresponding restriction to a time-slice, more precisely,

$$K = 1 + \frac{a}{2}\sum_{k=1}^{3}\big\{\gamma_k\big(\nabla_k + \nabla_k^*\big) - a\nabla_k^*\nabla_k\big\}. \tag{3.68}$$

---

[15]For an earlier application of these techniques to lattice field theory see (Taniguchi, 2005).

[16]Note that we only consider the case of vanishing boundary values. In the expression for the lattice path-integral we then suppress the dependence on the boundary source fields.

It is worth comparing at this point the action (3.66), with the corresponding result for the standard SF regularization (3.30). As one might have expected, the difference between the two definitions only relies in the structure of the Dirac operator close to the boundaries at $x_0 = 0, T$. In addition, for the specific discretization of the χSF we are considering, the dynamical field variables in (3.65) are different w.r.t. the standard SF case (3.27), since they also include the fields at the boundaries.

To conclude, we want to note that the χSF Dirac operator (3.67) satisfies the γ_5-hermiticity property of the standard Wilson operator, $(\gamma_5 D_{\mathrm{w}})^\dagger = \gamma_5 D_{\mathrm{w}}$, up to a flavour exchange, i.e.,

$$(\gamma_5 \tau^1 \mathcal{D}_W)^\dagger = \gamma_5 \tau^1 \mathcal{D}_W. \tag{3.69}$$

This property is enough to ensure that the χSF Dirac operator has a real determinant. As we will discuss in the next chapter, this is a fundamental requirement for the numerical simulation of the theory. Moreover, a well-defined eigenvalue problem is obtained for $(\gamma_5 \tau^1 \mathcal{D}_W)$. This allows to conclude that the lowest eigenvalue $\lambda_{\min}$ of the free χSF Dirac operator (3.67) is given by (Sint, 2011),

$$|\lambda_{\min}| = \frac{2}{a}\left| \sin\left(\frac{a\pi}{4T'}\right)\right| \overset{a\to 0}{\sim} \frac{\pi}{2T}, \qquad T' = T + a. \tag{3.70}$$

Fermionic zero-modes are thus excluded.[17]

3.4.3 Renormalization and O(a) improvement

In the previous subsection, we have introduced the lattice regularization of the χSF. For this construction, the correct chirally rotated boundary conditions are realized in the free theory, and the key features of the standard lattice formulation of the SF are maintained. In this concluding subsection, we thus want to study the renormalization of the theory in order to understand if the correct boundary conditions can be obtained also in the presence of the interactions. Once the proper boundary conditions are realized, automatic bulk O(a)-improvement is then expected to set in, in the chiral limit. As a result, the O(a) counterterms to the bulk action and operators will be irrelevant

---

[17]Similarly to the standard SF case, this statement can be extended to the continuum massless χSF Dirac operator defined for any smooth gauge potential (Sint, 2011).

for the improvement of $\gamma_5\tau^1$-even observables. Together with the renormalization of the boundary, we also want to understand if additional $O(a)$ boundary counterterms are present in the χSF w.r.t. the standard SF regularization. In this respect, we note that the discussion of the renormalization and $O(a)$ improvement of the χSF, is rather technical, and more involved than in the case of the standard SF regularization. In the following we thus simply summarize the main results and observations concerning this study, while leaving the details to the original reference (Sint, 2011). To conclude, it comes without saying that any bulk counterterm, as well as purely gluonic boundary counterterms, do not need be rediscussed since these are the same as for the standard SF case.

The boundary counterterms. In order to determine the allowed counterterms, we first need to identify the symmetries of the lattice theory as determined by the lattice action. In fact, it is easy to see that the symmetries of the lattice χSF are given by: charge conjugation, spatial lattice rotations, space and time reflections combined with a flavour exchange τ^1, and global U(1) vector like rotations with generator $\tau^3/2$. As in the standard regularization of the SF, indeed, the Wilson term breaks all axial symmetries. The additional structure of the χSF Dirac operator at the boundaries then explicitly breaks parity and time reflection (only recovered up to a flavour exchange), and two of the generators of the non-singlet vector rotations.[18]

Given the lattice symmetries, one can now list all fermionic operators of mass dimension 3 and 4. Their integrals over space taken at $x_0 = 0$ and $x_0 = T$, then define the possible counterterms to the lattice action that are needed to renormalize and $O(a)$ improve the boundary effects in the SF. In particular, note that we restrict ourselves to the case of vanishing quark-masses. Moreover, we discuss only the counterterms at $x_0 = 0$. The ones at $x_0 = T$, in fact, are related to the latter by time reflection combined with a flavour exchange.

---

[18]Note that we conventionally refer to vector and axial symmetries as defined in the standard SF base (cf. Section 2.1.1). In other words, vector transformations are defined as the ones that preserve the standard SF boundary conditions, while the remaining chiral-flavour transformations are identified with the axial transformations. These definitions are necessary once we consider the massless case (Sint, 2011).

Given these observations, after symmetrizing with respect to charge conjugation, we find the following 3 operators of mass dimension 3 (Sint, 2011),

$$\mathcal{O}_1 = \overline{\psi}\gamma_0\tilde{Q}_+\psi - \overline{\psi}\gamma_0\tilde{Q}_-\psi = \overline{\psi}i\gamma_5\tau^3\psi, \tag{3.71}$$

$$\mathcal{O}_2 = \overline{\psi}\tilde{Q}_+\psi, \tag{3.72}$$

$$\mathcal{O}_3 = \overline{\psi}\tilde{Q}_-\psi. \tag{3.73}$$

The operators of mass dimension 4 instead are 8 in total. Using partial integration and the field equations of motion, however, one can reduce their number to 3. These are conventionally taken to be (Sint, 2011),

$$\mathcal{O}_4 = \overline{\psi}\,\tilde{Q}_+\gamma_k D_k\psi - \overline{\psi}\overleftarrow{D}_k\gamma_k\tilde{Q}_+\psi, \tag{3.74}$$

$$\mathcal{O}_5 = \overline{\psi}\,\tilde{Q}_-\gamma_k D_k\psi - \overline{\psi}\overleftarrow{D}_k\gamma_k\tilde{Q}_-\psi, \tag{3.75}$$

$$\mathcal{O}_6 = \overline{\psi}\,\tilde{Q}_+\gamma_0\gamma_k D_k\psi + \overline{\psi}\overleftarrow{D}_k\gamma_k\gamma_0\tilde{Q}_+\psi. \tag{3.76}$$

As expected, due to the reduced symmetry of the χSF more counterterms are allowed than in the standard SF case. Specifically, one ends up with 3 $O(1)$ and 3 $O(a)$ fermionic boundary counterterms. Having these counterterms we can now proceed and discuss their inclusion in the lattice theory.

Lattice parametrization.   Starting from the boundary counterterms corresponding to $\mathcal{O}_3$ and $\mathcal{O}_5$, these can be directly included in the lattice action through a redefinition of the Dirac operator. More precisely, we can define an $O(a)$ improved χSF quark action it given by,

$$(S_I)_F = a^4 \sum_{\mathbf{x}\in\Gamma} \sum_{x_0=0}^{T} \overline{\psi}(x)\mathcal{D}\psi(x), \tag{3.77}$$

where we introduced the improved χSF Dirac operator,

$$\mathcal{D} = \mathcal{D}_W + \delta\mathcal{D}_{W,v} + \delta\mathcal{D}_{W,b} + m_0. \tag{3.78}$$

This is given in terms of the unimproved χSF Dirac operator $\mathcal{D}_W$ (cf. (3.67)), and the bulk and boundary counterterms, $\delta\mathcal{D}_{W,v}$, and $\delta\mathcal{D}_{W,b}$.

The bulk $O(a)$ counterterm $\delta \mathcal{D}_{W,v}$ is the same as in the standard SF regularization, and is given by (cf. (3.46)),

$$\delta \mathcal{D}_{W,v} \psi(x) = (1 - \delta_{x_0,0} - \delta_{x_0,T}) \, a \, c_{\mathrm{sw}}(g_0) \sum_{\mu,\nu=0}^{3} \tfrac{i}{4} \sigma_{\mu\nu} \widehat{F}_{\mu\nu}(x) \psi(x). \tag{3.79}$$

The boundary counterterm $\delta \mathcal{D}_{W,b}$, instead, contains the $O(1)$ and $O(a)$ counterterms corresponding to $\mathcal{O}_3$ and $\mathcal{O}_5$, and it is defined by (Sint, 2011),

$$\delta \mathcal{D}_{W,b} \psi(x) = (\delta_{x_0,0} + \delta_{x_0,T}) \Big[(z_f(g_0) - 1) + a \, (d_s(g_0) - 1) \mathbf{D}_s \Big] \psi(x). \tag{3.80}$$

In the above definition, $\mathbf{D}_s$ can be any lattice discretization of the spatial components of the continuum Dirac operator, $\gamma_k D_k$. In our setup, we consider,

$$\mathbf{D}_s = \frac{1}{2} \gamma_k (\nabla_k + \nabla_k^* - a \nabla_k^* \nabla_k), \tag{3.81}$$

which leads to a slightly simpler implementation in the simulation program. Note that the $O(a)$ counterterm proportional to $d_s(g_0)$ plays an analogous rôle to the $\tilde{c}_t(g_0)$ counterterm discussed in the standard SF regularization (cf. Section 3.3.2). The corresponding counterterms can be in fact related through the field equations of motion. The implementation adopted here, however, is more convenient in practice since it does not require any modification of the boundary quark fields (cf. (3.43)). For the specific χSF regularization we are considering, the value of $d_s(g_0)$ is then known to 1-loop order in perturbation theory (Vilaseca, 2013). The dimension 3 counterterm proportional to $z_f(g_0)$, instead, is a relevant operator and the corresponding coefficient $z_f(g_0)$ must be determined non-perturbatively. We will discuss this in more detail at the end of this section.

At this point, we are left with two $O(1)$ and two $O(a)$ boundary counterterms to be discussed. Considering first the terms corresponding to the operators $\mathcal{O}_2$ and $\mathcal{O}_4$, their contribution can be shown to manifests only in the two-point functions of the boundary fields $\zeta(\mathbf{x})$ and $\overline{\zeta}(\mathbf{y})$ at coinciding points $\mathbf{x} = \mathbf{y}$ (Sint, 2011). Similarly of course for $\zeta'(\mathbf{x})$ and $\overline{\zeta}'(\mathbf{y})$. As it will be discussed in detail in Chapter 5, however, these two-point functions can be generally avoided in practice and consequently the corresponding renormalization and improvement.

Finally, this leaves us with one O(1) and one O(a) boundary counterterms, which correspond to the operators $\mathcal{O}_1$ and $\mathcal{O}_6$, respectively. The presence of an additional O(1) boundary counterterm should not come as a surprise. Indeed, as already discussed in the case of the standard SF, one generally needs to renormalize the boundary values (cf. Section 3.1.4). In practice, the counterterm corresponding to $\mathcal{O}_1$ can thus be accounted for by the renormalization of the boundary quark fields that enter in correlation functions (cf. Section 3.3.1), i.e.,[19]

$$\zeta_R = Z_\zeta \zeta, \quad \bar\zeta_R = Z_\zeta \bar\zeta, \quad \zeta'_R = Z_\zeta \zeta, \quad \bar\zeta'_R = Z_\zeta \bar\zeta. \tag{3.82}$$

In this respect, we note that in the χSF the definition of the boundary quark fields (3.19) in correlation functions can be taken to be (cf. (3.35)),

$$\zeta(\mathbf{x}) = U_0(0,\mathbf{x})\tilde{Q}_-\psi(a,\mathbf{x}), \qquad \zeta'(\mathbf{x}) = U_0(T-a,\mathbf{x})^\dagger \tilde{Q}_+\psi(T-a,\mathbf{x}),$$
$$\bar\zeta(\mathbf{x}) = \overline\psi(a,\mathbf{x})\tilde{Q}_- U_0(0,\mathbf{x})^\dagger, \qquad \bar\zeta'(\mathbf{x}) = \overline\psi(T-a,\mathbf{x})\tilde{Q}_+ U_0(T-a,\mathbf{x}). \tag{3.83}$$

We stress, however, that this representation is correct as long as Wick contractions of boundary quark fields at the same boundary are avoided (Sint, 2011). Moreover, the effect of the remaining O(a) counterterm can be shown to lead to a redefinition of these boundary quark fields, which specifically reads (Sint, 2011),

$$\zeta(\mathbf{x}) \to [1 + \bar{d}_s(g_0)a\mathbf{D}_s]\zeta(\mathbf{x}),$$
$$\bar\zeta(\mathbf{x}) \to \bar\zeta(\mathbf{x})[1 - \bar{d}_s(g_0)a\mathbf{D}_s], \tag{3.84}$$

and similarly for $\zeta'(\mathbf{x})$ and $\bar\zeta'(\mathbf{x})$, where $\bar{d}_s(g_0)$ is the corresponding improvement coefficient. On the other hand, this O(a) counterterm can be neglected in most practical applications. Indeed, the counterterm $\mathcal{O}_6$ is $\gamma_5\tau^1$-odd, and thus contributes only at O(a^2) in $\gamma_5\tau^1$-even correlation functions (see below).

To conclude, the situation is not as bad as it might have seemed at first. In practice, the main new feature of the χSF formulation w.r.t. the standard SF regularization is given by the determination of the renormalization parameter $z_f(g_0)$. We thus conclude the section and chapter with a discussion about this important point.

---

[19]The role of $\mathcal{O}_1$ might become more clear if one chirally rotates this operator back to the standard SF base, i.e. $\overline\psi i\gamma_5\tau^3\psi \xrightarrow{R} \overline\psi'\psi'$. Considering then the boundary conditions for the fields, the operator obtained is the one responsible for the renormalization of the boundary values in the SF (cf. (3.16)).

Renormalization of z_f. In order to better understand the rôle of the counterterm proportional to z_f, it is useful to look at the corresponding operator $\mathcal{O}_3$ in the standard SF base. Applying a chiral rotation to $\mathcal{O}_3$ we obtain,

$$\overline{\psi}\tilde{Q}_-\psi \quad \xrightarrow{R} \quad \overline{\psi}'P_+i\gamma_5\tau^3\psi'. \tag{3.85}$$

This term explicitly breaks parity, and two of the generators of flavour symmetry. The lattice symmetries of the χSF are thus not enough to prevent the appearance of this counterterm that consequently needs to be fine tuned in order to recover the proper symmetries, or equivalently boundary conditions, in the continuum limit. In this respect, we note that in the standard SF base, the $\gamma_5\tau^1$-transformation (3.55) corresponds to the discrete SU(2) flavour transformation,

$$\psi' \to -\tau^2\psi' \qquad \overline{\psi}' \to -\overline{\psi}'\tau^2. \tag{3.86}$$

From this perspective, it is clear the rôle of z_f in the argument of automatic O(a)-improvement: it restores the relevant continuum symmetry needed to prove the result.

Given these observations we conclude that, since parity and flavour symmetry are good continuum symmetries of the SF, the renormalization parameter z_f has to be finite i.e. a scale-independent function of the bare coupling g_0 (Sint, 2011). The careful reader might have noticed that we already anticipated this result with our notation. In particular, the tree-level value of $z_f(g_0)$ is given by $z_f(0) = 1$ (Sint, 2011). This can be interpreted as the fact that the chirally rotated boundary conditions are correctly realized for the free theory. However, when the interactions are included, the boundary conditions are not protected by any lattice symmetry and this parameter needs to be renormalized. In particular, since the counterterm corresponding to z_f is a relevant operator at the boundaries, we expect that z_f needs to be determined non-perturbatively.

From the above discussion, it is also clear how the renormalization parameter $z_f(g_0)$ can be fixed. In practice, we can consider any lattice observable which is a pure source of parity and/or flavour symmetry breaking effects. The renormalization condition that defines $z_f(g_0)$ at a given g_0 is then simply obtained by requiring the given observable to vanish (Sint, 2011). In particular, we note that a class of these

observables is given by the $\gamma_5 \tau^1$-odd correlation functions. It is indeed clear that any non-trivial value for these quantities is a consequence of the aforementioned symmetry breaking by the regularization.

Once $z_f(g_0)$ has been tuned, and the quark-masses are set to zero, automatic bulk $O(a)$ improvement is expected to hold in the χSF. Specifically, this means that $\gamma_5 \tau^1$-even observables will be free of all $O(a)$ contributions corresponding to $\gamma_5 \tau^1$-odd counterterms (cf. Section 2.2.4). These include in particular the $O(a)$ contributions coming from the bulk action, the $O(a)$ counterterms associated to operator insertions in the volume of the lattice, and also the boundary counterterm proportional to $\bar{d}_s(g_0)$. On the other hand, some $O(a)$ effects will still be present due to a couple of $\gamma_5 \tau^1$-even boundary counterterms. As we have seen, these are given by the $O(a)$ counterterm proportional to $d_s(g_0)$, and if only spatially constant gauge fields are considered at the boundaries, the pure gauge counterterm proportional to $c_t(g_0)$ (cf. Section 3.3.2). Note that in the χSF the fermionic contribution to this improvement coefficient will be different w.r.t. the standard SF regularization. Its value has been in fact computed to 1-loop order in perturbation theory in (Vilaseca, 2013). Interestingly, the result obtained is much smaller than in the standard SF regularization. Together with the very small 1-loop coefficient of d_s (Vilaseca, 2013), this gives us confidence that a perturbative estimate of these coefficients might be good enough in practice. Finally, we recall that the complementary feature of automatic $O(a)$ improvement is that all $\gamma_5 \tau^1$-odd observables will be pure $O(a)$ lattice artifacts. In particular, they will contain all the effects corresponding to $\gamma_5 \tau^1$-odd counterterms (cf. Section 2.2.4).

To conclude, a crucial question one needs to address is whether the non-perturbative tuning of z_f is feasible in practice. As just mentioned, automatic $O(a)$ improvement is obtained by tuning simultaneously z_f, and the bare quark masses m_0 to their critical value m_{crit}. In principle, one could expect these conditions to be quite independent, at least close to the continuum limit. Any dependence of the critical mass m_{crit} on z_f, indeed, is a pure lattice artifact. In a non-perturbative determination, however, it is difficult to tell a priori which is the size of these discretization effects at the values of the lattice spacing covered by current simulations.

As a last remark, we note that in the unimproved theory the renormalization parameter z_f can be determined non-perturbatively only up to $O(a)$ ambiguities. This means that different renormalization conditions lead to determinations of z_f which differ by $O(a)$ effects. Similarly to the determination of the chiral point, one might thus wonder if this ambiguity in the tuning of z_f can spoil the argument of automatic $O(a)$ improvement (cf. Section 2.2.4). In fact, as for the case of the critical mass, the effect of an $O(a)$ ambiguity in z_f can be described by an insertion in the Symanzik effective action of the corresponding counterterm multiplied by an $O(a)$ coefficient. One then concludes that this counterterm is $\gamma_5 \tau^1$-odd, and thus it will only contribute to $O(a^2)$ in $\gamma_5 \tau^1$-even quantities.

4
Simulation algorithm

In this chapter, we present some details of the numerical implementation of the χSF in our simulation program. We will keep this technical discussion rather short. Essentially, we will focus on the main techniques that have been developed, and simply give an overview of how the χSF Dirac operator can be efficiently included in dynamical lattice QCD simulations. This will allow us in particular to discuss some of the tests that have been performed in order to check the reliably of the code.

Specifically, we start the chapter with a short review of the main algorithm on which modern simulations are based on, namely, the Hybrid Monte Carlo (Duane, Kennedy, Pendleton and Roweth, 1987). The presentation merely serves to introduce the notation, and some basic concepts needed in the following. For a more complete presentation we recommend the following set of lectures on which our short review is based (Kennedy, 2006; Lüscher, 2010a).

After this short introduction, we will discuss in some detail the main algorithmic tools that have been implemented for an efficient simulation program. In this respect, note that the code we developed is based on the openQCD[1] package of (Lüscher and Schaefer, 2013), which offers an advanced simulation program for Wilson-type fermions including the standard SF set-up presented in Section 3.2. Our simulation strategies then naturally derive from this work. The inclusion of the χSF Dirac operator in the package, however, is not entirely straightforward. Indeed, as we shall see, the peculiar matrix properties of the χSF Dirac operator w.r.t. to the standard SF one, forced us to redefine some of the methods implemented in the original code.

We conclude the chapter presenting some of the more stringent tests we have performed on our implementation.

[1] http://luscher.web.cern.ch/luscher/openQCD/

4.1 The Hybrid Monte Carlo

4.1.1 Statistical interpretation of the functional integral

The physical information of the lattice theory is contained in its correlation functions. As we have seen, these have the path-integral representation (cf. (2.26)),

$$\langle \mathcal{O} \rangle = \frac{1}{\mathcal{Z}} \int [\mathcal{D}U][\mathcal{D}\psi][\mathcal{D}\overline{\psi}] \, \mathcal{O}[U, \psi, \overline{\psi}] \, e^{-S[U,\psi,\overline{\psi}]}. \tag{4.1}$$

The basic goal of lattice QCD can be summarized in practical terms as the numerical evaluation of these path-integrals. In particular, due to the generally high number of integration variables in these integrals, exact integration methods are not applicable, and the evaluation has to proceed stochastically. Lattice QCD simulations are then based on Monte Carlo methods, and specifically on Markov chains and the concept of importance sampling.

The first complication that arises in the evaluation of the lattice path-integrals, is that the quark fields are represented in terms of Grassmann valued fields. At present, no practical method exists for a direct simulations of this type of fields.[2] The theory that has to be simulated is then the one obtained after the integration of the quark fields. In the case of two mass-degenerate Wilson-quarks, for example, the resulting partition function assumes the form,

$$\mathcal{Z} = \int \mathcal{D}[U] \{\det D(U)\}^2 e^{-S_{\mathrm{G}}(U)}, \qquad \mathcal{D}[U] = \prod_{x,\mu} \mathrm{d}U_\mu(x), \tag{4.2}$$

where $D(U)$ denotes the massive Dirac operator in the presence of the gauge field U. Assuming that the determinant, $\det D$, is real,

$$p(U) = \frac{1}{\mathcal{Z}} e^{-S(U)}, \qquad S(U) = S_{\mathrm{G}}(U) - \ln|\det D(U)|^2, \tag{4.3}$$

defines a normalized probability density on the space of gauge fields.

The generic lattice expectation value (4.1) can then be rewritten as,

$$\langle \mathcal{O} \rangle = \int \mathcal{D}[U] \, p(U) \mathcal{O}(U), \tag{4.4}$$

where the operator $\mathcal{O}(U)$ may contain terms resulting from the integration of the quark fields.

---

[2]Some attempts have been made for example in (Creutz, 1998).

Given this reinterpretation, lattice QCD resembles a classical statistical system where the states are given by gauge field configurations, and the expectation values of generic observables are defined by ensemble averages. This suggests the idea that these expectation values can be estimated stochastically by generating an ensemble of representative gauge field configurations $\{U_1, \ldots, U_N\}$, distributed according to the probability $\mathcal{D}[U]p(U)$. The given expectation value is then approximated by the average over the ensemble, i.e.,

$$\langle \mathcal{O} \rangle = \frac{1}{N} \sum_{i=1}^{N} \mathcal{O}(U_i) + \mathrm{O}(N^{-1/2}). \tag{4.5}$$

The central limit theorem assures that, asymptotically, the correct expectation values are obtained up to correction of $\mathrm{O}(N^{-1/2})$.

In practice, representative gauge field ensembles are constructed through Markov chains. The general procedure of evaluating integrals outlined above then goes under the name of importance sampling (see e.g. (Kennedy, 2006; Lüscher, 2010a)). The difficult task of lattice QCD is to find efficient algorithms that generate representative gauge field configurations with the desired probability distribution.

4.1.2 Towards the Hybrid Monte Carlo

Lattice QCD simulations are made difficult by the necessity of including the quark determinant in the probability distribution (4.3). Indeed, the determinant depends non-locally on the gauge field, and simple local algorithms as the ones commonly used for pure gauge theories are not practical.[3] One thus needs to find an alternative, more efficient way, to deal with this non-locality. Because of this reason, today lattice QCD simulations generally rely on some variant of the so-called Hybrid Monte Carlo (HMC) algorithm (Duane, Kennedy, Pendleton and Roweth, 1987).

The starting point of the HMC is the introduction in the theory of a $\mathfrak{su}(3)$-valued field,

$$\Pi_\mu(x) = \Pi_\mu^a(x)T^a, \qquad \Pi_\mu^a(x) \in \mathbb{R}. \tag{4.6}$$

---

[3]We refer to (Lüscher, 2010a) for a discussion of the algorithms for the pure gauge theory.

The rôle given to this field is that of canonical conjugate momentum of the gauge field U. In particular, the theory is now described by the Hamiltonian function,

$$H(\Pi, U) = \tfrac{1}{2}(\Pi, \Pi) + S(U), \qquad (\Pi, \Pi) = \sum_{x,\mu} \Pi_\mu^a(x)\Pi_\mu^a(x). \tag{4.7}$$

Note that, the introduction of this field and consequent interpretation, does not alter the physical content of the theory since,

$$\langle \mathcal{O} \rangle = \int \mathcal{D}[U]\mathcal{O}(U)e^{-S(U)} = \text{constant} \times \int \mathcal{D}[\Pi]\mathcal{D}[U]\mathcal{O}(U)e^{-H(\Pi,U)}. \tag{4.8}$$

This reinterpretation however suggests the following idea to generate an ensemble of gauge fields with the correct probability distribution.

One starts by considering the Hamiltonian equations of motion associated to the corresponding classical statistical system. In the context of lattice QCD, these are generally referred to as the molecular dynamics (MD) equations, and are defined by,

$$\partial_t \Pi_\mu(x,t) = -F_\mu(x,t), \qquad F_\mu^a(x,t) = \partial_{x,\mu}S(U(t)),$$
$$\partial_t U_\mu(x,t) = \Pi_\mu(x,t)U_\mu(x,t), \tag{4.9}$$

where the derivative over the gauge group $\partial_{x,\mu}$ is defined in Appendix A.3. The fields now depend on the additional time coordinate t. This fictitious time parameter simply parameterizes the evolution of the fields in field space. In particular, note that the MD equations are deterministic equations. The corresponding solutions $\Pi_\mu(x,t)$ and $U_\mu(x,t)$ at time t, are uniquely determined by the initial values of the fields at $t = 0$.

A sequence of properly distributed gauge fields U can now be obtained as follows. Given a field of initial momenta $\Pi_\mu(x,0) \equiv \Pi_\mu(x)$, and a starting gauge field $U_\mu(x,0) \equiv U_\mu(x)$, a new gauge field $U'_\mu(x)$ is obtained by integrating the MD equations up to a given time $t = \tau$, i.e., $U'_\mu(x) \equiv U_\mu(x,\tau)$. The corresponding momenta field $\Pi_\mu(x,\tau)$ is then discarded, and resampled according to the Gaussian probability density, $p(\Pi) \propto e^{-\frac{1}{2}(\Pi,\Pi)}$. The chain hence continues starting from the new momenta $\Pi'(x)$ so obtained, and the latest gauge configuration $U'_\mu(x)$. This ideal algorithm can be shown to be ergodic, and to lead to the desired probability distribution (see e.g. (Lüscher, 2010a)).

4.1.3 Numerical integration of the MD equations and accept-reject step

In practice, the MD equations (4.9) need to be integrated numerically. This means that the time interval $[0, \tau]$ is divided in N steps of size ϵ, and a given integration scheme is applied that gives the correct results for $\epsilon \to 0$. Here we do not want to enter into the details of any specific integration scheme, and we refer the reader to the extensive study in (Omelyan, Mryglod and Folk, 2003). We note however that, in general, so-called symplectic integrators are employed. These discrete integration schemes have the nice property that they preserve the time-reversibility of the solutions of the MD equations, and also the phase-space integration measure $\mathcal{D}[\Pi]\mathcal{D}[U]$. As we will comment shortly, these are two fundamental conditions for the correctness of the algorithm. We also mention that, in general, it is convenient from the numerical point of view to integrate different contributions to the MD forces with different resolutions ϵ, depending on their magnitude (Sexton and Weingarten, 1992). It is in fact intuitive that it is better to integrate more accurately the larger contributions to the forces, while using larger step-sizes for the smaller ones. This strategy is clearly more advantageous if the larger contributions to the forces are also the cheaper ones to evaluate numerically. In lattice QCD simulations, for example, this is generally the case since the contribution to the forces deriving from the gauge action is normally larger in magnitude and certainly cheaper to evaluate, than the fermionic contributions.

Given these observations, the main consequence of the numerical integration of the MD equations is that the Hamilton of the system is not preserved along the MD evolution. More precisely, for fixed step-size ϵ the difference,

$$\Delta H(\Pi, U) = \{H(\Pi(\tau), U(\tau)) - H(\Pi(0), U(0))\}_{\Pi(0)=\Pi, U(0)=U}, \qquad (4.10)$$

does not vanish in general. If not corrected, this can be shown to lead to an inexact algorithm. This means that the probability distribution of gauge fields that we obtain integrating the MD equations numerically at finite ϵ, does not correspond to the desired distribution we would obtain for $\epsilon = 0$. A possible solution to this problem is simply to repeat the evaluation of our observables by running the algorithm for different values of ϵ, and then extrapolate the results for $\epsilon \to 0$. Fortunately, this expensive procedure

can be avoided. In fact, the algorithm can be corrected simply by accepting the gauge field configuration obtained after the numerical integration of the MD equations with probability (Duane, Kennedy, Pendleton and Roweth, 1987),

$$P_{\text{acc}} = \min\{1, e^{-\Delta H(\Pi, U)}\}. \tag{4.11}$$

Provided that the numerical integrator is time reversible, and preserves the phase-space integration measure $\mathcal{D}[\Pi]\mathcal{D}[U]$, this leads to an exact algorithm.

To conclude, we want to note that even though the numerical integration of the MD equations does not conserve the Hamiltonian H, it is possible to show that a "shadow" Hamiltonian $\widetilde{H}$ is in fact conserved (Kennedy, Silva and Clark, 2013). Asymptotically, this coincides with the Hamiltonian H up to $O(\epsilon^n)$ corrections, i.e. $\widetilde{H} = H + O(\epsilon^n)$, where the value of n depends on the so-called *order* of the discrete integration scheme employed.[4] Even though only asymptotic, the analytic control provided by the shadow Hamiltonian on the form of the step-size errors, suggests interesting applications for the optimization of the MD integrators (Clark, Joo, Kennedy and Silva, 2011).

4.1.4 Pseudo-fermion action and final algorithm

The algorithm presented so far can in principle be applied to simulate the target distribution (4.3). A straightforward application of the algorithm, however, is not feasible in practice. A direct computation of the force deriving from the fermionic action indeed, requires the evaluation of the quark determinant. Given the high number of degrees of freedom of the problem this is clearly unfeasible.

This problem can be overcome by using a pseudo-fermion representation of the quark determinant, of the form,

$$|\det D(U)|^2 = \text{constant} \times \int \mathcal{D}[\phi] e^{-S_{\text{pf}}(U,\phi)},$$
$$S_{\text{pf}}(U, \phi) = (\phi, [D(U)^\dagger D(U)]^{-1}\phi), \qquad \mathcal{D}[\phi] = \prod_{x,A,\alpha} \mathrm{d}\phi_{A\alpha}(x)\mathrm{d}\phi_{A\alpha}(x)^*. \tag{4.12}$$

---

[4]This reminds of Symanzik's effective theory now extended to the 5d theory which includes the time coordinate t. It is difficult, however, to push this suggestive analogy very far, since the HMC as a field theory in 5d does not seem to be renormalizable, and in fact not even local (Lüscher and Schaefer, 2011).

Here the pseudo-fermion fields ϕ carry the same indices as a quark field ψ. Instead of being Grassmann valued field, though, they are complex valued fields. Note that we also introduced the natural scalar product $(\cdot, \cdot)$ on the space of such fields. In fact, as we shall see, more complicated representations of the quark determinant, involving several different pseudo-fermion fields, are used in practice to improve the efficiency of the simulations. We will comment on this later, in the next section.

To conclude, we now have all the basic ingredients of the HMC. We can thus schematically summarize the main steps of the algorithm as follows:

(a) A momentum field $\Pi_\mu(x)$, and a pseudo-fermion field $\phi(x)$ are generated randomly accordingly to the probability density: $p(\Pi, \phi) \propto \exp\{-\frac{1}{2}(\Pi, \Pi) - S_{\mathrm{pf}}(U, \phi)\}$.

(b) The MD equations are integrated from time $t = 0$ to some time $t = \tau > 0$, taking $\Pi_\mu(x)$ and $U_\mu(x)$ as the initial values.

(c) The new gauge field $U'_\mu(x)$ is set to the gauge field $U_\mu(x, \tau)$ obtained in (b) with probability,

$$P_{\mathrm{acc}} = \min\{1, e^{-\Delta H(\Pi, U)}\}. \tag{4.13}$$

In particular, if the proposed field is rejected, $U'_\mu(x)$ is set to the original field, i.e. $U'_\mu(x) \equiv U_\mu(x, 0)$.

4.2 The χSF **in numerical simulations**

Having introduced the basic concepts of the simulation algorithm, we now want to discuss in detail the numerical implementation of the χSF. We stress again that the code we developed is based on the `openQCD` package. As a result, most of the techniques that will presented in the following have been originally developed for this code. These are described in detail in the dedicated code documentation,[5] or alternatively, in the more condensed presentation of (Lüscher and Schaefer, 2013). However, substantial work had to be done in order to adjust the existing program for the standard SF regularization to the χSF. Apart from the obvious changes in the Dirac operator, this mostly concerned the evaluation of the different types of fermionic forces integrated in the HMC. We will now present these modifications in detail.

[5] http://luscher.web.cern.ch/luscher/openQCD/

4.2.1 Frequency splitting of the quark-determinant

In Section 4.1.1, we recalled that an essential ingredient for the numerical simulation of the theory is that once all fermionic species are integrated out, the product of the resulting determinants of the Dirac operators must be real and positive. As noticed, the Wilson-Dirac operator for two mass-degenerate quarks with χSF boundary conditions satisfies this property (cf. Section 3.4.2). Considering the improved operator $\mathcal{D}$ of (3.78), the hermiticity of $(\gamma_5\tau^1\mathcal{D})$ implies indeed for its flavour diagonal components,

$$\mathcal{D} = \mathrm{diag}(\mathcal{D}^{(1)}, \mathcal{D}^{(2)}) \qquad \gamma_5\mathcal{D}^{(1)}\gamma_5 = (\mathcal{D}^{(2)})^\dagger, \tag{4.14}$$

and therefore,

$$\det(\mathcal{D}) = \det(\mathcal{D}^{(1)})\det(\mathcal{D}^{(2)}) = \det\left[(\mathcal{D}^{(1)})^\dagger(\mathcal{D}^{(1)})\right] \geq 0. \tag{4.15}$$

Given this result, one can apply the HMC algorithm as described in the previous section, using for example the simple pseudo-fermion representation (4.12) for the quark determinant (4.15). Some time ago, however, it has been noticed that numerical simulations can be greatly stabilized by considering more elaborate representations of the quark-determinant (Hasenbusch, 2001; Hasenbusch and Jansen, 2003).

In order to present the specific representation we considered, we first need to discuss the inclusion of a twisted-mass term in the Dirac operator. As the reader might recall, we briefly commented on the possibility of adding a twisted-mass to the quarks in the context of automatic $O(a)$ improvement (cf. Section 2.2.4). On the other hand, an additional motivation for introducing a twisted-mass term is given by the fact that such a term provides a sharp infrared cutoff in the spectrum of the Wilson Dirac operator (Frezzotti, Grassi, Sint and Weisz, 2001). Without going into the details, this generally helps in the simulation of Wilson-fermions at small physical quark masses, since it prevents the occurrence of nearly zero eigenvalues of the Dirac operator. Small eigenvalues in fact can make the computation of the corresponding fermionic forces very difficult, and might even destabilize the simulations (see e.g. the discussions in (Del Debbio *et al.*, 2006; Lüscher and Palombi, 2008; Lüscher and Schaefer, 2013)).

Introducing a twisted-mass term in the χSF Dirac operator, the corresponding determinant reads ($\mu \geq 0$),

$$\det(\mathcal{D} + i\mu\gamma_5\tau^3) = \det(\mathcal{D}^{(1)} + i\mu\gamma_5)\det(\mathcal{D}^{(2)} - i\mu\gamma_5)$$

$$= \det\left[(\mathcal{D}^{(1)} + i\mu\gamma_5)^\dagger(\mathcal{D}^{(1)} + i\mu\gamma_5)\right] \tag{4.16}$$

$$= \det\left[(\mathcal{D}^{(1)})^\dagger(\mathcal{D}^{(1)}) + i\mu\gamma_5\Delta\mathcal{D} + \mu^2\right] \geq 0,$$

where we defined $\Delta\mathcal{D} = \mathcal{D}^{(2)} - \mathcal{D}^{(1)}$. For the specific lattice discretization we are considering, this term is gauge-link-independent and localized at the boundaries, i.e.,

$$\Delta\mathcal{D} = 2(\gamma_5 P_-\delta_{x_0,0} + \gamma_5 P_+\delta_{x_0,T}). \tag{4.17}$$

Note that the presence of this term is peculiar of the χSF, and is related to the fact that the γ_5-hermiticity of the operator $\mathcal{D}$ is only valid up to a flavour exchange. Indeed, in the standard SF case, it is easy to see that the linear term in μ is absent (see below). In conclusion, the expression (4.16) clearly shows the rôle of the twisted-mass as an infrared regulator for the zero-modes of the Dirac operator.

The new representation of the quark determinant is now obtained by considering the simple rewriting,

$$\det((\mathcal{D}^{(1)} + i\gamma_5\mu_0)^\dagger(\mathcal{D}^{(1)} + i\gamma_5\mu_0))$$

$$= \det((\mathcal{D}^{(1)} + i\gamma_5\mu_n)^\dagger(\mathcal{D}^{(1)} + i\gamma_5\mu_n)) \prod_{k=0}^{n-1} \det\left\{\frac{\det((\mathcal{D}^{(1)} + i\gamma_5\mu_k)^\dagger(\mathcal{D}^{(1)} + i\gamma_5\mu_k))}{\det((\mathcal{D}^{(1)} + i\gamma_5\mu_{k+1})^\dagger(\mathcal{D}^{(1)} + i\gamma_5\mu_{k+1}))}\right\}.$$

$$\tag{4.18}$$

where we introduced several different twisted-masses $0 \leq \mu_0 < \ldots < \mu_n$. In particular, if non-zero the lowest mass μ_0 can serve as infrared regulator to be reweighed away, or it may be interpreted as a physical twisted-mass of the quark doublet (Lüscher and Schaefer, 2013). Given the factorization (4.18), the basic idea is then to represent each term that appears in the product thought a separate pseudo-fermion representation (4.12). As a result, the pseudo-fermion action $S_{\rm pf}$ corresponding to the factorized determinant is given by the sum of different contributions associated with the different pseudo-fermion fields $\phi_0, \ldots, \phi_n$, namely,

$$S_{\rm pf} = \sum_{k=0}^{n} S_{{\rm pf},k}, \tag{4.19}$$

where,

$$S_{\mathrm{pf},n} = \left(\phi_n, \left[(\mathcal{D}^{(1)} + i\gamma_5\mu_n)^\dagger(\mathcal{D}^{(1)} + i\gamma_5\mu_n))\right]^{-1}\phi_n\right), \tag{4.20}$$

while,

$$S_{\mathrm{pf},k} = \left(\tilde{\phi}_k, \left[(\mathcal{D}^{(1)} + i\gamma_5\mu_k)^\dagger(\mathcal{D}^{(1)} + i\gamma_5\mu_k))\right]^{-1}\tilde{\phi}_k\right),$$

$$\tilde{\phi}_k = \gamma_5(\mathcal{D}^{(2)} - i\gamma_5\mu_{k+1})\phi_k. \tag{4.21}$$

for $k = 0, \ldots, n-1$. In the MD evolution each component of the total pseudo-fermion action will contribute with the corresponding force. In particular, we immediately see that independently from the number of terms that appear in the product (4.18), only two types of forces need to be considered: the one originating from the action type (4.20), and the one associated with the type (4.21).

The technique presented above, was firstly proposed in (Hasenbusch, 2001; Hasenbusch and Jansen, 2003), and is generally referred to as Hasenbusch (twisted-mass) preconditioning. This factorization effectively works as a frequency splitting of the quark determinant. This seems to reduce the fluctuations in the corresponding forces along the MD trajectory, and thus stabilize the simulations (see e.g. (Schaefer, 2012)). In practice this means that, for a given P_{acc} and τ, the twisted-masses can be tuned such that larger step-sizes ϵ can be considered for the numerical integration of the MD equations.[6] In particular, it has been noticed that the twisted-masses $\mu_0, \ldots, \mu_n$ can be generally tuned such that a hierarchy in the magnitude of the different forces resulting from the determinant splitting is obtained. The Hasenbusch preconditioning can then be efficiently combined with a multiple step integration of these forces (Urbach, Jansen, Shindler and Wenger, 2006).

To conclude, we will now study in detail the resulting types of forces that appear due to the factorization of the quark determinant. In this respect, we want to note that while the force computation deriving from the action (4.20) needed minor changes w.r.t. the original code, the ones associated with (4.21) instead had to be redefined. The basic motivation is due to the following observation.

---

[6]Note that, in fact, there is not solid theoretical understanding of why such splitting stabilizes the simulations. This means that the tuning of the twisted-masses is poorly guided, and essentially based on numerical experiments. In any case, different ideas to obtain a frequency splitting of the quark-determinant can be found in e.g. (Lüscher, 2005; Clark and Kennedy, 2007).

Considering the standard SF Dirac operator (3.45), including a twisted-mass term, the resulting determinant for two mass-degenerate quark fields reads,

$$\det\left[(D + i\mu\gamma_5)^\dagger(D + i\mu\gamma_5)\right] = \det(DD^\dagger + \mu^2) \geq 0, \tag{4.22}$$

where we used the γ_5-hermiticity property $\gamma_5 D \gamma_5 = D^\dagger$. In particular by defining the operator $Q = \gamma_5 D$, we simply obtain,

$$\det\left[(D + i\mu\gamma_5)^\dagger(D + i\mu\gamma_5)\right] = \det\left[(Q - i\mu)(Q + i\mu)\right]. \tag{4.23}$$

We then see that the operators in square brackets trivially commute, even without resorting to the properties of the determinant. In the case of the χSF instead we have,

$$\det\left[(\mathcal{D}^{(1)} + i\mu\gamma_5)^\dagger(\mathcal{D}^{(1)} + i\mu\gamma_5)\right] = \det\left[(\mathcal{Q}^\dagger - i\mu)(\mathcal{Q} + i\mu)\right], \tag{4.24}$$

where we defined $\mathcal{Q} = \gamma_5 \mathcal{D}^{(1)}$, and by using $\gamma_5 \mathcal{D}^{(1)} \gamma_5 = (\mathcal{D}^{(2)})^\dagger$, we have $\mathcal{Q}^\dagger = \gamma_5 \mathcal{D}^{(2)}$. The main difference in this case is that $\mathcal{Q}^\dagger \neq \mathcal{Q}$, and in particular,

$$[\mathcal{Q}^\dagger, \mathcal{Q}] = (\mathcal{D}^{(1)})^\dagger \mathcal{D}^{(1)} - (\mathcal{D}^{(2)})^\dagger \mathcal{D}^{(2)} \neq 0. \tag{4.25}$$

In other words, in the χSF case the operator $\mathcal{Q}$ is non-hermitian and non-normal. As we shall see more explicitly shortly, this in practice reduces the flexibility of the pseudo-fermion representation, in particular when ratios of determinants are taken. In fact, once a form of the pseudo-fermion action is specified, e.g. (4.21), the different matrix contributions do not commute.

The force deriving from a quark doublet. Given the factorization (4.18), we have seen that the first type of contribution to the pseudo-fermion action is given by (4.20). For the derivation of the corresponding MD force, it is convenient to rewrite this contribution as,

$$\begin{aligned} S_{\text{pf}}^{(1)} &= \left(\phi, \left[(\mathcal{D}^{(1)} + i\gamma_5\mu)^\dagger(\mathcal{D}^{(1)} + i\gamma_5\mu))\right]^{-1}\phi\right), \\ &= \left((\mathcal{D}^{(2)} - i\gamma_5\mu))^{-1}\gamma_5\phi, (\mathcal{D}^{(2)} - i\gamma_5\mu))^{-1}\gamma_5\phi\right), \\ &\equiv (\psi, \psi), \end{aligned} \tag{4.26}$$

where we used that $\gamma_5 \mathcal{D}^{(1)} \gamma_5 = (\mathcal{D}^{(2)})^\dagger$, and we defined $\psi = (\mathcal{D}^{(2)} - i\gamma_5\mu)^{-1}\gamma_5\phi$. This form also suggests how the pseudo-fermion fields can be actually obtained. As discussed

in Section 4.1.4, the pseudo-fermions indeed need to be generated at the beginning of the MD evolution according to the probability density $p(\phi, U) \propto e^{-S_{\text{pf}}(U)}$. From the expression (4.26), it is clear that this can be achieved by simply generating Gaussian-distributed fields ξ i.e. $p(\xi) \propto e^{-\frac{1}{2}(\xi,\xi)}$, and then computing,

$$\phi = \gamma_5 (\mathcal{D}^{(2)} - i\gamma_5 \mu)\xi. \tag{4.27}$$

The MD force corresponding to (4.26) is also easy to derive since (cf. eq. (4.9)),

$$F_{x,\mu}^{(1)} = \partial_{x,\mu} S_{\text{pf}}^{(1)} = \partial_{x,\mu}(\psi, \psi) = 2 \operatorname{Re}(\psi, \partial_{x,\mu}\psi). \tag{4.28}$$

Using then the identity $AA^{-1} = 1$, with A a general gauge-link dependent matrix, the simple relation $\partial_{x,\mu} A^{-1} = -A^{-1}(\partial_{x,\mu} A)A^{-1}$, is obtained. From this identity we can rewrite the expression (4.28) more explicitly as,

$$F_{x,\mu}^{(1)} = -2 \operatorname{Re}(\chi, \gamma_5(\partial_{x,\mu}\mathcal{D}^{(2)})\psi), \tag{4.29}$$

where,

$$\chi = (\mathcal{D}^{(1)} + i\gamma_5\mu)^{-1}\gamma_5\psi = \left[(\mathcal{D}^{(1)} + i\gamma_5\mu)^\dagger(\mathcal{D}^{(1)} + i\gamma_5\mu)\right]^{-1}\phi, \tag{4.30}$$

$$\psi = (\mathcal{D}^{(2)} - i\gamma_5\mu)^{-1}\gamma_5\phi. \tag{4.31}$$

Note that, the gauge group derivative of the χSF Dirac operator is independent of the flavour considered, i.e., $\partial_{x,\mu}(\mathcal{D}^{(2)} - \mathcal{D}^{(1)}) = 0$ (cf. (4.17)). In fact this derivative is equivalent to the one obtained from the standard SF Dirac operator. The explicit expression is given in Appendix B. In the case of the χSF, however, since the quark-fields are dynamical at $x_0 = 0, T$, the pseudo-fermion fields are non-zero at these time-slices, and consequently χ and ϕ. The force (4.29) is thus non-vanishing for all dynamical gauge link variables.[7]

To conclude, we obtain the field χ by solving the normal equation in (4.30) using a standard Conjugate Gradient (CG) solver. Note that in the force computation, the field ψ can then be obtained by a simple matrix multiplication without further inversions, i.e.,

$$\gamma_5(\mathcal{D}^{(1)} + i\gamma_5\mu)\chi = \psi. \tag{4.32}$$

---

[7]We remind that these are defined as the gauge fields $U_\mu(x)$ with $0 \leq x_0 < T$ for $\mu = 0$, and $0 < x_0 < T$ for $\mu = 1, 2, 3$.

Force deriving from the ratio of determinants. We now discuss the second type of forces which derives from the pseudo-fermion action (4.21). These have been obtained by applying straightforwardly the results discussed in (Hasenbusch, 2001; Hasenbusch and Jansen, 2003). For later convenience we will first recall the general strategy as presented in the given references, and then simply list and comment the results we derived for our specific case. This will also allow us to adopt a more compact notation.

As we have seen, the starting point is the factorization,

$$\det(V^\dagger V) = \det(W^\dagger W)\frac{\det(V^\dagger V)}{\det(W^\dagger W)} = \det(W^\dagger W)\det((W^{-1})^\dagger(V^\dagger V)W^{-1}), \quad (4.33)$$

where V is our original Dirac operator, while W is the so-called *preconditioner*. For the moment, we do not assume any specific form or relation between V and W. In particular, these operators do not generally commute. Focusing now on the second determinant defined on the r.h.s. of (4.33), this can be represented through a pseudo-fermion representation defined by the action (cf. (4.21)),

$$\begin{aligned} S_{\text{pf}}^{(2)} &= (W^\dagger\phi, (V^\dagger V)^{-1}W^\dagger\phi), \\ &= ((WV^{-1})^\dagger\phi, (WV^{-1})^\dagger\phi), \\ &= (\psi, \psi), \end{aligned} \quad (4.34)$$

where $\psi = (WV^{-1})^\dagger\phi$. In this form, it is explicit that the specific pseudo-fermion representation has been chosen such that the corresponding pseudo-fermions can be easily obtained. In this case indeed, given some Guassian-distributed fields ξ, correctly distributed pseudo-fermion fields can be simply generated as,

$$\phi = (VW^{-1})^\dagger\xi. \quad (4.35)$$

Note that the form of (4.34), offers the suggestive interpretation that the effect of the preconditioning matrix W is to replace the original pseudo-fermion fields ϕ, with some "effective" pseudo-fermions fields, given by $\tilde\phi = W^\dagger\phi$.

The force corresponding to (4.34) can be easily derived, and is given by,

$$F_{x,\mu}^{(2)} = -2\operatorname{Re}(\chi, \partial_{x,\mu}V^\dagger\psi) + 2\operatorname{Re}(\chi, \partial_{x,\mu}W^\dagger\phi), \quad (4.36)$$

where

$$\chi = (V^\dagger V)^{-1} W^\dagger \phi, \tag{4.37}$$

$$\psi = (WV^{-1})^\dagger \phi = V\chi. \tag{4.38}$$

Given this general expression, we can now consider our specific case defined in (4.21). This is in fact equivalent to choosing,

$$V = (\mathcal{Q} + i\mu_0), \qquad W = (\mathcal{Q} + i\mu_1), \tag{4.39}$$

where for simplicity we defined the two generic twisted-masses that occur as $\mu_0 < \mu_1$. We remind that $\mathcal{Q} = \gamma_5 \mathcal{D}^{(1)}$. In this specific case clearly, $\partial_{x,\mu} V^\dagger = \partial_{x,\mu} W^\dagger$, and the expression (4.36) simplifies to,

$$F_{x,\mu}^{(2)} = -2\mathrm{Re}\,(\chi, \partial_{x,\mu} V^\dagger \psi'), \tag{4.40}$$

where $\psi' = \psi - \phi$. In terms of the flavour diagonal Dirac operators, the final result for the force reads,

$$F_{x,\mu}^{(2)} = -2\mathrm{Re}\,(\chi, \gamma_5(\partial_{x,\mu}\mathcal{D}^{(2)})\psi'), \tag{4.41}$$

where,

$$\chi = [(\mathcal{D}^{(1)} + i\gamma_5\mu_0)^\dagger(\mathcal{D}^{(1)} + i\gamma_5\mu_0)]^{-1}\tilde{\phi},$$
$$\tilde{\phi} = \gamma_5(\mathcal{D}^{(2)} - i\gamma_5\mu_1)\phi. \tag{4.42}$$

and,

$$\psi' = \gamma_5(\mathcal{D}^{(1)} + i\gamma_5\mu_0)\chi - \phi. \tag{4.43}$$

Note that, the above expression could be reduced to,

$$\psi' = i(\mu_0 - \mu_1)\gamma_5(\mathcal{D}^{(2)} - i\gamma_5\mu_0)^{-1}\phi, \tag{4.44}$$

where the cancellation between the two terms in (4.43) is done analytically, and is thus expected to be numerically better behaved. Unfortunately, however, this would require an additional inversion of the Dirac operator at each step of MD trajectory. This solution is too expensive in terms of computational effort, and we then opted for

the original representation (4.43), which only requires a single matrix multiplication and vector subtraction once χ has been computed.

Finally, note that the pseudo-fermion fields are obtained by first solving the normal equation,

$$[(\mathcal{D}^{(1)} + i\gamma_5\mu_1)^\dagger(\mathcal{D}^{(1)} + i\gamma_5\mu_1)]\phi' = \gamma_5(\mathcal{D}^{(2)} - i\gamma_5\mu_0)\xi, \tag{4.45}$$

where ξ are Gaussian-distributed fields, and then computing,

$$\phi = \gamma_5(\mathcal{D}^{(1)} + i\gamma_5\mu_1)\phi'. \tag{4.46}$$

Differently from the determination of the χ field, the inversion of the Dirac operator here is required for the (generally) larger twisted-mass μ_1. The computation is thus expected to be less expensive.

To conclude, we want to note that in the case of the standard SF, an analogous computation of the force would have involved the operators,

$$V = (Q + i\mu_0), \qquad W = (Q + i\mu_1), \tag{4.47}$$

where, we remind, $Q = \gamma_5 D$. In this case, V and W commute with their hermitian conjugates $V^\dagger$ and $W^\dagger$. The pseudo-fermion action (4.34) can then be rewritten as,

$$\begin{aligned}
S_{\mathrm{pf}}^{(2)} &= ((WV^{-1})^\dagger\phi, (WV^{-1})^\dagger\phi), \\
&= (\phi, (W^\dagger W)(V^\dagger V)^{-1}\phi),
\end{aligned} \tag{4.48}$$

which for the SF case explicitly reads,

$$\begin{aligned}
S_{\mathrm{pf}}^{(2)} &= (\phi, (DD^\dagger + \mu_1^2)(DD^\dagger + \mu_0^2)^{-1}\phi), \\
&= (\phi, (1 + (\mu_1^2 - \mu_0^2)(DD^\dagger + \mu_0^2)^{-1}\phi).
\end{aligned} \tag{4.49}$$

The corresponding force computation can thus be nicely recast in the previous simpler case of a single quark determinant (Lüscher and Schaefer, 2013),

$$F_{x,\mu}^{(2)} = (\mu_1^2 - \mu_0^2)\partial_{x,\mu}S_{\mathrm{pf}}^{(1)}, \tag{4.50}$$

where for the standard SF we have (cf. eq. (4.26)),

$$S_{\mathrm{pf}}^{(1)} = (\phi, (DD^\dagger + \mu_0^2)^{-1}\phi). \tag{4.51}$$

4.2.2 Even-odd preconditioning

Another common technique to speed-up lattice QCD simulations is based on even-odd preconditioning (see e.g. (Lüscher, 2010a).) In this section we comment on the specific implementation that has been considered, in particular in conjunction with the Hasenbusch preconditioning just presented.

A lattice point x is classified to be even or odd depending on whether the sum of its coordinates $x_0 + x_1 + x_2 + x_3$, is even or odd. In particular, any quark field can be split into two parts,

$$\psi = \psi_e + \psi_o, \tag{4.52}$$

where ψ_e (ψ_o) has support on the even (odd) sites of the lattice only. If then the lattice points are labeled such that the even come first and the odd come after, the χSF Dirac operator assumes the block structure,

$$\mathcal{D} = \begin{pmatrix} \mathcal{D}_{ee} & \mathcal{D}_{eo} \\ \mathcal{D}_{oe} & \mathcal{D}_{oo} \end{pmatrix}. \tag{4.53}$$

The operators $\mathcal{D}_{eo}$ and $\mathcal{D}_{oe}$ simply include the hopping terms that connect odd to even and even to odd points, respectively. Note that these components of the χSF Dirac operator are trivial in flavour space. The non-trivial flavour structure is in fact contained in the diagonal part $M \equiv \mathcal{D}_{ee} + \mathcal{D}_{oo}$, which is given by (cf. (3.78)),

$$M(x) = \begin{cases} 4 + m_0 + c_{\text{sw}} \sum_{\mu\nu=0}^{3} \frac{i}{4}\sigma_{\mu\nu}\widehat{F}_{\mu\nu}(x), & \text{if } 0 < x_0 < T - a, \\ z_f + 3d_s + m_0 + i\gamma_5 P_- \tau^3, & \text{if } x_0 = 0, \\ z_f + 3d_s + m_0 + i\gamma_5 P_+ \tau^3, & \text{if } x_0 = T. \end{cases} \tag{4.54}$$

Given these observations, the even-odd preconditioning is based on the following result. The generic Dirac equation $\mathcal{D}^{(i)}\psi = \eta$ for the source field η, can be solved by first solving,

$$\hat{\mathcal{D}}^{(i)}\psi_e = \eta_e - \mathcal{D}_{eo}(\mathcal{D}_{oo}^{(i)})^{-1}\eta_o, \tag{4.55}$$

for ψ_e, where

$$\hat{\mathcal{D}}^{(i)} = \mathcal{D}_{ee}^{(i)} - \mathcal{D}_{eo}(\mathcal{D}_{oo}^{(i)})^{-1}\mathcal{D}_{oe}, \tag{4.56}$$

is the even-odd preconditioned Dirac operator. (Note that, $\hat{\mathcal{D}}^{(i)}$ acts inside the subspace of fields defined on the even sites only.) Once the solution ψ_e is given, the odd field components of ψ can be obtained simply as,

$$\psi_o = (\mathcal{D}_{oo}^{(i)})^{-1}\{\eta_o - \mathcal{D}_{oe}\psi_e\}. \tag{4.57}$$

Solving the Dirac equation in this way is generally advantageous e.g. 2-3 times faster. In fact, $\mathcal{D}_{oo}^{(i)}$ does not couple different lattice points, and can then be easily inverted. The expensive part of solving the Dirac equation is thus limited to half of the space-time volume i.e. the even sites only (cf. (4.55)).

In addition, even-odd preconditioning comes with the factorization of the quark determinant,

$$\det \mathcal{D}^{(i)} = \det \mathcal{D}_{oo}^{(i)} \det \hat{\mathcal{D}}^{(i)}. \tag{4.58}$$

In this respect, note that differently from the standard SF case, for the χSF Dirac operator $\mathcal{D}_{eo}\psi(x) \neq 0$ at the boundaries $x_0 = 0, T$ (cf. (3.78)). As a consequence, the operator product that defines $\hat{\mathcal{D}}^{(i)}$ involves the inverse of $\mathcal{D}_{oo}^{(i)}$ on all odd sites x in the range $0 \leq x_0 \leq T$. However, while a numerical inversion is needed to invert $\mathcal{D}_{oo}^{(i)}$ in the bulk of the lattice, at the boundaries this can be done on a piece of paper. Only in the bulk in fact the space diagonal part of the Dirac operator depends non-trivially on the gauge field (cf. (4.54)). Consequently, the determinant $\det \mathcal{D}_{oo}^{(i)}$ is given by a product of determinants one for each odd point in the time range $0 \leq x_0 \leq T$. As we will comment later in this section, though, the contributions from the boundaries $x_0 = 0, T$ can be neglected in practice.

Given the factorization (4.58), one can think of combining it with the Hasenbusch twisted-mass preconditioning (4.18). In this case, if the twisted-mass is introduced only as an infrared regulator, one could consider including it only on the even sites of the lattice (Lüscher and Schaefer, 2013). One thus introduces the projector 1_e on the subspace of quark fields that vanish on the odd sites. Its action on a generic spinor field ψ is defined as,

$$1_e\psi(x) = \begin{cases} \psi(x) & \text{if } x \text{ is even,} \\ 0 & \text{if } x \text{ is odd.} \end{cases} \tag{4.59}$$

The Dirac equation with the twisted-mass on the even sites then reads,

$$(\mathcal{D}^{(i)} + i\mu\gamma_5 1_e)\psi(x) = \eta(x). \tag{4.60}$$

This can be solved analogously as discussed before: first solving the even-odd precon-
ditioned system,

$$(\hat{\mathcal{D}}^{(i)} + i\mu\gamma_5)\psi_e = \eta_e - \mathcal{D}_{\mathrm{eo}}(\mathcal{D}^{(i)}_{\mathrm{oo}})^{-1}\eta_o, \tag{4.61}$$

and then obtaining ψ_o as in (4.57).

Combining now the factorization of the quark determinant (4.58) with (4.18), one
obtains (Lüscher and Schaefer, 2013),

$$\det((\mathcal{D}^{(1)} + i\mu_0\gamma_5 1_e)^\dagger(\mathcal{D}^{(1)} + i\mu_0\gamma_5 1_e))$$
$$= \det((\mathcal{D}^{(1)}_{\mathrm{oo}})^\dagger\mathcal{D}^{(1)}_{\mathrm{oo}})\det((\hat{\mathcal{D}}^{(1)} + i\mu_n\gamma_5 1_e)^\dagger(\hat{\mathcal{D}}^{(1)} + i\mu_n\gamma_5 1_e))\times$$
$$\times \prod_{n=0}^{n-1} \det\left\{\frac{\det((\hat{\mathcal{D}}^{(1)} + i\mu_k\gamma_5 1_e)^\dagger(\hat{\mathcal{D}}^{(1)} + i\mu_k\gamma_5 1_e))}{\det((\hat{\mathcal{D}}^{(1)} + i\mu_{k+1}\gamma_5 1_e)^\dagger(\hat{\mathcal{D}}^{(1)} + i\mu_{k+1}\gamma_5 1_e))}\right\}, \tag{4.62}$$

where we will generally consider the case with $\mu_0 = 0$. Similarly to (4.18), the idea
is to represent each term in the product (4.62) though a separate pseudo-fermion
representation. Note that in this case, the pseudo-fermion fields $\phi_{0,e}, \ldots, \phi_{n,e}$, need
to be defined only on the even sites of the lattice. The pseudo-fermion action S_{pf}
corresponding to the factorized determinant (4.62) is then given by,

$$S_{\mathrm{pf}} = S_{\mathrm{det}} + \sum_{k=0}^{n} S_{\mathrm{pf},k}, \tag{4.63}$$

where the $S_{\mathrm{pf},k}$ are defined analogously to the expressions (4.20) and (4.21), by simply
replacing $\mathcal{D}^{(i)}$ with $\hat{\mathcal{D}}^{(i)}$, $\phi_k \to \phi_{e,k}$, and also $\mu_k \to \mu_k 1_e$. The new component in the
action (4.63), is given by the contribution of the *small determinant* $\det((\mathcal{D}^{(1)}_{\mathrm{oo}})^\dagger\mathcal{D}^{(1)}_{\mathrm{oo}})$.
This is given by,

$$S_{\mathrm{det}} = -\mathrm{Tr}\log(1_e + (\mathcal{D}^{(1)}_{\mathrm{oo}})^\dagger\mathcal{D}^{(1)}_{\mathrm{oo}}). \tag{4.64}$$

Note that in the case of the χSF, $\mathcal{D}^{(i)}_{\mathrm{oo}}$ is hermitian except at the boundaries $x_0 = 0, T$.

We will now conclude the section presenting the derivation of the three different
types of forces that appear in the case of even-odd Hasenbusch preconditioning.

The force deriving from the quark doublet: even-odd. As just seen, the first type of contribution that enters in the pseudo-fermion action (4.63), is given by,

$$
\begin{aligned}
S_{\text{pf}}^{(4)} &= \left(\phi_e, \left[(\hat{\mathcal{D}}^{(1)} + i\mu\gamma_5 1_e)^\dagger(\hat{\mathcal{D}}^{(1)} + i\mu\gamma_5 1_e)\right]^{-1}\phi_e\right), \\
&= \left((\hat{\mathcal{D}}^{(2)} - i\mu\gamma_5 1_e)^{-1}\gamma_5\phi_e, (\hat{\mathcal{D}}^{(2)} - i\mu\gamma_5 1_e)^{-1}\gamma_5\phi_e\right), \\
&= \left((\mathcal{D}^{(2)} - i\mu\gamma_5 1_e)^{-1}\gamma_5\phi_e, 1_e(\mathcal{D}^{(2)} - i\mu\gamma_5 1_e)^{-1}\gamma_5\phi_e\right), \\
&\equiv (\psi, 1_e\psi),
\end{aligned}
\tag{4.65}
$$

where we defined $\psi = (\mathcal{D}^{(2)} - i\mu\gamma_5 1_e)^{-1}\gamma_5\phi_e$. Note that $\gamma_5\tau^1$-hermiticity also holds for $\hat{\mathcal{D}}^{(i)}$, and has been used to derive the expression above. Similarly to the case of (4.26), the representation (4.65) clearly shows that properly distributed pseudo-fermion fields can be generated from Gaussian-distributed fields ξ_e simply as,

$$
\phi_e = \gamma_5(\hat{\mathcal{D}}^{(2)} - i\mu\gamma_5 1_e)\xi_e.
\tag{4.66}
$$

where both ϕ_e and ξ_e are defined only on the even sites of the lattice.

The representation (4.65), is also convenient when considering the derivation of the corresponding MD force. Indeed, this is simply given by,

$$
F_{x,\mu}^{(4)} = \partial_{x,\mu}S_{\text{pf}}^{(4)} = \partial_{x,\mu}(\psi, 1_e\psi) = 2\,\text{Re}\,(\psi, 1_e\partial_{x,\mu}\psi).
\tag{4.67}
$$

In particular, we can avoid taking the gauge-group derivative of the preconditioned operator $\hat{\mathcal{D}}^{(i)}$, and only work with $\partial_{x,\mu}\mathcal{D}^{(i)}$. The explicit form of force $F_{x,\mu}^{(4)}$, is in fact given by (cf. (4.29)),

$$
F_{x,\mu}^{(4)} = -2\,\text{Re}\,(\chi, \gamma_5(\partial_{x,\mu}\mathcal{D}^{(2)})\psi),
\tag{4.68}
$$

where,

$$
\chi = (\mathcal{D}^{(1)} + i\mu\gamma_5 1_e)^{-1}\gamma_5 1_e\psi,
\tag{4.69}
$$

$$
\psi = (\mathcal{D}^{(2)} - i\mu\gamma_5 1_e)^{-1}\gamma_5\phi_e.
\tag{4.70}
$$

To conclude, note that the χ and ψ fields can be efficiently computed by solving the even-odd preconditioned Dirac equation (cf. (4.55) and (4.57)). Indeed, it is easy to show that the χ field is given by,

$$\chi_e = [(\hat{\mathcal{D}}^{(1)} + i\mu\gamma_5 1_e)^\dagger (\hat{\mathcal{D}}^{(1)} + i\mu\gamma_5 1_e)]^{-1}\phi_e,$$

$$\chi_o = -(\mathcal{D}^{(1)}_{oo})^{-1}\mathcal{D}_{oe}\chi_e.$$

(4.71)

This can be easily inferred from the definition of χ in (4.69), considering that the pseudo-fermion field ϕ_e is only defined on the even points of the lattice. Secondly, once χ is obtained, a bit more subtle is the determination of ψ, which is given by,

$$\psi_e = \gamma_5(\hat{\mathcal{D}}^{(1)} + i\mu\gamma_5 1_e)\chi_e$$

$$\psi_o = -(\mathcal{D}^{(2)}_{oo})^{-1}\mathcal{D}_{oe}\psi_e.$$

(4.72)

As we can see, $\mathcal{D}^{(2)}_{oo}$ is used to obtain the odd components of ψ. This is because, ψ is in principle computed through the inversion of $\mathcal{D}^{(2)}$ and not of $\mathcal{D}^{(1)}$ (cf. (4.70)).

Finally, we note that the computation of the action (4.65) only requires the even components of ψ, since $S_{\mathrm{pf}} = (\psi, 1_e\psi) = (\psi_e, \psi_e)$.

Force deriving from the ratio of determinants: even-odd. The second type of contribution that enters in (4.63) is defined from (4.21) by simply replacing the Dirac operator $\mathcal{D}^{(i)}$ with $\hat{\mathcal{D}}^{(i)}$, and restricting the pseudo-fermion fields and twisted-masses to the even sites of the lattice only (cf. (4.62)). The general presentation of the Hasenbusch preconditioning outlined before in this section (see (4.33) and relative discussion), can then be trivially extended to the even-odd preconditioned case. In particular, the pseudo-fermion representation can be similarly defined in terms of the action (cf. (4.34)),

$$S^{(5)}_{\mathrm{pf}} = (\hat{W}^\dagger\phi_e, (\hat{V}^\dagger\hat{V})^{-1}\hat{W}^\dagger\phi_e),$$

$$= ((\hat{W}\hat{V}^{-1})^\dagger\phi_e, (\hat{W}\hat{V}^{-1})^\dagger\phi_e),$$

$$= (\psi_e, \psi_e),$$

(4.73)

where $\psi_e = (\hat{W}\hat{V}^{-1})^\dagger\phi_e$. As one can immediately see, the only difference w.r.t. to the case in (4.34) is that now the pseudo-fermion fields live on the even sites only, and we consider the even-odd preconditioned Dirac operators $\hat{V}$ and $\hat{W}$. These will be specified shortly.

It comes without saying that, the pseudo-fermions can be obtained from Guassian-distributed fields ξ_e as,

$$\phi_e = (\hat{V}\hat{W}^{-1})^\dagger \xi_e, \tag{4.74}$$

and that assuming, $\partial_{x,\mu}\hat{V}^\dagger = \partial_{x,\mu}\hat{W}^\dagger$, the expression for the force is given by,

$$F_{x,\mu}^{(5)} = -2\,\mathrm{Re}\,(\chi_e, \partial_{x,\mu}\hat{V}^\dagger \psi_e'), \tag{4.75}$$

where

$$\chi_e = (\hat{V}^\dagger \hat{V})^{-1}\hat{W}^\dagger \phi_e, \tag{4.76}$$

$$\psi_e' = (\hat{W}\hat{V}^{-1})^\dagger \phi_e - \phi_e = \hat{V}\chi_e - \phi_e. \tag{4.77}$$

The preconditioned operators that we now choose, are the ones expected and given by,

$$\hat{V} = (\hat{Q} + i\mu_0), \qquad \hat{W} = (\hat{Q} + i\mu_1), \tag{4.78}$$

where $\hat{Q} = \gamma_5 \hat{D}^{(1)}$. From the general expression of the force (4.75), it is clear that in this case we have the complication of computing the derivative of the preconditioned operator $\hat{D}^{(2)}$. On the other hand, it is possible to show that the force $F_{x,\mu}^{(5)}$ can be in fact rewritten in terms of the derivative of the standard Dirac operator $\mathcal{D}^{(2)}$, and fields χ and ψ that live on all sites of the lattice. Such derivation is simple, but rather lengthy. It is thus not presented here. In a few words, the idea is to compute analytically the derivative of the preconditioned operator (4.56) by considering its expression in terms of the components $\mathcal{D}_{ee}^{(2)}, \mathcal{D}_{oo}^{(2)}, \mathcal{D}_{eo}, \mathcal{D}_{oe}$. Then, by recombining the pieces opportunely together, one can prove the relation (cf. (4.41)),

$$F_{x,\mu}^{(5)} = -2\,\mathrm{Re}\,(\chi_e, \gamma_5(\partial_{x,\mu}\hat{D}^{(2)})\psi_e'), = -2\,\mathrm{Re}\,(\chi, \gamma_5(\partial_{x,\mu}\mathcal{D}^{(2)})\psi'), \tag{4.79}$$

where,

$$\chi_e = [(\hat{D}^{(1)} + i\mu_0\gamma_5 1_e)^\dagger(\hat{D}^{(1)} + i\mu_0\gamma_5 1_e)]^{-1}(\hat{D}^{(1)} + i\mu_1\gamma_5 1_e)\phi_e,$$
$$\chi_o = -(\mathcal{D}_{oo}^{(1)})^\dagger \mathcal{D}_{oe}\chi_e. \tag{4.80}$$

and,

$$\psi_e' = \gamma_5(\hat{D}^{(1)} + i\mu_0\gamma_5 1_e)\chi_e - \phi_e$$
$$\psi_o' = -(\mathcal{D}_{oo}^{(2)})^\dagger \mathcal{D}_{oe}\psi_e'. \tag{4.81}$$

The standard Dirac operator $\mathcal{D}^{(2)}$ thus provides the odd components of the fields as expected from the solution of the even-odd preconditioned Dirac equation (cf. (4.57)).

Force deriving from the small determinant. To conclude, we want to briefly comment on how to treat the contribution to the pseudo-fermion action deriving from small determinant $\det((\mathcal{D}_{oo}^{(1)})^{\dagger}\mathcal{D}_{oo}^{(1)})$. We recall that this is given by,

$$S_{\text{det}} = -\text{Tr}\log(1_e + (\mathcal{D}_{oo}^{(1)})^{\dagger}\mathcal{D}_{oo}^{(1)}) = -\sum_{x\,\text{odd}} \text{tr}\log[(M^{(1)}(x))^{\dagger}M^{(1)}(x)], \qquad (4.82)$$

where $M^{(1)}$ indicates the upper flavour component of the matrix M in (4.54). First of all, note the matrix $\mathcal{D}_{oo}^{(1)}$, and so $M^{(1)}(x)$, are non-hermitian only for $x_0 = 0, T$ (cf. (4.54)). In particular, at these values of x_0 the matrix $M^{(1)}(x)$ is gauge link independent. For all practical purposes, we can then restrict the sum on the r.h.s of (4.82) to all odd points x with $0 < x_0 < T$. In fact, since the contributions at $x_0 = 0, T$ are independent from the gauge fields, the action at these time slices is constant along the MD trajectory. Consequently, these contributions cancel when we consider the accept-reject step in the HMC. In addition, they will not contribute to the MD forces either once we take the gauge-group derivative of the action. In conclusion, one can proceed in the exact same way as in the standard SF case (Lüscher and Schaefer, 2013). We then report the expression for the force corresponding to (4.82) in Appendix B.

4.3   Tests on the implementation

Given the details of our implementation, in this concluding section we want to present the results of some consistency checks we have performed. In this respect, note that the main modifications w.r.t. the original `openQCD` package have been the following. First of all, we have implemented the χSF Dirac operator, which also required some modifications of the communication routines for the fields, and of the CG solver. Secondly, the computation of the forces, actions, and pseudo-fermion generation, has been modified according to what we described in the previous section.[8] The integration of the MD equations, and the other details of the HMC, however, have been left unchanged. This said, the main tests that have been performed are:

---

[8]The author is grateful to John Bulava for his help in checking the implementation of the χSF Dirac operator, field communications, and CG solver.

- The application of the χSF Dirac operator $\mathcal{D}^{(i)}$ on random test sources has been compared with the results obtained from an independent implementation.[9] This included different lattice parameters, MPI parallelizations, and machines.

- The solution of the Dirac equation $\mathcal{D}^{(i)}\psi = \eta$ has been tested analogously. In particular, the results for several non-trivial fermionic correlation functions have been compared with an independent determination.

- Given the results above, we have tested the solution of the Dirac equation using even-odd preconditioning (cf. (4.55) and (4.57)). This is a strong check on the preconditioned Dirac operator $\hat{\mathcal{D}}^{(i)}$, and its components: $\mathcal{D}_{\mathrm{eo}}$, $\mathcal{D}_{\mathrm{oe}}$, $\mathcal{D}_{\mathrm{ee}}^{(i)}$, and $\mathcal{D}_{\mathrm{oo}}^{(i)}$.

- As we will discuss in more detail in the next subsection, we have checked the consistency between the MD action, and force computations. Similarly, we have also checked the consistency between the action computation, and pseudo-fermion generation.

- Finally, we have preformed some extensive simulations of $N_{\mathrm{f}} = 2$ $\mathrm{O}(a)$-improved Wilson-fermions with χSF boundary conditions, in order to check the statistical agreement among the different types of preconditioning on a set of observables.

For completeness, in the next subsections we present the details of the results of the last two tests listed above.

4.3.1   Force, and action computation

There are several ways to check the consistency between the computation of the pseudo-fermion action, and the corresponding forces. We note however that, in general, these kinds of tests do not detect a consistent error between the force and action evaluation, as in the case for example where the Dirac operator is not well-implemented. For this reason, it is important to check the latter independently, as we discussed above. This said, a way to probe the consistency between the forces and actions is suggested in the original `openQCD` package. The idea is to compare the computation of the force, with a numerical gauge-group derivative of the corresponding action.

---

[9]The author thanks Stefan Sint for having provided these crosschecks.

More precisely, starting from a given pseudo-fermion field $\phi(x)$, gauge field $U_\mu(x)$, and momenta field $\Pi_\mu(x) = \Pi_\mu^a(x)T^a$, one defines,

$$S_\epsilon^\Pi = \frac{2}{3}S_{\rm pf}(\phi, U_\epsilon^\Pi) - \frac{1}{12}S_{\rm pf}(\phi, U_{2\epsilon}^\Pi), \qquad (U_\epsilon^\Pi)_\mu(x) = e^{\epsilon\Pi_\mu(x)}U_\mu(x), \qquad (4.83)$$

where ϵ is a small parameter i.e. $\epsilon \ll 1$. In fact, only the dynamical links are changed in the above transformation. It is then easy to show that,

$$\frac{dS}{dt} \equiv \frac{1}{\epsilon}(S_\epsilon^\Pi - S_{-\epsilon}^\Pi) \xrightarrow{\epsilon \to 0} F = \sum_{x,\mu} \Pi_\mu^a(x)\partial_{x,\mu}^a S_{\rm pf}. \qquad (4.84)$$

As anticipated, the evaluation of the two terms above permits to check the consistency between force and action computation.

In Table 4.1 we present some results we have obtained for a given choice of lattice parameters, for the different actions and forces introduced in Section 4.2. Note that we adopt the following notation:

- STD: standard single pseudo-fermion representation of the quark determinant. The associated force and action are: $F_\mu^{(1)}(x)$ and $S_{\rm pf}^{(1)}$ (cf. (4.29) and (4.26)).

- HAS: Hasenbusch (twisted-mass) factorization of the quark determinant (4.18), and corresponding pseudo-fermion representation. In particular, here we consider the case with only two pseudo-fermions. Then, the associated force and action for the single ratio of determinants are: $F_\mu^{(2)}(x)$ and $S_{\rm pf}^{(2)}$ (cf. (4.41) and (4.34)).

- EO: single pseudo-fermion representation of the even-odd preconditioned quark-determinant (4.58), excluding the contribution of the small determinant (4.64). The associated force and action are: $F_\mu^{(4)}(x)$ and $S_{\rm pf}^{(4)}$ (cf. (4.68) and (4.65)).

- EO+SDET: as above but including the contribution from the small determinant.

- EO+HAS: Hasenbusch (twisted-mass) factorization of the even-odd preconditioned quark determinant (4.62), and corresponding pseudo-fermion representation. In particular, here we consider the case with only two pseudo-fermions. Then, the associated force and action for the single ratio of determinants are: $F_\mu^{(5)}(x)$ and $S_{\rm pf}^{(5)}$ (cf. (4.79) and (4.73)),

In Table 4.1 we also include a comparison of the action computation with the corresponding pseudo-fermion generation. This is obtained by firstly generating some

Gaussian-distributed fields ξ with action $S = \frac{1}{2}(\xi, \xi)$. Then, given the fields ξ, one can compute the pseudo-fermion fields ϕ as discussed in the previous section, and evaluate the corresponding action $S_{\text{pf}}^{(i)}$. If the generation of the fields ϕ is correct, the two actions should coincide i.e. $S = S_{\text{pf}}^{(i)}$.

Table 4.1 Results for the consistency checks of the action and force computations, and pseudo-fermion generation. The results are obtained for a given pseudo-fermion field ϕ, gauge field configuration U, and momenta Π. The lattice considered has: $L/a = T/a = 8$. The values for the twisted-masses are $a\mu_0 = 0.1$ and $a\mu_1 = 1.0$. The CG solver residuum is res $= 10^{-12}$, and $\epsilon = 10^{-4}$.

|	STD	EO	EO + SDET	HAS	EO+HAS
$\left\|\frac{\mathrm{d}S}{\mathrm{d}t}/F - 1\right\|$	3.12e-08	2.44e-08	3.86e-08	9.47e-08	3.77e-07
$\left\|S - S_{\text{pf}}\right\|$	1.50e-08	8.50e-09	4.80e-09	2.50e-08	1.5e-08

As we can see from the table, the results are generally good for both tests, and for all types of preconditioning. They are indeed consistent with the ones (roughly) expected, considering the size of the lattice volume, and the chosen CG residuum.

To conclude, in order to check the consistency of the force and action computation as integrated into the HMC, we have performed the following additional test. Given an initial pseudo-fermion field ϕ, gauge configuration U, and momenta configuration Π, we have integrated numerically the MD equations up to a fixed time $t = \tau$ for several different values of the step-size ϵ. We have then measured the difference ΔH in the Hamiltonian at the beginning, and at the end of the MD trajectories as in (4.10). If the computation of the action and forces is consistent, we then expect $\Delta H \propto \epsilon^n$, where n depends on the order of the numerical integrator.

In Figure 4.1, we present the results for a 2nd and 4th order integrator for some given lattice parameters, and different values of the integration step-size ϵ at fixed $\tau = 2$. The details of the numerical integrators can be found in (Lüscher and Schaefer, 2013). Note that we consider simulations of $N_{\text{f}} = 2$ O(a)-improved Wilson-fermion with χSF boundary conditions, and we employ both Hansenbush and even-odd preconditioning. Without entering into the details, in principle we expect for the given 2nd and 4th

Fig. 4.1: $|\Delta H|$ as a function of the step-size. Data obtained from a single trajectory of length $\tau = 2$, for fixed ϕ, U, and Π. The simulations considered are for $N_{\mathrm{f}} = 2$ O(a)-improved Wilson-fermions with χSF boundary conditions; both Hasenbusch and even-odd preconditioning are used. The lattice considered has $L/a = T/a = 8$, and the twisted-masses are given by $a\mu_0 = 0.0$ and $a\mu_1 = 1.2$. Note that the gauge force is integrated on a much finer time-scale through a 4th order integrator.

(a) 2nd order integrator

(b) 4th order integrator
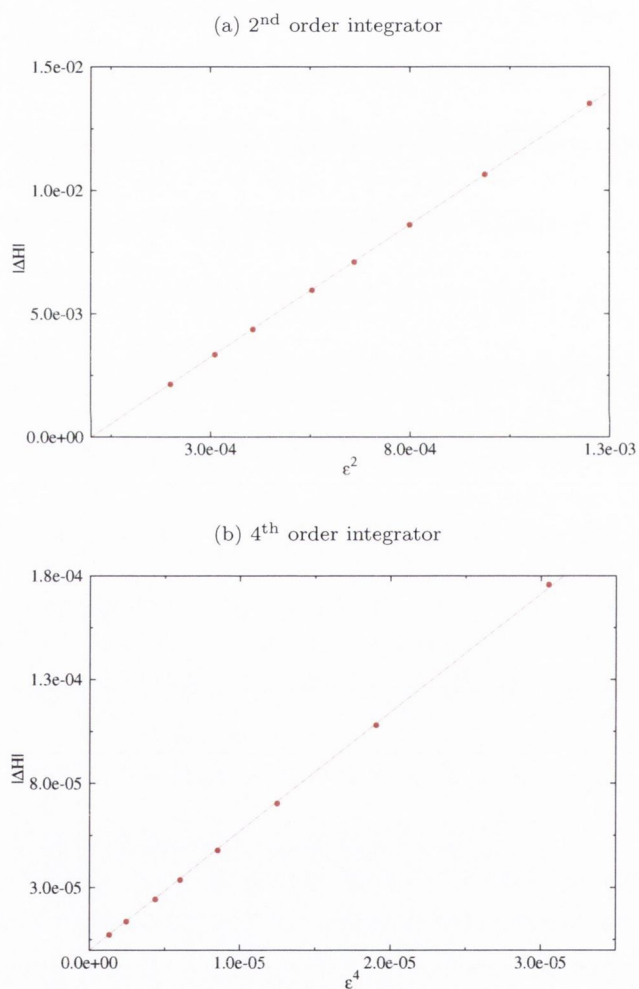
order integrators: $\Delta H \propto \epsilon^2$ and $\Delta H \propto \epsilon^4$, respectively; this assuming that the value of ϵ is small enough that higher-order terms in ϵ are negligible in ΔH.

As we can see from the figure, this is nicely the case. Note that the results at each ϵ are obtained from a single MD trajectory, and the line on the plot is a linear fit of the data constrained to zero.

4.3.2   Check on the preconditionings

In this concluding subsection, we present some tests we have performed in order to check the equivalence of the different types of preconditioning implemented. More precisely, for a given choice of lattice parameters, we have computed a set of different observables using simulations where different representations of the quark determinant have been employed. If the preconditionings are all well-implemented, we then expect the results from the different simulations to agree within their statistical uncertainties.

Specifically, for the test we have considered simulations of $N_f = 2$ $O(a)$-improved massless Wilson-fermions with χSF boundary conditions. The given lattice parameters are: $L/a = T/a = 6$, and $\beta = 6/g_0^2 = 5.6$. The observables we have studied then are the average plaquette (Plaq), and the energy density as defined through the Gradient flow (Lüscher, 2010b). In particular, we have measured two different discretizations of the energy density denoted in the following by W_{act} and Y_{act}. The details of these discretizations are unimportant for the present discussion. Note however that, W_{act} and Y_{act}, have been computed for a value of the flow time t specified by $c = \sqrt{8t}/L = 0.3$. This is in general a sensible value to obtain a good statistical precision for these observables (Fritzsch and Ramos, 2013). Finally, we have generated roughly 240.000 MD trajectories of length $\tau = 2$, corresponding to 480.000 molecular dynamics units (MDU). In particular, the plaquette has been measured at each trajectory finding an integrated autocorrelation time of $\tau_{\text{int}} \sim 4 - 5\,\text{MDU}$, while the Gradient flow observables every 5 trajectories without detecting any autocorrelation.

In Table 4.2, we report the results of the simulations for the three observables considered, and the different types of preconditioning. Similarly to the previous subsection, we adopt the following notation:

- STD: standard single pseudo-fermion representation of the quark determinant. The twisted-mass is set to zero i.e. $a\mu_0 = 0.0$.

- HAS: Hasenbusch factorization of the quark determinant (4.18) considering two pseudo-fermions with twisted-masses: $a\mu_0 = 0.0$, and $a\mu_1 = 1.2$.

- EO: single pseudo-fermion representation of the even-odd preconditioned quark-determinant (4.58). The twisted-mass is set to zero i.e. $a\mu_0 = 0.0$.

- EO+HAS : Hasenbusch factorization of the even-odd preconditioned quark determinant (4.62) considering two pseudo-fermions with twisted-masses: $a\mu_0 = 0.0$, and $a\mu_1 = 1.2$.

Note that we have set the twisted-mass μ_0 to zero, as otherwise a reweighting would have been needed to compare the results with and without even-odd preconditioning.

Table 4.2 Results for the average plaquette, and Gradient flow energy densities W_{act}, and Y_{act}, for different types of preconditioning.

$\mathcal{O}$	STD	HAS	EO	EO+HAS
Plaq	1.89463(4)	1.89469(5)	1.89469(5)	1.89466(5)
Y_{act}	377.8(1)	377.8(1)	377.8(1)	377.9(1)
W_{act}	732.5(2)	732.4(2)	732.4(2)	732.6(2)

As we can see from the results in the table, the precision on the plaquette is very good. Nevertheless very good agreement is found between all preconditionings. Similar conclusions can be drawn for the Gradient flow energy densities. In this case, it is interesting to note that the difference between W_{act} and Y_{act}, which is roughly a factor 2, is in fact a pure discretization effect.

To conclude, just to give an idea about timings, we report in Table 4.3 the average time taken by the different simulations to compute a single trajectory. Note that the P_{acc} has been tuned in order to be roughly equal in all runs i.e. $P_{\mathrm{acc}} \sim 0.90-0.95$. As we can see from the table, the gain from the even-odd preconditioning is evident, almost a factor 4. A bit surprisingly, also the Hasenbusch preconditioning helps considerably, even though we have considered a very small lattice volume. Finally, note that if

the two preconditionings are combined together, an overall factor of 5 in speed up is obtained. These results remarkably show the effectiveness of these preconditionings.

Table 4.3 Average time per trajectory for the different preconditionings.

	Time (s)
STD	31
HAS	17
EO	8
EO+HAS	6

5
The chirally rotated SF at work

In the previous chapter we discussed in detail the numerical implementation of the χSF, and presented some consistency checks on the basic algorithm. Assuming the correctness of the latter, in this concluding chapter we want to study some applications of the method. In particular, we are interested in providing evidence for the two main features expected from the χSF with Wilson-fermions, namely: the universality of its continuum limit with the standard SF regularization, and the realization of automatic $O(a)$ improvement in the chiral limit. Note that these properties have been confirmed in detailed studies in the quenched approximation (Sint and Leder, 2010; Lopez, Jansen, Renner and Shindler, 2013a; Lopez, Jansen, Renner and Shindler, 2013b), and recently also to 1-loop order in perturbation theory (Vilaseca, 2013). In this work, the non-trivial question we want to answer is whether these features also hold when the non-perturbative continuum limit of the full theory is considered. In this respect, we will focus on the theory with $N_{\mathrm{f}} = 2$ dynamical massless Wilson-fermions with χSF boundary conditions. For this case in fact, many results are available for comparison with the standard SF regularization.

The chapter thus begins by setting-up the connection between SF and χSF. More precisely, starting from a standard set of SF correlation functions, we study formally in the continuum their chiral rotation. We then determine the corresponding set of χSF correlation functions, and the expected universality relations. The corresponding lattice correlation functions and $O(a)$ counterterms are also commented.

Secondly, given the universality relations we will study their consequences on the lattice. As we already remarked, on the lattice these relations are expected to be valid among properly renormalized lattice correlation functions up to discretization effects. The idea is thus simply to define a suitable set of observables and test whether

the expected universality relations are correctly recovered in the continuum limit. As we shall see, as a by-product of this investigation we will determine several finite renormalization constants of interest related to the breaking of chiral symmetry by Wilson-fermions. In addition, these observables will provide a non-trivial check for automatic $O(a)$ improvement in the χSF. Indeed, by studying the continuum limit of these quantities we will be able to determine if the expected scaling is realized.

Before presenting any results, however, a crucial issue needs to be addressed first. As presented, the correct chirally rotated boundary conditions are obtained in the continuum limit only if the finite renormalization parameter $z_f(g_0)$ is properly tuned (cf. Section 3.4.3). As also discussed, this parameter can be fixed by imposing at finite lattice spacing parity and/or flavour restoration on a given observable. On the other hand, in order to obtain automatic $O(a)$ improvement one needs to simultaneously tune the quark masses to zero. At finite lattice spacing this simultaneous tuning of z_f and the bare quark masses might present some difficulty due to the presence of discretization effects. It is thus important to understand whether the tuning is feasible at the relevant values of the lattice spacing in simulations.

Finally, the chapter is concluded with a detailed analysis of the correctness of the simulations. Specifically, this includes: a study of the reversibility and measure preserving properties of the MD integrator in the HMC, an estimation of the longest autocorrelation times in the simulations, and an investigation of the ergodicity of the algorithm in sampling the topological sectors.

5.1 Correlation functions and universality relations

As anticipated, in this section we want to present the χSF correlation functions and corresponding universality relations that will be studied later in the chapter. To this end, after some comments on the specific set-up we are considering, we will introduce a set of suitable correlation functions in the standard SF base. Then, by performing the proper chiral rotation we will obtain the corresponding correlation functions in the χSF, and derive the universality relations of interest. The section is thus concluded with a discussion of the corresponding lattice correlation functions, and their $O(a)$

counterterms. Note that most of the details here presented can be found in a condensed form in (Sint and Leder, 2010).[1]

5.1.1 Flavour structure

So far we have assumed the quark fields to be doublets consisting of an up and down type quarks, i.e.,

$$\psi = \begin{pmatrix} \psi_u \\ \psi_d \end{pmatrix}. \tag{5.1}$$

In practice, however, it is convenient to look at the correlation functions obtained in a theory with four flavours of quarks. In the following, the quark fields will be then assumed to be of the form,

$$\psi = \begin{pmatrix} \psi_u \\ \psi_d \\ \psi_{u'} \\ \psi_{d'} \end{pmatrix}, \tag{5.2}$$

where we consider two up and two down type flavours of quarks.

Given this definition, the chiral rotation (3.58) is redefined as,

$$\psi' = R(\alpha)\psi, \qquad \overline{\psi}' = \overline{\psi}R(\alpha), \qquad R(\alpha) = e^{i\alpha\gamma_5(\mathbb{1}_2 \otimes \frac{\tau^3}{2})}, \tag{5.3}$$

where, $\mathbb{1}_2 \otimes \tau^3 = \text{diag}(1, -1, 1, -1)$. The χSF boundary conditions (3.62) are also modified accordingly, and are now specified by the projectors,

$$\tilde{Q}_\pm = \text{diag}(Q_\pm, Q_\mp, Q_\pm, Q_\mp), \qquad Q_\pm = \tfrac{1}{2}(1 \pm i\gamma_0\gamma_5). \tag{5.4}$$

After this short remark we can proceed and present the correlation functions of interest in the standard SF base.

5.1.2 SF correlation functions

The SF correlation functions that we are interested in involve the quark-bilinear fields introduced in the context of the WIs (cf. Section 2.1.2 and Section 2.2.3). Differently

---

[1] The author thanks Stefan Sint and Björn Leder for sharing several notes before publication. The presentation given in this section is based on this material.

from our original presentation, however, here we work with operators with definite flavour assignment instead of isospin index. This means that, for example, we consider the axial and vector currents specified by,

$$A_\mu^{f_1 f_2} = \overline{\psi}_{f_1} \gamma_\mu \gamma_5 \psi_{f_2}, \qquad V_\mu^{f_1 f_2} = \overline{\psi}_{f_1} \gamma_\mu \psi_{f_2}, \tag{5.5}$$

where the flavour indices f_1 and f_2 stand for u, d and eventually u', d'. Obviously these operators can be obtained from the definitions given in (2.13) and (2.19), by simply taking appropriate linear combinations of the generators of the flavour group. In particular, note that in the following we only consider flavour non-singlet operators. We thus exclude any operator with flavour assignment $f_1 = f_2$.

In addition to the flavour currents presented above, we also study the scalar and pseudo-scalar densities (cf. (2.20) and (2.17)),

$$S^{f_1 f_2} = \overline{\psi}_{f_1} \psi_{f_2}, \qquad P^{f_1 f_2} = \overline{\psi}_{f_1} \gamma_5 \psi_{f_2}, \tag{5.6}$$

and the tensor density (cf. (2.46)),

$$T_{\mu\nu}^{f_1 f_2} = \overline{\psi}_{f_1} i\sigma_{\mu\nu} \psi_{f_2}. \tag{5.7}$$

For completeness we then include the pseudo-tensor density,

$$\widetilde{T}_{\mu\nu}^{f_1 f_2} = \overline{\psi}_{f_1} i\gamma_5 \sigma_{\mu\nu} \psi_{f_2}, \tag{5.8}$$

since this is naturally obtained from a chiral rotation of the tensor density.

The SF correlation functions of interest are now defined as two-point functions of the quark bilinear operators introduced above, and bilinears of the zero-momentum components of the boundary fields, $\zeta(\mathbf{y}), \ldots, \overline{\zeta}(\mathbf{z})$. Specifically, we first consider the bilinear boundary operator (3.21) with definite flavour assignment, namely,

$$\mathcal{O}_5^{f_1 f_2} = \int d^3\mathbf{y} d^3\mathbf{z}\, \overline{\zeta}_{f_1}(\mathbf{y}) P_+ \gamma_5 \zeta_{f_2}(\mathbf{z}). \tag{5.9}$$

Note that comparing with the definition (3.21) an additional projector P_+ appeared. However, taking into account the boundary conditions for the fields it is easy to see that this projector is in fact redundant (cf. (3.20)). On the other hand, it is useful to remind us which are the non-Dirichlet field components at the boundaries.

Given this definition, we can now introduce the first set of boundary-to-bulk SF correlation functions defined by (Lüscher, Sint, Sommer and Weisz, 1996; Lüscher and Weisz, 1996; Sint and Weisz, 1997),

$$f_X(x_0) = -\frac{1}{2}\left\langle X^{f_1 f_2}(x)\mathcal{O}_5^{f_2 f_1}\right\rangle_{(P_+)}, \tag{5.10}$$

where X stands for $X = A_0, V_0, S, P$. As a first remark, note that due to translation invariance in the spatial directions, these correlation functions only depend on x_0. Secondly, f_V and f_S are odd under parity and consequently vanish (cf. Section A.6.2). This is also true on the lattice with standard SF boundary conditions. These correlation functions, however, are still interesting since at finite lattice spacing not all of their chirally rotated counterparts are automatically zero. This because, as discussed, the lattice χSF explicit breaks parity, which is only recovered up to a flavour exchange.

In addition to the f_X correlation functions, we can consider correlation functions involving fields with an open spatial index k. In order to define these, we first need to introduce the bilinear boundary operator,

$$\mathcal{O}_k^{f_1 f_2} = \int d^3\mathbf{y}\, d^3\mathbf{z}\, \overline{\zeta}_{f_1}(\mathbf{y})\gamma_k P_-\zeta_{f_2}(\mathbf{z}). \tag{5.11}$$

Given this definition, the new set of correlation functions is specified by,

$$k_Y(x_0) = -\frac{1}{6}\sum_{k=1}^{3}\left\langle Y_k^{f_1 f_2}(x)\mathcal{O}_k^{f_2 f_1}\right\rangle_{(P_+)}, \tag{5.12}$$

where the fields Y_k stand for the bilinear quark-fields, $Y_k = A_k, V_k, T_{0k}, \widetilde{T}_{0k}$. Note that, in this case, parity symmetry implies $k_A = k_{\widetilde{T}} = 0$.

Finally, we define the boundary-to-boundary correlators,

$$f_1 = -\frac{1}{2}\left\langle \mathcal{O}_5^{f_1 f_2}\mathcal{O}_5'^{f_2 f_1}\right\rangle_{(P_+)}, \qquad k_1 = -\frac{1}{6}\sum_{k=1}^{3}\left\langle \mathcal{O}_k^{f_1 f_2}(x)\mathcal{O}_k'^{f_2 f_1}\right\rangle_{(P_+)}, \tag{5.13}$$

where the source fields at upper-time boundary are given by,

$$\mathcal{O}_5'^{f_1 f_2} = \int d^3\mathbf{y}\, d^3\mathbf{z}\, \overline{\zeta}'_{f_1}(\mathbf{y})P_-\gamma_5\zeta'_{f_2}(\mathbf{z}), \tag{5.14}$$

$$\mathcal{O}_k'^{f_1 f_2} = \int d^3\mathbf{y}\, d^3\mathbf{z}\, \overline{\zeta}'_{f_1}(\mathbf{y})\gamma_k P_+\zeta'_{f_2}(\mathbf{z}). \tag{5.15}$$

To conclude, we note that if only non-singlet operators are considered, the flavour indices on the correlation functions are redundant in the case of standard SF boundary

conditions. This is true both in the continuum and on the lattice, since in both cases the Dirac operator and boundary conditions are trivial in flavour space. Hence, one has for example that: $f_X^{uu'} = f_X^{dd'} = f_X^{ud} = f_X^{du}$, and similarly for the k_Y functions, and the boundary-to-boundary correlators. However, it is important to specify the exact flavour assignment once we consider the rotation of these correlation functions to the χSF base. The chiral rotation, indeed, distinguishes between up and down quark-flavours (cf. (5.3)), and thus different flavour assignments correspond to different χSF correlation functions. Note that, at least in the continuum, this does not mean that flavour symmetries are broken by the χSF boundary conditions, but rather that the flavour symmetries of the standard SF assume a different form in the χSF (Sint, 2011).

5.1.3 χSF correlation functions and universality relations

Given the SF correlation functions presented in the previous subsection, it is now easy to derive the corresponding χSF correlation functions. Indeed, these are obtained by simply considering the relation (3.63) now defined in terms of the transformation (5.3). More precisely, we have,

$$\langle O[R(\pi/2)\psi, \overline{\psi}R(\pi/2)]\mathcal{Q}^{f_1 f_2}\rangle_{(\tilde{Q}_+)} = \langle O[\psi, \overline{\psi}]\mathcal{O}^{f_1 f_2}\rangle_{(P_+)}, \tag{5.16}$$

where O is a generic quark bilinear operator, while the χSF bilinear source field $\mathcal{Q}^{f_1 f_2}$ is obtained by chirally rotating the bilinear SF boundary field $\mathcal{O}^{f_1 f_2}$. In Appendix C, we collected the results for the operators $\mathcal{Q}^{f_1 f_2}$ corresponding to the SF boundary fields $\mathcal{O}_5^{f_1 f_2}$ and $\mathcal{O}_k^{f_1 f_2}$.

Having these definitions, the χSF correlation functions related to the SF correlators f_X can be easily found. Indeed, if we define the χSF two-point functions g_X of the operators $X = V_0, A_0, S, P$, as,

$$g_X^{f_1 f_2}(x_0) = -\frac{1}{2}\left\langle X^{f_1 f_2}(x)\mathcal{Q}_5^{f_2 f_1}\right\rangle_{(\tilde{Q}_+)}, \tag{5.17}$$

it is easy to work out the following universality relations (Sint and Leder, 2010),

$$f_A = g_A^{uu'} = g_A^{dd'} = -ig_V^{ud} = ig_V^{du}, \tag{5.18}$$

$$f_P = ig_S^{uu'} = -ig_S^{dd'} = g_P^{ud} = g_P^{du}, \tag{5.19}$$

$$f_V = g_V^{uu'} = g_V^{dd'} = -ig_A^{ud} = ig_A^{du}, \tag{5.20}$$

$$f_S = ig_P^{uu'} = -ig_P^{dd'} = g_S^{ud} = g_S^{du}. \tag{5.21}$$

Thus, choosing different flavour combinations in the SF correlation functions, and applying the corresponding chiral rotation, we can obtain several non-trivial relations among χSF correlation functions with different flavour assignment and quark-bilinear insertions. In fact we note that, given our definition of the boundary fields in the χSF, the corresponding transformation properties of the correlation functions are simply found by considering the chiral transformations of the quark-bilinears X.

Analogously to the case of the g_X functions, if we introduce the χSF correlation functions of the bilinear fields $Y_k = A_k, V_k, T_{0k}, \widetilde{T}_{0k}$, defined by,

$$l_Y^{f_1 f_2}(x_0) = -\frac{1}{6} \sum_{k=1}^{3} \left\langle Y_k^{f_1 f_2}(x) \mathcal{Q}_k^{f_2 f_1} \right\rangle_{(\tilde{Q}_+)}, \tag{5.22}$$

the following universality relations with the SF correlation functions k_Y are easy to derive (Sint and Leder, 2010),

$$k_V = l_V^{uu'} = l_V^{dd'} = -il_A^{ud} = il_A^{du}, \tag{5.23}$$

$$k_A = l_A^{uu'} = l_A^{dd'} = -il_V^{ud} = il_V^{du}, \tag{5.24}$$

$$k_T = il_{\widetilde{T}}^{uu'} = -il_{\widetilde{T}}^{dd'} = l_T^{ud} = l_T^{du}, \tag{5.25}$$

$$k_{\widetilde{T}} = il_T^{uu'} = -il_T^{dd'} = l_{\widetilde{T}}^{ud} = l_{\widetilde{T}}^{du}. \tag{5.26}$$

Finally, we can define the boundary-to-boundary χSF correlators,

$$g_1^{f_1 f_2} = -\frac{1}{2} \left\langle \mathcal{Q}_5^{f_1 f_2} \mathcal{Q}_5'^{f_2 f_1} \right\rangle_{(\tilde{Q}_+)}, \tag{5.27}$$

$$l_1^{f_1 f_2} = -\frac{1}{6} \sum_{k=1}^{3} \left\langle \mathcal{Q}_k^{f_1 f_2} \mathcal{Q}_k'^{f_2 f_1} \right\rangle_{(\tilde{Q}_+)}, \tag{5.28}$$

where again we collected the results for the boundary fields $\mathcal{Q}'^{f_1 f_2}$ corresponding to the SF source fields $\mathcal{O}_5'^{f_1 f_2}$ and $\mathcal{O}_k'^{f_1 f_2}$ in Appendix C.

It is then easy to find the universality relations,

$$f_1 = g_1^{uu'} = g_1^{dd'} = g_1^{ud} = g_1^{du}, \tag{5.29}$$

$$k_1 = l_1^{uu'} = l_1^{dd'} = l_1^{ud} = l_1^{du}. \tag{5.30}$$

In conclusion, we obtained several formal relations between χSF and SF correlation functions. However, as discussed, once we move to the lattice these relations are not expected to be exact anymore. Even at zero quark-mass, indeed, the Wilson bulk action is not invariant under the chiral rotation (5.3), and the general relations (5.16) can not be derived. On the other hand, we expect these relations to be valid up to discretization effects among properly renormalized lattice correlation functions, such that once the continuum limit is taken the universality relations are recovered. In the next section, we will investigate in detail some of the consequences of this expectation. Before that, we conclude this section with a short discussion on the lattice definition of the χSF correlation functions here introduced, and their O(a) counterterms.

5.1.4 χSF correlation functions on the lattice

Given the formal continuum definition of the χSF correlation functions, it is easy to define their lattice counterparts. First of all, the bilinear quark fields X and Y are easily regularized on the lattice (cf. Section 2.1.2 and Section 2.2.3). In this respect, we recall that in the case of the vector current one can either consider the local (cf. (2.13)) or point-split definition (cf. (2.35)). The latter does not requite any finite renormalization, and in addition satisfies for degenerate quark masses the conservation law (2.34). Note that this relation holds in the interior of the lattice volume, independently from the specific χSF boundary conditions considered.

Secondly, as we have seen, the lattice boundary source fields are obtained from their continuum counterparts by simply replacing the space integrals with spatial sums (cf. (3.34)). As an example, if we consider the continuum field (C.1), the corresponding lattice field reads,

$$\mathcal{Q}_5^{uu'} = a^6 \sum_{\mathbf{y},\mathbf{z}\in\Gamma} \bar{\zeta}_u(\mathbf{y})\gamma_0\gamma_5 Q_-\zeta_u(\mathbf{z}). \tag{5.31}$$

In particular we remind that when inserted in correlation functions, the boundary fields are equivalent to the following expressions in terms of quark fields,

$$\zeta(\mathbf{x}) = U_0(0, \mathbf{x})\tilde{Q}_-\psi(a, \mathbf{x}), \qquad \zeta'(\mathbf{x}) = U_0(T - a, \mathbf{x})^\dagger \tilde{Q}_-\psi(T - a, \mathbf{x}), \qquad (5.32)$$

$$\overline{\zeta}(\mathbf{x}) = \overline{\psi}(a, \mathbf{x})\tilde{Q}_+U_0(0, \mathbf{x})^\dagger, \qquad \overline{\zeta}'(\mathbf{x}) = \overline{\psi}(T - a, \mathbf{x})\tilde{Q}_+U_0(T - a, \mathbf{x}). \qquad (5.33)$$

As discussed in Section 3.4.3, this representation is correct only if Wick contractions of boundary fields at the same boundary are not present in the correlation functions. In the following, we will avoid the appearance of these contributions by choosing proper flavour assignments in the two-point functions. Moreover, note that we leave out the $O(a)$ boundary counterterm proportional to $\bar{d}_s(g_0)$ (cf. (3.84)). For most of the applications we will consider this is in fact not relevant.

Given these observations, it is now straightforward to determine the corresponding lattice expressions for the χSF correlation functions presented in the previous subsection. In particular, we can study their transformation properties w.r.t. the lattice symmetries, in order to determine some exact relations among different correlation functions or specific properties of individual correlators. In this respect, we collected some of these results in Appendix C. Here we just want to mention that in practice we can restrict ourselves to consider only correlation functions with flavour assignment uu' and ud, since the flavour combinations dd' and du are related to the former by exact lattice relations. Furthermore all correlation functions are found to be either real, purely imaginary or vanishing exactly.

To conclude, it is important for our analysis later on to identify the $O(a)$ operators counterterms to the lattice χSF correlation functions here introduced. As discussed, for this type of correlation functions, the $O(a)$ operator counterterms are determined by the corresponding counterterms to the quark-bilinears X and Y inserted in the bulk of the lattice volume (cf. Section 3.3). In fact, however, the given counterterms might contribute or not to the corresponding correlators g_X or l_Y. More precisely, given the results in Section 2.2.3, we obtain that for the vector correlators,

$$g_{V_I}^{f_1 f_2}(x_0) = g_V^{f_1 f_2}(x_0), \qquad (5.34)$$

$$l_{V_I}^{f_1 f_2}(x_0) = l_V^{f_1 f_2}(x_0) + c_V(g_0)\, a\tilde{\partial}_0 l_T^{f_1 f_2}, \qquad (5.35)$$

where V_I indicates as usual the improved (local) vector current (2.45). As we can see, the O(a) counterterm proportional to the spatial derivatives of the tensor correlator does not contribute to the g_V functions. This can be easily understood by noticing that in the χSF translation invariance is preserved along the spatial directions. Secondly, we remind that if the point-split vector $\widetilde{V}_\mu$ (cf. (2.35)) is considered in (5.35) instead of the local current, a different improvement coefficient $c_{\widetilde{V}}(g_0)$ is needed.

For the axial vector correlators the situation is somehow the other way around, namely,

$$g_{A_I}^{f_1 f_2}(x_0) = g_A^{f_1 f_2}(x_0) + c_A(g_0) \, a\tilde{\partial}_0 g_P^{f_1 f_2}, \tag{5.36}$$

$$l_{A_I}^{f_1 f_2}(x_0) = l_A^{f_1 f_2}(x_0). \tag{5.37}$$

Then, for the tensor and pseudo-tensor correlator we have,

$$l_{T_I}^{f_1 f_2}(x_0) = l_T^{f_1 f_2}(x_0) + c_T(g_0) \, a\tilde{\partial}_0 l_V^{f_1 f_2}, \tag{5.38}$$

$$l_{\widetilde{T}_I}^{f_1 f_2}(x_0) = l_{\widetilde{T}}^{f_1 f_2}(x_0) + c_{\widetilde{T}}(g_0) \, a\tilde{\partial}_0 l_A^{f_1 f_2}. \tag{5.39}$$

Finally, the scalar and pseudo-scalar correlators do not need any operator improvement, as we have seen, i.e.,

$$g_{P_I}^{f_1 f_2}(x_0) = g_P^{f_1 f_2}(x_0), \tag{5.40}$$

$$g_{S_I}^{f_1 f_2}(x_0) = g_S^{f_1 f_2}(x_0). \tag{5.41}$$

At this point, the reader might wonder why we considered this type of boundary-to-bulk and boundary-to-boundary correlation functions for our study. The reason is that thanks to the projection to zero momentum of both quark and anti-quark fields at the boundary, these correlation functions are expected to have in general milder cutoff effects and better statistical precision than gauge invariant correlation functions involving only bulk operators (see e.g. (Della Morte, Sommer and Takeda, 2009)).

5.2   Renormalization conditions and O(a) improvement

Given the universality relations between SF and χSF correlation functions presented in the previous section, a non-trivial question now is whether these relations are correctly

recovered once the continuum limit of the properly renormalized lattice correlation functions is taken. In this section, we will thus define a set of suitable observables that will allow us to address this question. In addition, the investigation of these quantities will give us the opportunity to confirm whether the property of automatic $O(a)$ is at work as expected for the χSF.

More precisely, in the next subsection we will define several ratios of χSF two-point functions which are expected to converge to a common continuum limit due to some universality relation. In fact, at finite lattice spacing these ratios are related to finite renormalization constants originating from the breaking of chiral symmetry by Wilson-fermions (cf. Section 2.1.3). Similarly, we will also consider ratios of boundary-to-boundary correlators which are again expected to converge to the same continuum limit because of some universality relation. Finally, we will define the basic tools to study the non-perturbative running of the quark-masses in the SF and χSF. More precisely, we will introduce a finite-volume renormalization scheme for the pseudo-scalar density, and the corresponding step-scaling function. Studying the continuum limit of these functions will then provide a direct test of the universality between SF and χSF.

5.2.1   Renormalization conditions from universality relations

The starting point is given by the formal continuum relations (5.18)-(5.21) and (5.23)-(5.26). As discussed, on the lattice these relations are expected to be valid up to discretization effects among properly renormalized correlation functions. Starting from this assumption, we consider the following set of relations involving the $\gamma_5\tau^1$-even boundary-to-bulk two-point functions,

$$(g_A^{uu'})_R = (-ig_V^{ud})_R + O(a^2), \qquad (ig_S^{uu'})_R = (g_P^{ud})_R + O(a^2),$$

$$(l_V^{uu'})_R = (-il_A^{ud})_R + O(a^2), \qquad (il_{\widetilde{T}}^{uu'})_R = (l_T^{ud})_R + O(a^2). \qquad (5.42)$$

Note that if automatic $O(a)$ improvement is at work, the expected discretization effects in these relations are of other $O(a^2)$. This will be presented in detail in Section 5.2.4.

Given the above relations, we remind that the renormalization of the correlation functions we are considering simply involves the renormalization of the boundary fields

with the appropriate factors Z_ζ, and the renormalization of the quark-bilinears X and Y. More precisely, we have,

$$(g_X)_R = Z_\zeta Z_X g_X, \qquad (l_Y)_R = Z_\zeta Z_Y l_Y, \tag{5.43}$$

where Z_X and Z_Y correspond to the renormalization factors of the quark bilinear X and Y, respectively. Considering a definite example we have,

$$Z_\zeta^2 Z_A g_A^{uu'} = -i Z_\zeta^2 Z_V g_V^{ud} + \mathrm{O}(a^2), \tag{5.44}$$

and consequently,

$$\frac{g_A^{uu'}}{-i g_V^{ud}} = \frac{Z_V}{Z_A} + \mathrm{O}(a^2). \tag{5.45}$$

As we can see, the ratio of these bare correlation functions corresponds, up to cutoff effects, to the ratio of the finite renormalization constants related to the local vector and axial currents (cf. Section 2.1.3). This ratio is then expected to have a well-defined continuum limit simply given by 1, which could be verified explicitly.

For the purpose of our analysis, however, it is more convenient to somehow turn the tables. Once the validity of the universality relations is assumed, we can use the ratio of bare two-point functions to actually *define* a renormalization condition for the finite renormalization constants. By comparing different definitions of these renormalization factors also including determinations from the standard SF, we will then be able to assess if the assumed hypothesis of universality was well founded. As we will discuss in more detail later in this section, the advantage of this approach is that the difference between these definitions is expected to scale to the continuum limit as $\mathrm{O}(a^2)$. This is easy to verify numerically, and the actual scaling will provide a check for automatic $\mathrm{O}(a)$ improvement. The continuum limit of (5.45), instead, is reached only logarithmically with a due to the contribution of the finite renormalization constants. A direct verification of the approach of this ratio to 1 is then more difficult to perform through non-perturbative studies. This, however, is a possible approach to consider in order to verify universality in perturbation theory (Vilaseca, 2013).

This said, the renormalization conditions for the finite renormalization constants can be simply obtained by imposing the validity of the expected continuum relations

on properly renormalized lattice correlation functions. Given the relation (5.44) for example, we can define (Sint and Leder, 2010),

$$\frac{Z_V}{Z_A} \equiv \left.\frac{g_A^{uu'}(x_0)}{-ig_V^{ud}(x_0)}\right|_{x_0=\frac{T}{2}}. \tag{5.46}$$

Note that it is convenient to measure the correlation functions in the middle of the lattice in order to maximize the distance from the boundaries, and thus minimize the corresponding cutoff effects. The actual renormalization condition is then specified by several other details related to the specific χSF set-up, as for example the boundary conditions for the fields and the geometry. These will be discussed in the next section.

Given the relation (5.46), we note that if we use the point-split discretization of the vector current we can obtain directly the renormalization factor for the local axial current Z_A, specifically,

$$Z_A^g \equiv \left.\frac{-ig_{\widetilde{V}}^{ud}(x_0)}{g_A^{uu'}(x_0)}\right|_{x_0=\frac{T}{2}}. \tag{5.47}$$

Considering then other universality relations in (5.42), the renormalization of the axial current can also be defined by the ratio,

$$Z_A^l \equiv \left.\frac{il_{\widetilde{V}}^{uu'}(x_0)}{l_A^{ud}(x_0)}\right|_{x_0=\frac{T}{2}}. \tag{5.48}$$

The renormalization of the local vector current instead, can be obtained by comparing matrix elements of the local and point-split vector currents as,

$$Z_V^g \equiv \left.\frac{g_{\widetilde{V}}^{ud}(x_0)}{g_V^{ud}(x_0)}\right|_{x_0=\frac{T}{2}}, \qquad Z_V^l \equiv \left.\frac{l_{\widetilde{V}}^{uu'}(x_0)}{l_V^{uu'}(x_0)}\right|_{x_0=\frac{T}{2}}. \tag{5.49}$$

Given the above definitions, we can also consider the somehow "mixed" definition of the axial current renormalization defined by,

$$Z_A^{lg} \equiv \left.\frac{Z_V^g \, il_V^{uu'}(x_0)}{l_A^{ud}(x_0)}\right|_{x_0=\frac{T}{2}}. \tag{5.50}$$

This will be useful later on in our scaling studies.

Finally, in similar fashion, from the relations (5.42) we can define finite ratios of scale-dependent renormalization constants belonging to the same chiral multiplet, e.g.,

$$\frac{Z_P}{Z_S} \equiv \left.\frac{ig_S^{uu'}(x_0)}{g_P^{ud}(x_0)}\right|_{x_0=\frac{T}{2}}, \qquad \frac{Z_T}{Z_{\widetilde{T}}} \equiv \left.\frac{il_{\widetilde{T}}^{uu'}(x_0)}{l_T^{ud}(x_0)}\right|_{x_0=\frac{T}{2}}. \tag{5.51}$$

To conclude, a few observations are in order. Firstly, note that in principle we could define the renormalization conditions above in terms of the corresponding improved correlation functions (5.34)-(5.41). Just to give some examples we could then have,

$$
Z_{A_I}^g \equiv \left. \frac{-i g_{\tilde{V}}^{ud}(x_0)}{g_{A_I}^{uu'}(x_0)} \right|_{x_0 = \frac{T}{2}}, \qquad Z_{A_I}^l \equiv \left. \frac{i l_{\tilde{V}_I}^{uu'}(x_0)}{l_A^{ud}(x_0)} \right|_{x_0 = \frac{T}{2}}, \qquad Z_{V_I}^l \equiv \left. \frac{l_{\tilde{V}_I}^{uu'}(x_0)}{l_{V_I}^{uu'}(x_0)} \right|_{x_0 = \frac{T}{2}}. \qquad (5.52)
$$

However, if automatic $O(a)$ improvement holds the insertion of the $O(a)$ operator counterterms will only affects the results at $O(a^2)$.

In this respect, a second important remark is the following. The relations (5.46)-(5.52) only determine the finite renormalization factors up to $O(a^2)$ effects. Depending on the choice of the lattice size, the boundary values of the fields, or other kinematical parameters like x_0, different results for Z_V and Z_A will be obtained. One could then think that it is better to assign a systematic error to the normalization constants by studying these variations in detail. Since however it is difficult to judge which choices of parameters are "the more reasonable", this error estimates will turn out to be rather subjective. It is thus better to simply define the normalization constants through a particular normalization condition (Lüscher, Sint, Sommer and Wittig, 1997*b*; Guagnelli *et al.*, 2001). The physical matrix elements of the renormalized currents that one is interested in must then be calculated for a range of lattice spacings so as to be able to extrapolate the data to the continuum limit. The results obtained in this way are guaranteed to be independent of the chosen normalization condition, because any differences in the normalization constants of $O(a^2)$ extrapolate to zero together with the cutoff effects associated with the matrix elements. In particular note that also for these finite renormalization constants, a renormalization condition is not only specified by the boundary conditions for the fields and the geometry of the χSF, but also by the condition of constant physical spatial extent L. This said, it is always important to study different renormalization conditions in order to verify that the given definition of the renormalization constants does not have accidentally large $O(a^2)$ effects, which might render the continuum limit extrapolations difficult to be performed.

Finally, the fact that these finite renormalization constants can be obtained from the expected universality relations between the SF and χSF should not come as a

surprise. As discussed in Section 2.1.3, a possibility to determine these renormalization factors was simply to impose on a set of properly renormalized lattice correlation functions, the validity of some continuum WIs. In order words, one is imposing the restoration of chiral symmetry at finite lattice spacing on a set of observables. Here, the idea is the same, since the universality relations between SF and χSF are a simple manifestation of the chiral symmetry of the massless QCD action once considered in a finite volume with SF boundary conditions.

5.2.2 Flavour symmetry restoration

Other interesting observables can be obtained by considering the χSF boundary-to-boundary correlation functions. This corresponds to study the universality relations (5.29). Analogously to what we discussed in the previous subsection, on the lattice we expect these relations to be realized as,

$$(g_1^{uu'})_R = (g_1^{ud})_R + \mathrm{O}(a^2), \qquad (l_1^{uu'})_R = (l_1^{ud})_R + \mathrm{O}(a^2). \tag{5.53}$$

Note that again we have anticipated the expected $\mathrm{O}(a^2)$ scaling for these $\gamma_5\tau^1$-even correlation functions. We then remind that the renormalization of these two-point functions is simply determined by the multiplicative renormalization of the boundary quark fields, i.e.,

$$(g_1^{f_1 f_2})_R = Z_\zeta^4 g_1^{f_1 f_2}, \qquad (l_1^{f_1 f_2})_R = Z_\zeta^4 l_1^{f_1 f_2}. \tag{5.54}$$

Consequently the ratios,

$$\frac{g_1^{uu'}}{g_1^{ud}} = 1 + \mathrm{O}(a^2), \qquad \frac{l_1^{uu'}}{l_1^{ud}} = 1 + \mathrm{O}(a^2), \tag{5.55}$$

have a well-defined continuum limit, and should approach 1 with $\mathrm{O}(a^2)$ corrections. These observables thus offer some interesting probes for the realization of the correct relations in the continuum limit. In particular, since these ratios involve the same basic correlation function with different flavour assignments, they are a clear indicator of the breaking of flavour symmetry by the χSF with Wilson-fermions.

5.2.3   The running of the quark masses

So far we have only looked at universality relations involving χSF correlation functions. Even though the relations are implicitly based on the equivalence with some common SF correlator, we would like to consider some explicit example of the relation between SF and χSF. In this respect, we study the renormalization of the pseudo-scalar density, which as seen is related to the renormalization of the quark masses (cf. Section 2.1.3). The idea is to compare the determination of the renormalization factor Z_P as obtained from the SF and χSF. Of course, it is natural to define renormalization conditions in the SF and χSF such that the same renormalization scheme is obtained for the renormalized matrix elements of the pseudo-scalar density. In this way, the ratio of the renormalization factors Z_P's computed with the SF and χSF is expected to converge to 1 in the continuum limit.

Given this observation a simple definition for the renormalization constant Z_P in the SF and χSF can be obtained as (Capitani, Lüscher, Sommer and Wittig, 1999; Sint and Leder, 2010),

$$\frac{(f_P)_R}{\sqrt{(f_1)_R}} = \frac{f_P}{\sqrt{f_1}}\bigg|_{\text{tree}}, \qquad \frac{(g_P^{ud})_R}{\sqrt{(g_1^{ud})_R}} = \frac{g_P^{ud}}{\sqrt{g_1^{ud}}}\bigg|_{\text{tree}}, \tag{5.56}$$

where at a given value of the bare coupling g_0 we require the renormalized matrix elements to be equal to their tree level values. Note that in the above expressions, the boundary-to-boundary correlators f_1 and g_1^{ud} are used to cancel the boundary quark field renormalization factors Z_ζ.[2] The resulting expressions for the renormalization constant of the pseudo-scalar density are then given by,

$$Z_P^{\text{SF}}(g_0, L/a) = c(L/a)\frac{\sqrt{3f_1}}{f_P(x_0)}\bigg|_{x_0=\frac{T}{2}}, \qquad Z_P^{\chi\text{SF}}(g_0, L/a) = c'(L/a)\frac{\sqrt{3g_1^{ud}}}{g_P^{ud}(x_0)}\bigg|_{x_0=\frac{T}{2}}, \tag{5.57}$$

where the factors c and c' are chosen such that $Z_P^{\text{SF}/\chi\text{SF}}(0, L/a) = 1$. We stress that we defined a finite-volume renormalization scheme for Z_P by fixing the renormalization

---

[2] At this point we want to mention that the renormalization constants Z_ζ are not expected to be equal between the standard SF and χSF. Indeed, the ratio of these renormalization factors in the two set-ups is given by a finite function of g_0 that only approaches 1 in the continuum limit. This somehow limits the flexibility in defining suitable quantities to test universality. In particular, note that consequently the relation $f_P = g_P^{ud} + O(a^2)$ does not hold, but instead one has $f_P = g_P^{ud} + O(g_0^2)$.

scale in terms of the physical spatial extent of the volume L. To do this consistently we have to require $\rho = T/L$ to be a fixed ratio, and similarly for all other dimensionfull quantities that enter in the definition of Z_P (cf. Section 2.3.3). This will be commented in detail in the next section. Given these definitions we then expect,

$$\frac{Z_P^{\mathrm{SF}}}{Z_P^{\chi\mathrm{SF}}} = 1 + \mathrm{O}(a^2). \tag{5.58}$$

Related to the renormalization factor Z_P, another interesting quantity to consider is the corresponding step scaling function (cf. Section 2.3.3). As we have seen, a definition of a renormalized quark mass can be obtained as (cf. (2.31)),

$$m_R(\mu) = \lim_{a \to 0} Z_m(g_0, a\mu)\, m_{\mathrm{PCAC}}(g_0, am_0(g_0))\big|_{\bar{g}(\mu)}, \; Z_m(g_0, a\mu) = \frac{Z_A(g_0)}{Z_P(g_0, a\mu)}, \tag{5.59}$$

where $\bar{g}(\mu)$ is a given renormalized coupling which is kept fixed in order to keep the renormalization scale μ constant while approaching the continuum limit. The scheme for the quark masses is then implicitly specified by the renormalization scheme of Z_P. In particular, we can define a finite-volume scheme by considering the definition of Z_P given in (5.57), and as a renormalized coupling the SF coupling $\bar{g}^2(L)$ (Della Morte *et al.*, 2005*a*). In this way the renormalization scale of the quark masses is given in terms of the box size L, and finite size scaling can be applied to determine the running.

In practice, we recall, this is done by considering the step scaling function $\sigma_P(u)$ defined by (cf. Section 2.3.3),

$$\sigma_P(u) = \lim_{a \to 0} \Sigma_P(u, a/L), \qquad \Sigma_P(u, a/L) = \frac{Z_P(g_0, 2L/a)}{Z_P(g_0, L/a)}\bigg|_{u = \bar{g}^2(L)}. \tag{5.60}$$

From the definition (5.59), it is then easy to conclude that,

$$\sigma_P(u) = \frac{m_R(\mu)}{m_R(\mu/2)}, \qquad \mu = L^{-1}. \tag{5.61}$$

As anticipated, the step-scaling function describes the running of the quark masses. In particular, this function can be evaluated non-perturbatively through numerical simulations by applying the recipe (5.60). Eventually, once high-energies are reached the results can be compared with perturbation theory, and the conversion to other perturbative schemes is possible. For our analyze, however, the important observation is that we expect the step scaling function obtained from the lattice SF and χSF to be equal in the continuum limit.

5.2.4 Automatic $O(a)$ improvement

In the previous subsections, we introduced several interesting quantities in order to investigate the expected universality of the SF and χSF. Since a continuum limit is involved in this analyze, it is natural to exploit these observables to study also whether automatic $O(a)$ improvement is realized as expected for the χSF. The expectation is that, once the bare quark masses are tuned to their critical value, and the boundary renormalization parameter $z_f(g_0)$ is properly determined, then $O(a)$ contributions corresponding to $\gamma_5\tau^1$-odd counterterms will be absent in $\gamma_5\tau^1$-even observables (cf. Section 3.4). On the contrary, $\gamma_5\tau^1$-odd observables will be pure discretization effects, and will contain all these $O(a)$ contributions. As discussed, this in practice means that for $\gamma_5\tau^1$-even observables the $O(a)$ counterterms coming from the bulk action, and the operator insertions in the interior of the volume do not contribute at $O(a)$. The remaining $O(a)$ effects are thus localized at the boundaries, and correspond to the $O(a)$ operators counterterms proportional to $c_t(g_0)$ and $d_s(g_0)$.

On the other hand, in (5.42) and (5.53) we expressed the expectation that the universality relations among $\gamma_5\tau^1$-even correlation functions are valid up to $O(a^2)$ effects. This seems to contradict the conclusion above, since in principle $O(a)$ boundary contributions are present. However, it is possible to show that these $O(a)$ terms do not contribute in these specific relations. In Appendix D.1, we offer a simple proof of this result. Here we just want to mention that this conclusion is not a feature of automatic $O(a)$ improvement. Indeed, it simply relies on the fact that the correlators involved in these relations are expected to have a common continuum limit, and the $\gamma_5\tau^1$-even $O(a)$ boundary counterterms are invariant under chiral rotations. As a result, the observables we derived from universality relations involving $\gamma_5\tau^1$-even χSF correlation functions are fully $O(a)$ improved. Of course, similar conclusions apply to suitable universality relations between SF and χSF correlation functions (cf. (5.58)). Note however that in this case, the determination from the SF requires all the necessary (bulk) $O(a)$ improvement as otherwise $O(a)$ contaminations will enter in the relations.

In the case of the finite renormalization constants discussed in Section 5.2.1, this means that any change in the details of the renormalization conditions will effect the

results only at $O(a^2)$. As anticipated indeed, any difference in determinations obtained from different renormalization conditions is a pure discretization effect. We then expect for example the definitions Z_A^g and Z_A^l (or Z_A^{lg}) to differ by $O(a^2)$ terms, and similarly for Z_V^g and Z_V^l.

To conclude, automatic $O(a)$ improvement can be also verified by studying the $\gamma_5\tau^1$-odd correlation functions. As said, these are expected to be pure $O(a)$ effects. In particular, the correlators that are not trivially zero due to some exact lattice symmetry of the χSF are given by (cf. Appendix C.2),

$$g_A^{ud}, \qquad g_P^{uu'}, \qquad l_V^{ud}, \qquad l_T^{uu'}. \tag{5.62}$$

Note that in practice, we can simply consider the bare correlation functions in order to verify automatic $O(a)$ improvement. In fact, the corresponding renormalization factors only contribute logarithmically in a while taking the continuum limit. Note also that the x_0-derivatives of the above correlators correspond to the $O(a)$ counterterms of the $\gamma_5\tau^1$-even correlation functions we considered in the definition of the finite renormalization constants Z_V and Z_A (cf. Section 5.1.4). If these correlators are pure $O(a)$ effects, it is then clear that they can only contribute to $O(a^2)$ in the determination of these finite constants.

Finally, we just want to mention the possibility that $\gamma_5\tau^1$-odd observables could be exploited to determine some of the $O(a)$ improvement coefficients. In fact, they offer a source of pure cutoff effects that could be used to impose suitable improvement conditions. On the other hand, the problem that occurs with these observables is that it is difficult to isolate the $O(a)$ contribution coming from a specific source. Indeed, these correlation functions include contributions from the bulk action and operators, and also boundary counterterms. In addition, one should consider the effect coming from the $O(a)$ uncertainty in the tuning of the critical mass and z_f. In conclusions, a straightforward application of this idea is not practical, and some more elaborate strategy needs to be devised.

5.3 The lattice setup

In the previous section, we defined the observables that will be investigated and their expected features. Before presenting the corresponding results, however, we need to specify the lattice set-up. This includes: the boundary conditions for the fields, the χSF geometry, the choice of the lattice action, and the renormalization conditions for the bare parameters, g_0, m_0, and z_f. The renormalization of the latter is done by requiring three given observables to assume some prescribed values while the bare coupling $g_0 \to 0$. The specification of these observables is what defines our *line of constant physics* (LCP). Regarding the boundary conditions for the fields, we recall that these consist of the gauge boundary fields, C and C', and the angle θ that defines the spatial periodicity of the quark fields (cf. Section 3.1). In the following, we consider the boundary gauge fields to vanish, namely $C = C' = 0$. The angle θ, instead, is taken to be equal to zero if not specified otherwise. Finally, the χSF geometry is simply defined by the condition $T = L$. Given these definitions, we now describe the lattice action in detail.

5.3.1 Lattice action

In order to choose the lattice action, we need to consider that we want to compare our results with previous standard SF determinations. In particular, we would like to compare the results for the finite renormalization constants defined in Section 5.2.1. Since this is clearly done at finite lattice spacing, to do it consistently we have to choose the very same bulk lattice action as in the standard SF regularization. In the following, we thus study the theory with $N_f = 2$ non-perturbatively O(a)-improved Wilson-fermions. More precisely, we consider the action as specified by (3.22), and (3.77), where the value of the improvement coefficient $c_{\mathrm{sw}}(g_0)$ has been tuned non-perturbatively (Jansen and Sommer, 1998). As we will comment on shortly, this plays to our advantage. In principle, if automatic O(a)-improvement holds, we would not need to tune this coefficient in order to eliminate the O(a) contributions coming from the bulk action in our $\gamma_5 \tau^1$-even observables. However, the absence of these bulk O(a) contributions is expected to help significantly in the determination of the critical

quark mass and z_f (cf. Section 5.3.3). On the other hand, note that by considering an improved bulk action, the property of automatic $O(a)$ improvement can be verified only through the study of the $O(a)$ contributions coming from the operator improvement.

To conclude, in order to completely specify the lattice action, we need to define the values for the improvement coefficients corresponding to the two $\gamma_5\tau^1$-even $O(a)$ boundary counterterms. Specifically, we consider $c_t(g_0)$ and $d_s(g_0)$ as given by 1-loop order perturbation theory (Vilaseca, 2013).[3] As commented, however, we expect our determinations to be independent at $O(a)$ from these contributions (cf. Section 5.2.4). Finally, note that for the convenience of the reader we collected the expressions for these improvement coefficients, together with $c_{\mathrm{sw}}(g_0)$, in Table 5.1.

Table 5.1 $O(a)$ improvement coefficients for the χSF lattice action.

Coefficient	Expression	Notes
$c_{\mathrm{sw}}(g_0)$	$\dfrac{1-g_0^2\,0.454-g_0^4\,0.175+g_0^6\,0.012+g_0^8\,0.045}{1-g_0^2\,0.720}$	
$c_t(g_0)$	$1+g_0^2(0.006888\times N_{\mathrm{f}}-0.08900)$	
$d_s(g_0)$	$0.5-g_0^2(0.0009\times C_F)$	$C_F=\frac{N^2-1}{2N}$

5.3.2 Lines of constant physics (LCPs)

In this subsection we present the details of the LCPs considered. More precisely, we will first discuss how the bare coupling is renormalized, and later introduce the precise renormalization conditions for the quark-masses and z_f. As anticipated, since we are considering finite-volume renormalization schemes for the renormalization factors, the physical spatial extent L of the volume needs to be kept fixed while approaching the continuum limit. This defines our condition for the renormalization of the bare coupling. Given some values of the bare coupling g_0 then, we have to tune our lattice size L/a such that L is constant in physical units. In the following, we present two sets of lattice parameters which correspond to quite some different physical regimes. On one hand, we will consider values of the lattice spacing typical of non-perturbative large volume simulations. The finite volumes we will consider thus have $L\sim 0.6\,\mathrm{fm}$.

---

[3]We warmly thank Pol Vilaseca for sharing his results before publication.

These will be mostly used for the determination of the finite renormalization constants. Secondly, we will enter in the "femto-universe", in order discuss the running of the quark masses. The finite volumes in this case are pretty tiny with $L < 0.25\,\mathrm{fm}$.

LCP$_0$: hadronic regime. For the first LCP we are considering, the range of bare couplings and thus lattice spacings is fixed by the large volume simulations performed with $N_\mathrm{f} = 2$ non-perturbatively O(a)-improved Wilson-fermions. The details of the corresponding lattice ensembles can be found in (Fritzsch *et al.*, 2012). In particular, in the latter work the lattice spacing a has been determined in physical units in terms of the Kaon decay constant F_K, for the values of the bare coupling of interest. Given these results, it is easy to define a set of L/a's for the given g_0's such that the physical L is constant.

Table 5.2 Lattice parameters that define the two sets LCP$_0$ and PT.

	β	L/a	a (fm)	$\kappa_\mathrm{crit}(\beta)$	$z_f(\beta)$
LCP$_0$	5.2	8	0.0755(9)(7)	0.1356491(36)	1.2824(07)
	5.3	9.2*	0.0658(7)(7)	-	-
	5.5	12	0.0486(4)(5)	0.1367093(27)	1.3112(10)
	5.7	16	0.0379(15)	0.1367058(36)	1.3061(21)
PT	7.2	8	-	0.1341925(15)	1.2296(04)
	8.4	8	-	0.1325594(11)	1.1901(02)
	9.6	8	-	0.1313952(11)	1.1617(02)

*This point was not directly simulated. Some interpolation instead was considered. See text and Appendix D.3.

The idea is simply to fix L at the coarsest lattice spacing by choosing some value of L/a. This choice is in principle arbitrary and only guided by the condition $L/a \gg 1$, which guarantees that cutoff effects are under control for our finite-volume observables. After some careful analysis we chose the value of $L/a = 8$, which corresponds to a physical spatial extent of $L \sim 0.6\,\mathrm{fm}$. The values for L/a corresponding to the

other lattice spacings are then easily inferred from the condition $L = \text{const.}$[4] The results are collected in Table 5.2, together with the values of the lattice spacing in physical units, the values of the bare coupling $\beta = 6/g_0^2$, and the tuned values for $z_f(g_0)$ and $\kappa_{\text{crit}}(g_0) = (2m_{\text{crit}}(g_0) + 8)^{-1}$.[5] Note that for latter convenience, we will refer to this set of lattice parameters as LCP_0. As we shall see, for this choice of parameters cutoff effects turn out to be relatively small for most of the observables we considered. Moreover, the resulting lattice volumes are also small, and extensive numerical simulations could be thus performed.

Given the results in Table 5.2, some specifications are in order. First of all, note that of course we can only simulate at integer values of L/a. In the table we thus reported the closest integer values that satisfy the condition $L = \text{const.}$ For the value of the bare coupling given by $\beta = 5.3$, however, this would have corresponded to a lattice size of $L/a = 9$, and our algorithm can only simulate L/a-even lattices. Consequently, we decided to interpolate our observables at the "exact" value of L/a determined by the condition $L = \text{const.}$ i.e. $L/a = 9.2$. The details of this interpolation are discussed in Appendix D.3. For the other values of L/a instead, we have estimated the systematic effects on our observables due to the deviation from the exact values of L/a. This is also discussed in the Appendix, more precisely Appendix D.2. We invite the reader to consult these appendices only after the discussion in the next section, when the specific observables we considered have been introduced.

Finally, note that in Table 5.2 we also reported a set of lattice parameters referred to as PT. This includes three relatively high values of β at fixed lattice size $L/a = 8$. These parameters of course do not satisfy the condition of constant physical L. Nevertheless, we will consider this set to have an idea of how our non-perturbative results connect to their perturbative predictions, and to other non-perturbative determinations at high-β.

---

[4]Note that the error on the value of L and consequently on L/a deriving from the uncertainty in the lattice spacing a can be neglected in practice.

[5]The physical value of the lattice spacing for $\beta = 5.7$ was not available from non-perturbative determinations. We thus had to estimate it using the values at larger β's and the results for the 3-loop perturbative running of the bare coupling (Bode and Panagopoulos, 2002).

Table 5.3 Lines of constant physics corresponding to the non-perturbative running of the quark-masses.

LCP	L/a	$\beta = 6/g_0^2$	$u = \bar{g}_{\mathrm{SF}}^2(L)$	$\kappa_{\mathrm{crit}}(\beta)$	$z_f(\beta)$
	6	6.6085	2.0146(56)	0.1352428(24)	1.2580(3)
LCP$_3$	8	6.8217	2.014(10)	0.1348340(22)	1.2452(5)
	12	7.09300	2.014(20)	0.1343877(15)	1.2370(4)
	6	6.1330	2.488(11)	0.1360800(30)	1.2777(6)
LCP$_2$	8	6.3229	2.479(13)	0.1357386(20)	1.2688(4)
	12	6.63164	2.479(25)	0.1351926(11)	1.2570(3)
	6	5.6215	3.326(20)	0.1366258(43)	1.2896(8)
LCP$_1$	8	5.8097	3.334(19)	0.1365442(19)	1.2902(6)
	12	6.11816	3.334(49)	0.1361290(20)	1.2831(7)

LCP$_{1,2,3}$: femto-universe. As discussed, we want to investigate the universality of the continuum limit between the standard SF and the χSF by studying the running of the quark-masses at high-energy. To this end, we will consider the three LCPs defined in Table 5.3. For these values of the lattice parameters indeed, previous standard SF determinations are available for the quantities of interest (Della Morte *et al.*, 2005*a*). In particular, note that in this case the condition $L = $ const. is implicitly enforced by fixing the SF coupling $\bar{g}_{\mathrm{SF}}^2(L)$ to a prescribed value (cf. Section 5.2.3). For later reference, the corresponding values for the SF coupling are then also reported in the table together with their errors. Finally, we note that for these ensembles the fermionic angle θ has been set to $\theta = 0.5$ in order to match the renormalization scheme for the pseudo-scalar density adopted in (Della Morte *et al.*, 2005*a*).

This concludes our discussion on the renormalization of the bare coupling. We will now address the renormalization of the quark-masses and z_f.

5.3.3   Tuning of m_0 and z_f

In order to discuss the renormalization conditions for the quark masses and z_f, we start recalling that the (renormalized) quark-masses need to be tuned to zero in order to define a mass-independent scheme for our renormalization constants (cf. Section 2.3). This is also a necessary condition to obtain automatic O(a) improvement. The second condition, instead, is the renormalization of the χSF boundary conditions which amounts to fixing the boundary coefficient z_f (cf. Section 3.4.3).

To fix the quark-masses one then simply tunes the PCAC mass (2.30) to zero at each value of the bare coupling g_0. In particular, to completely specify the definition of PCAC mass, we set $\mathcal{O}_{\text{ext}} = \mathcal{Q}_5^{ud}$ in (2.30) and require,

$$m_{\text{PCAC}}(g_0, m_{\text{crit}}(g_0)) = \left.\frac{\partial_0 g_A^{ud}(x_0)}{2g_P^{ud}(x_0)}\right|_{x_0=\frac{T}{2}} \overset{!}{=} 0. \tag{5.63}$$

This defines the critical value $m_{\text{crit}}(g_0)$ for the bare quark masses. In particular, note that since we are not considering the improved axial current A_I (cf. (2.44)) in the above definition, our determination of the critical mass will suffer from O(a) ambiguities, even though the bulk action is improved. As discussed, however, this does not affect $\gamma_5\tau^1$-even functions at O(a) but only at O(a^2).

Regarding the tuning of $z_f(g_0)$ instead, we impose the criteria of parity/flavour symmetry restoration on some suitable observable. A convenient set of observables is given by the $\gamma_5\tau^1$-odd correlation functions (5.62). Specifically, we then consider the condition,

$$g_A^{ud}(x_0)|_{x_0=\frac{T}{2}} \overset{!}{=} 0. \tag{5.64}$$

As we shall see, this correlation function offers a good sensitivity on z_f, and also a good statistical precision. Similarly to the case of m_{crit}, the determination of z_f so obtained will suffer from O(a) ambiguities. Hence, if another $\gamma_5\tau^1$-odd correlation function is used to determine z_f, the difference between these two determinations will scale as O(a) to the continuum limit. However, as argued for the critical mass, this ambiguity will only effect $\gamma_5\tau^1$-even functions at O(a^2). In this respect, we want to note that these expectations have been extensively confirmed in perturbation theory (Vilaseca, 2013), and also in the quenched approximation (Sint and Leder, 2010).

To conclude, once the renormalization conditions above are imposed on the bare quark-masses and z_f, we expect automatic $O(a)$ improvement to be realized. However, the practical question now is how difficult it is to force these conditions within a good precision in numerical simulations. Before moving to discuss the results, we will address this important issue in the following paragraph.

Tuning strategy. In principle one would expect that close to the continuum limit, the determinations of $m_{\text{crit}}(g_0)$ and $z_f(g_0)$ are rather independent. These parameters indeed are both functions of the bare coupling only. However, at a generic value of the lattice spacing, cutoff effects create an interdependence between these two parameters which a priori is hard to quantify. In general, the tuning of m_0 and z_f need then to be performed simultaneously. A possible strategy one can pursue is the following.

We consider simulations at different values of m_0, and for each m_0 we choose a given set of z_f's, then:

1. At fixed z_f, we compute $m_{\text{PCAC}}(m_0, z_f)$, $\forall m_0$, and determine m_{crit} by requiring $m_{\text{PCAC}}(m_{\text{crit}}, z_f) = 0$. This gives $m_{\text{crit}} \equiv m_{\text{crit}}(z_f)$.

2. At fixed z_f, we compute $g_A^{ud}(m_0, z_f)$, $\forall m_0$, and interpolate in m_0 to get $g_A^{ud}(m_{\text{crit}}(z_f), z_f) \equiv f(z_f)$, which is now only function of z_f.

3. We determine the value z_f^* by requiring $f(z_f^*) = 0$.

4. At fixed m_0, we interpolate $m_{\text{PCAC}}(m_0, z_f)$ in z_f to get $m_{\text{PCAC}}(m_0, z_f^*)$.

5. m_{crit}^* is determined by requiring $m_{\text{PCAC}}(m_{\text{crit}}^*, z_f^*) = 0$.
   Analogously one can interpolate and get $m_{\text{crit}}^* = m_{\text{crit}}(z_f^*)$ from 1.

6. Check that $g_A^{ud}(m_{\text{crit}}^*, z_f^*) = 0$; if not go back to 3. and iterate.

Basically, one thus has to solve a minimization problem in two variables, and if the interdependence is strong it could be difficult to satisfy the two conditions within a good precision. In the quenched approximation however, it has been observed that once the bulk action is improved, the PCAC mass turns out to be rather independent from z_f (Sint and Leder, 2010). From the point of view of the strategy discussed above, this means that in practice: $m_{\text{crit}}(z_f) \simeq \text{const} \rightarrow m_{\text{crit}}^*$. Hence, in most of the cases one can make the two conditions be satisfied independently: one first tunes to zero

quark-masses, and then determines z_f at the given critical mass. As we now show with an explicit example also in dynamical simulations this result seems to hold. More precisely, the PCAC mass does not depend much on z_f if the two parameters are close to their critical values.

As an example consider the results for the PCAC mass shown in Figure 5.1. As one can see from the figure, the values of $m_{\rm PCAC}$ do not depend much on z_f in the given range. As we will comment on shortly, this range is in fact a typical range to obtain a good tuning for z_f. These measurements are for $L/a = 8$ and $\beta = 5.2$, namely the coarsest lattice we considered along the LCP given by LCP_0 (cf. Table 5.2). The situation is thus expected to be even better for the other lattices at smaller values of the lattice spacing. In fact, this is what we observe.
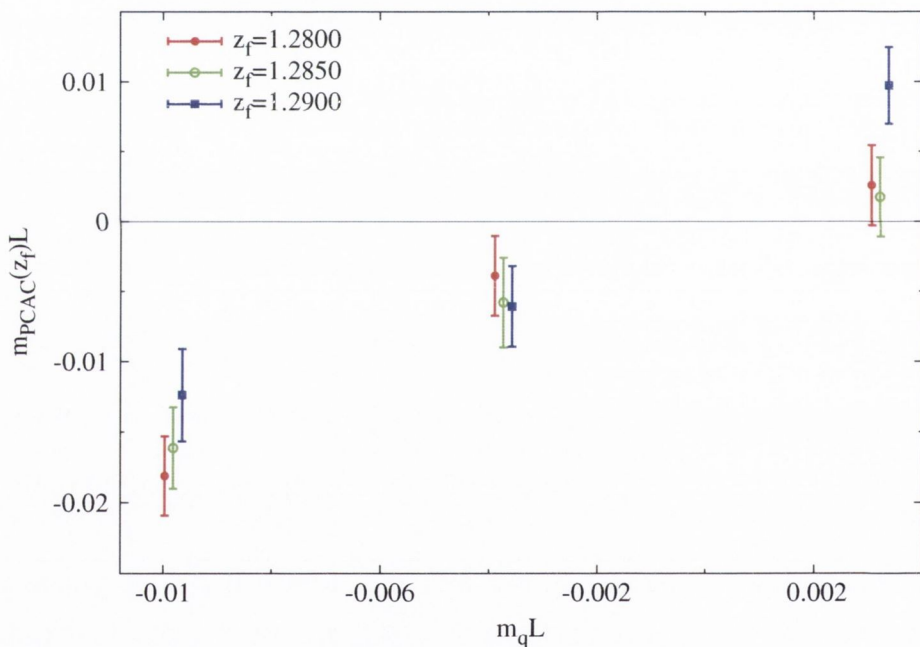

Fig. 5.1: Value of $m_{\rm PCAC}$ for $L/a = 8$, $\beta = 5.2$, and three different values of z_f. $m_q = m_0 - m^*_{\rm crit}$, where $m^*_{\rm crit}$ has been determined from a constant fit of the three $m_{\rm crit}(z_f)$.

In this situation, as anticipated the critical mass turns out to be rather independent on z_f. After some experimentation one thus ends up with a range of m_0 and z_f close to their critical values. Given these ranges, one can then generally obtain a single value of $m_{\text{crit}} \equiv m^*_{\text{crit}}$ that ensures that the PCAC mass vanishes within some desired precision over the whole range of z_f's. [6] Once this value is determined, one interpolates the given renormalization condition for z_f at m^*_{crit}. This is what we show for example in Figure 5.2, which is the result for g_A^{ud} and $g_P^{uu'}$ interpolated to zero quark-masses. We recall that our renormalization condition for z_f is based on $g_A^{ud} = 0$. In the figure however we also consider the eventual tuning based on a different $\gamma_5 \tau^1$-odd function, namely $g_P^{uu'}$. As discussed the difference in the determination of z_f from these two different correlators is an O(a) effect. As we can see, the two determinations z_f^{A*} and z_f^{P*} corresponding to g_A^{ud} and $g_P^{uu'}$, respectively, are in fact pretty close and within error compatible (the errors are not shown for readability of the plot.) This suggests that these O(a) effects are relatively small.

To conclude, this was just a quick illustration of how the tuning looks like. The main point we want to stress is that, similarly to what has been concluded in the quenched approximation, also in the dynamical case the tuning of the additional renormalization parameter is relatively straightforward, at least for the case where the bulk action is improved. In fact, if one is relatively close to the critical values of m_0 and z_f the two conditions can be implemented independently in practice. In this respect, note that if the value of the critical mass is known from a previous standard SF determination, this could be used as part of the definition of the LCP. In this case, one simply has to tune z_f for the given value of the critical mass (Sint and Leder, 2010). Indeed, since the critical mass is determined through the PCAC relation, it is expected to be independent from the specific boundary conditions employed, up to discretization effects. However, we did not follow this strategy since we wanted to acquire familiarity with the tuning. Moreover, if the O(a) effects between the SF and χSF determinations of the critical mass are large, this might induce large O(a^2) effects in the χSF results.

---

[6]This can be obtained in practice by a weighted fit over the different $m_{\text{crit}}(z_f)$ in the given range of z_f for example.
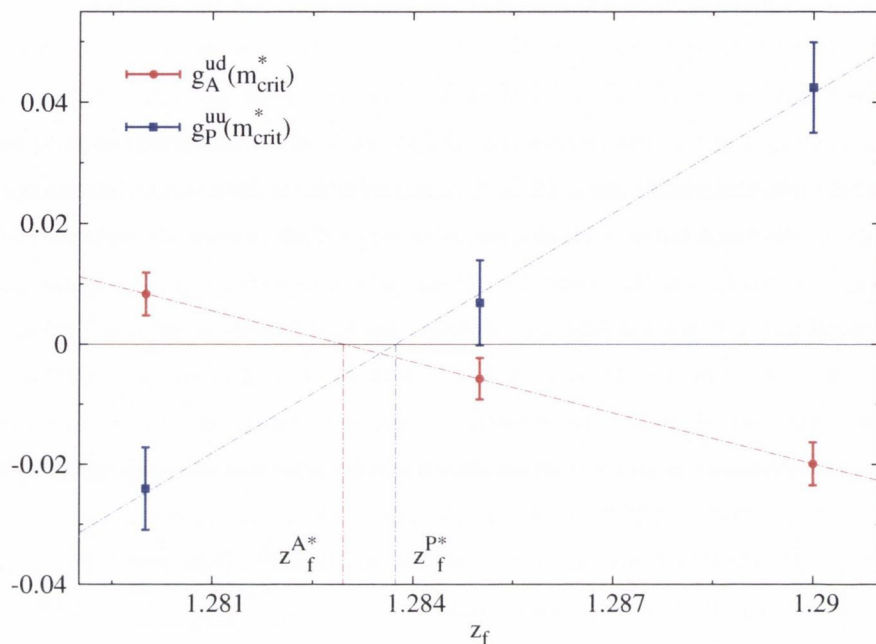
Fig. 5.2: Results for g_A^{ud} and $g_P^{uu'}$ interpolated at zero quark-mass for $L/a = 8$, and $\beta = 5.2$.

5.4 Determination of Z_V and Z_A

Having introduced the lattice setup and discussed the tunning of the bare quark-masses and z_f, we can now present our results. We thus start with the finite renormalization constants Z_V and Z_A. Specifically, we first compare our determinations with previous standard SF computations. We then study the scaling to the continuum limit of the difference between different definitions of these renormalization factors. As we shall see, the $O(a^2)$ scaling expected from automatic $O(a)$-improvement is nicely realized, and cutoff effects are generally small in these observables. In order to provide further evidence to this conclusion, we will compare the results for the finite renormalization constants for two different LCPs. In addition, the x_0 dependence of our definitions will be investigated.

5.4.1 Z_V: a first look

We start from the results for the renormalization of the local vector current Z_V, which is the simplest case to study. We note indeed that its determination does not rely on any universality relation between the SF and χSF, but simply on the universality between the matrix elements of the local and point-split vector currents. Moreover, the results from the standard SF, Z_V^{SF}, are quite accurate and provide a stringent comparison (Della Morte, Hoffmann, Knechtli, Sommer and Wolff, 2005b).
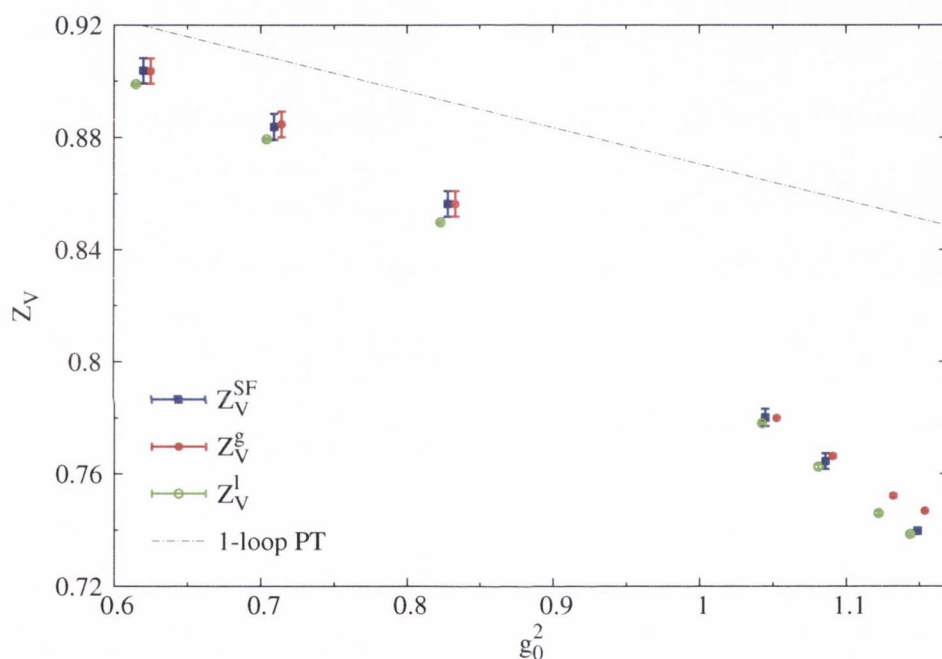
Fig. 5.3: Results for the renormalization of the local vector current as a function of g_0. This includes a comparison between the χSF determinations Z_V^g and Z_V^l, and the standard SF determination Z_V^{SF}. The 1-loop perturbative result is also given. The set of lattice parameters is the one corresponding to LCP_0 and PT. Note that the points have been slightly shifted in g_0^2 in order to improve the readability of the plot.

In Figure 5.3, we present our results for Z_V (cf. (5.49)) as a function of g_0 for the line of constant physics defined by LCP_0, and the set of lattice parameters given

by PT (cf. Table 5.2). The first thing to note is that, apart from Z_V^g at the largest value of the bare coupling, our results nicely agree within errors with the standard SF determination. This of course does not have to be the case since in general we expect $O(a^2)$ differences, assuming that automatic $O(a)$ is at work for our results. The conclusion is thus simply that these $O(a^2)$ effects are smaller than the statistical uncertainly in the standard SF determination. Note however that given our precision we can resolve some differences between our two definitions Z_V^g and Z_V^l, at the largest values of the bare coupling. This can be better seen in Figure 5.4, where we provide a zoom of Figure 5.3 on the results corresponding to LCP_0 only. As we can see from this figure the spread of our determinations is in fact compatible with an $O(a^2)$ effect. If we consider for example the relative difference between Z_V^g and Z_V^l at the largest value of the bare coupling, since the corresponding lattice size is $L/a = 8$, we would expect (roughly): $1 - Z_V^g/Z_V^l \sim 1/64 \sim 1.5\%$, which is in fact the case. We will investigate this in more detail shortly, in order to check if also the scaling of these differences to the continuum limit is the expected one.

To conclude, a few observations are in order. First of all, we want to comment on the higher precision of our determinations. In this respect, note that the errors shown in the figures are not only statistical but include an estimate of the main systematics. These are related to the fact that the conditions: $L = $ const., $m_{PCAC} = 0$, and for the χSF case also, $g_A^{ud} = 0$, are only satisfied within some precision. The details of our error estimates is given in Appendix D.2. Here we just want to mentioned that through dedicated numerical simulations and the information from the tuning runs, we have estimated the derivative of our renormalization factors w.r.t. these three quantities in order to propagate the corresponding uncertainties in our determinations. Moreover, note also that to have a fairer comparison between our and the standard SF determination, one should increase our errors by roughly a fact two in order to compensate for the different statistic.[7] This said, however, still our determinations turn out to be much more precise. We believe that the origin of the higher precision is

---

[7]We believe this to be a conservative statement, even though it is difficult to access the effective statistic on Z_V^{SF} since no autocorrelations are provided in the corresponding reference. We thus have estimated those based on our runs.
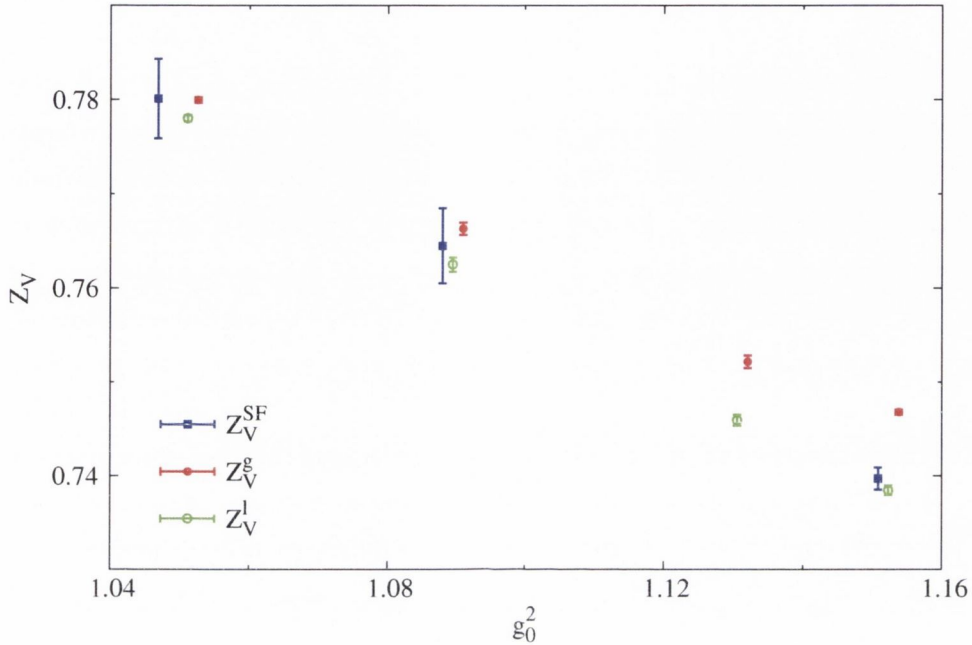
Fig. 5.4: Results for the renormalization of the local vector current as a function of g_0. This includes a comparison between the χSF determinations Z_V^g and Z_V^l, and the standard SF determination Z_V^{SF}. The set of lattice parameters is the one corresponding to LCP$_0$. Note that the points have been slightly shifted in g_0^2 in order to improve the readability of the plot.

due to the fact that our definitions are given by simple ratios of two-point functions (cf. (5.49)). In particular, we have noticed that considering only the statistical errors, the ratio of such correlation functions is of O(10) times more precise than the individual correlators.[8] In the standard SF case, instead, Z_V is obtained through a WI. This results in having to compute the more complicated ratio of a three-point function involving two boundary source fields and the local vector current, with a two-point boundary-to-boundary correlator (see e.g. (Della Morte, Hoffmann, Knechtli, Sommer and Wolff, 2005b)).

---

[8]Of course this statement depends on the given lattice parameters and other details. Here we just want to give a rough idea of the size of the statistical correlations of these two-point functions.

Going back to Figure 5.3, we also want to briefly comment on the data corresponding to the set PT. This includes the data with $g_0^2 < 1$. As discussed these determinations do not lie on a LCP since it is L/a and not L which is fixed while $g_0 \to 0$. The difference between the different determinations is thus expected to scale as $O(g_0^2)$. However, note that the errors include a rough estimate for the deviation from the condition $L = \text{const}$. Surprisingly, the definition Z_V^l is not much sensitive to these $O(g_0^2 a^2)$ effects. We will notice a similar behavior in the Z_A determination from the standard SF later on. Consequently the results from the different determinations all agree, and seem to smoothly connect with the perturbative 1-loop results. Note that this corresponds to the determination for $L/a \to \infty$ (see e.g. (Della Morte, Hoffmann, Knechtli, Sommer and Wolff, 2005b) and references therein). In this respect, it would be interesting to compare the results with perturbation theory at finite L/a. Using these results might also help in further reducing the differences in our determinations.

Table 5.4 Values for Z_V from the χSF corresponding to LCP$_0$.

β	L/a	Z_V^g	Z_V^l
5.2	8	0.74680(26)	0.73844(51)
5.3	9.2	0.75217(67)	0.74592(59)
5.5	12	0.76632(67)	0.76251(76)
5.7	16	0.77997(29)	0.77801(36)

Finally, in Table 5.4 we report our final results for Z_V corresponding to the line of constant physics given by LCP$_0$.

5.4.2 Z_A: a first look

Similarly to the previous subsection, we now want to compare our results for Z_A with the standard SF determination, Z_A^{SF}. We recall that our definitions are given by (5.47), (5.48), and (5.50). In Figure 5.5 we present the corresponding results for the line of constant physics given by LCP$_0$, and the set of parameters referred to as PT. The results for the standard SF are also shown, as well as the 1-loop perturbative prediction. The corresponding details of these results and the definition of Z_A can be found
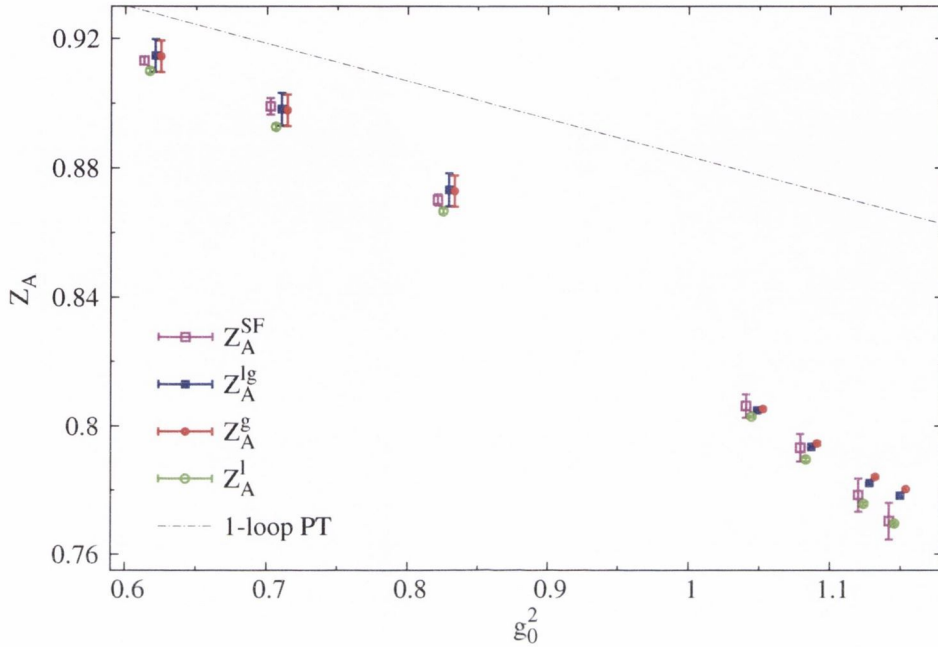
Fig. 5.5: Results for the renormalization of the local axial current as a function of g_0. This includes a comparison between the χSF determinations Z_A^g, Z_A^l, Z_A^{lg}, and the standard SF determination Z_A^{SF}. The 1-loop perturbative result is also given. The set of lattice parameters is the one corresponding to LCP_0 and PT. Note that the points have been slightly shifted in g_0^2 in order to improve the readability of the plot.

in (Della Morte, Hoffmann, Knechtli, Sommer and Wolff, 2005b; Della Morte, Sommer and Takeda, 2009; Fritzsch *et al.*, 2012). In particular, note that a first update of Z_A has been given by the Alpha Collaboration in (Della Morte, Sommer and Takeda, 2009), since large cutoff effects have been observed in their first computation along the line of constant physics given by LCP_0 (Della Morte, Hoffmann, Knechtli, Sommer and Wolff, 2005b). The updated SF results for Z_A, thus correspond to a different LCP defined by the values of $\beta = 5.2, 5.4, 5.7$, and the larger lattice resolutions $L/a = 12, 16, 24$. The results for Z_A at the values of g_0 where the large volume simulations were performed have then been obtained through a proper interpolation in g_0. The latest updated results used in Figure 5.5 can be found in (Fritzsch *et al.*, 2012).
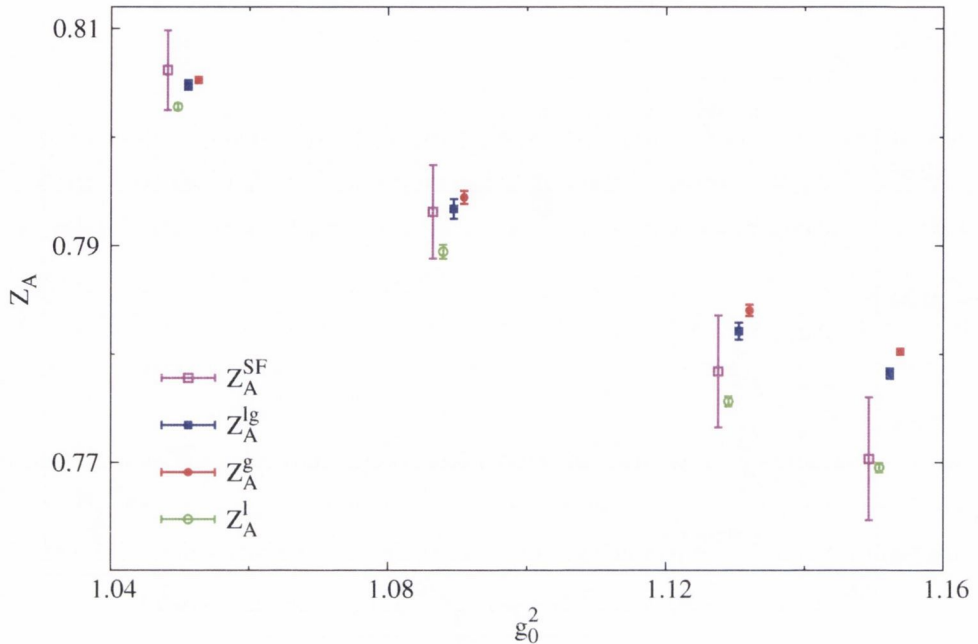
Fig. 5.6: Results for the renormalization of the local axial current as a function of g_0. This includes a comparison between the χSF determinations Z_A^g, Z_A^l, Z_A^{lg}, and the standard SF determination Z_A^{SF}. The set of lattice parameters is the one corresponding to LCP_0. Note that the points have been slightly shifted in g_0^2 in order to improve the readability of the plot.

Similarly to the case of Z_V, we see good agreement between ours and the standard SF determination. In this case, however, the errors in the latter computation are much larger. This can be better seen in Figure 5.6, where we consider only the results in the range of bare couplings corresponding to LCP_0. We also notice that given our precision we can resolve some differences between the different χSF definitions for Z_A. In particular, again as for the case of Z_V, the size of these differences is small and compatible with an $\mathrm{O}(a^2)$ effect. This will be investigated more in detail in the next subsection.

To conclude, we want to note that the standard SF determination of Z_A is much more involved than the corresponding χSF determination. In the standard SF, Z_A

is obtained through a WI. As a result, one has to consider the ratio of a four-point function involving two boundary source fields and two axial currents, with a two-point boundary-to-boundary correlator. The precision of this determination is thus expected to be generally lower than in the case of the χSF where only two-point functions are involved. In addition, for the standard SF determination the improved axial current A_I needs to be considered in order to obtain an O(a) improved definition. The corresponding determination of the improvement coefficient c_A needs thus to be performed first (see e.g. (Della Morte, Hoffmann and Sommer, 2005c) for the details of this computation).

Finally, in Table 5.5 we collect our final results for Z_A corresponding to the line of constant physics given by LCP$_0$ and the three definitions.

Table 5.5 Values for Z_A from the χSF corresponding to LCP$_0$.

β	L/a	Z_A^g	Z_A^l	Z_A^{lg}
5.2	8	0.78026(29)	0.76950(45)	0.77820(47)
5.3	9.2	0.78406(52)	0.77564(48)	0.78214(80)
5.5	12	0.79448(59)	0.78948(64)	0.79342(91)
5.7	16	0.80527(29)	0.80280(32)	0.80482(43)

After this discussion on Z_V and Z_A, we can conclude that our results look sensible and in fact very promising. In the next subsection, we thus present a series of tests that we performed on the size and nature of the cutoff effects in these determinations. This will both serve us as a check for automatic O(a) improvement, as well as for corroborating the robustness of our results.

5.4.3 Z_V and Z_A: a closer look

As anticipated, in this subsection we collected a few observations on the nature and size of cutoff effect in our Z_V and Z_A determinations. We now present these in detail.

Scaling of $Z_{V,A}$ differences.   We here present the continuum limit extrapolation of the differences between different renormalization conditions that define Z_V and

Z_A. We study this along the line of constant physics given by LCP_0. We recall that if automatic $O(a)$-improvement is at work, we expect these differences to scale like $O(a^2)$ (cf. Section 5.2.4). The results we obtained are shown in Figure 5.7.
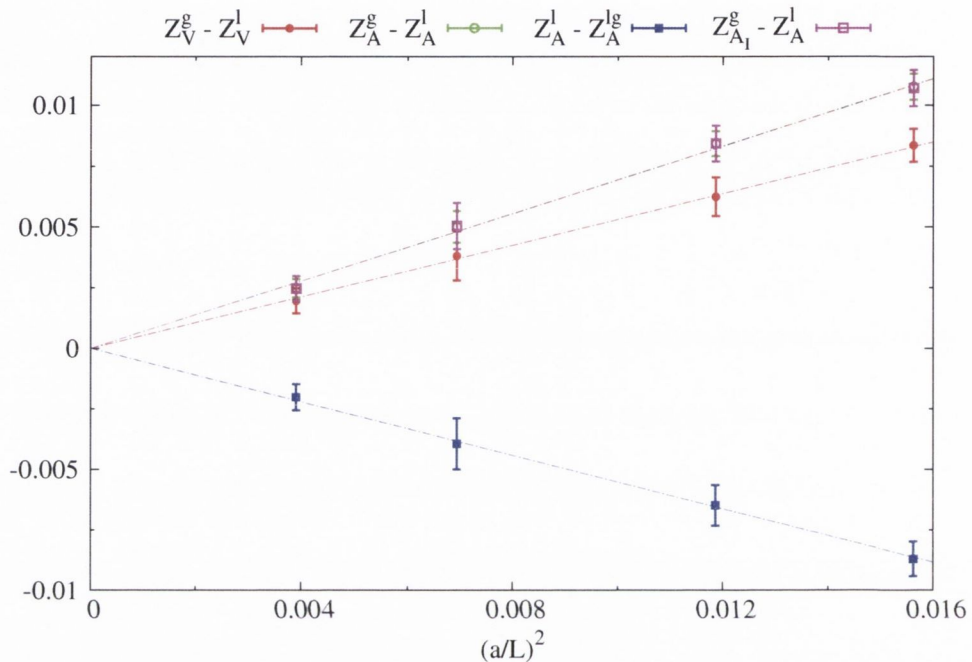

Fig. 5.7: Continuum limit extrapolations for the differences between different χSF definitions of Z_V and Z_A along the line of constant physics defined by LCP_0.

Note that, since L is fixed in physical units, the continuum limit is obtained by simply taking $a/L \to 0$. As we can see, the difference between our two definitions of Z_V, as well as the differences among several definitions of Z_A, nicely extrapolates to zero with the expected $O(a^2)$ scaling. Note that the lines on the plot are given in fact by linear fits in $(a/L)^2$ constrained to pass from zero. We want to stress again that this result is non-trivial. Indeed, as mentioned, even though our bulk action is $O(a)$ improved, the full improvement of our determinations would generally require the corresponding (bulk) $O(a)$ operator improvement. As an example Z_V^l would require the improvement of both the local and point-split vector currents (cf. (5.52)).

In order to corroborate the above observation further, in Figure 5.7 we considered the effect of substituting Z_A^g with the corresponding improved definition $Z_{A_I}^g$ (cf. (5.52)) in the difference $Z_A^g - Z_A^l$, where the improvement coefficient for the axial current, c_A, has been fixed to its non-perturbative value (Della Morte, Hoffmann and Sommer, 2005c). As we can see, (a bit surprisingly) there is basically no effect of the $O(a)$ operator counterterm within the errors. This give us confidence to interpret the result as the fact that the $O(a)$ operator improvement only contributes as an $O(a^2)$ effect, which in this case turns out to be very small. To conclude, as already noticed in the previous subsections, also the (relative) differences between the different definitions are small. In fact, we have only $\sim 1.0 - 1.5\%$ differences at the coarsest lattice spacing.

Comparison with an alternative LCP.   Given the results presented so far, it seems that cutoff effects in our determinations of Z_V and Z_A are generally small and have the expected scaling to the continuum limit. In order to have another estimate of the size of cutoff effects, we thus decided to compute our finite renormalization constants at the coarsest lattice spacing for a different lattice resolution L/a. More precisely, at the value of the bare coupling specified by $\beta = 5.2$, we considered a lattice with $L/a = 12$ instead of $L/a = 8$. This would correspond to a LCP where $L \sim 0.9$ fm. As discussed, we then expect the dependence on L/a at fixed bare coupling g_0 to be an $O(a^2)$ effect.

Table 5.6 Comparison between the results for different finite renormalization constants between two lattices with $L/a = 8$ and $L/a = 12$ at fixed $\beta = 5.2$. Note that for the convenience of the reader the relative difference between the results of the two ensembles is also given in per cent.

L/a	Z_V^g	Z_V^l	Z_P/Z_S	Z_A^g	Z_A^l	Z_A^{lg}
8	0.7468(3)	0.7384(5)	0.7923(5)	0.7803(3)	0.7695(4)	0.7782(5)
12	0.7334(4)	0.7304(8)	0.7385(22)	0.7732(7)	0.7636(7)	0.7667(8)
$\sim\%$	1.8	1.1	6.8	0.9	0.8	1.5

In Table 5.6, we report the values we obtained for our finite renormalization factors

for the two lattice sizes $L/a = 8, 12$ at fixed $\beta = 5.2$. For later convenience we also included the determination of Z_P/Z_S. As we can see, the (relative) difference between the Z_V and Z_A determinations on the two lattices is small, and generally of the order of a couple of per cent. This is not case though for the ratio Z_P/Z_S which shows more pronounced cutoff effects. We will discuss this in more detail in a later section.

x_0–**dependence of** Z_V **and** Z_A. The last quantities we have looked at in order to study the size of cutoff effects in our finite renormalization constants, are related to their x_0 dependence. As discussed, we normally measure the ratio of our two-point functions in the definition of the Z factors at $x_0 = T/2$, i.e. in the middle of the lattice volume. This we argued generally leads to smaller cutoff effects since it maximizes the distance from the boundaries where the $O(a)$ (and higher) boundary counterterms are localized.[9] However, any other value of x_0 in the bulk of the lattice is equally good in principle and should lead to $O(a^2)$ differences in the results.[10]

Given these observation, we then studied the quantities defined by,

$$\Delta Z \equiv Z(3T/4) - Z(T/2), \qquad (L\tilde{\partial}_0 Z)(T/2), \qquad (5.65)$$

where Z is our generic finite renormalization factor. In order words, we looked at the difference between the Z factors at $x_0 = 3T/4$ and $x_0 = T/2$, and at the x_0-derivative at $x_0 = T/2$. Note that, the latter has to be multiplied by L in order to obtain a dimensionless quantity that scales to a finite value in the continuum limit.

In Figure 5.8 we thus present the results for the continuum limit extrapolations of these quantities as a function of $(a/L)^2$ along the LCP defined by LCP_0.[11] As we can see, regarding ΔZ the differences are generally small and below a couple of per cent also at the coarsest lattice spacing. The only Z factor that stands out is Z_A^g, but still cutoff effects are of the order of just a few per cent.

---

[9]We recall that in fact the $O(a)$ boundary counterterms are not expected to contribute to the finite renormalization constants. Higher-orders are however certainly present.

[10]We obviously exclude the point $x_0 = a$ where the boundary source fields are localized, as otherwise contact terms will originate between the boundary fields and the quark-bilinears.

[11]Note that for ΔZ we omitted the value for $L/a = 9.2$ since the interpolation is not straightforward in this case.
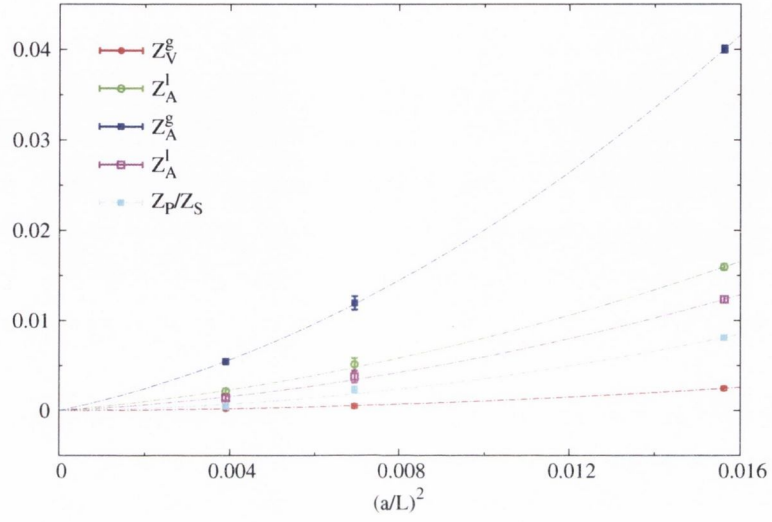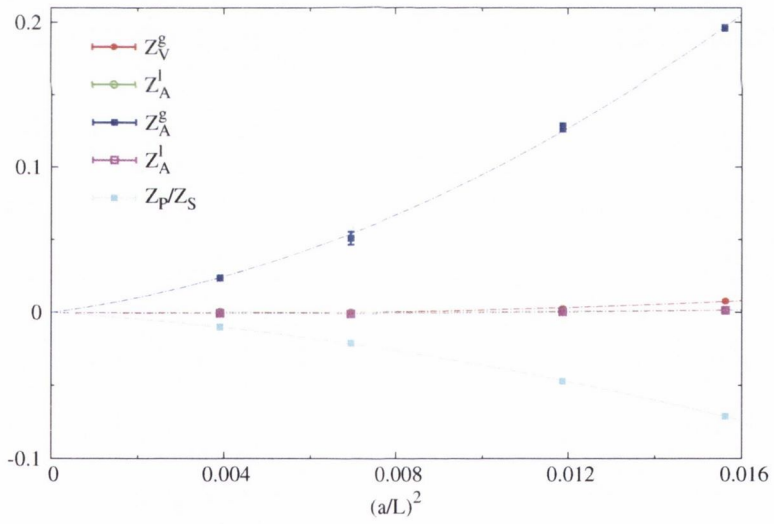
(a) ΔZ

(b) $L\tilde{\partial}_0 Z$

Fig. 5.8: Continuum limit extrapolations for ΔZ and $L\tilde{\partial}_0 Z$ along the line of constant physics given by LCP_0.

What is clear from the figure is that these differences cannot be described by a simple $O(a^2)$ effect over the whole range of lattice spacings considered. Some higher-order contributions are indeed present. In the plots, we thus show a fit of the data that contains a linear and quadratic term in $(a/L)^2$, and it is constrained to pass through zero for $a \to 0$.[12] In this way, we had at least a single degree of freedom for the fit to (roughly) judge its quality. In fact, the fit nicely describes the data, and we thus conclude that even though some higher order effects seem to be enhanced in this quantity they correctly extrapolate to zero in the continuum limit.[13]

Concerning the slope $L\tilde{\partial}_0 Z$ at $x_0 = T/2$ similar conclusions can be drawn. In this case we also have an additional point at $L/a = 9.2$ which fits on our fitting curves. The thing that we want to note here is that in this case also the ratio Z_P/Z_S shows some sizable cutoff effects at the largest values of the lattice spacing.

This concludes our discussion on Z_V and Z_A. As we have seen, our determinations are solid and much more precise than the standard SF determinations. In fact, here we have only presented a comparison of these determinations with results from the standard SF. Our computation of Z_A, however, turns out to be very precise also if compared with other determinations, where for example twisted-mass fermions and several different methods have been employed (Constantinou *et al.*, 2010). On the other hand, since the gauge action is different in this case we could not directly compare.

5.5 Determination of Z_P/Z_S

In the previous section, we discussed in some detail the determination of the finite renormalization constants Z_V and Z_A using the χSF. As discussed in Section 5.2.1, however, the universality relations among χSF correlation functions allow us to easily define also renormalization conditions for the ratio of scale-dependent renormalization factors belonging to the same chiral multiplet (cf. (5.51)). As an example of this application, in this section we briefly present the determination of the ratio Z_P/Z_S.

---

[12]We also tried a cubic instead of a quartic term in a/L, which describes the data equally well.

[13]Note that a similar discussion on the enhancement of cutoff effects in some SF correlation functions for this range of physical parameters can be found in (Della Morte, Sommer and Takeda, 2009).

More precisely, we will consider the finite renormalization factor defined by,

$$Z^{l,g} = \frac{Z_P}{Z_S Z_A^{l,g}}.$$

(5.66)

Note that the two definitions simply differ by the choice of Z_A. This renormalization factor Z in interesting since it gives the ratio of the bare quark mass difference over the corresponding PCAC mass difference. It is thus of interest for the tuning of the quark masses in the non-degenerate case. Similarly to the case of Z_V and Z_A, also in this case we compare our results with previous SF determinations for $N_f = 2$ non-perturbatively $O(a)$ improved Wilson-fermions. The details of the latter computation can be found in (Fritzsch, Heitger and Tantalo, 2010).
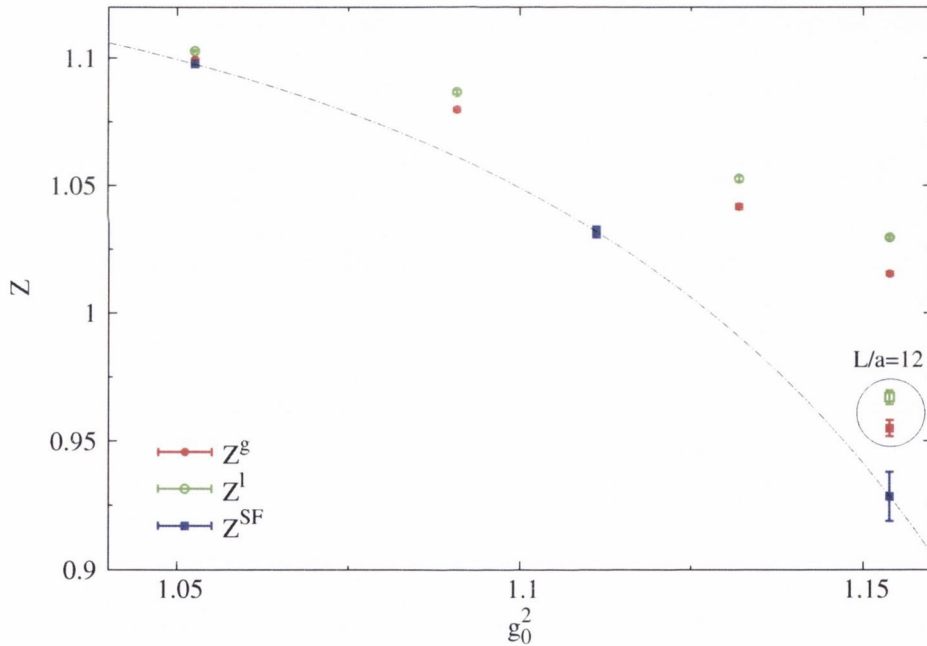

Fig. 5.9: Results for the finite renormalization factor Z as a function of g_0. This includes a comparison between the χSF determinations Z^g, Z^l, and the standard SF determination Z^{SF}. The set of lattice parameters is the one corresponding to LCP$_0$. Circled instead are the results of a determination at $\beta = 5.2$ and $L/a = 12$.

In Figure 5.9 we report our results for the renormalization factor Z along the LCP given by LCP_0. The standard SF determination, Z^{SF}, is also shown. Note that we included the result of a fit for the corresponding mean value over the range of g_0 of interest. As we can see from the plot, excluding the value at the coarsest lattice spacing, the χSF and SF determinations have similar precision. On the other hand, we can resolve some sizable discretization effects. For the largest value of the bare coupling, $\beta = 5.2$, indeed the relative difference between χSF and SF determinations is of the order of $\sim 10\%$. The difference however disappears quite quickly as we approach the continuum limit, and for $\beta = 5.7$ it is reduced to $\sim 0.1\%$. This is much faster than an $O(a^2)$ effect, since we would expect in this case a reduction by a factor of four. The difference between our two determinations of Z instead is only dictated by Z_A and thus as already noticed is small.

To conclude, we want to note that the difference between the SF and χSF determinations at the coarsest lattice spacing is significantly reduced if we consider our results for $L/a = 12$ instead of $L/a = 8$. In fact, in this case the relative difference goes down to $\sim 4\%$, as can be seen also from the plot. This suggests that the LCP defined by $L/a = 12$ at $\beta = 5.2$, and which corresponds to $L \sim 0.9\,\text{fm}$, is probably more suited for a reliable computation of the Z factor through the χSF.

Finally, for completeness, in Figure 5.10 we report the determination of Z including the set of lattice parameters corresponding to PT. As we can see, the results slowly move towards the 1-loop perturbative determination (Guagnelli *et al.*, 2001) for the largest values of g_0.

5.6 Automatic O(a) improvement

In the previous sections, studying different finite renormalization constants we gave evidence that automatic O(a) improvement holds for our χSF determinations. More precisely, we have shown that several non-trivial $\gamma_5\tau^1$-even observables have corrections w.r.t. their continuum values of O(a^2), even though the corresponding O(a) operator improvement has not been implemented. To complete this analysis, in this section we want to present some results on the complementary feature expected from automatic O(a) improvement, namely that $\gamma_5\tau^1$-odd observables are pure O(a) effects.
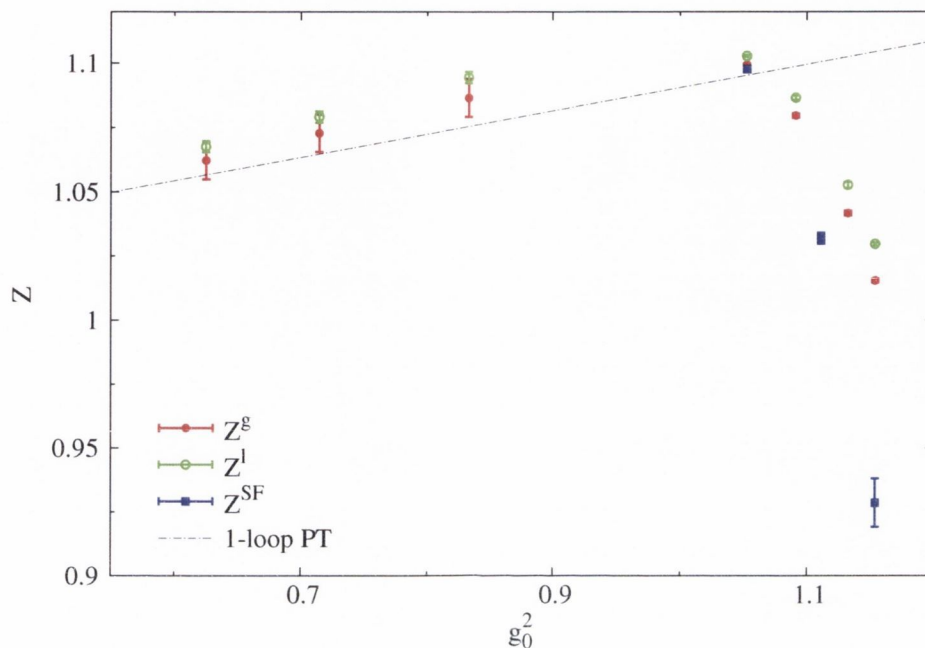
Fig. 5.10: Results for the renormalization factor Z as a function of g_0. This includes a comparison between the χSF determinations Z^g, Z^l, and the standard SF determination Z^{SF}. The 1-loop perturbative result is also given. The set of lattice parameters is the one corresponding to LCP_0 and PT.

For this study we consider the bare $\gamma_5 \tau^1$-odd correlation functions corresponding to (5.62), and in addition some alternative discretization of the latter (see below). Note that we exclude g_A^{ud} since this has been used for the tuning of z_f, and thus is automatically zero within errors. As discussed already, in practice we can simply focus on the bare correlation functions since they are anyway expected to vanish as $O(a)$ effects up to logarithmic corrections. In particular, the correlation functions we consider are the only $\gamma_5 \tau^1$-odd correlators among those we introduced that do not vanish identically because of some exact lattice symmetry.

Given these observations, in Figure 5.11 we present the results for the continuum limit extrapolation of the $\gamma_5 \tau^1$-odd two-point functions considered along the line of constant physics defined by LCP_0. As we can see from the plot, with the exception of
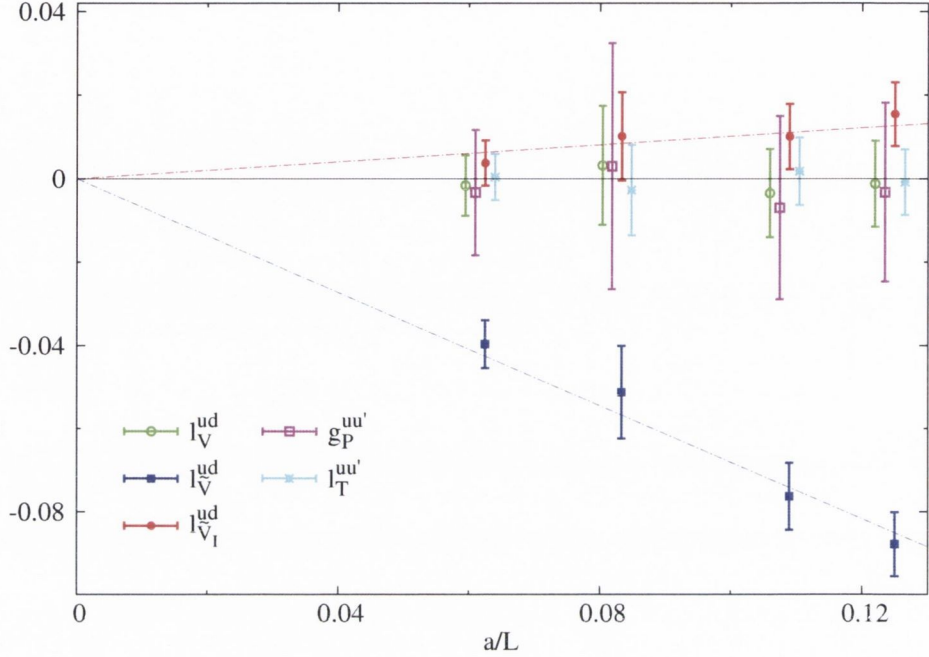
Fig. 5.11: Continuum limit extrapolations for a set of $\gamma_5\tau^1$-odd correlation functions along the line of constant physics given by LCP_0.

the single correlation function $l^{ud}_{\widetilde{V}}$, all other $\gamma_5\tau^1$-odd correlators are zero within errors. We are thus tempted to conclude that once the bulk action is improved, the remaining cutoff effects corresponding to the bulk $\mathrm{O}(a)$ operator counterterms, and eventually some $\mathrm{O}(a)$ boundary counterterms, and the $\mathrm{O}(a)$ ambiguities in the determination of the critical mass and z_f, are generally small.

Going back to $l^{ud}_{\widetilde{V}}$, we see instead a clear $\mathrm{O}(a)$ scaling to the continuum limit. The results for $l^{ud}_{\widetilde{V}}$ indeed are described rather well by a linear fit in a/L constrained to zero. These sizable $\mathrm{O}(a)$ effects in $l^{ud}_{\widetilde{V}}$, we argue, can be attributed to the corresponding $\mathrm{O}(a)$ operator counterterm. As we can see from the plot indeed, if we consider the bulk $\mathrm{O}(a)$ improved definition $l^{ud}_{\widetilde{V}_I}$ (cf. (5.35)), where $c_{\widetilde{V}}$ is set to its tree-level value $c^{(0)}_{\widetilde{V}} = \frac{1}{2}$, the corresponding results are compatible with zero. To conclude, note that also l^{ud}_V and $l^{uu'}_T$ do in principle have $\mathrm{O}(a)$ contributions coming from the insertion of the bulk operators V_k and T_{0k}, respectively (cf. (5.34) and (5.38)). In this case, however,

the respective improvement coefficients c_V and c_T are zero at tree-level, and their 1-loop corrections are small (Sint and Weisz, 1998). We thus expect that in general the contribution of the corresponding $O(a)$ counterterms is smaller than for the case of $l_{\widetilde{V}}^{ud}$.

5.7   Results from the femto-universe: Z_P

In this section, we want to investigate the universality of the continuum limit between the SF and χSF by studying the running of the quark masses at high-energy. More precisely, we want to compare the results for the scale-dependent renormalization of the pseudo-scalar density, Z_P, and the corresponding step-scaling function (cf. Section 5.2.3). To this end, we will consider the LCPs defined by: LCP_1, LCP_2, and LCP_3 (cf. Table 5.3). As discussed, in this case the LCP is defined in terms of the SF coupling $\bar{g}^2(L)$, which implicitly fixes the physical spatial extent L of our space-time lattice. In fact, for the range of (renormalized) couplings we have chosen, the resulting volumes are pretty tiny with $L < 0.25\,\text{fm}$. We thus suggestively refer to these volumes as the *femto-universe* (Lüscher, 1998a). Note that on these ensembles we have also conducted a similar scaling analysis as the one presented in Section 5.4.3 and 5.6. Since analogous conclusions were found, we decided to collect the results in Appendix D.4. What we will present instead is a discussion on flavour symmetry restoration (cf. Section 5.2.2).

Before moving to the results, let us mention that for the determinations on these ensembles we have included estimates for the systematics effects coming from the finite precision on the tuning to zero quark-mass, as well as for the tuning of z_f. However, apart from the study of the step scaling functions, we did not include an estimate for the finite precision on the condition $\bar{g}^2(L) = \text{const}$. This in fact is not straightforward since the derivative of our observables w.r.t. the SF coupling needs to be determined, either analytically or numerically. We did not do this yet. On the other hand, as we will discuss, even without including these systematics the qualitative picture that will emerge is the expected one.

5.7.1 The running of the quark-masses

Ratio of pseudo-scalar renormalization factors. The first quantity we consider is the ratio of Z_P factors defined in (5.58). As discussed, in this ratio the universal divergent part cancels between the SF and χSF renormalization constants leaving only a finite regular function of the lattice spacing. The corresponding results for this ratio for the three ensembles LCP_1, LCP_2, and LCP_3 are presented in Figure 5.12. Note that more precisely we look at the quantity,

$$R \equiv 1 - \frac{Z_P^{\chi\text{SF}}}{Z_P^{\text{SF}}}, \tag{5.67}$$

where we subtracted the expected continuum limit of the ratio. We recall that the values for Z_P^{SF} can be found in (Della Morte *et al.*, 2005*a*).
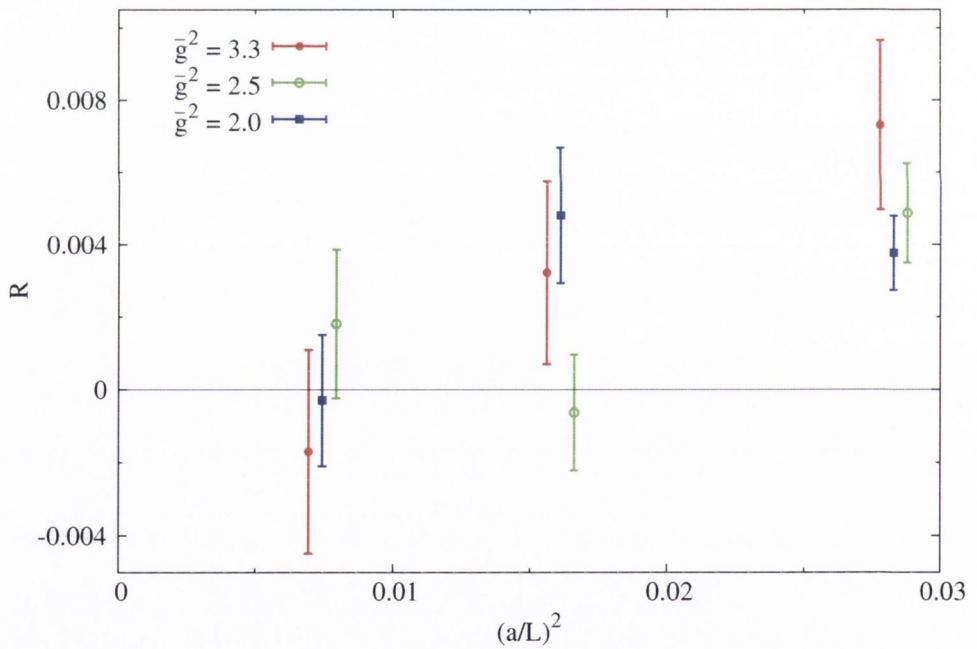

Fig. 5.12: Continuum limit extrapolations for the relative difference R (5.67) of Z_P factors computed from the SF and χSF. The lines of constant physics considered are specified by the value of the SF coupling $\bar{g}^2$, and are given by LCP_1, LCP_2, and LCP_3.

As we can see, the agreement between SF and χSF is generally good, indicating that cutoff effects are small. In fact, the relative difference R between the corresponding Z_P factors is never greater than 1%, even for the largest value of the SF coupling and smallest lattice size L/a considered. The scaling of this ratio however is not evident. In particular it is not clear whether $L/a = 6$ does or does not belong to the scaling region. An additional point at a larger value of L/a would thus be desirable to make definite conclusions. On the other hand, already at $L/a = 12$ the ratio has the expected continuum value within errors for all three values of the SF coupling.
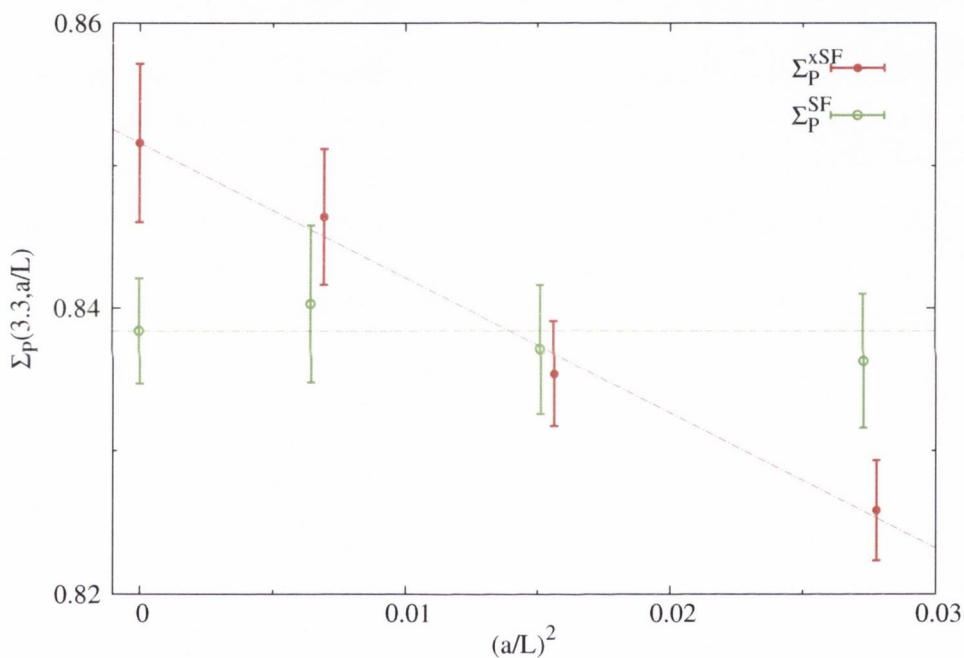

Fig. 5.13: Continuum limit extrapolation for the lattice step-scaling function $\Sigma_P^{\chi \mathrm{SF}}$ and Σ_P^{SF} obtained from the χSF and SF, respectively. The line of constant physics is defined by LCP_1.

Step-scaling function of Z_P. The second observable we considered is the step-scaling function of Z_P (cf. eq. (5.60)). More precisely, we studied the continuum limit of the lattice step-scaling function Σ_P as obtained from the χSF, and compared the

results with the corresponding SF determination (Della Morte *et al.*, 2005*a*). Note that we considered a single value of the SF coupling $\bar{g}^2(L)$. The computation of the step-scaling function in fact requires the evaluation of Z_P for the double lattices with $L'/a = 2L/a$, and it then involves lattices up to $L/a = 24$. These are relatively demanding in terms of computer resources, and we thus decided to focus only on the most non-perturbative case by choosing the largest coupling.

The corresponding results are shown in Figure 5.13. Note that the error due to the uncertainty in the SF coupling was added in quadrature to the statistical error of $\Sigma_P^{\chi SF}$. The latter has been estimated using the 1-loop result for the derivative of $\Sigma_P^{\chi SF}$ with respect to $\bar{g}^2$ (Della Morte *et al.*, 2005*a*). This is in fact universal so that we could use the result for the standard SF. The resulting correction is very tiny, and it increases the error of $\Sigma_P^{\chi SF}$ by at most 5% at the the largest coupling and lattice.

Going back to the results in the figure, we find good agreement between the SF and χSF determinations of the step-scaling function already at finite lattice spacing, indicating that cutoff effects are relatively small w.r.t. the statistical uncertainties. The results for $L/a > 6$ in fact are compatible within a single standard deviation, while the values at $L/a = 6$ only differ by (roughly) 2 standard deviations. On the other hand, due to the slightly better precision in our determinations and the value obtained for $L/a = 6$, we could not simply fit our results to a constant as in the standard SF case. A linear continuum extrapolation in $(a/L)^2$ was needed in order to obtain a good χ^2.[14] Our resulting continuum value then turned out to be slightly higher and less accurate than the SF determination. However, the two agree within two standard deviations.

To conclude, we obtained a non-trivial check of universality between the standard SF and the χSF also from the study of scale-dependent renormalization factors. This suggest to combine the results from the SF and χSF in a joint continuum extrapolation in order to improve the accuracy of the determination.

---

[14]We note that in principle the step-scaling function has $O(a)$ discretization errors coming from the boundaries. There in fact we only have improvement at 1-loop order in perturbation theory. The relevant question for these continuum limit extrapolations is thus whether these effects are small compared to the statistical precision on the results, such that in practice a linear behavior in a^2 well describes the data.

5.7.2   Flavour symmetry restoration

To conclude, we briefly present some results on the ratio of the boundary-to-boundary correlators (5.55). More precisely, in Figure 5.14 we consider the continuum limit of these ratios for the three lines of constant physics LCP_1, LCP_2, and LCP_3. As noticed, these ratios are expected to converge to 1 in the continuum with $O(a^2)$ corrections. We thus considered linear fits in $(a/L)^2$ constrained to pass through 1.
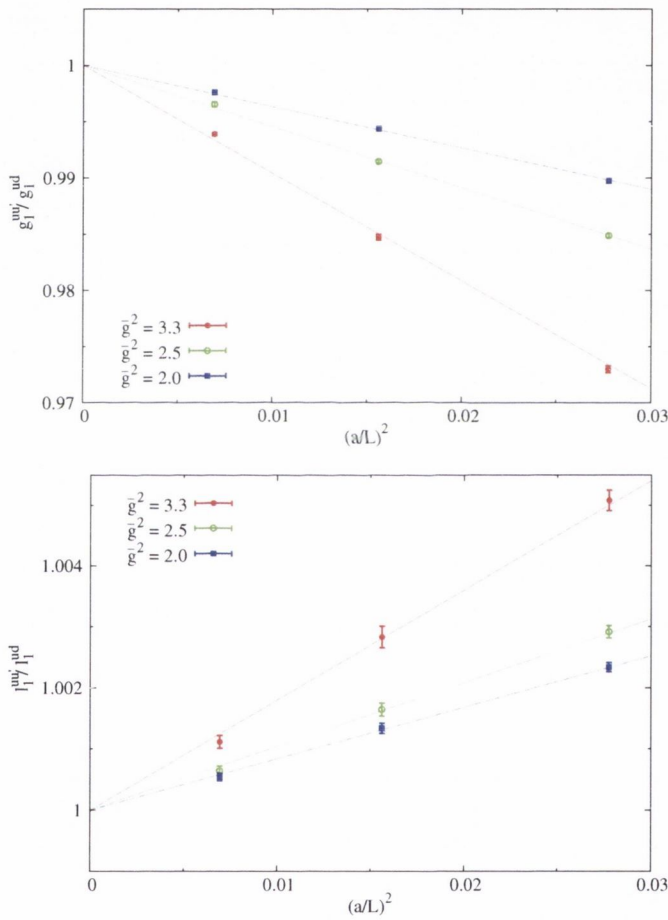

Fig. 5.14: Continuum limit extrapolations for ratios of boundary-to-boundary correlation functions for the lines of constants physics given by LCP_1, LCP_2, and LCP_3

As we can see from the figure, the values we obtained for these ratios are very precise. The ratios of l_1 correlators then nicely follow the expected $O(a^2)$ scaling for all values of the SF coupling and including all lattice sizes. Note also that, the violations from the continuum limit are very tiny in this case and of the order of at most 0.5%.

For the case of the g_1 functions the situation is similar at the two smallest values of the SF coupling, which extrapolate to 1 with the proper $O(a^2)$ scaling. The corrections from the continuum value however are more pronounced than in the case of the l_1 functions but yet quite small i.e. of the order of $\sim 1.5\%$. For the largest value of the SF coupling instead, we see some tension for the value of the g_1's ratio at $L/a = 12$. On the other hand, as mentioned, in these determinations we did not include the systematic errors due to the statistical uncertainty on the SF coupling. Note that this is in general twice as large for the largest lattice sizes on a given LCP (cf. Table 5.3). We thus suspect that this contribution is important for these ratios of correlation functions due to their high-precision, and that our errors are then underestimated. In any case, we conclude that the expected scaling is qualitatively confirmed.

5.8   Some checks on the simulations

To conclude this chapter, we want to present some of the checks we performed on our simulations in order to support the reliability of our determinations. Specifically, these include: a study of the reversibility and area preservation of the MD integrator in the HMC, an estimate of the longest autocorrelation times in our simulations, and a discussion on the ergodicity of the algorithm in sampling the different topological sectors.

5.8.1   Reversibility and area preservation in the MD equations

The first issue that we want to address is the integration of the MD equations in the HMC. As discussed in Section 4.1.3 indeed, in order for the algorithm to be exact, the numerical integrator needs to satisfy two basic properties: time reversibility, and preservation of the phase-space measure. In principle, these properties are guaranteed if symplectic integrators are employed. In practice, however, rounding errors in the integration of the MD equations, and a "sloppy" solution of the Dirac equation along

the MD trajectory can compromise these basic properties (see (Joo *et al.*, 2000)). In particular, the latter issue can be quite problematic if, as in our case, one uses chronological inversions to speed up the solution of the Dirac equation along the MD trajectory (see (Lüscher, 2010*a*)). In this case indeed the reversibility of the algorithm can be severely violated. In the following we will thus investigate if our choices of parameters for the numerical integrator were sensible in this respect. Note that we will focus only on the simulations belonging to LCP_0. These in fact were the more delicate from a numerical point of view.

In order to study the time reversibility and area preservation of the algorithm we need to introduce a suitable set of observables. In this respect, from the hypothesis of area preservation of the integrator one can easily derive the following relation (see e.g. (Montvay and Münster, 1997)),

$$\langle e^{-\Delta H} \rangle = 1, \tag{5.68}$$

where ΔH is the difference in the Hamiltonian between the end and starting point of a trajectory (cf. (4.10)).

A second useful quantity to consider is given by,

$$\delta H(\Pi, U) = \{H(\Pi''(\tau), U''(\tau)) - H(\Pi(0), U(0)\}_{\Pi(0)=\Pi, U(0)=U}, \tag{5.69}$$

where $\Pi''(\tau)$ and $U''(\tau)$ are obtained by integrating the MD equations up to a time $t = \tau$ starting from the initial conditions $\Pi''(0) \equiv -\Pi(\tau)$, and $U''(0) \equiv U(\tau)$. If the integrator was exactly time-reversible, we would then expect the difference in the Hamiltonians (5.69) to be zero. In particular, note that $1/\delta H$ gives an estimate of the frequency with which we make a mistake in the accept-reject step along the HMC history. It is then important that this quantity is much longer than the total length of our runs.

Analogously to the difference in the energy (5.69), one can look directly at the difference between the gauge fields U and U''. This can be done by introducing some suitable norm on the space of gauge fields. In our case we consider,

$$\delta U(U) \equiv \max_{\substack{x,\mu, \\ i,j}} |U''^{ij}_\mu(x) - U^{ij}_\mu(x)|, \tag{5.70}$$

where i, j indicate the row and column indices of the given link variable. In (5.70) we are thus looking at the maximum absolute deviation in the gauge field, component by component, after integrating the MD equations back-and-forth a given trajectory. Again if the integrator was exactly time-reversible, we would expect this quantity to be exactly zero.

Table 5.7 Reversibility checks for the ensembles in LCP_0. The maximum (max), minimum (min), and average (avr) values for δH and δU are given.

L/a	β	δH			δU		
		min	max	avr	min	max	avr
8	5.2	1.21e-09	1.38e-06	2.52e-07	7.81e-10	1.04e-08	1.36e-09
12	5.5	5.60e-10	2.08e-06	5.15e-07	1.11e-09	1.07e-08	1.76e-09
16	5.7	4.20e-08	5.67e-06	1.21e-06	1.28e-09	1.59e-08	2.05e-09
8*	5.3	5.00e-12	1.71e-07	2.45e-08	6.45e-11	1.17e-09	1.23e-10
10	5.3	5.84e-09	1.31e-06	3.43e-07	1.09e-09	6.56e-09	1.88e-09
12	5.3	5.06e-10	2.38e-06	6.58e-07	1.44e-09	1.15e-08	2.81e-09
12	5.2	3.42e-10	2.69e-06	6.03e-07	1.72e-09	1.86e-08	3.53e-09

* A smaller CG residuum has been used.

In Table 5.7, we present the results for (5.69) and (5.70) for the ensembles in LCP_0. The measure has been performed by considering (roughly) $300 - 500$ trajectories of the corresponding ensemble. As we can see from the table, the values are generally very good (e.g. compare with the discussion in (Joo *et al.*, 2000)).[15] In particular, the values of δH are such that the frequency of mistakes in our accept-reject step is extremely rare given the length of our runs (cf. Table 5.9).

To conclude, in Table 5.8 we also report the results for (5.68). Note that the different replicas r_i for the given ensembles have been investigated separately. As we can see

[15]We note that there is no solid theoretical argument for judging the goodness of these numbers, since the effects of the rounding are very difficult to infer, especially those related to the iterative solution of the Dirac equation in the integration of the MD equations.

Table 5.8 Checks on the area preservation for the ensembles in LCP_0. Note that the different replicas r_i have been studied separately.

L/a	β	$\langle e^{-\Delta H} \rangle$			
		r_1	r_2	r_3	r_4
8	5.2	1.0012(11)	1.0009(12)		
12	5.5	0.9952(23)	0.9947(22)	1.0036(23)	
16	5.7	1.0011(39)	1.0039(40)	1.0087(39)	
8	5.3	0.9988(11)	1.0008(17)		
10	5.3	0.9998(21)	1.0012(20)	1.0026(21)	1.0009(20)
12	5.3	0.9986(38)	1.0051(41)	1.0018(40)	
12	5.2	0.9965(23)	1.0006(21)	1.0010(21)	

from the table, the condition is generally well-satisfied. In particular, three standard derivations differences from the expected condition are not unusual. This because this expectation value is in general dominated by "spikes" in ΔH related to the occurrence of small eigenvalues of the Wilson Dirac operator along the MD trajectories.

5.8.2 Autocorrelations and topology

In order to study the reliability of our statistical error estimates, we have analyzed the autocorrelations in our simulations. Only if the latter are reliably determined indeed, our error estimate can be trusted. To this end, we have considered three different observables, namely: the average plaquette (Plaq), a given discretization of the Yang-Mills action at positive flow time Y_{act} (Lüscher, 2010b), and the topological charge at positive flow time summed over the whole space-time volume Q_{top} (Lüscher, 2010b). In particular, the flow observables have been measured for a value of the flow time specified by $c = \sqrt{8t}/L \sim 0.5$. We note that, in general, observables defined through the Yang-Mills gradient flow are good indicators for potentially long autocorrelations in our simulations (Lüscher and Schaefer, 2013). These observables can in fact be used to estimate the exponential autocorrelation time τ_{exp}, or at least to have a lower-bound for it. In addition, differently from the case of the plaquette, the autocorrelations of

these observables have a well-defined continuum limit, so that their scaling can be studied (Lüscher, 2010b).

In Table 5.9, we present our results for the ensembles along the LCP given by LCP_0. The autocorrelations have been estimated as discussed in (Wolff, 2004). In particular, a general criteria for a proper determination of the autocorrelations in our simulations is that the length of our runs should be at least of the order of $100\,\tau_{\text{exp}}$ (Schaefer, Sommer and Virotta, 2011; Schaefer, 2012). If we take as τ_{exp} the longest of the autocorrelation times we have measured, this condition is generally satisfied for each of the replicas of our ensembles.

Table 5.9 Integrated autocorrelation times for the average plaquette (Plaq), the flow Yang-Mills action (Y_{act}), and the flow topological charge Q_{top}, for the ensembles along the LCP given by LCP_0. The total number of trajectories of the different ensembles are also given in terms of the corresponding replica sets.

| L/a	β	$\tau_{\text{int}}(\text{Plaq})$	$\tau_{\text{int}}(Y_{\text{act}})$	$\tau_{\text{int}}(Q_{\text{top}})$	traj. (MDU)
8	5.2	6.0(3)	14(1)	7.0(5)	40000×2
12	5.5	4.8(3)	41(8)	- *	8000×3
16	5.7	4.7(4)	42(9)	11(2)	6000×3
8	5.3	5.7(2)	10.0(5)	10.8(6)	$80000 + 40000$
10	5.3	5.5(3)	35(5)	48(7)	10000×4
12	5.3	5.6(4)	100(25)	95(23)	8000×3
12	5.2	7.2(6)	59(11)	37(6)	10000×3

Before concluding, we want to note that for $L/a = 12$ and $\beta = 5.5$ we could not determine the autocorrelation function for the topological charge. This was due to a peculiar behavior of the latter. This can be seen in more detail in Figure 5.15, where we show the topological charge distribution along the MC history of three of the ensembles of LCP_0.[16] As we can see from the figures, the system gets quickly frozen in the trivial

---

[16]Note that for the scope of illustration, for each given ensemble we patched the different replica histories one after the other.

topological sector $Q_{\text{top}} = 0$ as the lattice spacing is decreased. Already at the coarsest lattice spacing, however, the topological charge does not show much excursion outside this sector, which then seems to be the only relevant one at this physical volume. On the other hand, at the intermediate lattice spacing corresponding to $\beta = 5.5$ the topological charge rapidly jumps to -1 and stays around this value for roughly 150 MDU. This did not allow us to determine the corresponding autocorrelation function along the MC history. In this respect, we note that these rapid excursions of the topological charge to non-trivial sectors in relatively small volumes are not unexpected in simulations of the SF (see e.g. (Jansen and Sommer, 1998)).

To conclude, the relevant general question is how the sampling of the topological sectors in simulations does affect the determination of our specific observables within our precision (Schaefer, Sommer and Virotta, 2011). In this respect, we note that renormalization factors and parameters can in principle be defined such that only contributions from the trivial topological sector are considered (Fritzsch, Ramos and Stollenwerk, 2013). In this way one can avoid in practice the consequences of a bad sampling of the topological charge as we approach the continuum limit of the SF. In our case, however, this is not an issue since the physical volume is small enough that only the trivial topological sector actually contributes to the SF path integral. Indeed, the restriction of our renormalization factors, and renormalization conditions for m_{PCAC} and z_f, to the trivial topological sector, does not have any influence within the final errors.

Fig. 5.15: Topological charge distribution. Lattice spacing dependence. $L \sim 0.60$ fm.

(a) $L/a = 8$, $\beta = 5.2$

(b) $L/a = 12$, $\beta = 5.5$

(c) $L/a = 16$, $\beta = 5.7$
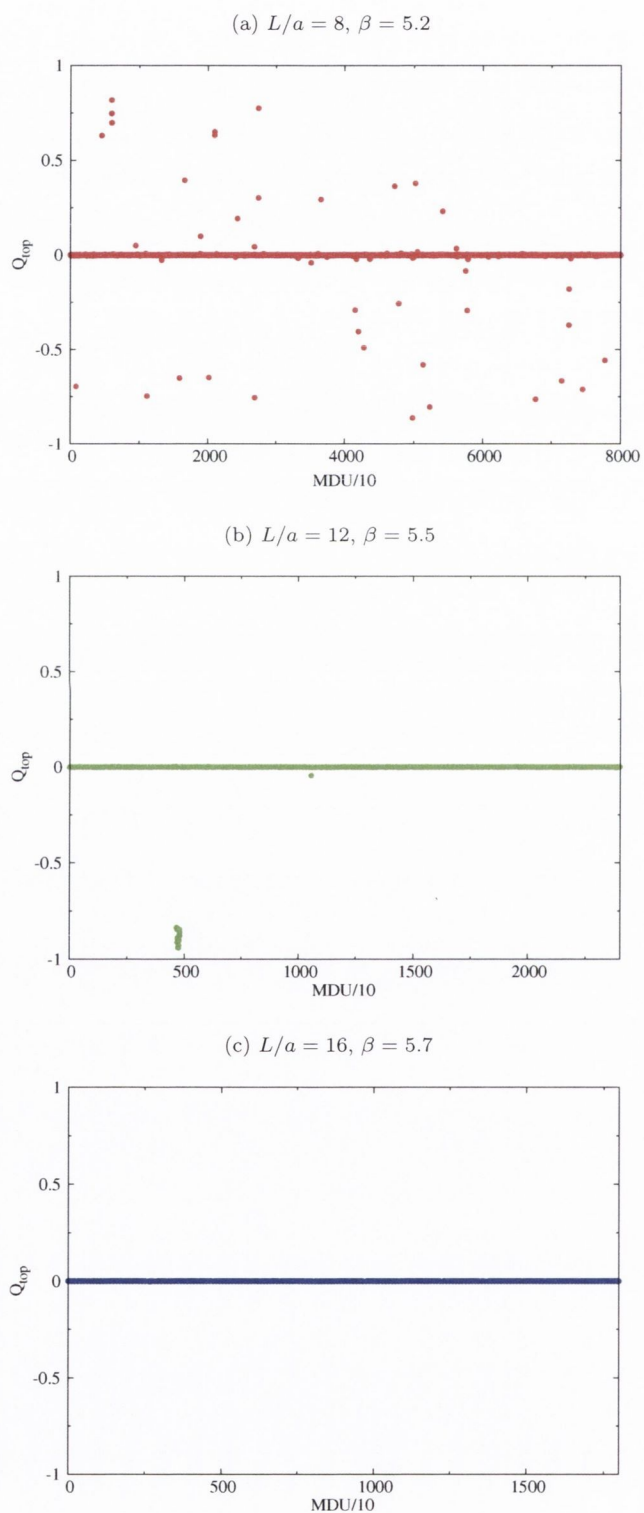
6
Conclusions

In this work, we presented a first complete study of the chirally rotated Schrödinger functional with dynamical Wilson-fermions. The first important conclusion that we draw is that the expectations from the results in perturbation theory (Sint, 2011; Vilaseca, 2013), and in the quenched approximation (Sint and Leder, 2010; Lopez, Jansen, Renner and Shindler, 2013b; Lopez, Jansen, Renner and Shindler, 2013a) are confirmed. More precisely, through the detailed analysis of several different observables over a wide range of parameters, we have given substantial evidence for the existence and universality of the continuum limit of the χSF. In particular, the property of automatic $O(a)$ improvement has been shown to be realized as expected after the proper renormalization of the theory.

Secondly, the universality relations offer a novel method for the computation of the finite renormalization constants related to the breaking of chiral symmetry by Wilson-fermions (Sint and Leder, 2010). In this work we investigated this possibility in detail. The results show that these determinations are very competitive and robust. Due to the property of automatic $O(a)$ improvement, several different definitions can be studied without having to perform the corresponding improvement. This allows to control carefully the size of cutoff effects in the determinations, and eventually choose the more precise and solid definition for the given renormalization constant. Moreover, their evaluation in terms of simple ratios of two-point functions gives very accurate predictions.

In this respect, we want to note that our results for the renormalization of the axial current, Z_A, improve significantly on previous SF determinations. The total error on this quantity indeed has been reduced by a factor 10. This result can have an important impact on the computations performed in large volume simulations with

Wilson-fermions. In fact, the renormalization of the axial current is a fundamental ingredient in the present strategy for the determination of the lattice spacing at the bare couplings of interest (Fritzsch *et al.*, 2012). In particular, the precision on Z_A has been so far the dominant source of error in this determination. Improving the accuracy on the lattice spacing is then crucial, since this quantity enters in the conversion of any dimensionless lattice result to physical units.

Table 6.1 Comparison between the lattice spacings a^{SF} and $a^{\chi\mathrm{SF}}$, as determined using Z_A^{SF} and Z_A^l, respectively.

β	a^{SF} (fm)	$a^{\chi\mathrm{SF}}$ (fm)
5.2	0.0755(9)(7)	0.0747(2)
5.3	0.0658(7)(7)	0.0648(2)
5.5	0.0486(4)(5)	0.0480(2)

We thus want to show the effect of our results for Z_A on the determination of the lattice spacing a. In Table 6.1, we present a comparison of the values obtained for a using the standard SF determination, Z_A^{SF}, and our most precise determination Z_A^l (cf. Table 5.5). The strategy followed for the computation is the same as in (Fritzsch *et al.*, 2012). As we can see from the table, the new preliminary values for the lattice spacing are at least 3 times more precise than the previous results.[1]

To conclude, the χSF provides a competitive tool for solving non-perturbative renormalization problems on the lattice. As a future application of the method, it is thus natural to address the renormalization of more complicated operators. These in particular include four quark-operators relevant for the determination of electro-weak hadronic matrix elements.

---

[1] The author warmly thanks Stefano Lottini for having provided these results.

Appendix A
Useful definitions

The notation conventions presented in this Appendix are taken from (Lüscher, Sint, Sommer and Weisz, 1996).

A.1 Index conventions

Lorentz indices $\mu, \nu, \ldots$ are taken from the middle Greek alphabet and run from 0 to 3. Latin indices $k, l, \ldots$ run from 1 to 3 and are used to label the components of the spatial vectors. For the Dirac indices capital letters $A, B, \ldots$ from the beginning of the alphabet are taken. They run from 1 to 4. Color vectors in the fundamental representation of $\mathrm{SU}(N)$ carry indices $\alpha, \beta, \ldots$ ranging from 1 to N, while for vectors in the adjoint representation, Latin indices $a, b, \ldots$ running from 1 to $N^2 - 1$ are employed. By abuse of notation such indices are also used for the flavor label of the axial current and density. Repeated indices are always summed over unless otherwise stated and scalar products are taken with euclidean metric.

A.2 Dirac matrices

We choose a chiral representation for the Dirac matrices, where

$$\gamma_\mu = \begin{pmatrix} 0 & e_\mu \\ e_\mu^\dagger & 0 \end{pmatrix}. \tag{A.1}$$

The 2×2 matrices e_μ are taken to be,

$$e_0 = -1 \qquad e_k = -i\sigma_k, \tag{A.2}$$

with σ_k the Pauli matrices. In is then easy to check that

$$\gamma_\mu^\dagger = \gamma_\mu, \qquad \{\gamma_\mu, \gamma_\nu\} = 2\delta_{\mu\nu}. \tag{A.3}$$

Furthermore, if we define $\gamma_5 = \gamma_0\gamma_1\gamma_2\gamma_3$, we have,

$$\gamma_5 = \begin{pmatrix} 1 & 0 \\ 0 & -1 \end{pmatrix}. \tag{A.4}$$

In particular, $\gamma_5 = \gamma_5^\dagger$ and $\gamma_5^2 = 1$.

Having introduced γ_5 one can also introduce the chiral projects:

$$P_R = \frac{1 + \gamma_5}{2}, \qquad P_L = \frac{1 - \gamma_5}{2}. \tag{A.5}$$

Finally, the hermitian matrices

$$\sigma_{\mu\nu} = \frac{i}{2}[\gamma_\mu, \gamma_\nu] \tag{A.6}$$

are explicitly given by

$$\sigma_{0k} = \begin{pmatrix} \sigma_k & 0 \\ 0 & -\sigma_k \end{pmatrix}, \qquad \sigma_{ij} = -\epsilon_{ijk}\begin{pmatrix} \sigma_k & 0 \\ 0 & \sigma_k \end{pmatrix}, \tag{A.7}$$

where ϵ_{ijk} is the totally anti-symmetric tensor with $\epsilon_{123} = 1$.

A.3 Gauge group

The Lie algebra $\mathfrak{su}(N)$ of $SU(N)$ can be defined as the space of complex $N \times N$ matrices $X_{\alpha\beta}$ which satisfy

$$X^\dagger = -X, \qquad \mathrm{tr}\{X\} = 0, \tag{A.8}$$

where $X^\dagger$ denotes the adjoint matrix and $\mathrm{tr}\{X\} = X_{\alpha\alpha}$ is the trace of X. We may choose a basis T^a, $a = 1, 2, \ldots, N^2 - 1$, in this space such that

$$\mathrm{tr}\{T^a T^b\} = -\frac{1}{2}\delta^{ab}. \tag{A.9}$$

For $N = 2$, for example, the standard basis is

$$T^a = \frac{\tau^a}{2i}, \qquad a = 1, 2, 3, \tag{A.10}$$

where τ^a denote the Pauli matrices. With these conventions the structure constants f^{abc}, defined through

$$[T^a, T^b] = f^{abc}T^c, \tag{A.11}$$

are real and totally ant-symmetric under permutations of the indices.

If $\mathcal{F}(U)$ is a differentiable function of the gauge field, its derivative with respect to the link variable $U_\mu(x)$ in the direction of the generator T^a is defined by

$$\partial^a_{x\mu}\mathcal{F}(U) = \frac{d}{dt}\mathcal{F}(U_t)\bigg|_{t=0}, \quad U_t(y,\nu) = \begin{cases} e^{tT^a}U_\mu(x) & \text{if } (y,\nu)=(x,\mu), \\ U_\nu(y) & \text{otherwise.} \end{cases} \tag{A.12}$$

In particular, in the case of a scalar function $\mathcal{F}(U)$, the combination,

$$\partial_{x,\mu}\mathcal{F}(U) \equiv T^a \partial^a_{x\mu}\mathcal{F}(U), \tag{A.13}$$

is a vector field with values in $\mathfrak{su}(N)$ that transform under the adjoint representation of the gauge group.

A.4   Lattice derivatives

Ordinary forward and backward lattice derivatives act on colour singlet functions $f(x)$ as

$$\partial_\mu f(x) = \frac{1}{a}[f(x+a\hat{\mu}) - f(x)], \tag{A.14}$$

$$\partial^*_\mu f(x) = \frac{1}{a}[f(x) - f(x-a\hat{\mu})], \tag{A.15}$$

where $\hat{\mu}$ denotes the unit vector in the direction μ. Another useful discretization of the continuum derivative is given by the average of the forward and backward lattice derivatives,

$$\tilde{\partial}_\mu f(x) \equiv \frac{1}{2}(\partial^*_\mu + \partial_\mu)f(x) = \frac{1}{2a}[f(x+a\hat{\mu}) - f(x-a\hat{\mu})]. \tag{A.16}$$

The gauge covariant derivatives instead, act on quark fields as,

$$\nabla_\mu \psi(x) = \frac{1}{a}[\lambda_\mu U_\mu(x)\psi(x+a\hat{\mu}) - \psi(x)], \tag{A.17}$$

$$\nabla^*_\mu \psi(x) = \frac{1}{a}[\psi(x) - \lambda^*_\mu U^\dagger_\mu(x-a\hat{\mu})\psi(x-a\hat{\mu})], \tag{A.18}$$

The origin of the phase factors,

$$\lambda_\mu = e^{ia\theta_\mu/L}, \qquad \theta_0 = 0, \qquad -\pi < \theta_k \le \pi, \tag{A.19}$$

is explained in Section 3.2.2. They depend on the spatial extent L of the lattice and are all equal to 1 on the infinite or periodic lattice. The left action of the lattice derivative operators is then defined as,

$$\overline{\psi}(x)\,a\overleftarrow{\nabla}_\mu = \overline{\psi}(x+a\hat{\mu})U_\mu^\dagger(x)\lambda_\mu^* - \overline{\psi}(x), \tag{A.20}$$

$$\overline{\psi}(x)\,a\overleftarrow{\nabla}_\mu^* = \overline{\psi}(x) - \overline{\psi}(x-a\hat{\mu})U_\mu(x-a\hat{\mu})\lambda_\mu]. \tag{A.21}$$

A.5   Continuum fields and their discretization

An SU(N) gauge potential in the continuum theory is a vector field $A_\mu(x)$ with values in the Lie algebra $\mathfrak{su}(N)$. It can thus be written as,

$$A_\mu(x) = A_\mu^a(x)T^a, \tag{A.22}$$

with real functions $A_\mu^a(x)$. The associated field tensor,

$$F_{\mu\nu}(x) = \partial_\mu A_\nu(x) - \partial_\nu A_\mu(x) + [A_\mu(x), A_\nu(x)], \tag{A.23}$$

may be decomposed similarly and the right and left action of the covariant derivative D_μ is defined by

$$D_\mu\psi(x) = (\partial_\mu + A_\mu + i\theta_\mu/L)\psi(x) \tag{A.24}$$

$$\overline{\psi}(x)\overleftarrow{D}_\mu = \overline{\psi}(x)(\overleftarrow{\partial}_\mu - A_\mu - i\theta_\mu/L). \tag{A.25}$$

The Abelian gauge field $i\theta_\mu/L$ appearing here has been introduced in Section 3.13.

Finally, note that a lattice discretization of the field strength tensor (A.23) can be obtained as,

$$\widehat{F}_{\mu\nu}(x) = \frac{1}{8a^2}\{Q_{\mu\nu}(x) - Q_{\nu\mu}(x)\}, \tag{A.26}$$

where the matrices $Q_{\mu\nu}(x)$ are defined as,

$$\begin{aligned}
Q_{\mu\nu}(x) = {} & U_\mu(x)U_\nu(x+a\hat{\mu})U_\mu(x+a\hat{\nu})^{-1}U_\nu(x)^{-1} \\
& + U_\nu(x)U_\mu(x-a\hat{\mu}+a\hat{\nu})^{-1}U_\nu(x-a\hat{\mu})^{-1}U_\mu(x-a\hat{\mu}) \\
& + U_\mu(x-a\hat{\mu})^{-1}U_\nu(x-a\hat{\mu}-a\hat{\nu})^{-1}U_\mu(x-a\hat{\mu}-a\hat{\nu})U_\nu(x-a\hat{\nu}) \\
& + U_\nu(x-a\hat{\nu})^{-1}U_\mu(x-a\hat{\nu})U_\nu(x+a\hat{\mu}-a\hat{\nu})U_\mu(x)^{-1}.
\end{aligned} \tag{A.27}$$

This defines the so-called *clover* definition of the lattice field strength tensor.

A.6   Discrete symmetry transformations

A.6.1   Charge conjugation

Under charge conjugation the gauge field transformations according to

$$U_\mu(x) \to U_\mu(x)^*. \tag{A.28}$$

The transformations law for the quark and anti-quark fields reads,

$$\psi(x) \to C^{-1}\overline{\psi}(x)^T, \quad \overline{\psi}(x) \to -\psi(x)^T C, \tag{A.29}$$

where C is a 4×4 matrix satisfying

$$\gamma_\mu^* = -C\gamma_\mu C^{-1}. \tag{A.30}$$

If the Dirac matrices are chosen as specified in Appendix A.2, we may take $C = i\gamma_0\gamma_2$ so that $C^{-1} = C^\dagger = C$.

It follows from these definitions that the Wilson action is invariant under charge conjugation. This is both true in infinite volume and in the Schrödinger functional. In the latter case the transformation is applied to the field variables at all sites of the lattice including the boundaries $x_0 = 0$ and $x_0 = T$.

A.6.2   Parity

A parity transformation is defined as,

$$\psi(x) \to \gamma_0\psi(\tilde{x}), \quad \overline{\psi}(x) \to \overline{\psi}(\tilde{x})\gamma_0, \quad \tilde{x} = (x_0, -\mathbf{x}). \tag{A.31}$$

while the gauge fields transform as,

$$U_0(x) \to U_0(\tilde{x}), \quad U_k(x) \to U_k(\hat{x})^\dagger, \quad \hat{x} = (x_0, -\mathbf{x} - a\hat{k}). \tag{A.32}$$

We here assume periodic boundary conditions for the fields in the spatial directions (or an infinite spatial extend). Similar consideration as for charge conjugation then apply.

A.6.3   Time-reflection

A time-reflection transformation is defined as,

$$\psi(x) \to i\gamma_0\gamma_5\psi(\check{x}), \quad \overline{\psi}(x) \to \overline{\psi}(\check{x})i\gamma_0\gamma_5, \quad \check{x} = (T - x_0, \mathbf{x}). \tag{A.33}$$

while the gauge fields transform as,

$$U_0(x) \to U_0(\check{x})^\dagger, \quad U_k(x) \to U_k(\check{x}), \quad \check{x} = (T - x_0 - a, \mathbf{x}). \tag{A.34}$$

Here we assume the case of a finite temporal extent of the lattice volume given by T.

Appendix B
Molecular dynamics forces

The results reported here are taken from the documentation of `openQCD`.[1]

The force field

$$F_\mu(x) = -2\operatorname{Re}(\chi, \gamma_5 \partial_{x,\mu} \mathcal{D}^{(2)}\psi) \tag{B.1}$$

is a sum of two terms,

$$F_\mu^{\mathrm{sw}}(x) = -2\operatorname{Re}(\chi, \gamma_5 \partial_{x,\mu}(\mathcal{D}_{\mathrm{ee}}^{(2)} + \mathcal{D}_{\mathrm{oo}}^{(2)})\psi), \tag{B.2}$$

$$F_\mu^{\mathrm{hop}}(x) = -2\operatorname{Re}(\chi, \gamma_5 \partial_{x,\mu}(\mathcal{D}_{\mathrm{eo}} + \mathcal{D}_{\mathrm{oe}})\psi). \tag{B.3}$$

In order to give the explicit expression is it convenient to introduce the matrices,

$$X_{\mu\nu}(x) = i\sum_{A=1}^{4}\left\{(\gamma_5\sigma_{\mu\nu}\psi)_A \otimes \chi_A(x)^\dagger + (\psi \leftrightarrow \chi)\right\}, \tag{B.4}$$

$$X_\mu(x) = \sum_{A=1}^{4}\left\{(\gamma_5(1-\gamma_\mu)\psi)_A(x+a\hat\mu) \otimes \chi_A(x)^\dagger + (\psi \leftrightarrow \chi)\right\}. \tag{B.5}$$

The sums in these equations run over the Dirac index of the spinors involved and the tensor products are taken in colour space, i.e. both $X_{\mu\nu}(x)$ and $X_\mu(x)$ are 3×3 complex matrices in colour space.

Given these definitions, the force (B.2) is given by

$$F_\mu^{\mathrm{sw}}(x) = \partial_{x,\mu}S_{\mathrm{sw}} = -\tfrac{1}{8}c_{\mathrm{sw}}(g_0)\sum_{\mathbf{y}\in\Gamma}\sum_{y_0=a}^{T-a}\operatorname{Re}\operatorname{tr}\{(\partial_{x,\mu}Q_{\rho\sigma}(y))X_{\rho\sigma}(y)\}, \tag{B.6}$$

with $Q_{\mu\nu}$ defined as in (A.27).

The force (B.3) instead is given by,

$$F_\mu^{\mathrm{hop}}(x) = \mathcal{P}\{U_\mu(x)X_\mu(x)\}, \tag{B.7}$$

where

$$\mathcal{P}\{m\} = \tfrac{1}{2}(m - m^\dagger) - \tfrac{1}{6}\text{tr}(m - m^\dagger), \tag{B.8}$$

projects any complex 3×3 matrix m to $\mathfrak{su}(3)$. Note that, $F_\mu^{\text{hop}}(x)$ is defined for all x such that $0 \leq x_0 < T$ for $\mu = 0$, and $0 < x_0 < T$ for $\mu = 1, 2, 3$.

Finally, as we have seen the contribution to the pseudo-fermion action given by the small determinant is,

$$S_{\text{det}} = -\text{Tr}\log(1_e + (\mathcal{D}_{\text{oo}}^{(1)})^\dagger \mathcal{D}_{\text{oo}}^{(1)}) = -\sum_{x\,\text{odd}} \text{tr}\log[(M^{(1)}(x))^\dagger M^{(1)}(x)]. \tag{B.9}$$

The corresponding force then reads,

$$F_\mu^{\text{det}}(x) = \partial_{x,\mu} S_{\text{det}} = -\tfrac{1}{4}c_{\text{sw}}(g_0) \sum_{y\,\text{odd}} \text{Re}\,\text{tr}\{(\partial_{x,\mu} Q_{\rho\sigma}(y))\tilde{X}_{\rho\sigma}(y)\}, \tag{B.10}$$

where y is odd with $0 < y_0 < T$, and

$$\tilde{X}_{\mu\nu}(x) = i \sum_{A=1}^{4} \{\sigma_{\mu\nu}(M^{(1)}(x))^{-1}\}_{AA}. \tag{B.11}$$

Appendix C
Correlation functions

In this Appendix we want to present some results on the χSF correlation functions presented in Section 5.1.3. Firstly, we give the definition for the boundary source fields. Secondly, we give the explicit expressions for the correlation functions. Finally, given these expressions we list some exact symmetry properties valid on the lattice.

C.1 Boundary source fields

The χSF boundary fields are defined as follows.

At $x_0 = 0$ we have,

$$\mathcal{Q}_5^{uu'} = \int d^3\mathbf{y}\, d^3\mathbf{z}\, \overline{\zeta}_u(\mathbf{y})\gamma_0\gamma_5 Q_- \zeta_{u'}(\mathbf{z}), \tag{C.1}$$

$$\mathcal{Q}_5^{dd'} = \int d^3\mathbf{y}\, d^3\mathbf{z}\, \overline{\zeta}_d(\mathbf{y})\gamma_0\gamma_5 Q_+ \zeta_{d'}(\mathbf{z}), \tag{C.2}$$

$$\mathcal{Q}_5^{ud} = \int d^3\mathbf{y}\, d^3\mathbf{z}\, \overline{\zeta}_u(\mathbf{y})\gamma_5 Q_+ \zeta_d(\mathbf{z}), \tag{C.3}$$

$$\mathcal{Q}_5^{du} = \int d^3\mathbf{y}\, d^3\mathbf{z}\, \overline{\zeta}_d(\mathbf{y})\gamma_5 Q_- \zeta_u(\mathbf{z}), \tag{C.4}$$

and,

$$\mathcal{Q}_k^{uu'} = \int d^3\mathbf{y}\, d^3\mathbf{z}\, \overline{\zeta}_u(\mathbf{y})\gamma_k Q_- \zeta_{u'}(\mathbf{z}), \tag{C.5}$$

$$\mathcal{Q}_k^{dd'} = \int d^3\mathbf{y}\, d^3\mathbf{z}\, \overline{\zeta}_d(\mathbf{y})\gamma_k Q_+ \zeta_{d'}(\mathbf{z}), \tag{C.6}$$

$$\mathcal{Q}_k^{ud} = \int d^3\mathbf{y}\, d^3\mathbf{z}\, \overline{\zeta}_u(\mathbf{y})\gamma_0\gamma_k Q_+ \zeta_d(\mathbf{z}), \tag{C.7}$$

$$\mathcal{Q}_k^{du} = \int d^3\mathbf{y}\, d^3\mathbf{z}\, \overline{\zeta}_d(\mathbf{y})\gamma_0\gamma_k Q_- \zeta_u(\mathbf{z}). \tag{C.8}$$

At $x_0 = T$ instead,

$$Q_5'^{uu'} = -\int d^3\mathbf{y}d^3\mathbf{z}\,\overline{\zeta}_u'(\mathbf{y})\gamma_0\gamma_5 Q_+\zeta_{u'}'(\mathbf{z}), \tag{C.9}$$

$$Q_5'^{dd'} = -\int d^3\mathbf{y}d^3\mathbf{z}\,\overline{\zeta}_d'(\mathbf{y})\gamma_0\gamma_5 Q_-\zeta_{d'}'(\mathbf{z}), \tag{C.10}$$

$$Q_5'^{ud} = \int d^3\mathbf{y}d^3\mathbf{z}\,\overline{\zeta}_u'(\mathbf{y})\gamma_5 Q_-\zeta_d'(\mathbf{z}), \tag{C.11}$$

$$Q_5'^{du} = \int d^3\mathbf{y}d^3\mathbf{z}\,\overline{\zeta}_d'(\mathbf{y})\gamma_5 Q_+\zeta_u'(\mathbf{z}), \tag{C.12}$$

and,

$$Q_k'^{uu'} = \int d^3\mathbf{y}d^3\mathbf{z}\,\overline{\zeta}_u'(\mathbf{y})\gamma_k Q_+\zeta_{u'}'(\mathbf{z}), \tag{C.13}$$

$$Q_k'^{dd'} = \int d^3\mathbf{y}d^3\mathbf{z}\,\overline{\zeta}_d'(\mathbf{y})\gamma_k Q_-\zeta_{d'}'(\mathbf{z}), \tag{C.14}$$

$$Q_k'^{ud} = -\int d^3\mathbf{y}d^3\mathbf{z}\,\overline{\zeta}_u'(\mathbf{y})\gamma_0\gamma_k Q_-\zeta_d'(\mathbf{z}), \tag{C.15}$$

$$Q_k'^{du} = -\int d^3\mathbf{y}d^3\mathbf{z}\,\overline{\zeta}_d'(\mathbf{y})\gamma_0\gamma_k Q_+\zeta_u'(\mathbf{z}). \tag{C.16}$$

C.2 Explicit expressions and symmetry properties

Before giving the explicit expressions for the correlation functions defined in Section 5.1.3, it is convenient to introduce the following definitions. We first introduce the propagators for the up and down type flavours defined by,

$$M^u = \int d^3\mathbf{y}\,S_u(x;0,\mathbf{y})Q_-, \qquad M^d = \int d^3\mathbf{y}\,S_d(x;0,\mathbf{y})Q_+, \tag{C.17}$$

where on the r.h.s. we employ a continuum notation. These however should be interpreted on the lattice as e.g.,

$$\int d^3\mathbf{y}\,S_u(x;0,\mathbf{y})Q_- \quad \to \quad a^3\sum_{\mathbf{y}} S_u(x;0,\mathbf{y})U_0(0,\mathbf{y})^\dagger Q_-, \tag{C.18}$$

and similarly for M^d.

Given these definitions, after some algebra one arrives at the following explicit expressions for the g_X-functions,

$$g_X^{uu'}(x_0) = \frac{1}{2}\left\langle \mathrm{tr}\left\{ M^d(x)^\dagger \gamma_5 \Gamma_X M^u(x)\gamma_0 \right\}\right\rangle_G, \tag{C.19}$$

$$g_X^{dd'}(x_0) = \frac{1}{2}\left\langle \mathrm{tr}\left\{ M^u(x)^\dagger \gamma_5 \Gamma_X M^d(x)\gamma_0 \right\}\right\rangle_G, \tag{C.20}$$

$$g_X^{ud}(x_0) = \frac{1}{2}\left\langle \mathrm{tr}\left\{ M^d(x)^\dagger \gamma_5 \Gamma_X M^d(x) \right\}\right\rangle_G, \tag{C.21}$$

$$g_X^{du}(x_0) = \frac{1}{2}\left\langle \mathrm{tr}\left\{ M^u(x)^\dagger \gamma_5 \Gamma_X M^u(x) \right\}\right\rangle_G, \tag{C.22}$$

and similarly for the l_Y-functions

$$l_Y^{uu'}(x_0) = \frac{1}{6}\sum_{k=1}^{3}\left\langle \mathrm{tr}\left\{ M^d(x)^\dagger \gamma_5 \Gamma_Y M^u(x)\gamma_k\gamma_5 \right\}\right\rangle_G, \tag{C.23}$$

$$l_Y^{dd'}(x_0) = \frac{1}{6}\sum_{k=1}^{3}\left\langle \mathrm{tr}\left\{ M^u(x)^\dagger \gamma_5 \Gamma_Y M^d(x)\gamma_k\gamma_5 \right\}\right\rangle_G, \tag{C.24}$$

$$l_Y^{ud}(x_0) = \frac{1}{6}\sum_{k=1}^{3}\left\langle \mathrm{tr}\left\{ M^d(x)^\dagger \gamma_5 \Gamma_Y M^d(x)\gamma_0\gamma_k\gamma_5 \right\}\right\rangle_G, \tag{C.25}$$

$$l_Y^{du}(x_0) = \frac{1}{6}\sum_{k=1}^{3}\left\langle \mathrm{tr}\left\{ M^u(x)^\dagger \gamma_5 \Gamma_Y M^u(x)\gamma_0\gamma_k\gamma_5 \right\}\right\rangle_G. \tag{C.26}$$

In order to introduce the boundary-to-boundary correlator, we also define the matrices,

$$L^u = Q_+ \frac{1}{L^3}\int \mathrm{d}^3\mathbf{x}\, M^u(T,\mathbf{x}), \qquad L^d = Q_- \frac{1}{L^3}\int \mathrm{d}^3\mathbf{x}\, M^d(T,\mathbf{x}). \tag{C.27}$$

On the lattice these read e.g.,

$$L^u = Q_+ \frac{a^3}{L^3}\sum_{\mathbf{x}} U_0(T-a,\mathbf{x})^\dagger M^u(T-a,\mathbf{x}). \tag{C.28}$$

Given these definition it is then easy to show that,

$$g_1^{uu'} = \frac{1}{2}\left\langle \mathrm{tr}\left\{ (L^d\gamma_0)^\dagger \gamma_0 L^u \right\}\right\rangle_G, \tag{C.29}$$

$$g_1^{dd'} = \frac{1}{2}\left\langle \mathrm{tr}\left\{ (L^u\gamma_0)^\dagger \gamma_0 L^d \right\}\right\rangle_G, \tag{C.30}$$

$$g_1^{ud} = \frac{1}{2}\left\langle \mathrm{tr}\left\{ (L^u)^\dagger L^u \right\}\right\rangle_G, \tag{C.31}$$

$$g_1^{du} = \frac{1}{2}\left\langle \mathrm{tr}\left\{ (L^d)^\dagger L^d \right\}\right\rangle_G, \tag{C.32}$$

and,

$$l_1^{uu'} = \frac{1}{6} \sum_{k=1}^{3} \left\langle \mathrm{tr}\left\{ \left(L^d \gamma_5 \gamma_k\right)^\dagger \gamma_5 \gamma_k L^u \right\} \right\rangle_G, \tag{C.33}$$

$$l_1^{dd'} = \frac{1}{6} \sum_{k=1}^{3} \left\langle \mathrm{tr}\left\{ \left(L^u \gamma_5 \gamma_k\right)^\dagger \gamma_5 \gamma_k L^d \right\} \right\rangle_G, \tag{C.34}$$

$$l_1^{ud} = \frac{1}{6} \sum_{k=1}^{3} \left\langle \mathrm{tr}\left\{ \left(L^u \gamma_5 \gamma_0 \gamma_k\right)^\dagger \gamma_5 \gamma_0 \gamma_k L^u \right\} \right\rangle_G, \tag{C.35}$$

$$l_1^{du} = \frac{1}{6} \sum_{k=1}^{3} \left\langle \mathrm{tr}\left\{ \left(L^d \gamma_5 \gamma_0 \gamma_k\right)^\dagger \gamma_5 \gamma_0 \gamma_k L^d \right\} \right\rangle_G. \tag{C.36}$$

Once the explicit expressions are obtained, it is also easy to work out some properties and relations for the χSF correlation functions using the exact symmetries on the lattice. These are collected in Table C.1.

Table C.1 Transformation properties of some χSF correlation functions under: complex conjugation (c.c.), parity combined with a flavour exchange ($P \times \tau^1$), and charge conjugation combined with complex conjugation ($C + $c.c.). Note that with "avr." we indicate properties satisfied by the correlators only after the average over the gauge fields is taken, while with "conf." we denote properties that hold for any gauge field configuration. The parity w.r.t. the $\gamma_5 \tau^1$-transform is also listed for completeness.

	c.c.	$P \times \tau^1$	$C + $c.c.	$\gamma_5 \tau^1$	avr.	conf.
$g_1^{uu'}$	$g_1^{dd'}$	$g_1^{dd'}$	$g_1^{uu'}$	$+$	Re	$-$
g_1^{ud}	g_1^{ud}	g_1^{du}	g_1^{du}	$+$	Re	Re
$g_A^{uu'}$	$g_A^{dd'}$	$g_A^{dd'}$	$g_A^{uu'}$	$+$	Re	$-$
g_A^{ud}	g_A^{ud}	g_A^{du}	g_A^{du}	$-$	Re	Re
$g_P^{uu'}$	$g_P^{dd'}$	$g_P^{dd'}$	$g_P^{uu'}$	$-$	Re	$-$
g_P^{ud}	g_P^{ud}	g_P^{du}	g_P^{du}	$+$	Re	Re
$g_S^{uu'}$	$g_S^{dd'}$	$-g_S^{dd'}$	$g_S^{uu'}$	$+$	Im	$-$
g_S^{ud}	g_S^{ud}	$-g_S^{du}$	g_S^{du}	$-$	$\emptyset$	Re
$g_V^{uu'}$	$-g_V^{dd'}$	$-g_V^{dd'}$	$-g_V^{uu'}$	$-$	$\emptyset$	$-$
g_V^{ud}	$-g_V^{ud}$	$-g_V^{du}$	$-g_V^{du}$	$+$	Im	Im
$l_1^{uu'}$	$l_1^{dd'}$	$l_1^{dd'}$	$l_1^{uu'}$	$+$	Re	$-$
l_1^{ud}	l_1^{ud}	l_1^{du}	l_1^{du}	$+$	Re	Re
$l_A^{uu'}$	$-l_A^{dd'}$	$-l_A^{dd'}$	$-l_A^{uu'}$	$-$	$\emptyset$	/
l_A^{ud}	$-l_A^{ud}$	$-l_A^{du}$	$-l_A^{du}$	$+$	Im	Im
$l_V^{uu'}$	$l_V^{dd'}$	$l_V^{dd'}$	$l_V^{uu'}$	$+$	Re	$-$
l_V^{ud}	l_V^{ud}	l_V^{du}	l_V^{du}	$-$	Re	Re
$l_T^{uu'}$	$l_T^{dd'}$	$l_T^{dd'}$	$l_T^{uu'}$	$-$	Re	$-$
l_T^{ud}	l_T^{ud}	l_T^{du}	l_T^{du}	$+$	Re	Re
$l_{\tilde{T}}^{uu'}$	$l_{\tilde{T}}^{dd'}$	$-l_{\tilde{T}}^{dd'}$	$l_{\tilde{T}}^{uu'}$	$+$	Im	$-$
$l_{\tilde{T}}^{ud}$	$l_{\tilde{T}}^{ud}$	$-l_{\tilde{T}}^{du}$	$l_{\tilde{T}}^{du}$	$-$	$\emptyset$	Re

Appendix D
More on the chirally rotated SF at work

D.1 On the improvement of renormalization factors from universality relations

In Section 5.2.4, we commented on the fact that the $\gamma_5\tau^1$-even $O(a)$ boundary counterterms do not contribute to the universality relations involving $\gamma_5\tau^1$-even correlators. In order to show this result we will consider an explicit example.

Let us start from the universality relation,

$$(g_A^{uu'})_R = (-ig_{\tilde{V}}^{ud})_R + O(a^2). \tag{D.1}$$

The idea is simply to study the Symanzik's expansion of the ratio,

$$\frac{(-ig_{\tilde{V}}^{ud})_R}{(g_A^{uu'})_R}. \tag{D.2}$$

First of all, given the observations in Section 5.2.4 the Symanzik's expansion for the individual observables reads (cf. Section 2.2.4),

$$(g_{\tilde{V}}^{ud})_R = (g_{\tilde{V}}^{ud})_0 - a\big[(g_{\tilde{V},c_{sw}}^{ud})_0 + (g_{\tilde{V},d_s}^{ud})_0 + (g_{\tilde{V},c_t}^{ud})_0\big] + O(a^2), \tag{D.3}$$

$$(g_A^{uu'})_R = (g_A^{uu'})_0 - a\big[(g_{A,c_{sw}}^{uu'})_0 + (g_{A,d_s}^{uu'})_0 + (g_{A,c_t}^{uu'})_0 - c_A(\partial_0 g_P^{uu'})_0\big] + O(a^2). \tag{D.4}$$

First of all, note that we indicated with $(g_X^{f_1 f_2})_0$ the continuum correlation functions corresponding to the lattice correlation functions on the l.h.s. of the above relations. Secondly, we considered explicitly the insertion of all possible $O(a)$ counterterms that appear. For example, $(g_{\tilde{V},c_{sw}}^{ud})_0$ indicates the insertion in $(g_{\tilde{V}}^{ud})_0$ of the $O(a)$ counterterm corresponding to the bulk action and proportional to the improvement coefficient c_{sw}. Similarly for the other counterterms. However, as discussed in Section 5.2.4, the $\gamma_5\tau^1$-odd $O(a)$ counterterms do not contribute to $\gamma_5\tau^1$-even correlation functions, and

are thus crossed out in the above equations. As anticipated, the only remaining cutoff effects are the ones associated with the $\gamma_5\tau^1$-even $O(a)$ boundary operators and proportional to c_t and d_s. Once however we consider the ratio of the above correlation functions, we obtain,

$$\frac{(-ig_{\widetilde{V}}^{ud})_R}{(g_A^{uu'})_R} = \frac{(-ig_V^{ud})_0 - a\left[(-ig_{V,d_s}^{ud})_0 + (-ig_{V,c_t}^{ud})_0\right]}{(g_A^{uu'})_0 - a\left[(g_{A,d_s}^{uu'})_0 + (g_{A,c_t}^{uu'})_0\right]} + O(a^2)$$

$$= \frac{-i(g_V^{ud})_0}{(g_A^{uu'})_0}\left\{1 - a\left[\frac{(g_{V,d_s}^{ud})_0}{(g_V^{ud})_0} + \frac{(g_{V,c_t}^{ud})_0}{(g_V^{ud})_0} - \frac{(g_{A,d_s}^{uu'})_0}{(g_A^{uu'})_0} - \frac{(g_{A,c_t}^{uu'})_0}{(g_A^{uu'})_0}\right]\right\} + O(a^2).$$

$$(D.5)$$

If we now remind that the universality relations are valid exactly for the continuum correlation functions, we then have that: $(-ig_V^{ud})_0 = (g_A^{uu'})_0$. Consequently, noticing that the counterterms proportional to d_s and c_t are invariant under a chiral rotation, we hence have: $(-ig_{V,d_s}^{ud})_0 = (g_{A,d_s}^{uu'})_0$, and similarly for the c_t counterterm. We then conclude that the term in square brackets in the above equation is zero, and thus,

$$\frac{(-ig_{\widetilde{V}^{ud}})_R}{(g_A^{uu'})_R} = 1 + O(a^2). \qquad (D.6)$$

Similar conclusions can be derived for Z_V, Z_P/Z_S, $Z_T/Z_{\widetilde{T}}$, and general universality relations between SF and χSF correlation functions.

D.2 Systematic error estimates

In this Appendix we want to describe how we have estimated the systematic errors of our renormalization constants associated with the deviation from the given line of constant physics. We will distinguish three sources of systematic, that are related to the finite precision with which we unavoidably impose the following conditions,

$$m = 0, \qquad g_A^{ud} = 0, \qquad L = \text{const.}, \qquad (D.7)$$

where m is the PCAC mass for this section. Note that for the latter discussion, it is more convenient to look at the condition $g_A^{ud} = 0$ as a condition for z_f rather than g_A^{ud}. Note also that for definiteness we consider the case of the line of constant physics given by LCP_0. A similar strategy has been used for LCP_1, LCP_2, and LCP_3, although in this case we neglected the systematic due to the condition on L. The procedure we used to estimate these systematics has then been the following.

We considered the systematic error on a given (finite) Z factor has given by,

$$(dZ_{\mathrm{sys}})^2 \equiv (dZ_{z_f})^2 + (dZ_m)^2 + (dZ_L)^2, \tag{D.8}$$

where dZ_m, dZ_{z_f}, dZ_L, are the error estimates for the systematics due to the condition on the PCAC mass, z_f, and L, respectively. These have been estimated as follows.

Starting from dZ_{z_f}, we have,

$$(dZ_{z_f})^2 \equiv \left(\frac{\partial Z}{\partial z_f}\right)^2 (dz_f)^2 + \left(\frac{\partial Z}{\partial mL}\right)^2 \left(\frac{dmL}{dz_f}\right)^2 (dz_f)^2, \tag{D.9}$$

were dmL/dz_f is the derivative of the PCAC mass w.r.t z_f, multiplied by L. Note that the derivatives are in principle evaluated at the conditions (D.7), in practice we have computed them at our tuned values. Given the above expression, the derivative $\frac{\partial Z}{\partial z_f}$ has been estimated as follows. We have generated two ensembles at $L/a = 8$, $\beta = 5.2$ where z_f has been varied of plus and minus 2% w.r.t. our tuned value.[1] All other bare parameters have been kept fixed. The derivatives of our renormalization factors w.r.t. z_f have then been computed using a symmetric finite difference approximation. Using the (less accurate) results from the tuning runs of the other ensembles of LCP_0, we could confirm that the value of the derivative at $L/a = 8$ is an upper bound for the derivatives at the larger values of L/a.[2] Similarly, from the tuning runs we could also estimate that $\frac{dmL}{dz_f}$ is zero to good approximation. This is simply the observation we made already that the PCAC mass does not depend much on z_f, close to the critical values. The corresponding contribution in (D.9) has thus been neglected. Finally, for dz_f we have considered,

$$dz_f = \left(\frac{\partial g_A^{ud}}{\partial z_f}\right)^{-1} dg_A^{ud}. \tag{D.10}$$

where dg_A^{ud} is the residual value of g_A^{ud} on the tuned ensembles, and for $\frac{\partial g_A^{ud}}{\partial z_f}$ we have taken the value computed at $L/a = 8$ and $\beta = 5.2$. In fact this derivative is not a cutoff effect, and we thus used the tuning runs to estimate the continuum limit of it.

---

[1] We also checked that with a variation of z_f of 5% compatible results were obtained.

[2] Note that $\frac{\partial Z}{\partial z_f}$ is a cutoff effect. The value at $L/a = 8$ is thus expected to be an overestimation for larger L/a's, if we are in the scaling region for this quantity. Within our precision, this seems to be the case.

Within our precision $\frac{\partial g_A^{ud}}{\partial z_f}$ turns out to be basically constant along LCP_0. The value we obtained is roughly given by $\frac{\partial g_A^{ud}}{\partial z_f} \sim -2.5$.

The second contribution in (D.8) is given by

$$(\mathrm{d}Z_m)^2 \equiv \left(\frac{\partial Z}{\partial mL}\right)^2 (\mathrm{d}mL)^2 + \left(\frac{\partial Z}{\partial z_f}\right)^2 \left(\frac{\mathrm{d}z_f^*}{\mathrm{d}mL}\right)^2 (\mathrm{d}mL)^2. \qquad (\text{D.11})$$

The derivatives w.r.t. the PCAC mass $\frac{\partial Z}{\partial mL}$ have been estimated similarly to the derivative w.r.t. z_f. We generated a single ensemble in this case at $L/a = 8$ and $\beta = 5.2$, where the (bare) PCAC mass has been increased by roughly $30\,\text{MeV}$. We have then estimated the derivative with an asymmetric finite difference. Note that, this derivative is a cutoff effect, and so we have used the tuning runs in order to judge whether the value at $L/a = 8$ offered an upper bound for it along LCP_0. This is in fact the case. The derivative $\frac{\mathrm{d}z_f^*}{\mathrm{d}mL}$ instead is not a cutoff effect. We have estimated its value along LCP_0 using again the tuning runs. In fact within our precision, this quantity turned out to be pretty constant along our LCP_0, and roughly equal to $\frac{\mathrm{d}z_f^*}{\mathrm{d}mL} \sim -1$.[3] To conclude with this systematic effect, we have taken $\mathrm{d}mL$ to be the residual PCAC mass am at the tuned ensembles, multiplied by L/a.

For the last contribution in (D.8) we have simply taken,

$$(\mathrm{d}Z_L)^2 \equiv \left(L\frac{\partial Z}{\partial L}\right)^2 \left(\frac{\mathrm{d}L}{L}\right)^2 \qquad (\text{D.12})$$

In this case we have estimated this derivative for each ensemble along LCP_0 through a dedicated simulation. More precisely, in order to estimate the value for the ensemble at $L/a = 12$ and $\beta = 5.5$, we have done a simulation at $L/a = 8$ and $\beta = 5.5$ keeping all other bare parameters fixed. The derivative has then been evaluated using an asymmetric finite difference.[4] Similarly for the ensemble at $L/a = 16$ and $\beta = 5.7$, we have generated a corresponding ensemble at $L/a = 12$ and $\beta = 5.7$. Note that the ensemble at $L/a = 8$, $\beta = 5.2$, is by definition on the LPC, and we thus do not need to take this systematic into account. Regarding the ensemble at $L/a = 9.2$ instead,

---

[3] Note that, the corresponding value obtained from tree-level perturbation theory is given by $\frac{\mathrm{d}z_f^*}{\mathrm{d}mL} \sim -0.3$ (Vilaseca, 2013).

[4] Note that in this case the denominator in this numerical derivative is of $O(1)$, what we are getting is thus a really rough estimate.

we have performed an interpolation of our observables to the exact value of L/a given by the condition of constant L using the results of simulations at different L/a's (cf. Section D.3). This was done as otherwise the systematic effect related to L would have been to large, and would have spoiled the good precision of our determinations. Finally, note that in (D.12) we neglected the contributions coming from the variation of the PCAC mass, and the condition on z_f w.r.t. L. On the other hand, using the results from the interpolation at $\beta = 5.3$, we could get a good estimate for dZ_L at this β. Considering that this is an $O(a^2)$ effect, we concluded that the systematic errors dZ_L we have estimated on the other ensembles using (D.12) are already conservative. We have also checked that including these contributions increases the systematic error by roughly 20% only at the value of $\beta = 5.5$. For $\beta = 5.7$ instead these are negligible. Given these observations, we decided to neglect these contributions also for $\beta = 5.5$.

Finally, the values of dL/a that enter in (D.12) have been estimated as: $dL/a = L^{\text{ext}}/a - L/a$, where L^{ext}/a are the exact values of L/a that we would need to satisfy the condition $L = $ const. These are obtained by simply using the values of the lattice spacings in Table 5.2. We remind that the uncertainty on the lattice spacing can be neglected in practice. L/a instead is the value at which we simulated. In fact, these deviations are tiny i.e. $dL/L \sim 0.03$ for the two ensembles at $\beta = 5.5$. and $\beta = 5.7$.

To conclude with the systematics, a few words about the points in the ensemble PT. dZ_m, dZ_{z_f} have been estimated as described above. Regarding dZ_L instead, we have simulated an ensemble at $\beta = 7.2$ and $L/a = 16$, and we have taken the difference between the corresponding Z determinations as a systematic on Z. The same error has been used for the other points at $\beta = 8.4, 9.6$. In this case estimating the derivative would have been in fact pointless since dL is of $O(10)$.

The gradient flow coupling. Some additional information about our simulations can be extracted from flow observables at very little extra cost. Specifically we looked at the gradient flow coupling in finite volume with SF boundary conditions (Fritzsch and Ramos, 2013). For this coupling the renormalization scale is set by $\mu = L^{-1}$, and the flow time at which is measured is specified by the ratio $c = \sqrt{8t}/L$, which

Fig. D.1: Continuum limit extrapolations for the gradient flow coupling along the line of constant physics defined by LCP_0. Three different renormalization schemes are considered.
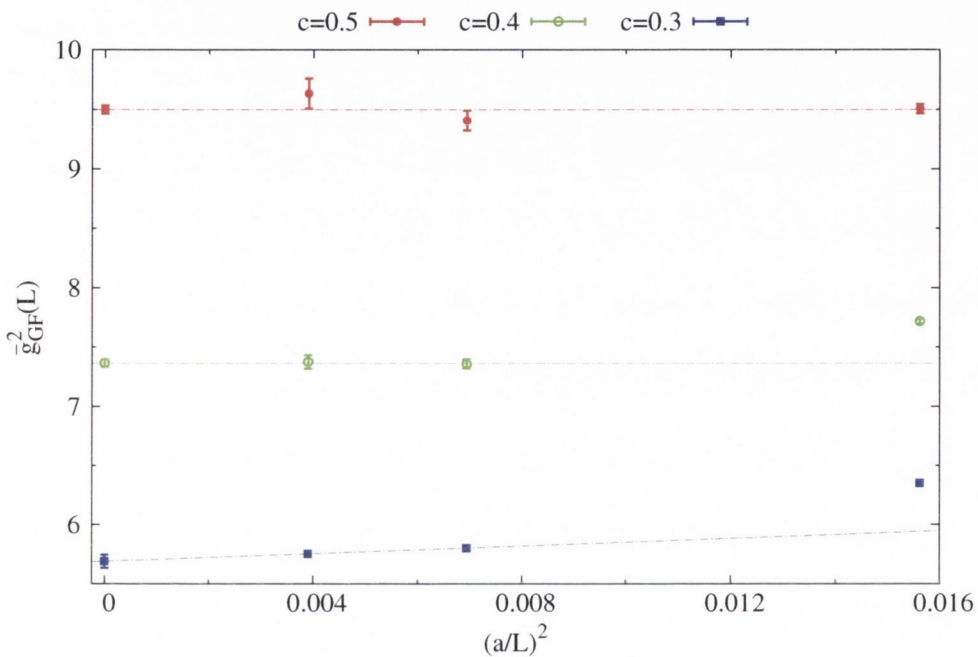
has to be kept fixed while taking the continuum limit.[5] In particular, different values of c correspond to different renormalization schemes. For our analysis, the important observation is that by measuring this observable we can gain some insight on how well the condition $L = $ const. is satisfied on our ensembles. Indeed, if the condition is well-satisfied, the gradient flow coupling should smoothly approach its continuum limit value at the renormalization scale $\mu = L^{-1}$, with the expected scaling. Specifically, one would expect some $O(a)$ lattice artifacts coming from the boundaries. However, if these effects are small within our precision, we could in principle expect an a^2 scaling, or even a constant.

[5] Note that in the SF one has to pick up a time slice where to measure the energy density that defines the coupling. In the following we take $x_0 = T/2$.

Given these observations, in Figure D.1 we present the continuum limit extrapolations of the gradient flow (GF) coupling $\bar{g}_{\mathrm{GF}}^2(L)$ for three different schemes c.[6] Note that the value at $\beta = 5.3$ is not available. In this case in fact an interpolation in L/a is non-trivial since this quantity is scale dependent. As we can see from the plot, as we move towards bigger values of c the statistical precision on the coupling decreases for a fixed number of gauge configurations, but also cutoff effects. These are general features of the GF coupling in finite volume (see (Fritzsch and Ramos, 2013)). Thus, considering the results for $c = 0.5$, we can conclude that qualitatively the condition of constant L is well-satisfied on our ensembles. Note that this is a non-trivial result, in particular considering that the value for L/a at $\beta = 5.7$ has been estimated using bare lattice perturbation theory.

D.3   Details on the interpolation at $\beta = 5.3$

We here comment on the determination of the finite renormalization constants Z_V and Z_A at $\beta = 5.3$, since this provides indirect evidence for the automatic $\mathrm{O}(a)$ improvement of these determinations. Similar results hold for the ratio Z_P/Z_S. This case however is less interesting since this ratio is improved once the action is improved.

As discussed in Section 5.3.2, for this value of the bare coupling the LCP condition $L \sim 0.6\,\mathrm{fm}$ would require a lattice size of $L/a \sim 9.2$ (cf. Table 5.2). However, as mentioned our simulation code can only simulate even lattice sizes L/a. In order to determine the renormalization factors for the required value of L/a, we then exploited the cutoff dependence of $Z_{V,A}$. More precisely, at fixed $\beta = 5.3$ we have simulated three different lattice sizes corresponding to $L/a = 8, 10, 12$. If the determinations are $\mathrm{O}(a)$ improved, we expect the results for $Z_{V,A}$ on these lattices to differ by cutoff effects of $\mathrm{O}(a^2)$. We can then use this dependence to actually interpolate the results at the given vale of $L/a = 9.2$.

In Figure D.2 we reported our results for Z_V and Z_V at fixed $\beta = 5.3$ and for the different lattice sizes $L/a = 8, 10, 12$. As we can see, the dependence on $(a/L)^2$ is nicely linear, meaning that higher order terms in a are negligible within our precision.

---

[6]The author wants to thank Alberto Ramos for providing several routines for the computation of the GF coupling.
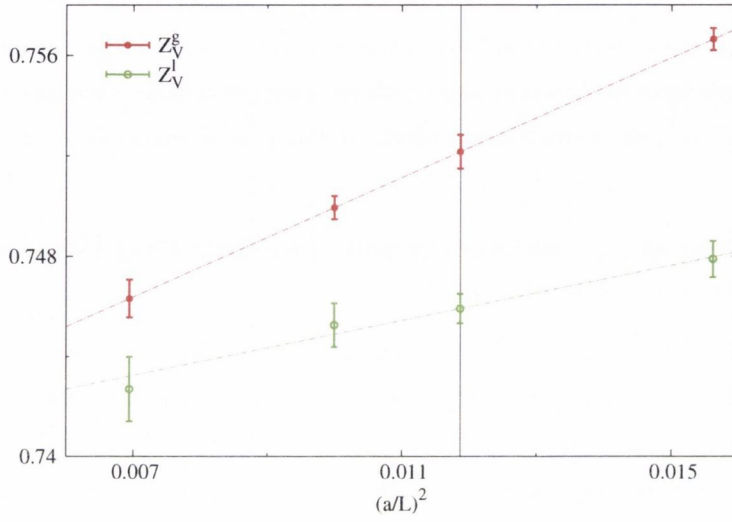
(a) Z_V
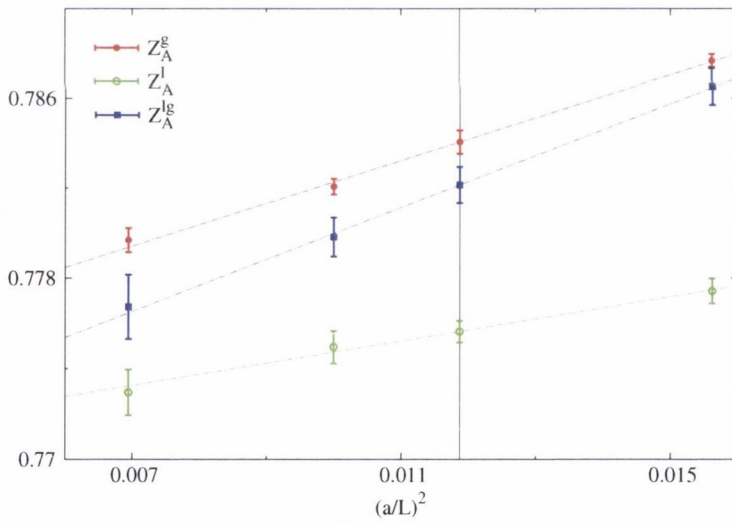
(b) Z_A

Fig. D.2: Z_V and Z_A interpolations for $\beta = 5.3$. Three different lattice sizes have been considered: $L/a = 8, 10, 12$.

Due to this linear dependence, it is then easy to interpolate the results to the desired value of $L/a = 9.2$. These are marked on the plot by a black vertical line. Note that, the renormalization constants defined in terms of the l-functions only, generally have a milder dependence on L/a than those defined using g-functions. Overall however, all definitions of $Z_{V,A}$ show small cutoff effects at this (not so small) value of the lattice spacing.

D.4   Scaling of $Z_{A,V}$ differences and automatic O(a) improvement from the femto-universe

Z_V and Z_A **differences.**   Similarly to what done in Section 5.4.3, we considered the continuum limit extrapolation of the differences between different definitions of Z_V and Z_A along the LCPs given by LCP$_1$, LCP$_2$, and LCP$_3$. We collected the results obtained for the three different values of the SF coupling in Figure D.3. Note that, we fit the data through a linear fit in $(a/L)^2$, including only the points at $L/a = 8, 12$. The fit is then constrained to pass through zero. Looking at the deviation from the fitting line thus permits to judge whether the $L/a = 6$ lattice belongs or not to the scaling region. As we can see, similar conclusions as in Section 5.4.3 can be drawn. In particular, the O(a^2) scaling is obtained for the largest values of L/a, and the effect of the O(a) improvement of the axial current in the definition of Z_A^g does not affect the results within errors.

Automatic O(a) improvement.   Here we propose a study of the $\gamma_5 \tau^1$-odd correlation functions considered in Section 5.6, along the LCPs defined by LCP$_1$, LCP$_2$, and LCP$_3$. The results are collected in Figure D.4. Similarly to what noticed there, the only (literally) odd function that shows some sizable cutoff effects is $l_{\widetilde{V}}^{ud}$. Remarkably, all other correlators are zero within errors along all LCPs. In this case however, including the O(a) operator counterterm to $l_{\widetilde{V}}^{ud}$ using the tree-level value for $c_{\widetilde{V}}$ simply changes the sign of the cutoff effects (cf. results for $l_{\widetilde{V}_I}^{ud}$). As we can see though, the contribution of the operator counterterm is an O(a) effect that properly vanishes in the continuum limit. In conclusion, we confirm our expectation that O(a) cutoff effects are generally small in these correlation functions.
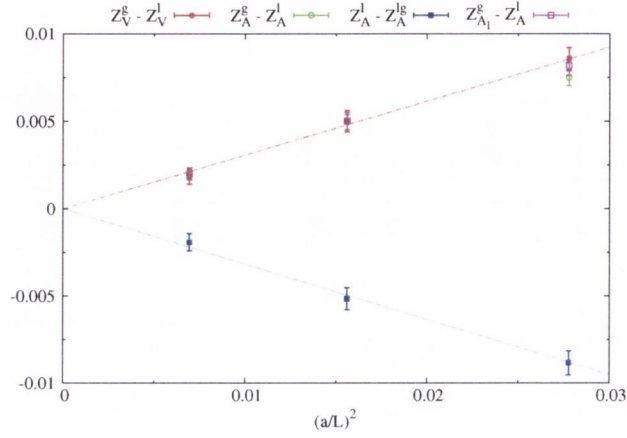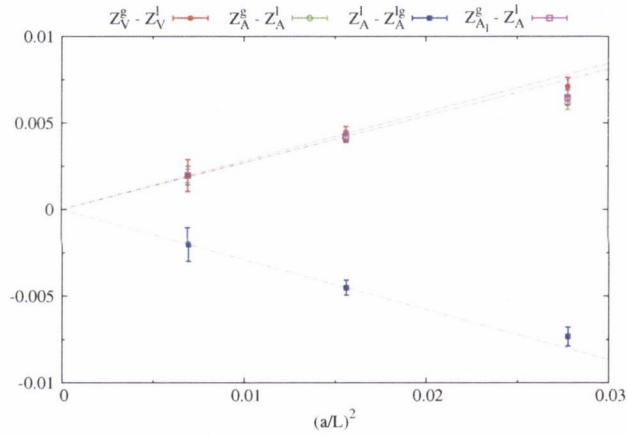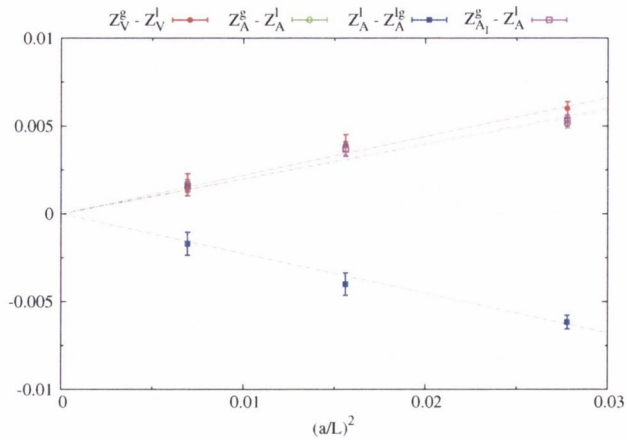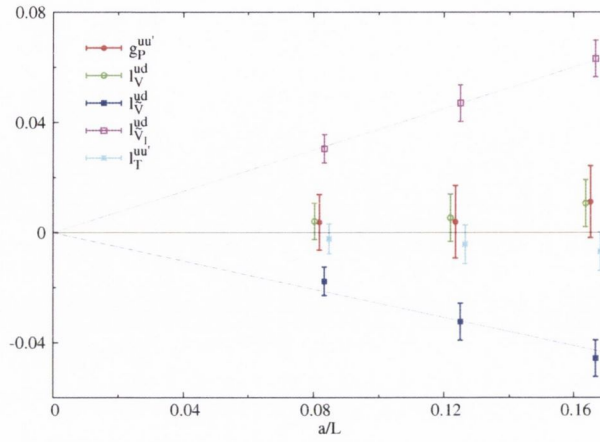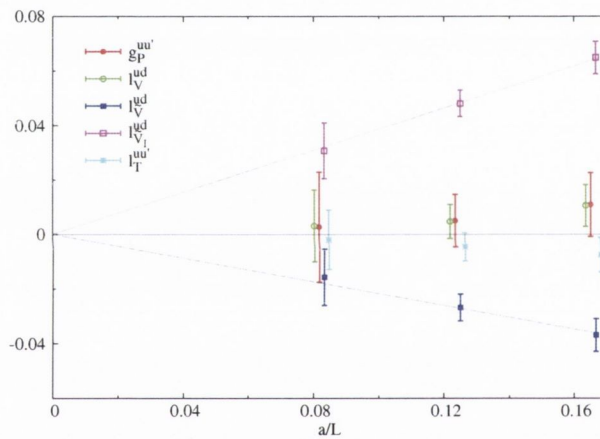
(a) $\bar{g}^2(L) = 3.3$
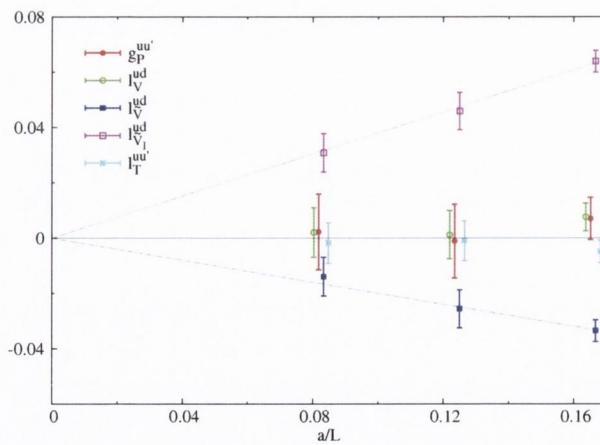

(b) $\bar{g}^2(L) = 2.5$

(c) $\bar{g}^2(L) = 2.0$

Fig. D.3: Continuum limit extrapolations for the differences between different χSF definitions of Z_V and Z_A along the lines of constant physics defined by LCP$_1$, LCP$_2$, and LCP$_3$.

(a) $\bar{g}^2(L) = 3.3$

(b) $\bar{g}^2(L) = 2.5$

(c) $\bar{g}^2(L) = 2.0$

Fig. D.4: Continuum limit extrapolations for a set of $\gamma_5\tau^1$-odd correlation functions along the lines of constant physics given by LCP_1, LCP_2, and LCP_3.

References

Abbott, L.F. (1982). *Acta Phys. Polon.*, **B13**, 33.

Aitchison, I.J.R. and Hey, A.J.G. (2004). *Gauge Theories in Particle Physics* (3rd edn). Graduate Student Series in Physics.

Aoki, S. and Bär, O. (2006). *Phys. Rev.*, **D74**, 034511.

Becirevic, D. et al. (2003). *Nucl. Phys. Proc. Suppl.*, **119**, 442–445.

Bochicchio, M. et al. (1985). *Nucl. Phys.*, **B262**, 331.

Bode, A. and Panagopoulos, H. (2002). *Nucl. Phys.*, **B625**, 198–210.

Bode, A., Weisz, P., and Wolff, U. (1999). *Nucl. Phys.*, **B540**, 491–499.

Bode, A., Weisz, P., and Wolff, U. (2000). *Nucl. Phys.*, **B576**, 517–539.

Brambilla, M. et al. (2013). *PoS*, **LATTICE2013**, 325.

Capitani, S., Lüscher, M., Sommer, R., and Wittig, H. (1999). *Nucl. Phys.*, **B544**, 669–698.

Chiu, T. W. (2013). *J. Phys. Conf. Ser.*, **454**, 012044.

Clark, M.A., Joo, B., Kennedy, A.D., and Silva, P.J. (2011). *Phys. Rev.*, **D84**, 071502.

Clark, M.A. and Kennedy, A.D. (2007). *Phys. Rev. Lett.*, **98**, 051601.

Collins, J. C. (1986). *Renormalization: An Introduction to Renormalization, the Renormalization Group and the Operator-Product Expansion*. Cambridge Monographs on Mathematical Physics.

Collins, J. C., Manohar, A. V., and Wise, M. B. (2006). *Phys. Rev.*, **D73**, 105019.

Constantinou, M. et al. (2010). *JHEP*, **1008**, 068.

Creutz, M. (1998). *Phys. Rev. Lett.*, **81**, 3555–3558.

Del Debbio, L. et al. (2006). *JHEP*, **0602**, 011.

Della Morte, M. et al. (2005*a*). *Nucl. Phys.*, **B729**, 117–134.

Della Morte, M., Hoffmann, R., Knechtli, F., Sommer, R., and Wolff, U. (2005*b*). *JHEP*, **0507**, 007.

Della Morte, M., Hoffmann, R., and Sommer, R. (2005*c*). *JHEP*, **0503**, 029.

Della Morte, M., Sommer, R., and Takeda, S. (2009). *Phys. Lett.*, **B672**, 407–412.

Donini, A. et al. (1995). *Phys. Lett.*, **B360**, 83–92.

Donoghue, J. F., Golowich, E., and Holstein, B. R. (1994). *Dynamics of the Standard Model*. Cambridge Monographs on Particle Physics, Nuclear Physics and Cosmology.

Duane, S., Kennedy, A.D., Pendleton, B.J., and Roweth, D. (1987). *Phys. Lett.*, **B195**, 216–222.

Ellis, R. K., Stirling, W. J., and Webber, B. R. (1996). *QCD and Collider Physics*. Cambridge Monographs on Particle Physics, Nuclear Physics and Cosmology.

Fodor, Z. et al. (2012). *JHEP*, **1211**, 007.

Frezzotti, R., Grassi, P. A., Sint, S., and Weisz, P. (2001). *JHEP*, **0108**, 058.

Frezzotti, R., Martinelli, G., Papinutto, M., and Rossi, G.C. (2006). *JHEP*, **0604**, 038.

Frezzotti, R. and Rossi, G.C. (2004). *JHEP*, **0408**, 007.

Frezzotti, R. and Rossi, G. (2005).

Fritzsch, P. et al. (2012). *Nucl. Phys.*, **B865**, 397–429.

Fritzsch, P., Heitger, J., and Tantalo, N. (2010). *JHEP*, **1008**, 074.

Fritzsch, P. and Ramos, A. (2013). *JHEP*, **1310**, 008.

Fritzsch, P., Ramos, A., and Stollenwerk, F. (2013). *PoS*, **Lattice2013**, 461.

Giusti, L. et al. (2001). *Int. J. Mod. Phys.*, **A16**, 3487–3534.

Golterman, M. (2009). *Applications of chiral perturbation theory to lattice QCD*. Lectures given at the Summer School: Modern perspectives in lattice QCD, Les Houches, August 3-28, 2009.

Gonzalez-Arroyo, A., Jurkiewicz, J., and Korthals-Altes, C.P. (1981). *Ground state metamorphosis for Yang-Mills fields on a finite periodic lattice*.

Gonzalez-Lopez, J. (2011). PhD thesis. Humboldt-Universität zu Berlin.

Gonzlez-Arroyo, A. and Okawa, M. (2013). *Phys. Rev.*, **D88**, 014514.

Gribov, V.N. (1978). *Nucl. Phys.*, **B139**, 1.

Gross, D. J. and Wilczek, F. (1973). *Phys. Rev. Lett.*, **30**, 1343–1346.

Guagnelli, M. et al. (2001). *Nucl. Phys.*, **B595**, 44–62.

Guagnelli, M. et al. (2006). *JHEP*, **0603**, 088.

Guagnelli, M. and Sommer, R. (1998). *Nucl. Phys. Proc. Suppl.*, **63**, 886–888.

Hasenbusch, M. (2001). *Phys. Lett.*, **B519**, 177–182.

Hasenbusch, M. and Jansen, K. (2003). *Nucl. Phys.*, **B659**, 299–320.

Hasenfratz, P. (1998). *Nucl. Phys.*, **B525**, 401–409.

Hesse, D. and Sommer, R. (2013). *JHEP*, **1302**, 115.

Jansen, K., et al. (1996). *Phys. Lett.*, **B372**, 275–282.

Jansen, K. and Sommer, R. (1998). *Nucl. Phys. Proc. Suppl.*, **63**, 853–855.

Joo, B. et al. (2000). *Phys. Rev.*, **D62**, 114501.

Kaplan, D. B. (1992). *Phys. Lett.*, **B288**, 342–347.

Kaplan, D. B. (2009). *Chiral Symmetry and Lattice Fermions*. Lectures given at the Summer School: Modern perspectives in lattice QCD, Les Houches, August 3-28, 2009.

Karsten, L. H. and Smit, J. (1981). *Nucl. Phys.*, **B183**, 103.

Kennedy, A.D. (2006). *Algorithms for dynamical fermions*. Lectures given at the Summer School: Perspectives in Lattice QCD, Nara, October 31 - November 14, 2005.

Kennedy, A.D., Silva, P.J., and Clark, M.A. (2013). *Phys. Rev.*, **D87**(3), 034511.

Kikukawa, Y. and Yamada, A. (1999). *Nucl. Phys.*, **B547**, 413–423.

Lellouch, Laurent (2011). *Flavor physics and lattice quantum chromodynamics*. Lectures given at the Summer School: Modern perspectives in lattice QCD, Les Houches, August 3-28, 2009.

Lepage, G. P. and Mackenzie, P. B. (1993). *Phys. Rev.*, **D48**, 2250–2264.

Lopez, J. Gonzalez, Jansen, K., Renner, D.B., and Shindler, A. (2013a). *Nucl.Phys.*, **B867**, 609–635.

Lopez, J. Gonzalez, Jansen, K., Renner, D.B., and Shindler, A. (2013b). *Nucl.Phys.*, **B867**, 567–608.

Lüscher, M. (1977). *Commun. Math. Phys.*, **54**, 283.

Lüscher, M. (1986a). *Commun. Math. Phys.*, **104**, 177.

Lüscher, M. (1986b). *Commun. Math. Phys.*, **105**, 153–188.

Lüscher, M. (1988). *Conf. Proc.*, **C880628**, 451–528.

Lüscher, M. (1998a). *Advanced lattice QCD*. Lectures given at the Summer School: Probing the Standard Model of Particle Interactions, July 28 - September 5, Les Houches, 1997.

Lüscher, M. (1998b). *Phys. Lett.*, **B428**, 342–345.

Lüscher, M. (2000). *Chiral gauge theories revisited*. Lectures given at the International School of Subnuclear Physics, 27 August - 5 September, Erica, 2000.

Lüscher, M. (2005). *Comput. Phys. Commun.*, **165**, 199–220.

Lüscher, M. (2006). *JHEP*, **0605**, 042.

Lüscher, M. (2010a). *Computational Strategies in Lattice QCD*. Lectures given at the Summer School: Modern perspectives in lattice QCD, Les Houches, August 3-28, 2009.

Lüscher, M. (2010b). *JHEP*, **1008**, 071.

Lüscher, M., Narayanan, R., Weisz, P., and Wolff, U. (1992). *Nucl. Phys.*, **B384**, 168–228.

Lüscher, M. and Palombi, F. (2008). *PoS*, **LATTICE2008**, 049.

Lüscher, M. and Schaefer, S. (2011). *JHEP*, **1104**, 104.

Lüscher, M. and Schaefer, S. (2013). *Comput. Phys. Commun.*, **184**, 519–528.

Lüscher, M., Sint, S., Sommer, R., and Weisz, P. (1996). *Nucl. Phys.*, **B478**, 365–400.

Lüscher, M., Sint, S., Sommer, R., Weisz, P., and Wolff, U. (1997a). *Nucl. Phys.*, **B491**, 323–343.

Lüscher, M., Sint, S., Sommer, R., and Wittig, H. (1997b). *Nucl. Phys.*, **B491**, 344–364.

Lüscher, M. and Weisz, P. (1985a). *Phys. Lett.*, **B158**, 250.

Lüscher, M. and Weisz, P. (1985b). *Commun. Math. Phys.*, **97**, 59.

Lüscher, M. and Weisz, P. (1996). *Nucl. Phys.*, **B479**, 429–458.

Lüscher, M., Weisz, P., and Wolff, U. (1991). *Nucl. Phys.*, **B359**, 221–243.

Maiani, L. and Martinelli, G. (1986). *Phys. Lett.*, **B178**, 265.

Martinelli, G. et al. (1993). *Phys. Lett.*, **B311**, 241–248.

Martinelli, G. et al. (1995). *Nucl. Phys.*, **B445**, 81–108.

Martinelli, G. et al. (1997). *Phys. Lett.*, **B411**, 141–151.

Montvay, I. and Münster, G. (1997). *Quantum Fields on a Lattice.* Cambridge Monographs on Mathematical Physics.

Narayanan, R. and Neuberger, H. (1995). *Nucl. Phys.*, **B443**, 305–385.

Narayanan, R. and Wolff, U. (1995). *Nucl. Phys.*, **B444**, 425–446.

Neuberger, H. (1998). *Phys. Lett.*, **B417**, 141–144.

Niedermayer, F. (1999). *Nucl. Phys. Proc. Suppl.*, **73**, 105–119.

Nielsen, H. B. and Ninomiya, M. (1981*a*). *Nucl. Phys.*, **B185**, 20.

Nielsen, H. B. and Ninomiya, M. (1981*b*). *Nucl. Phys.*, **B193**, 173.

Nielsen, H. B. and Ninomiya, M. (1981*c*). *Phys. Lett.*, **B105**, 219.

Omelyan, I. P., Mryglod, I. M., and Folk, R. (2003). *Comp. Phys. Commun.*, **151**, 272.

Osterwalder, K. and Seiler, E. (1978). *Annals Phys.*, **110**, 440.

Parisi, G. (1980). *World Sci. Lect. Notes Phys.*, **49**, 349–386.

Parisi, G. (1984). *Prolegomena to any future computer evaluation of the QCD mass spectrum.*

Parisi, G. (1985). *Nucl. Phys.*, **B254**, 58–70.

Perez-Rubio, P. and Sint, S. (2010). *PoS*, **LATTICE2010**, 236.

Politzer, H. D. (1973). *Phys. Rev. Lett.*, **30**, 1346–1349.

Reisz, T. (1989). *Nucl. Phys.*, **B318**, 417.

Reisz, T. and Rothe, H.J. (2000). *Nucl. Phys.*, **B575**, 255–266.

Rothe, H. J. (2012). *Lattice Gauge Theories: An Introduction.* World Scientific Lecture Notes in Physics.

Schaefer, S. (2012). *PoS*, **LATTICE2012**, 001.

Schaefer, S., Sommer, R., and Virotta, F. (2011). *Nucl.Phys.*, **B845**, 93–119.

Sexton, J.C. and Weingarten, D.H. (1992). *Nucl. Phys.*, **B380**, 665–678.

Sharpe, S. R. (2006). *Applications of Chiral Perturbation theory to lattice QCD.* Lectures given at the Workshop: Perspectives in Lattice QCD, Nara, Japan, Oct 31-Nov 11, 2005.

Sheikholeslami, B. and Wohlert, R. (1985). *Nucl. Phys.*, **B259**, 572.

Shindler, A. (2006). *PoS*, **LAT2005**, 014.

Sint, S. (1994). *Nucl. Phys.*, **B421**, 135–158.

Sint, S. (1995). *Nucl. Phys.*, **B451**, 416–444.

Sint, S. (2006). *PoS*, **LAT2005**, 235.

Sint, S. (2007*a*). *Lattice QCD with a chiral twist.*

Sint, S. (2007*b*). *PoS*, **LAT2007**, 253.

Sint, S. (2011). *Nucl. Phys.*, **B847**, 491–531.

Sint, S. and Leder, B. (2010). *PoS*, **LATTICE2010**, 265.

Sint, S. and Sommer, R. (1996). *Nucl. Phys.*, **B465**, 71–98.

Sint, S. and Weisz, P. (1997). *Nucl. Phys.*, **B502**, 251–268.

Sint, S. and Weisz, P. (1998). *Nucl. Phys. Proc. Suppl.*, **63**, 856–858.

Sommer, R. (1997). *Nonperturbative renormalization of QCD.* Lectures given at the 36th Internationale Universitätswochen für Kern- und Teilchen-physik: Computing Particles, Schladming, 1997.

Symanzik, K. (1981*a*). *Nucl. Phys.*, **B190**, 1.

Symanzik, K. (1981*b*). *Some Topic in Quantum Field Theory.* Presented at the 6th International Conference on Mathematical Physics, Berlin, August 1981.

Symanzik, K. (1983*a*). *Nucl. Phys.*, **B226**, 187.

Symanzik, K. (1983*b*). *Nucl. Phys.*, **B226**, 205.

't Hooft, G. (1973). *Nucl. Phys.*, **B61**, 455–468.

't Hooft, G. (1979). *Nucl. Phys.*, **B153**, 141.

Takeda, S. (2009*a*). *PoS*, **LAT2009**, 204.

Takeda, S. (2009*b*). *Nucl. Phys.*, **B811**, 36–65.

Taniguchi, Y. (2005). *JHEP*, **0512**, 037.

Testa, M. (1998). *JHEP*, **9804**, 002.

Urbach, C., Jansen, K., Shindler, A., and Wenger, U. (2006). *Comput. Phys. Commun.*, **174**, 87–98.

Vilaseca, P. (2013). PhD thesis. Trinity College Dublin.

Vladikas, A. (2011). *Three Topics in Renormalization and Improvement.* Lectures given at the Summer School: Modern perspectives in lattice QCD, Les Houches, August 3-28, 2009.

Weinberg, S. (1973). *Phys. Rev.*, **D8**, 3497–3509.

Weinberg, S. (2005). *The Quantum Theory of Fields, Volume 2: Modern Applications.* Cambridge University Press.

Weisz, P. (2010). *Renormalization and lattice artifacts.* Lectures given at the Summer School: Modern perspectives in lattice QCD, Les Houches, August 3-28, 2009.

Wilson, K. G. (1974). *Phys.Rev.*, **D10**, 2445–2459.

Wohlert, R. (1987). PhD thesis. DESY Hamburg.

Wolff, U. (1986). *Nucl. Phys.*, **B265**, 537.

Wolff, U. (2004). *Comput. Phys. Commun.*, **156**, 143–153.